Hydrometallurgical recycling of rare earth elements from secondary resources

Peelman, Sebastiaan

DOI
10.4233/uuid:17e8a268-130c-4c36-b235-ba9e7747c45f

Publication date
2019

Document Version
Final published version

Citation (APA)
Peelman, S. (2019). *Hydrometallurgical recycling of rare earth elements from secondary resources*. [Dissertation (TU Delft), Delft University of Technology]. https://doi.org/10.4233/uuid:17e8a268-130c-4c36-b235-ba9e7747c45f

Hydrometallurgical Recycling of Rare Earth Elements from Secondary Resources

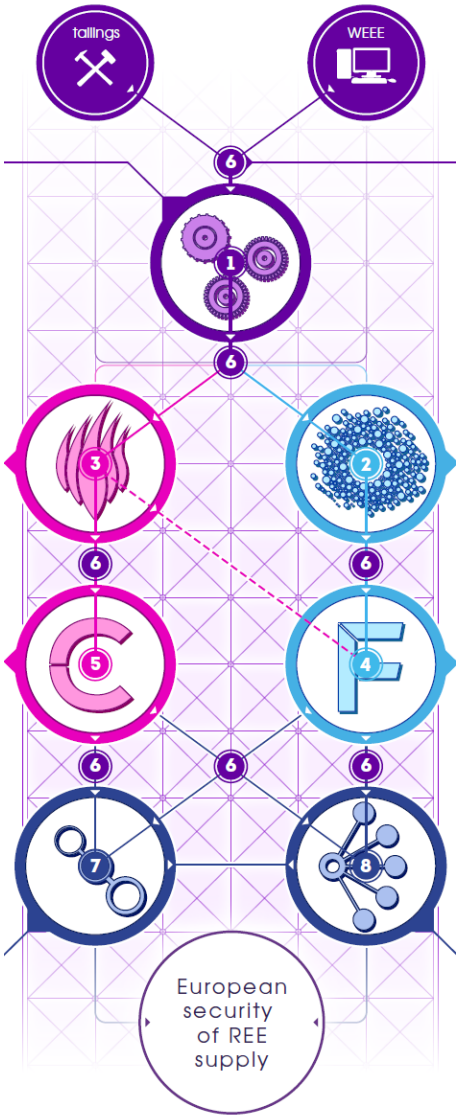

Sebastiaan Peelman

This work is funded by the FP7 REEcover project

Hydrometallurgical Recycling of Rare Earth Elements from Secondary Resources

Dissertation

for the purpose of obtaining the degree of doctor
at Delft University of Technology
by the authority of the Rector Magnificus Prof.dr.ir. T.H.J.J. van der Hagen
chair of the Board of Doctorates,
to be defended publicly on
Tuesday 23 April 2019 at 10:00 o'clock

by

Sebastiaan PEELMAN
Master of Science in Materials Engineering: Metallurgy
Ghent University, Belgium
born in Ghent, Belgium

This dissertation has been approved by the promotors.

Composition of the doctoral committee:

Rector Magnificus,	chairperson
Prof.dr.ir. J. Sietsma	Delft University of Technology, promotor
Dr. Y.Yang	Delft University of Technology, promotor

Independent members:

Prof.dr. A. Stankiewicz	Delft University of Technology
Prof.dr. R. Petrov	Ghent University
Prof.dr. T. Van Gerven	KU Leuven
Prof.dr. G. Tranell	Norwegian University of Science and Technology
Prof.dr. A. Jokilaakso	Aalto University

This research received financial support and was carried out as part of the FP7 REEcover project (Project ID: 603564).

Table of contents

Chapter 1: Introduction

1.1. The Rare Earth Elements

The Rare Earth Elements (REEs) are a group of 17 elements (15 lanthanides (La-Lu), plus Y and Sc) that are considered by the European Union as the most critical raw materials for the future. Reports from 2010, 2014 and 2017 [1-3], see Figure 1.1 from 2014, classify the REEs as the material group that has the highest supply risk of all critical materials, with the heavy REEs being more critical than the lights ones in the 2014 list. In the 2017 list, the criticality of the light REEs has risen to the level of the heavy REEs. But what are REEs, why are they important and what is the origin of the supply risk?

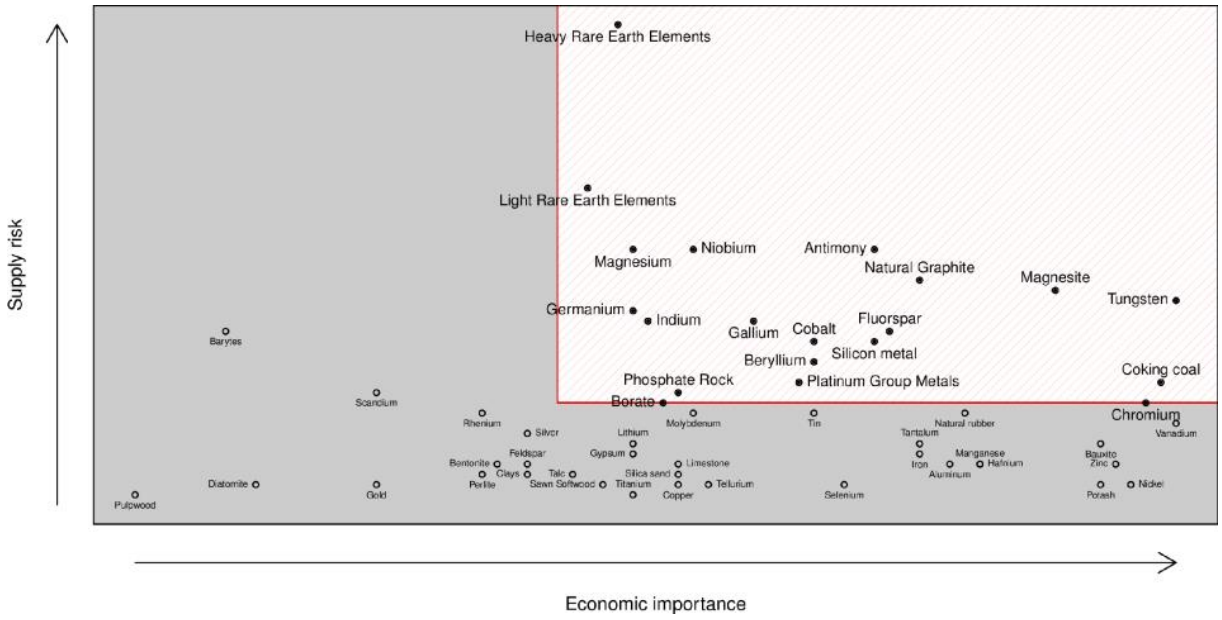

Figure 1.1: Analysis of the EU on the economic importance and supply risk of critical raw resources, the EU 2014 list [2]

1.1.1. The history of the Rare Earth Elements

The REEs were first discovered by C.A. Arrhenius near the Swedish town of Ytterby in 1787 [4]. What was unique about these elements is, that at the time, the REEs were thought to be a single element and not a collection of 17. Over a period of 160 years the elements began to be distinguished from one another until finally, with the discovery of Promethium in 1947, all 17 elements were identified as separate elements. This long period is a testament to the similarity of the chemical properties of these elements.

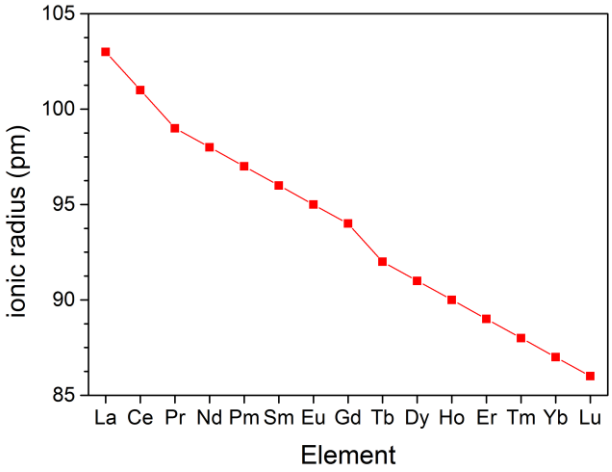

Figure 1.2: Ionic radii of the lanthanides ranked by atomic number, based on the data listed on [5]

The reason for the similarity in chemical properties amongst the REEs lies with the electron configuration of these elements. The lanthanides are the first series of elements in the periodic table where electrons fill the 4f atomic orbitals. These 4f orbitals lie beneath the already filled 5s, 5p and 6s orbitals, and consequently they are not part of the outer electron structure of the atom. As a result, the 4f electrons are effectively shielded from the chemical environment by the outer orbitals and do not participate in the formation of chemical bonds. This means that the 4f electrons do not contribute to the chemical properties of the lanthanides, at least not directly, which leads to the great similarity in chemical properties of all REEs. There is an indirect influence, however, as it would be impossible to separate them otherwise, which manifests itself as the lanthanide contraction.

The lanthanide contraction is a phenomenon where the decrease of ionic radii across the series is greater than those of the other series on the periodic table [5]. This strong decrease, as shown in Figure 1.2, is caused by the poor shielding effect that the 4f orbitals exert on the outer orbitals. Normally the orbitals that lie beneath the outer orbitals shield the outer electrons from the attraction of the positive nucleus. However, the effectiveness of this shielding decreases from s to p to d to f. Due to the poor shielding of the 4f orbitals, the outer electrons are drawn closer to the nucleus. This results in smaller than average ionic radii. The differences in ionic radii influence the chemical properties and allow the REEs to be distinguished from one another.

The chemical property that is most influenced by the lanthanide contraction is basicity, which is a measure of how easily a cation can lose anions or electrons. A high basicity means that the electrons (or anions) are less strongly bonded to the cation, which means that, due to the lanthanide contraction, the basicity of the lanthanides decreases from La to Lu. The decreasing basicity is the reason the REEs can be separated from one another and forms the basis of the REE separation technology.

1.1.2. The applications of Rare Earth Elements

The REEs have found applications in many different industries, such as polishing powder in the glass industry, alloying elements in the metallurgical industry and catalysts in the chemical and automotive industry [6]. The REEs also have their use in the medical world, as Gd is a key component for

contrasting agents for magnetic resonance imaging (MRI). The most prominent use, however, is in the production of high-tech consumer products and the development of green technologies. Here the REEs are an integral and irreplaceable part of two technologies: high strength permanent magnets and luminescent phosphors. REEs are also an important part of NiMH batteries, but these are being systematically replaced with Li-ion batteries.

The production of high strength permanent magnets is one of the most well-known applications of REEs and represents over 25% of the total REE consumption [7]. The REE magnet alloys, first SmCo and later NdFeB, are the strongest permanent magnets that are currently available in the market. These magnets are 2000 times stronger than ferrite magnets and have a multitude of uses, from small electric motors and speakers to electric vehicles and wind turbines.

REE luminescent phosphors have been a cornerstone in TV and display industry for decades. Due to their shielded 4f electrons, the REEs have very sharply defined emission lines, with several lines in the visual spectrum. With Eu-Y for red light, Tb for green light and Ce for blue light, the REEs are key in the production of monitors and displays [4].

1.1.3. The production of Rare Earth Elements

The name Rare Earth Elements is somewhat misleading, as these elements are not truly rare. The REEs are relatively abundant in the earth's crust, as can be seen in Figure 1.3 (a) [8], occurring in approximately the same amount as Cu. They are scarce, however, and this is another consequence of the lanthanide contraction. The lanthanide contraction gives the REEs ionic radii that are similar to the common rock-forming elements (like Ca), which allows them to occasionally replace these elements in the crystal lattice. As a result, the REEs are very dispersed, appearing in a multitude of different minerals in ppm levels. There are only a few REE minerals with a sufficiently high concentration of REEs to be mined economically. Of those minerals, bastnaesite, monazite and xenotime are the most important ones.

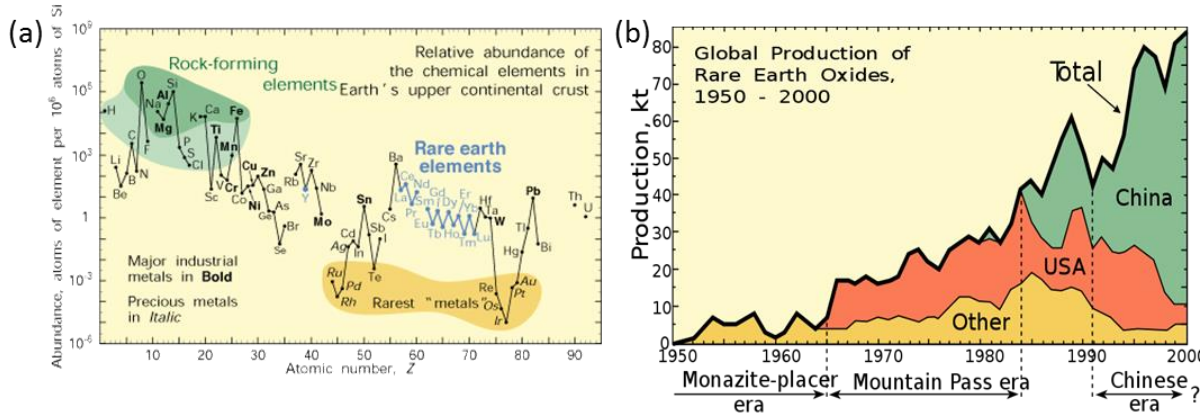

Figure 1.3: (a): Abundance of elements in the earth's crust. **(b):** History of the production of REEs, showing a transition of a USA dominated production to a China-dominated production. [8]

The history of REE production is defined by these minerals. An outline of the evolution of REE production is given in Figure 1.3 (b). The earliest production of REEs was focused on processing of monazite placer deposits on beach sands, which were easily exploited to produce a moderate amount

of REEs. However, REE production only became relevant in the mid-1960s, when the first major REE mine, the Mountain Pass mine in California, was opened. Bastnaesite was the main mineral that was mined there. Until 1980 the Mountain Pass mine was the main producer of the world's REEs. At this point, China entered the REE market with the Bayan Obo mine. The Bayan Obo mine is a massive Fe-Nb-REE deposit in Inner Mongolia, which represents almost 50% of the world's reserves of REEs. With the exploitation of the Bayan Obo mine China completely took over the production of REEs and is now the world's dominant supplier of REEs, with over 95% of REEs being produced there [7]. However, since 2016 Australia has increased its REE drastically, reducing China's market share to 80% [8].

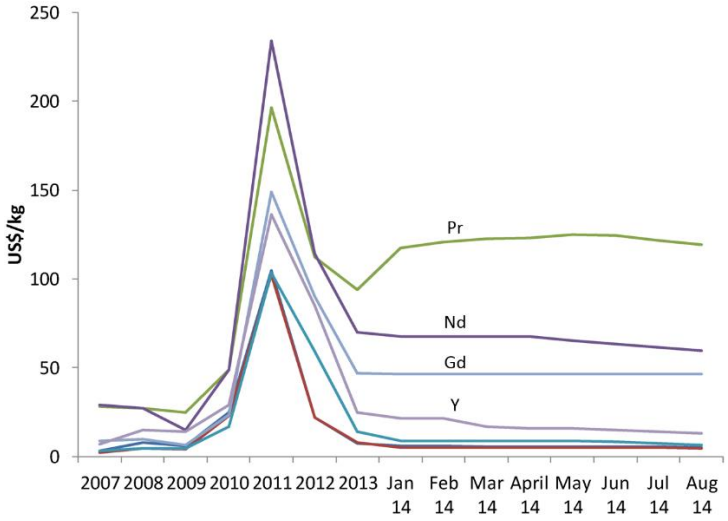

Figure 1.4: REE price evolution before and after the 2011 announcement of Chinese export restrictions, adapted from [9].

China's dominance of the REE market did not impose problems on the rest of the world as China's exports more than covered the demands of the other countries. However, when in 2011 China announced it was going to place export restrictions of its REEs the market spiked. Figure 1.4 [10] shows the evolution of the REE price before and after the announcement. It shows that the price of REEs exploded virtually overnight, with elements like Nd, crucial for magnet production, more than quintupled in value.

This rapid change in the REE market showed the European Union that the supply of the critical REEs is no longer secured. This is further exacerbated by the fact that the EU has no domestic REE production. The EU has no non-active mines like Mountain Pass and starting up a new mine is a time consuming and expensive process. These facts have made it clear to the EU that the REEs are now amongst its most critical raw material resources and the EU is now actively searching for ways to reduce the supply risk of REEs.

One of the paths the EU has chosen to help secure a domestic supply of REEs is recycling. The recycling of valuable materials is already commonplace, and even REE recycling has already been developed to some degree. However, existing REE recycling involves either production scrap or collected End-of-Life (EoL) products that are manually disassembled. The large majority of REEs containing products end up in general waste streams from which they are not or cannot be recycled. As of 2011 current recycling practices recover less than 1% of the total use of REEs [11]. In an effort to improve upon this

the EU has started several framework projects (FP7), which aim to recycle REEs from high-volume waste streams. These high-volume waste streams only contain a small fraction of REEs, often at the ppm level, but if they can be recycled successfully it would represent a considerable REE supply.

One of the FP7 projects that were started to investigate the possibility of recycling these high-volume waste streams is the REEcover project. The participation in this project forms the basis for this Ph.D. thesis.

1.2. The REEcover project

REEcover is a European Union (EU) FP7 project (Project ID: 603564) [12] created to tackle the problem of the EU's dependency on China for its REE supply. It aims to secure a domestic REE supply through the recycling of high-volume waste streams containing low concentrations of REEs. The waste streams in questions are mine tailings from the Kiruna iron ore mine and shredded "Waste Electrical and Electronic Equipment" (WEEE). The project consists of partners from industry and companies (LKAB, INUMETAL, Elemetal, Chemconserve, LCM, Metsol, BCC), research institutions (Tecnalia, SINTEF, SIMTEC) and universities (LTU, NTNU, TU Delft), each working towards the end goal of creating a European REE supply. The project is divided into several work packages, as shown in Figure 1.5, each responsible for a specific part of the total flowsheet.

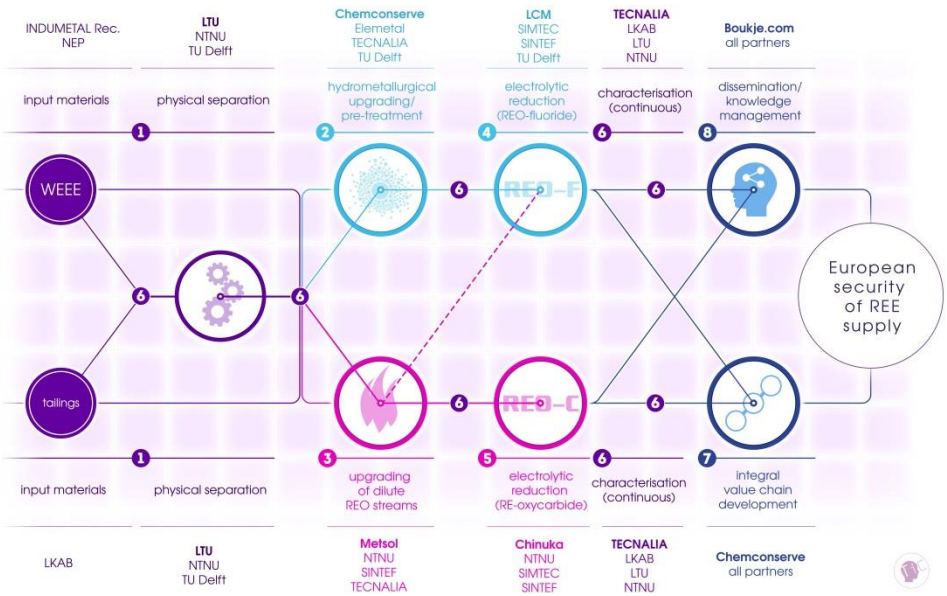

Figure 1.5: Project flowsheet for REEcover divided into its separate work packages [12]

The first part of the process is the physical upgrading of the input material to create a concentrate that is as rich in REEs as possible. This was achieved through a myriad of physical upgrading techniques, ranging from flotation to thermal demagnetisation and cryo-grinding. This part of the project was led by the Luleå University of Technology (LTU).

The next step is the extraction of the REEs from these upgraded concentrates. Two process routes were developed in parallel: a hydrometallurgical one and a pyrometallurgical one. The hydrometallurgical process route was developed at the Delft University of Technology (TU Delft) and forms the basis for this thesis. The pyrometallurgical process was developed at the Norwegian University of Science and Technology (NTNU). Both process routes aim to extract the REEs from the upgraded concentrates and produce an REE intermediary that is free from impurities. This intermediate REE product is then ready to be processed in the next step of the flowsheet, electrolytic reduction.

The next step in the flowsheet is the production of REE metal from the REE compounds that were produced. Traditionally this is achieved through reduction via molten salt electrolysis, but this project aims to improve on the existing technology. The molten salt electrolysis currently used in China is very energy intensive, as well as introducing high levels of pollution to the environment. The project partners at TU Delft and LCM aim to develop a more sustainable reduction technology, utilising the oxide-fluoride electrolysis system. The partners at SINTEF aim to develop an oxy-carbide reduction system.

The entire process is supported by several partners. Tecnalia offers analytical support for all partners, as well as supplying benchmarks and upkeep of the database. Chemconserve works together with all partners to provide an economic evaluation and construct detailed in-depth flowsheets for the developed processes. Finally, Boukje.com (BCC) organises and supports all dissemination of achieved results to the public and the EU, as well as handling administrative tasks and scheduling.

1.3. The goal of this work

The goal of this work is to study the possibilities for hydrometallurgical recycling of REEs from the WEEE and mine tailings. By studying the upgraded input materials supplied by our REEcover project partners and analysing existing technologies we aim to develop hydrometallurgical processes capable of extracting the REEs and producing a compound that is ready for the next step in REE metal production: the molten salt electrolysis. We will explore acid leaching, alkaline conversion, microwave-assisted processing, precipitation and solvent extraction, as possible means to achieve this goal.

Prior to the development of the recycling processes, a thorough analysis and characterisation of the input materials will be performed. From this analysis, the main REE phases and compounds present within the upgraded waste streams will be identified. Through this identification, the possible recycling approaches can be determined, and further understanding can be gained on how these REE compounds ended up in these waste streams.

During the development of the hydrometallurgical processes, attention is paid to the underlying chemistry and behaviour of the REEs, as well as to the viability of the process. We aim to build understanding on the behaviour of REEs in these low concentration waste streams, as well as to develop processes that have the potential to be up-scaled and be adopted by companies to actively recycle these waste streams industrially. To this effect economic constraints are considered, such as

energy use, consumption of chemicals and other raw materials and waste generation. Working within these constraints means that whenever possible the most simple and efficient processes will be used. High energy processes, such as roasting, will be avoided and instead low-temperature alternatives, such as corrosion (a low-temperature oxidation process), will be utilised. Complex chemical processes, such as solvent extraction, will only be utilised when required and be replaced with simpler ones, such as precipitation, provided the purity of the end product can be guaranteed.

The inherent value of the feed materials will also be considered, and other potential recyclable elements will be taken into account. For example, the mine tailings are rich in apatite and thus also represent a valuable resource for phosphorous. This is taken into consideration and the developed processes recover both the phosphorous and REEs from the mine tailings. In the case of the WEEE, the value of Cu and Zn in the scrap product stream is not to be dismissed, both can lead to additional value streams during WEEE recycling. Attention will also be paid to the metallic Fe, as this is the element that this waste stream is currently being recycled for. The developed processes will attempt to maintain the Fe recyclability after the REEs have been extracted from the WEEE.

In the end, several developed flowsheets will be presented that describe the recycling process from the raw material to the end product ready from molten salt electrolysis. The developed processes all adhere to the main project goals:

- They extract the REEs from the waste streams.
- The produced REE end product has minimal impurities.
- They are not complex and require little energy and chemicals, making them economically viable.
- The other critical/valuable elements in the input materials are co-extracted.
- They have the potential to be up-scaled and implemented into industrial operation.

1.4. Overview of this thesis

This thesis is built up from 8 chapters. This first chapter gives an overview of the chapters in the thesis and gives an introduction on what the REEs are, why they are important, how the EU aims to secure a domestic supply of REEs through recycling and how the REEcover project ties in to that goal.

The second chapter will give an overview of the literature that is available on the primary production of REEs, as well as take a look at what has already been developed in the field of REE recycling. This information will offer a basis to develop new recycling technologies for never before considered materials, by drawing parallels for existing processes based on similar, yet different, resources. By looking at the phosphoric acid industry we gain inspiration to recycle the mine tailings and from the principles of NdFeB recycling a new process can be designed to extract the REEs from shredded WEEE.

In the third chapter the materials, from which the REEs will be recycled, are analysed and characterised. By determining the mineralogy and chemical composition of both the mine tailings and shredded WEEE possible recycling approaches can be designed. Analysis of the mine tailings shows that, after physical upgrading, its primary component is the apatite mineral. This mineral is the primary resource for phosphoric acid production and is also known to be associated with REEs in minor

concentrations. Further analysis also shows the presence of monazite, which is one of the main REE minerals. Analysis of the fractions of a WEEE shredder product shows that the REEs concentrate in the ferrous fractions and that the main REE components are fragments of NdFeB magnets that adhere to the steel components of the shredded WEEE. Physical upgrading, through thermal demagnetisation, makes it possible to create an upgraded REE concentrate from which a hydrometallurgical recovery process can be designed.

The fourth chapter will discuss the processes that were developed to recycle the mine tailings. The goals for recycling the mine tailings are the recovery of the REEs and the recovery of the phosphorous. An analysis of phosphoric acid production processes forms the basis of the developed recycling process. Through acid dissolution of the upgraded mine tailings the phosphorous will be recovered as H_3PO_4 and through control of the leaching conditions, the REEs can be directed to the leach solution or leach residue. Based on this ability to control where the REEs end up after leaching, two divergent recycling flowsheets are developed. One will utilise the combined P and REE leach liquor and will use solvent extraction to separate them from one another. The other will concentrate the REEs into the low volume leach residue and process that residue via alkaline conversion to extract the REEs.

In the fifth chapter microwave assisted leaching is investigated as an alternative way to decompose monazite. Monazite is the primary REE component in the leach residue that is produced in chapter 4. In the work of chapter 4 alkaline conversion was utilised to decompose the monazite to only moderate success. Microwave-assisted leaching offers a better way to decompose monazite through the use of rapid heating, high temperatures and high pressure, which are all easily and efficiently achieved via microwave heating.

The sixth chapter discusses the development of the recycling process for the recovery of REEs from shredded WEEE. Through analysis of past technologies and consideration to the economy of the process, a new process was developed to oxidise the ferrous components in the WEEE. Via a corrosion process the Fe is oxidised to its 3+ state, which is crucial to achieve a measure of selectivity towards REEs when leaching the material. After this oxidative pre-treatment, the shredded WEEE can be leached with diluted H_2SO_4 and very high selectivity can be achieved (95% Nd and 5% Fe). From the resulting leach liquor the REEs can be recovered, without solvent extraction, through the use of double sulphate precipitation. This leads to a very efficient process, which requires only a minimal amount of chemicals and virtually no energy.

In the seventh chapter the hydrometallurgical processing of pyrometallurgically produced slags will be discussed. As part of the REEcover project the Norwegian University of Science and Technology (NTNU) focussed on recycling REEs from the WEEE via pyrometallurgy. This process yields a REE-rich slag phase, which has been separated from a metallic Fe phase. To extract the REEs from the pyrometallurgical slag, a hydrometallurgical leaching process is developed at TU Delft. Through the use of a fluxing agent (borax) an easily leachable slag is produced and in co-operation with Elemetal, a solvent extraction process is developed to finish the combined pyrometallurgical-hydrometallurgical process.

The eighth and final chapter serves as a closing chapter where the results of this research are summarised. All conclusions and observations will be reiterated and recommendations for future studies will be given.

References

[1] "Critical raw materials for the EU, Report of the Ad-hoc Working Group on defining critical raw materials", European Commission Enterprise and Industry, 2010.

[2] "Report on Critical Raw Materials for the EU, Report of the Ad hoc Working Group on defining critical raw materials", European Commission Enterprise and Industry, 2014.

[3] "Study on the review of the list of critical raw materials", Directorate-General for Internal Market, Industry, Entrepreneurship and SMEs (European Commission), 2017.

[4] N. Krishnamurthy and C. K. Gupta, "Extractive metallurgy of rare earths", CRC press, 2004.

[5] "Lanthanides & Actinides: Features of Lanthanide Chemistry". [Online]. Availible on: https://www.radiochemistry.org/periodictable/la_series/L6.html. (retrieved 28/02/2018)

[6] I. McGill, "Rare Earth Elements", in Ullmann's Encyclopedia of Industrial Chemistry, W.-V. V. G. & C. KGaA, Red. Weinheim, Germany: Wiley-VCH Verlag GmbH & Co. KGaA, 2000.

[7] M. Humphries, "Rare Earth Elements: the global supply chain", Congressional Research Service, CRS Report for Congress, 2013.

[8] G. B. Haxel, J. B. Hendrick, and G. J. Orris, "Rare Earth Elements—Critical Resources for High Technology", USGS factsheet, 2002.

[9] U.S. Geological Survey, "USGS 2015 Minerals Yearbook", 2016.

[10] N. Haque, A. Hughes, S. Lim, and C. Vernon, "Rare Earth Elements: Overview of Mining, Mineralogy, Uses, Sustainability and Environmental Impact", Resources, vol. 3, nr. 4, pp. 614–635, 2014.

[11] K. Binnemans et al., "Recycling of rare earths: a critical review", J. Clean. Prod., vol. 51, pp. 1–22, 2013.

[12] REEcover." [Online]. Available: https://cordis.europa.eu/project/rcn/110976_en.html (retrieved 09/09/2018)

Chapter 2: Literature review

Abstract

The recycling of Rare Earth Elements (REEs) from mine tailings and REE containing End-of-Life (EoL) scrap, two promising secondary resources, offers great opportunities to secure REE supply in Europe. The relatively low concentration of REE in mine tailings (1000-1500 ppm) and the variety in contaminants in the EoL scrap have made the extraction of REEs from these resources very challenging. This chapter provides a review of the past and present technologies for REE leaching used in primary REE production and in current REE recycling, as an important part of hydrometallurgical REE processing. Detailed studies of the existing processes are essential to properly understand and resolve the difficulties in REE recycling from these secondary resources. The known processes range from acid leaching with H_2SO_4, HCl or HNO_3 for primary ores, to leaching with NaCl or $(NH_4)_2SO_4$ of ion adsorbed clays, combined base and acid leaching for EoL lamp phosphors and selective acid leaching with thermal pre-treatment for magnet scraps. A comprehensive understanding of these processes is the key to applying them to REE recycling from secondary resources.[1]

[1] **Remark:** this chapter is published as: S. Peelman, Z. H. I. Sun, J. Sietsma, and Y. Yang, "Leaching of rare earth elements: review of past and present technologies", in *Rare Earths Industry technological, economic and environmental Implications,* Elsevier, pp 319-334, 2016.

2.1. Introduction

The rare earth elements (REEs) are a group of 17 chemically similar elements consisting of the lanthanides, Y and Sc. Their unique physical and chemical properties have made them essential as components (e.g. magnets, catalysts, batteries) in state-of-the-art applications or equipment. However, these same properties also make them difficult to mine and process, making them scarce in the market. A potential supply risk of REEs, environmental concerns in the primary REE industry and economic benefits promote research and development on processing of secondary resources, such as mine tailings and electronic waste or WEEE (waste electrical and electronic equipment) in the EU. Although significant investigations on REE extraction from secondary resources have been carried out and a variety of technologies have been developed or proposed, most of them are still in the stage of research or only suitable for some very specific secondary resources. No technologies currently exist that can extract REE from secondary resources like mine tailings and WEEE. The REE extraction efficiency and selectivity, together with the cost and engineering during process design, still require substantial optimisation before further commercialisation. In hydrometallurgical processing, leaching is a key step to dissolve REEs in the minerals or REE-bearing scrap or waste materials. However, the understanding of interactions between REE minerals in a low concentration and the leaching media, as well as the dissolution behaviour of different REE phases in WEEE, is at present not sufficient to develop a proper hydrometallurgical processing route to extract the REE from the secondary resources. In order to have a better view on the state of the art and to improve engineering possibilities of REE extraction from secondary resources, as well as to provide inspiration to develop new processes, the dominant leaching technologies that are currently in use in REE production were reviewed and are presented in this work.

2.2. Leaching technologies in primary REE production

The main REE minerals used in primary REE production are bastnaesite and monazite. Next to these, ion adsorbed clays, despite their substantially lower grade, are becoming more popular as a primary resource. This is a result of their easy, more environmentally friendly processing and unique REE distribution [1]. Table 2.1 gives a concise overview of the leaching technologies, both past and present, used in primary REE production.

2.2.1. Bastnaesite

Bastnaesite is a rare earth fluorocarbonate mineral, $REE(CO_3)F$ [6], which predominantly contains light rare earth elements[2]. After physical upgrading, bastnaesite ore concentrates contain between 40 to 60 wt.% REE [7] [8].

One of the main concerns in past bastnaesite processing technologies (see Table 2.1) was the inability to extract the REE fluorides. This has been successfully resolved in the current day technologies in two different ways: pre- and post-treatment with alkaline or sulphuric acid roasting. The alkaline treatment, developed by Kruesi and Duker of Molycorp [1], is a three-step process, defined by reactions

[2] La, Ce, Pr, Nd, Sm, Eu, Gd and Sc

$$REEF_3 \bullet RE_2(CO_3)_{3(s)} + 6HCl \rightarrow REEF_{3(s)} + 2REECl_3 + 3H_2O + 3CO_{2(g)} \quad (2.1)$$

$$REEF_{3(s)} + 3NaOH \rightarrow REE(OH)_{3(s)} + 3NaF \quad (2.2)$$

$$REE(OH)_{3(s)} + 3HCl \rightarrow REECl_3 + 3H_2O \quad (2.3)$$

Step I - reaction with a 31.5 wt.% HCl solution (1.8 kg/kg ore) to dissolve the REE carbonate and form REE chlorides; step II - reaction with NaOH (0.5 kg/kg) at 96°C to convert the remaining REE fluorides to hydroxides, which are then dissolved by leaching with HCl in step III. Alternative processes exist, which skip the first leaching step and instead the bastnaesite is first treated with alkaline and then leached with HCl [1]. This consumes more NaOH though as it converts all the REEs to hydroxides, not only the REE fluorides. Whether this compensates for elimination a step in the process depends on the economics of the operation.

Sulphuric acid roasting is the other main process currently used in industry to process bastnaesite. In the process, bastnaesite concentrate is heated in a 98% H_2SO_4 solution to 400 - 500°C for several hours. This decomposes the fluorocarbonate matrix, leading to the release of the CO_2 and HF gas. These emissions are becoming a serious environmental concern. The REEs are converted to their sulphates and can be selectively precipitated as Na double sulphates after leaching the roasted ore with a NaCl water solution. The sulphuric acid roasting process is currently in use at the Bayan Obo mine in China, making it the primary method for bastnaesite processing. The alkaline method was used by Molycorp at the Mountain Pass mine before the mine was closed [1].

Table 2.1: Summary of leaching technologies in primary REE production

Mineral	Process	REE yield	Remarks	Status	Ref.
Bastnaesite	1) HCl leach to remove non REE carbonate 2) Calcination of residue to form REO	85-90%	The oldest way to process bastnaesite concentrates	outdated	[1]
	Digestion with HNO_3 or H_2SO_4	98%	Acid choice depends on further processing: HNO_3 for solvent extraction H_2SO_4 for precipitation	outdated	[1]
	1) Roast at 620°C to drive off CO_2 2) 30% HCl leach	--	Ce^{3+} oxidises to Ce^{4+} during roasting → Ce will not leach REE fluorides will not leach, residue is marketable	outdated	[1]
	1) Alkaline conversion REF_3 → $RE(OH)_3$ 2) HCl leach	--	Process can be preceded with HCl leach to extract REE carbonates before alkaline conversion	In use	[1]
	1) Sulphuric acid roast 2) NaCl solution leach 3) Precipitation as Na double sulphates	--	Precipitates are converted to chlorides for further purification with solvent extraction	In use	[1]
Monazite	Digestion in hot H_2SO_4	--	Process conditions determine what is leached: only LREE or LREE+HREE+Th Does not yield a pure product	outdated	[1]
	1) Digestion in hot 60-70% NaOH 2) Washing residue with hot water 3) Leach with mineral acid of choice	98%	Ce cannot be leached if Mn is present Th is leached together with REE Na_3PO_4 is marketable by-product	In use	[1]-[2]
	1) Heat under reducing and sulphidizing atmosphere with $CaCl_2$ and $CaCO_3$ 2) Leach with 3% HCl	89%	Requires no fine grinding Th does not leach, remains in residue as ThO_2 No Mn problem	In use	[3]
Ion clay	Salt leach with $(NH_4)_2SO_4$	80-90%	Targets physisorbed REE through cation exchange	In use	[4]
	Leach with seawater	40%	Inefficient but cheap process	R&D	[5]
	Acid leach with strong acid (pH<1)	ALL	Dissolves entire clay, incurs significant additional costs	Not used	[4]

2.2.2. Monazite

Monazite is a rare earth phosphate mineral, $RE(PO_4)$, containing mostly light REE and some heavy REEs[3] (more than bastnaesite) [6]. Monazite can contain up to 70% REE, primarily Ce and La as well as significant concentrations of Nd, Pr and Sm. The Th content is also quite high, ranging from 4 to 12% which, due to the radioactive nature of Th, is an ever-present concern in monazite processing.

As shown in Table 2.1, the alkaline method is currently one of the main leaching technologies for monazite. The main reactions during alkaline leaching are

$$REEPO_{4(s)} + 3NaOH \rightarrow REE(OH)_{3(s)} + Na_3PO_4 \quad (2.4)$$

$$Th_3(PO_4)_{4(s)} + 12NaOH \rightarrow 3Th(OH)_{4(s)} + 4Na_3PO_4 \quad (2.5)$$

After the monazite mineral is digested in 60-70% NaOH at 140-150°C for 4 hours, the hydroxide residue is dissolved into a hot acidic solution. The acid is selected based on the subsequent separation process, i.e. HNO_3 for solvent extraction using TBP or H_2SO_4 for solvent extraction using amines of the solution. Na_3PO_4 is formed as a by-product which (after crystallisation) is sold to the fertiliser industry. This process requires extensive grinding of the monazite ore prior to treatment (particle size below 45 µm) so that extraction rates of 98% can be achieved even with relatively low-grade ores (e.g. Australian monazite 48.6% REE [3]). This process leaches the Th together with the REE which leads to safety concerns during the separation stage where the Th can be up concentrated to dangerous levels. Another concern is the presence of Mn^{4+} during alkaline processing, which oxidises Ce ($Ce^{3+} \rightarrow Ce^{4+}$) and form CeO_2, which will not dissolve in HCl [2].

An alternative method has been proposed by Merritt [3], in which the monazite ore is heated with $CaCl_2$ and $CaCO_3$ under a reducing and sulphidizing atmosphere. This leads to the conversion of REE phosphates to REE oxysulphides (REE_2O_2S) and oxychlorides (REEOCl), and chloroapatite ($Ca_5Cl(PO_4)_3$) is formed as a by-product. From this mixture, the REE can be selectively leached with 3% HCl. During the heating process Th is converted ThO_2, which is stable and does not dissolve in 3% HCl. The ThO_2 can be safely separated and disposed of together with the other residue. This process has three advantages over the alkaline process: (1) the conversion step is shorter (45 min vs 3-4 h in the alkaline digestion), (2) there is no necessity for extensive grinding, and (3) Th is stabilised as ThO_2 in the residue so that it isn't concentrated in further processing steps. However, the trade-off is that the REE recovery rate is lower than the alkaline method (89% vs 98%) and the by-product is not marketable, unlike the Na_3PO_4. Environmental concerns regarding the roasting operation should also be carefully considered.

2.2.3. Ion adsorbed clays

Ion adsorbed clays are becoming an increasingly important REE resource in the primary REE industry. These clays have alumina-silicate matrix onto which REE ions have been adsorbed. Although these clays have an average REE concentration of only 0.05-0.2 wt.%, their ease to process and relatively high heavy REE fraction make them a valuable REE resource [6]. These clays require no prior beneficiation process and contain very little radioactive elements, a constant concern with monazite processing.

[3] Tb, Dy, Ho, Er, Tm, Yb, Lu and Y

As given in Table 2.1, salt or low concentration acidic leaching of these clays to recover REEs is most frequently applied [9]. $(NH_4)_2SO_4$ and NaCl are the most commonly used leachants and the leaching reaction (6) (using $(NH_4)_2SO_4$ as an example) is given as follows [4]:

$$[Al_2Si_2O_5(OH)_4] \bullet REE^{3+}{}_{(s)} + 3NH_4{}^+ \rightarrow [Al_2Si_2O_5(OH)_4] \bullet (NH_4{}^+)_{3(s)} + REE^{3+} \quad (2.6)$$

The REEs in reaction (2.6) are not chemically bound to the alumina-silicate matrix, rather they are physisorbed. The cations of the leachant (here $(NH_4)^+$) displace the REE^{3+} cation from the matrix and transfer them into solution. The kinetics of the leaching process are very fast, equilibrium is achieved in around 10 min and the total REE extraction is between 80-90%. There have even been leaching trials in Madagascar using seawater as a leachant [5]. However, these trials only yielded recovery rates of around 40%, vastly inferior to the 80-90% achieved with $(NH_4)_2SO_4$. The industrial process currently used in China uses an ion clay with an REO concentration between 0.08 and 0.8 wt.% and a leachant of 7% NaCl and 1-2% $(NH_4)_2SO_4$ at a pH of 4. A recovery rate of up to 95% REO is achieved [10].

2.2.4. Discussion

The main REE resources in the primary industry are high grade concentrates with REE contents between 60-70% after physical upgrading. In both the bastnaesite and monazite minerals, REEs are present in compounds that are difficult to dissolve ($REEF_3$ and $REEPO_4$ respectively). The extraction technologies reflect this as both bastnaesite and monazite treatment are multi-step processes with the aim of first converting the REE to a more easily leachable compound before the actual leaching. All of these processes are energy intensive and environmentally hazardous. This is part of the reason that the primary REE industry has branched out to the low-grade ion clays. The other, more important, reason is of course the high fraction of heavy REE in these clays. It is from these technologies that the understanding of REE extraction behaviour originates. And it will be from these technologies that the keys for unlocking the REE from secondary resources will be found.

2.3. Leaching technologies in new and upcoming secondary REE resources

Next to the primary REE production, a range of secondary REE production routes have been established. Amongst these processes, the recovery of REE in the phosphoric acid industry, the recycling of EoL fluorescent lamps and the recycling of REE magnet production scrap stand out as the most developed. All of these technologies have in common that they are all hydrometallurgical processes. Thus, understanding the leaching behaviour of these REE-bearing secondary raw materials is key to the overall REE recovery.

2.3.1. REE recovery in the phosphoric acid industry

The main resource for phosphorous in the phosphoric acid industry is the apatite mineral. This mineral, $Ca_5(PO_4)_3(Cl,F,OH)$, is known to contain 0.1 to 1% REE [11]. The REEs in apatite are present as either REE^{3+} ions substituted on the Ca^{2+} ion sites of the apatite lattice (balanced with Na^+ ions) or as REE mineral inclusions, e.g. monazite inclusions. This has led many of the phosphoric acid producers to seek extracting and valorising the REEs in their process as a by-product. The REE are most commonly found in the fluorine variant of the apatite mineral [12], as such $Ca_5(PO_4)_3F$ will be used as the representative formula in this review.

The main reaction in the phosphoric acid production is as follows [13]:

$$Ca_5(PO_4)_3F_{(s)} + 5\,H_2SO_4 + x\,H_2O \rightarrow 3\,H_3PO_4 + 5\,CaSO_4 \cdot \frac{x}{5}H_2O_{(s)} + HF_{(g)} \quad (2.7)$$

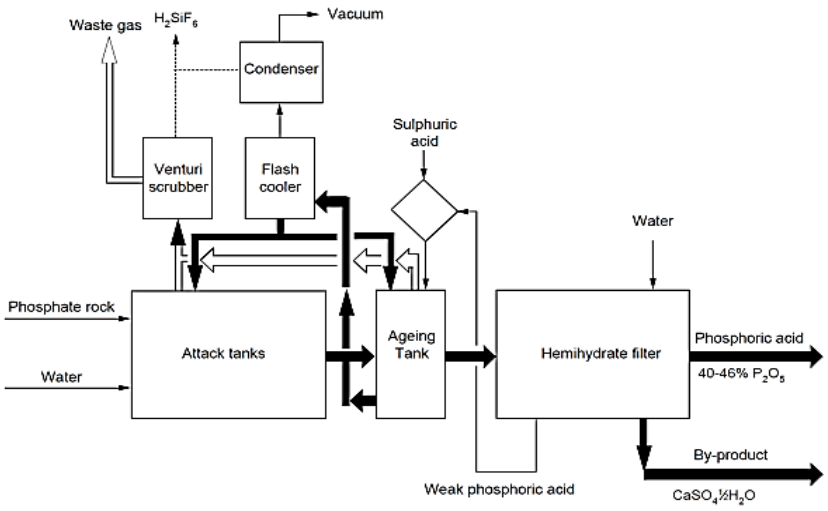

Figure 2.1: Hemihydrate process flow sheet [15]

The amount of water in the process determines the nature of the calcium sulphate by-product. In the conventional process, enough water is present to always form the dihydrate $CaSO_4 \bullet 2H_2O$. This process completely dissolves the apatite, transferring all REEs to the solution. However, the precipitation of the insoluble $CaSO_4$ (gypsum) formed during this reaction removes 80% of the REEs from the solution. This is caused by incorporation of the REE into the $CaSO_4$ crystal lattice during precipitation. Considering the amount of gypsum formed under typical processing conditions (5 tonnes of gypsum are formed per tonne of P_2O_5) [14] and the chemical stability of gypsum, these REEs are considered lost. This has promoted several different approaches by phosphoric acid producers to recover the REEs.

The first approach, proposed in 1980, was to ignore the REE losses to the gypsum and focus on the REEs remaining in solution. This method is applied to the purification process of the crude P_2O_5 (27%) to the commercial grade (54%) [12]. During this process a sludge of $CaSO_4 \bullet ½H_2O$ (hemihydrate) forms, which contains the REEs. This sludge is leached with HNO_3 with a leaching efficiency of around 80%. However, this process is inherently flawed for the production of REE, as most of the REEs are lost to the gypsum by-product in the first step. This has led to the second approach, the hemihydrate process [14]. This process (as shown in Figure 2.1 [15]) adapts the process parameters (i.e. water content) of the original process so that, instead of forming gypsum during the apatite digestion, $CaSO_4 \bullet ½H_2O$ (hemihydrate) is formed and precipitated. The precipitation of the hemihydrate captures nearly all the REEs in the solution (unlike gypsum which captures only 80%), and unlike gypsum, the hemihydrate is easily leached to extract the REEs. After precipitation, the hemihydrate is filtered and then leached with diluted H_2SO_4. This dissolves the hemihydrate and at the same time brings the REEs into solution. It was found that under these conditions the REEs in the solution inhibit the re-precipitation of gypsum, allowing for them to be removed through solvent extraction [14].

Some of the phosphoric acid producers have opted to completely redesign their process in order to make REE recovery easier. Instead of dissolving the apatite using H_2SO_4, it is dissolved with HNO_3 [16], with $Ca(NO_3)_2$ as a by-product. The advantage of this approach is that the solubility of $Ca(NO_3)_2$ can easily be controlled, allowing for the REE to be removed from the solution before it is co-precipitated. Also compared to gypsum, $Ca(NO_3)_2$ is a marketable product for the fertilizer industry. In Brazil [17] the possibility of using HCl is being explored as well. This process has both the advantage and disadvantage of producing $CaCl_2$ as a by-product. $CaCl_2$ cannot be precipitated from the solution, meaning no REEs can be lost this way. It also means, however, that the solution from which the REE must be separated contains a large amount of Ca, making it more difficult to achieve a high purity REE concentrate. Neither the HNO_3 nor HCl process has seen full-scale implementation in the industry. However, with the rising importance and decreasing availability of the REEs, these processes could one day replace the traditional H_2SO_4 process.

Parallel to these developments to extract the REEs during the production of phosphoric acid, there have been attempts to process the copious amount of REE containing gypsum already produced by the industry worldwide. In some countries, like Poland [18], the dumped gypsum represents the largest national REE resource. The most basic process was leaching the gypsum with 0.5-1 M H_2SO_4 at room temperature [11]. This process leaches about 50% of the REE from the gypsum without destroying the gypsum crystal structure. This makes the process efficient by limiting chemical consumption and makes the waste easy to handle. This process was partially improved by mechanical activation through ball milling the gypsum before leaching [19]. An alternative process uses $(NH_4)_2CO_3$ to react with $CaSO_4$ according to [11]:

$$(\mathrm{NH_4})_2\mathrm{CO_3} + \mathrm{CaSO_{4(s)}} \rightarrow (\mathrm{NH_4})_2\mathrm{SO_4} + \mathrm{CaCO_{3(s)}} \tag{2.8}$$

This process produces $(NH_4)_2SO_4$, which is valuable to the fertiliser industry, and $CaCO_3$. All REEs are incorporated into the lattice of $CaCO_3$, which is easily leached with HNO_3, also producing useful $Ca(NO_3)_2$. Alternatively, the $CaCO_3$ can be calcined to CaO and leached with $(NH_4)Cl$. This selectively dissolves the CaO, leaving a REE-rich residue [11].

2.3.2. Extracting REEs from red mud

Red mud, or bauxite residue, is the characteristic waste product of the Bayer process, where bauxite ore is converted into alumina. This residue is a hazardous waste that has been troubling the aluminium industry for a long time. There have been many attempts to use red mud as a secondary resource, as the metal content in this residue is quite high, especially Fe content (up to 60%), but none of these were very successful. Recently it has been discovered that the red mud also contains a minor REE fraction, ranging from 500 to 1700 ppm. What is especially interesting is that the Sc fraction is considerable, between 130 and 390 ppm [20].

Currently, experimental research is being carried out to extract the REE from the red mud [21]. Two approaches are being attempted: (1) physical upgrading of the red mud to obtain a REE concentrate prior to leaching, and (2) directly leaching the red mud [21]. The first approach aims to limit the volume of the residue that has to be treated so that chemical consumption and additional waste production can be minimised. However, most physical upgrading techniques fail to separate more than 20 wt.% of the REEs from the bulk of the mud. The second approach is to treat the red mud directly so that all REEs can be extracted. An example of such a process is the leaching with low concentration (0.5 M)

HNO_3 combined with dissolved SO_2 [20]. The SO_2 functions to keep the Fe from dissolving together with the REE. Recoveries of 80% for Sc and 95% for Y were obtained. The recovery of the light REEs was around 30-50%. The problem with this process is the considerable chemical consumption and the large amount of waste that is produced afterwards, both solid and liquid. The developments of these technologies are still ongoing, but as the REEs become more critical in our society they could become one of the solutions to solving the REE supply problem.

2.3.3. Recycling of lamp phosphor from EoL florescent lamps

Fluorescent lamp phosphors represent a valuable REE resource, especially for Y, Eu, and Tb. The main REE compounds in these lamps are: $Y_2O_3:Eu^{3+}$ (YOX), $LaPO_4:Ce^{3+}$, Tb^{3+} (LAP), $(Gd,Mg)B_5O_{12}:Ce^{3+},Tb^{3+}$ (CBT), $(Ce,Tb)MgAl_{11}O_{19}$ (CAT) and $BaMgAl_{10}O_{17}: Eu^{3+}$ (BAM). Some also contain chloroapatite ($(Sr,Ca,Ba,Mg)_5(PO_4)_3Cl:Eu^{3+}$) and halophosphate $(Sr,Ca)_{10}(PO_4)(Cl,F)_2$.

Among these REE compounds, the leaching of REEs from YOX was found to be the easiest [22], as they dissolve in relatively diluted acids (0.5 M H_2SO_4). In comparison, the REE in the other phosphors can only be leached at a sulphuric acid concentration of 18M (98wt.%) [22]. This is due to the fact that the REE in YOX are present as oxides, while the REEs in the other phosphors have much stronger chemical bonds. It was found that for these compounds the same leaching processes used in monazite processing were relatively effective [23]. Alternatively, a leachant of 4M HCl with H_2O_2 also proved moderately effective [23].

A typical leaching process of REEs from waste phosphor contains three stages. The ground phosphors are leached with 1.5 M H_2SO_4 to dissolve Y and Eu (from YOX). As this also dissolves some impurities (e.g. Ca, P, Mn, etc.), aqueous ammonia is added to the second stage. This keeps the impurities in the solution while converting the remaining undissolved REE into hydroxides, which precipitate out. The precipitates are leached with HCl in the third stage [24].

A different approach is the process developed by OSRAM A.G. with a patent in 2011 [25]. In this process, the multistep leaching targets specific compounds in the phosphors: 1) leaching with diluted HCl below 30°C leaches only the halophosphates; 2) increasing temperature to 60-90°C, the diluted HCl leaches YOX (alternatively dilute H_2SO_4 can also be used); 3) LAP is then dissolved with concentrated H_2SO_4 above 120°C (but below 230°C); 4) CAT and BAM are dissolved in 30% NaOH at 150°C in autoclave or in molten alkali. For acids, H_2SO_4 is preferred as it dissolves fewer impurities (Ca and Sr) compared to HCl or HNO_3 [22]. Also, applying ultrasound to the leaching systems increases the efficiency, regardless of the leachant [26].

2.3.4. Recycling of REE magnet scrap

There are two major REEs to be recovered from REE magnets: Nd from NdFeB magnets and Sm from SmCo magnets. Most recycling efforts of magnets are currently focused on the production scrap (so-called new scrap). As such, the input streams for magnet leaching are relatively pure. The leaching of SmCo scrap is relatively easy. It can completely dissolve in 3 M HCl, HNO_3 or H_2SO_4 [24]. Processes for SmCo leaching have not been further developed as the magnets have fallen out of favour with the rise of the cheaper and stronger NdFeB magnets.

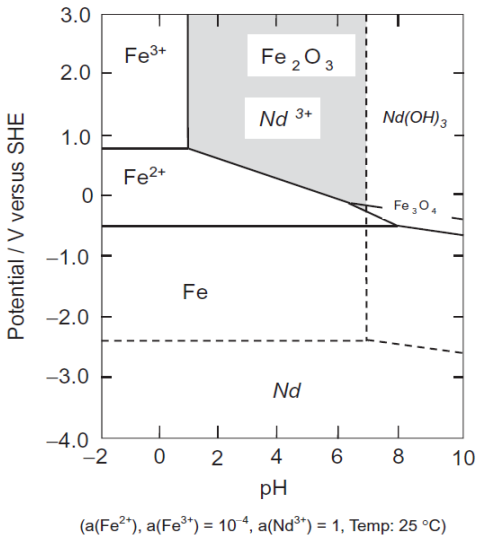

Figure 2.2: Pourbaix diagram Fe-H_2O and Nd-H_2O system [24]

For the NdFeB magnet scrap two different hydrometallurgical leaching routes are established: a total leaching route and a selective leaching route. In the total leaching route the scrap is fully dissolved with the aim to separate the Nd afterwards. Similar to the SmCo scrap, this is relatively straightforward as NdFeB easily dissolves in mineral acids. The choice of acid is mostly dependent on the subsequent separation process: H_2SO_4 for selective precipitation and HCl for solvent extraction [27]. HNO_3 is avoided since it produces nitrated waste water. Note that the solubility of rare earth elements decreases with increasing temperature, leading to lower leaching efficiencies at higher temperature. As the leaching efficiency is more important than leaching rate in magnet recycling, low temperatures are preferred [27]. Thus, most of these processes are done at room temperature.

In the selective leaching process, Nd is extracted from the magnets without dissolving Fe and B. This is achieved through a combination of roasting and leaching. The roasting is based on the Pourbaix diagram of Nd and Fe that is shown in Figure 2.2 [24].

The Pourbaix diagram reveals a joint stability region of solid Fe_2O_3 and dissolved Nd^{3+} in the pH range of 1 to 7. By exploiting this region, selective dissolution of Nd can be achieved. Roasting the magnet scrap for 6 h at 900°C (in air) converts the metallic iron to Fe_2O_3, which allows the Nd to be selectively dissolved by a 0.02 M HCl leach by the reactions

$$Nd_2O_{3(s)} + HCl \rightarrow NdCl_3 + H_2O \quad (2.9)$$

$$Fe_2O_{3(s)} + HCl \nrightarrow FeCl_3 + H_2O \quad (2.10)$$

Extraction ratios of 99% for Nd and less than 0.5% for Fe were achieved [24]. The same process without the roasting leached over 50% of the Fe.

Next to the low-temperature leaching system, there is also a high-temperature leaching system which used molten Mg to selectively dissolve the Nd from the NdFeB magnet alloy [23]. This process utilises the high solubility of Nd in liquid Mg at 800°C (65 at.%), compared to Fe and B which remains insoluble at 800°C. Thus, the Nd is selectively recovered in a Nd-Mg mixture. It can be separated from this mixture by vacuum distilling away the Mg, leaving pure Nd behind.

2.3.5. Discussion

Countries lacking primary REE resources are turning to what they do have and try to develop it as secondary resources. These potential secondary resources range from production waste or by-products, such as gypsum of the phosphoric acid industry and red mud from the aluminium industry, to the recycling of EoL REE-containing applications like lamp phosphors and magnets. Some producers of phosphoric acid are even considering redesigning their entire production process to be able to valorise the REEs present in their feedstock. Extraction technologies for these resources are being developed as either adaptations of the processes in the primary industry (lamp phosphors) or completely new processes (magnets). A summary of the possible secondary REE resources and their possible extraction processes is given in Table 2.2.

Table 2.2: Summary of possible secondary RE resources and their extraction

Secondary resource	REE content	Extraction technology	Yield	Remarks	Reference
Apatite rock	0.1-1 wt%	Conventional H_3PO_4 process	20% at best	Can be done without any changes to the process	[12-13]
		Hemihydrate process	80-85%	Implementable using standard equipment	[15]
		HNO_3 / HCl process	80%	Still in development	[16]
Phosphogypsum	0.3-0.4 wt%	H_2SO_4 leaching	50%	Does not decompose the gypsum	[18]
		$(NH_4)_2CO_3$ process	--	Valuable by-product	[11]
Red mud	0.05-0.17 wt%	Physical upgrading followed by leaching	< 20%	Low yield, low chemical consumption	[21]
		Direct leaching	Heavy REE: 80-90% Light REE: 30-50%	Many impurities, a lot of waste	[21]
Lamp phosphors	10-28 wt%	Sequential leaching	--	Extraction efficiency varies between steps and compound	[25]
SmCo magnets	23-33 wt% (pure)	Total dissolution	100%	Yield after solvent extraction: 70-95%	[24]
NdFeB magnets	26.7 wt% (pure)	Total dissolution	100%	Yield after solvent extraction: 96-99%	[27]
		Selective dissolution	96-99%	Yield depends on the tolerance on Fe dissolution	[24]

2.4. Recent progress and new leaching technologies for REE extraction

The history of primary REE production is one mired with environmental pollution in the form of hazardous emissions, copious amounts of both solid and liquid waste and of course the presence of radioactive material. As the primary industry moves forward, eliminating these hazards is becoming increasingly important. This, combined with the discovery of new REE resources, be they (very) low grade waste products from another industry (like mine tailings or gypsum from the phosphoric acid industry) or recycling of EoL REE-containing appliances (like magnets or lamp phosphors), drives the development of new technologies forward. Some of these developments include the reduction of hazardous emissions during bastnaesite processing, bioleaching and microwave assistance during leaching.

2.4.1. Progress in bastnaesite leaching

The environmental pollution caused by fluorine emissions during H_2SO_4 roasting of bastnaesite processing in China is becoming an increasing concern [28]. Due to this, processes have been developed to prevent the emission of fluorine. A first method revolves around only leaching the carbonate REE while leaving the REE fluorides in the residue. This is achieved by thermally activating the ore (400°C for 3 h) and then leaching it with HCl. The thermal activation enables the leaching of the carbonates at conditions in which the fluorides are unaffected. The reported leaching efficiency of this process is 94.6% for the carbonates and 0.07% for the fluorides [28].

A different method involves progress in the air roasting process mentioned in the discussion of established bastnaesite leaching processes. This process had already been proven ineffective in leaching the fluoride components, but the oxidation of Ce^{3+} to Ce^{4+} prevented Ce from being leached together with the other REEs and led to purification issues. The addition of thiourea [29] offered a solution to this problem. Thiourea prevents the oxidation of Ce, keeping it trivalent after roasting and thus allowing it to be leached with HCl together with other REEs. This allowed for the recovery of Ce and the non-fluoride bonded REE. These methods are not optimal, since not all REEs present in the bastnaesite are being extracted, leading to a less efficient process. However, considering the abundance of REEs in China, the Chinese REE industry can consider this loss in efficiency an acceptable trade-off for reducing the environmental impact of their REE extraction processes.

Another more efficient process involves the mechano-chemical activation of bastnaesite by milling it with NaOH powder [30]. In this process the bastnaesite concentrate is milled together with NaOH powder, followed by washing with water to remove the Na compounds and then leaching with HCl. These steps are performed at room temperature and can lead to a leaching efficiency of around 90%. This process generates no emissions and the F is bonded with Na as NaF. However, ball milling is very energy intensive and the process takes several hours.

2.4.2. Bioleaching

The field of bioleaching is being explored for REE extraction from low grade resources. The REE concentration of the resources is often below the 1% level, mostly around 0.5% even after physical upgrading. These resources include old mine tailings and ion adsorbed clays. As total leaching of these resources, using strong mineral acids and/or bases, leads to large amounts of waste and/or pollution and is very inefficient, alternative low cost and clean routes are being explored. In Egypt the possibility of using '*Acidithiobacillus ferrooxidans*' (bacteria often used in the bioleaching of copper [31]) to

bioleach low grade Gibbsite ore to recover the REE (0.49%) and U (0.05%) is being investigated [32]. Their initial results show a leaching efficiency of about 55% for REE and 49% for U. Other bacteria that are tested are '*Aspergillus ficuum*' and '*Pseudomonas aeruginosa*' [33] leading to slightly higher leaching efficiencies for REE's, around 75%. However, these bacteria are not as harmless to humans as '*Acidithiobacillus ferrooxidans*', thus safety can be an issue here.

Researchers in Japan have investigated the use of a blue-green algae named '*phormidium*' in combination with $(NH_4)_2SO_4$ for the extraction of REEs from ion adsorbed clays [34]. Like the process used in the primary production, in this process the ammonium ions displace the adsorbed REE^{3+} ions in the clays bringing them into solution, as well as several other adsorbed ions, mainly Al, Mn and Si. The difference with the primary industry is the presence of the algae, which selectively adsorbs the REE ions present in the solution. Leaching efficiencies between 40% (Dy, Gd) and 70% (Nd, Sm), dependent on the REE species, can be obtained, and the REE solution is almost devoid of impurities making subsequent separation processes easier. The advantage of this process, compared to other bioleaching systems, is that temperature and pH control is easy, and the leaching time is relatively short (3 h vs several days). Also, in Japan '*phormidium*' is easily obtained, as it needs to be removed from the local reefs to preserve said reefs. The waste of this process is also minimal and easily detoxified.

2.4.3. Microwave assisted leaching

Microwave assisted leaching is frequently used for improving mineral leaching efficiency [35]. However, for REE extraction concrete results have yet to be found. The principle of microwave assisted leaching is based on the fact that transition-metal-containing minerals are less transparent for microwaves than gangue minerals such as CaO, $CaCO_3$ and SiO_2 [35]. This leads to on-site heating at and around the metal-containing minerals, thus locally changing the leaching kinetics. As the leaching kinetics generally increase with increasing temperature, this leads to increased leaching rates at the metal-containing minerals, allowing for the leaching of the metal-containing minerals to be finished sooner and with less unwanted dissolved species originating from the gangue. Another effect of the localised and rapid heating is that it can fracture the surfaces of the metal-containing minerals due to thermal stresses, thereby effectively increasing the surface area [36] and further enhancing the leaching rate. Whereas microwave assisted leaching has not been applied to REE leaching at present, there is a growing interest in doing so. This interest originates from the successful implementation of microwave assisted leaching in Cu leaching from chalcopyrite and in Au leaching [36]. The effects observed there, e.g. removing reaction product from the surface through convective streams (Cu) or activating finely distributed metal-containing areas (Au), could be beneficial for REE leaching. Considering these current applications there is potential in applying the microwave technique to REE leaching, especially for low grade sources where the REEs are finely distributed in the material, sometimes in difficult to leach compounds (e.g. phosphates), such as in old mine tailings.

2.5. Conclusions

This brief review shows that there are a variety of leaching technologies that have been developed in the past, both for primary REE minerals and secondary resources. These in-market technologies were developed according to the mineralogy of REE ores, REEs occurrence and engineering feasibility. The main features are that these are all multi-step processes and that acid and alkaline are often interactively used in a single process. This proves that REE compounds are challenging to leach, even in the high grade primary resources. This review also shows that the technologies used in primary industry can offer a basis for developing technologies for recycling secondary resources as proven by the recycling of lamp phosphorous which uses the same technologies as monazite leaching. However, with the (very) low grade of other prospective secondary resources (like mine tailings and WEEE) the existing technologies will have to be adapted and refined. One promising method of doing so is microwave assisted leaching. Or technologies from other industries could be used as basis, like bioleaching.

In light of the increasing importance of secondary REE resources, this overview can provide a basis for developing more efficient processes for REE recovery from secondary resources, i.e. mine tailings and WEEE. For example, old mine tailings often contain a sizeable fraction of apatite and/or monazite. Drawing inspiration from current monazite processing and phosphoric acid production can lead to a workable process for REE recycling from these tailings. As for WEEE, many individual components (e.g. lamp phosphors and magnet scrap) of WEEE have been researched for REE recycling, but not for a mixed WEEE stream. However, knowledge of these individual components will be essential to develop a process for extracting REE from a mixed WEEE stream.

The main challenges will be overcoming the low concentration of REEs, both in the tailings and in the mixed WEEE, and the variety of contaminants. Here advancements in microwave assisted leaching or bioleaching show a promising future for low grade and/or difficult to leach secondary resources.

References

[1] N. Krishnamurthy and C. K. Gupta, Extractive metallurgy of rare earths. CRC press, 2004.

[2] V. I. Kuzmin, G. L. Pashkov, V. G. Lomaev, E. N. Voskresenskaya, and V. N. Kuzmina, "Combined approaches for comprehensive processing of rare earth metal ores," Hydrometallurgy, vol. 129–130, pp. 1–6, 2012.

[3] R. R. Merritt, "High temperature methods for processing monazite: I. Reaction with calcium chloride and calcium carbonate," J. Common Met., vol. 166, no. 2, pp. 197–210, 1990.

[4] G. A. Moldoveanu and V. G. Papangelakis, "Recovery of rare earth elements adsorbed on clay minerals: II. Leaching with ammonium sulfate," Hydrometallurgy, vol. 131–132, pp. 158–166, 2013.

[5] G. A. Moldoveanu and V. G. Papangelakis, University of Toronto - Tantalus Report, 2013.

[6] Y. Kanazawa and M. Kamitani, "Rare earth minerals and resources in the world," J. Alloys Compd., vol. 408–412, pp. 1339–1343, 2006.

[7] X. Feng et al., "Kinetics of rare earth leaching from roasted ore of bastnaesite with sulfuric acid," Trans. Nonferrous Met. Soc. China, vol. 23, no. 3, pp. 849–854, 2013.

[8] I. McGill, "Rare Earth Elements," in Ullmann's Encyclopedia of Industrial Chemistry, W.-V. V. G. & C. KGaA, Ed. Weinheim, Germany: Wiley-VCH Verlag GmbH & Co. KGaA, 2000.

[9] G. A. Moldoveanu and V. G. Papangelakis, "Recovery of rare earth elements adsorbed on clay minerals: I. Desorption mechanism," Hydrometallurgy, vol. 117–118, pp. 71–78, 2012.

[10] F. Shi, "Rare earth extraction technologies," Beijing: Metallurgical industry publishing, pp. 55–57, 2009.

[11] F. Habashi, "The recovery of the Lanthanides from phosphate rock," J. Chem. Technol. Biotechnol., vol. 35A, pp. 5–14, 1985.

[12] J. S. Preston, P. M. Cole, W. M. Craig, and A. M. Feather, "The recovery of rare earth oxides from a phosphoric acid by-product. Part 1: Leaching of rare earth values and recovery of a mixed rare earth oxide by solvent extraction," Hydrometallurgy, vol. 41, pp. 1–19, 1996.

[13] L. Wang et al., "Recovery of rare earths from wet-process phosphoric acid," Hydrometallurgy, vol. 101, no. 1–2, pp. 41–47, 2010.

[14] S. Zielinski, A. Szczepanik, M. Buca, and M. Kunecki, "Recovery of lanthanides from Kola apatite in phosphoric acid manufacture," J. Chem. Technol. Biotechnol., vol. 56, no. 4, pp. 355–360, 1993.

[15] A. E. van Nieuwenhuyse, "Production of Ammonium Nitrate and Calcium Ammonium Nitrate", vol. 4, 8 vols. Peterborough, England: Fisherprint Ltd, 2000.

[16] H. Li, F. Guo, Z. Zhang, D. Li, and Z. Wang, "A new hydrometallurgical process for extracting rare earths from apatite using solvent extraction with P350," J. Alloys Compd., vol. 408–412, pp. 995–998, 2006.

[17] F. Pereira and E. Bilal, "Phosphoric acid extraction and rare earth recovery from apatites of the Brazilian phosphatic ores," Romanian J. Miner. Depos., vol. 85, no. 2, pp. 49–52, 2012.

[18] A. Jarosiński, J. Kowalczyk, and C. Mazanek, "Development of the Polish wasteless technology of apatite phosphogypsum utilization with recovery of rare earths," J. Alloys Compd., no. 200, pp. 147–150, 1993.

[19] D. Todorovsky, A. Terziev, and M. Milanova, "Influence of mechanoactivation on rare earths leaching from phosphogypsum," Hydrometallurgy, vol. 45, no. 1–2, pp. 13–19, 1997.

[20] K. Binnemans et al. , “Recovery of rare earths from industrial waste residues: a concise review,” in Proceedings of the 3rd International Slag Valorisation Symposium: the Transition to Sustainable Materials Management, Leuven, Belgium, pp. 191–205, 2013.

[21] O. Petrakova, G. Klimentenok, A. Panov, and S. Gorbachev, “Application of Modern Methods for Red Mud Processing to Produce Rare Earth Elements.,” presented at the ERES 2014: 1ste European Rare Earth Resources Conference, Milos Greece, pp. 222–241, 2014.

[22] F. Yang et al., “Selective extraction and recovery of rare earth metals from phosphor powders in waste fluorescent lamps using an ionic liquid system,” J. Hazard. Mater., vol. 254–255, pp. 79–88, 2013.

[23] K. Binnemans et al., “Recycling of rare earths: a critical review,” J. Clean. Prod., vol. 51, pp. 1–22, 2013.

[24] M. Tanaka, et al., “Chapter 255 - Recycling of Rare Earths from Scrap,” in Handbook on the Physics and Chemistry of Rare Earths, vol. Volume 43, Jean-Claude G. Bünzli and Vitalij K. Pecharsky, Ed. Elsevier, pp. 159–211, 2013.

[25] R. Otto and A. Wojtalewicz-Kasprzak, “Method for recovery of rare earths from fluorescent lamps,” US20120027651 A1, 2012.

[26] C. Tunsu, C. Ekberg, and T. Retegan, “Characterization and leaching of real fluorescent lamp waste for the recovery of rare earth metals and mercury,” Hydrometallurgy, vol. 144–145, pp. 91–98, 2014.

[27] C.-H. Lee et al., “Selective Leaching Process for Neodymium Recovery from Scrap Nd-Fe-B Magnet,” vol. Vol. 44A, pp. 5825–5833, 2013.

[28] X. Bian, et al., “Study on Leaching Process of Activation Bastnaesite by HCl Solution,” Adv. Mater. Res., vol. 233–235, pp. 1406–1410, 2011.

[29] A. Yörükoğlu, A. Obut, and I. Girgin, “Effect of thiourea on sulphuric acid leaching of bastnaesite,” Hydrometallurgy, vol. 68, no. 1–3, pp. 195–202, 2003.

[30] Q. Zhang and F. Saito, “Non-thermal process for extracting rare earths from bastnaesite by means of mechanochemical treatment,” Hydrometallurgy, vol. 47, no. 2–3, pp. 231–241, 1998.

[31] K. Nowaczyk, A. Juszczak, F. Domka, and J. Siepak, “The use of Thiobacillus ferrooxidans bacteria in the process of chalcopyrite leaching,” Pol. J. Environ. Stud., vol. 7, pp. 307–312, 1998.

[32] H. A. Ibrahim and E. M. El-Sheikh, “Bioleaching Treatment of Abu Zeneima Uraniferous Gibbsite Ore Material for Recovering U, REEs, Al and Zn,” Res. J. Chem. Sci., vol. 4, no. Vol. 1, pp. 55–66, 2011.

[33] W. A. Hassanien, O. A. Desouky, and S. S. Hussien, “Bioleaching of some Rare Earth Elements from Egyptian Monazite using Aspergillus ficuum and Pseudomonas aeruginosa,” Walailak J. Sci. Technol., vol. 11, no. 9, pp. 809–823, 2014.

[34] J.-A. Kim et al., “Leaching of rare-earth elements and their adsorption by using blue-green algae,” Mater. Trans., vol. Vol. 52, no. No. 9, pp. 1799–1806, 2011.

[35] K. E. Haque, “Microwave energy for mineral treatment processes—a brief review,” Int. J. Miner. Process., vol. 57, no. 1, pp. 1–24, 1999.

[36] M. Al-Harahsheh and S. W. Kingman, “Microwave-assisted leaching—a review,” Hydrometallurgy, vol. 73, no. 3, pp. 189–203, 2004.

Chapter 3: Analysis and characterisation of the project materials

Abstract

Understanding the chemical composition and phase makeup of the raw materials is crucial to the development of their recycling processes. Thus, all the raw materials studied in the project, i.e. the apatite concentrate produced from the Kiruna mine tailings, the upgraded *Met-2* fraction produced from the shredded ferrous WEEE and the pyrometallurgical slags produced from the smelting of non-upgraded ferrous WEEE fraction *Met-1* and *Met-2*, were characterised in this research.

Characterisation of the apatite concentrate reveals that its major components are apatite, calcite and dolomite, and that there are traces of the REE bearing monazite as well. Chemical analysis of the concentrate shows an average REE concentration of 5000 ppm, primarily Ce (37 %), Nd (19 %), La (12 %) and Y (11 %). Other than REEs, the apatite concentrate contains a substantial concentration of valuable phosphorus (10-15 wt.% P). The main non-valuable element, i.e. the impurity, is Ca, which represents 34-37 wt.% of the concentrate.

XRD characterisation of the upgraded *Met-2* fraction indicates that the major components are metallic Fe and Fe oxides, with small fraction of CuO and SiO_2 present as well. REE particles were found using SEM/EDS as fragments of NdFeB magnets attached to the ferrous scrap. Chemical analysis of the material showed that it is predominantly composed of Fe (58 wt.%), with minor fractions of Zn (7.5 wt.%), Cu (2 wt.%) and Nd (1 wt.%).

Characterisation of the pyrometallurgical slags reveals that the slags formed from the smelting of the *Met-1* fraction are composed primary of Spinel phases, $(Mg,Fe,Al)O_4$, accompanied by a $Ca_3B_2O_6$ phase, which is formed due to the addition of $Na_2B_4O_7$ flux. Chemical analysis shows an average Nd concentration of 1.25 wt.%. The slags formed from the *Met-2* fraction have a mineralogy that is primarily silicate based and have an average Nd concentration of 1.4 wt.%.

3.1. Introduction

This chapter will introduce and analyse the input materials that will be investigated in this work. For each material its origin will be discussed, and an overview will be given of the processes the material underwent before they arrived at the Delft University of Technology for the development of their hydrometallurgical recycling processes. Then, a thorough characterisation of each material will be provided, including phase analysis and chemical composition. The materials that will be discussed are: mine tailings from LKAB, shredded WEEE from INDUMETAL, and slags produced by NTNU and Tecnalia.

3.2. Analysis setup and protocols

Characterisation of the raw materials is key in the development of their recycling processes. Without the knowledge of how the REEs occur within these materials, process design cannot start. In order to identify the REEs bearing compounds present, the input materials were analysed using XRD, XRF, ICP-OES, and SEM/EDS.

X-ray diffraction or XRD is a technique that utilises the diffraction patterns obtained when a material is irradiated with X-rays of a specific wavelength. The diffraction pattern, which is determined by the distance between the atoms in the crystal lattice, can be used to identify the crystal structures of phases present in the analysed material. For this work a Bruker D8 Advance diffractometer [1], [2] was used. The XRD analysis was performed on 100 mg samples deposited on a Si510 wafer, using Bragg-Brentano geometry and a Lynxeye position sensitive detector, Cu Kα radiation (λ = 0.15418 nm) generated at 45 kV and 40 mA, and a scatter screen height of 5 mm. The measurement scanned from 10° to 130° 2θ angle, with a step size of 0.034° and a counting time per step of 2 s.

X-ray fluorescence of XRF is a technique where a sample is irradiated with X-rays to ionise its atoms. When the ionised atoms return to their ground state they emit X-rays that are characteristic for each atomic species. These emitted X-rays are captured by a detector, which forms the XRF spectrum of the sample. From this spectrum the chemical composition of the sample can be derived. For this work a Panalytical Axios Max WD-XRF machine [3] was used.

Inductively coupled plasma-optical emission spectroscopy or ICP-OES is a technique which measures elemental concentration of a solution. The technique is based on the detection of photons, which are emitted when an exited atom returns to its relaxed state. Each element emits photons of a unique frequency, and the emission intensity is proportional to the elemental concentration. The atoms are excited when a sample solution is nebulised with an aerosol and is introduced to a high energy plasma. The emitted photons are captured by a detector to form the spectrum of the solution from which the chemical composition can be derived. For this work a SPECTRO ARCOS ICP-OES analyser [4] was used.

As ICP-OES can only be applied to liquid samples, solid samples must first be dissolved into a solution before they can be measured. To ensure full dissolution, the borax fusion method was used to fully dissolve the solid samples for ICP-OES measurement. This method uses an alkaline flux into which the solid sample is dissolved at high temperatures. After cooling the obtained fused glass is dissolved in an acidic solution. The flux used was prepared by mixing 1 g $Na_2B_4O_7$ and 1 g Na_2CO_3 with 0.2 g of sample in a platinum crucible. The mixture was then heated to 1000°C in a box furnace and held for 1 h. Finally, the resulting glass was dissolved in 150 ml 21 wt.% HNO_3 solution to obtain the solution for analysis.

Scanning Electron microscopy or SEM is a microscopy technique which uses electrons to create an image of the surface of a sample. The image can be constructed in two modes: secondary electron imaging (SEI) mode and back scattered electron (BSE) mode. The SEI mode uses the secondary electrons that are emitted from the surface of the sample after interaction of the surface atoms with the electron beam. The BSE mode on the other hand, uses the back scattered electrons of the beam after elastic scattering interaction with the atoms with the material. The intensity of back-scattered electrons is proportional to the atomic number of the atoms of the material. Thus, BSE offers a useful tool to find areas in a material which contain heavy elements (like REEs). Next to imaging, the SEM also offers chemical characterisation through energy-dispersive X-ray spectroscopy or EDS. EDS, like XRF, uses the X-rays that are emitted when exited atoms return to their ground state. However, instead of using X-rays, EDS uses the electron beam of the SEM to excite the atoms. Electrons do not have the penetration depth of X-rays (5 µm vs 50 µm - 5 mm), thus only the surface of the material can be analysed with EDS, and since the electron beam is narrow the analysis is also localised. The SEM/EDS use in this work is a JEOL JSM 6500F [5].

3.3. Mine tailings and apatite concentrate

3.3.1. Origin of the mine tailings and physical upgrading

The tailings that were used during this work originate from the tailings pond at the LKAB (Luossavaara-Kiirunavaara Aktiebolag) iron ore mine at Kiruna, Sweden. These tailings represent the waste rock that is produced during the mining of the iron ore. The tailings are deposited into a large waste pond, see Figure 3.1, after the iron ore has been removed from it. With its current mining practices, Kiruna produces approximately 8 Mtons of tailings per year. This has led to an accumulation of tailings in the pond to over a 100 Mtons through the years of mining operation. While some interest has been shown to process these tailings for their phosphorous content (4-8 wt.% P_2O_5) in the past, no viable processes were developed. However, with the increasing interest towards REEs, these mine tailings are again being reconsidered as a potential secondary REE resource.

Figure 3.1: Satellite photo of the tailings pond at the LKAB mine at Kiruna (picture courtesy of the REEcover project)

Exploration of the tailings has revealed that the tailings have an average REE content of 1200-1500 ppm. Considering the amounts of tailings being produced, this represents a potential annual production of 12 ktons of REE, without considering the 100 Mtons of tailings already present in the

tailing pond. The combination of a potential REE resource together with a phosphorous resource makes these tailings a potential candidate for recycling.

However, a material that only contains 1200 ppm of REEs and 4-8 wt.% of phosphorous does not make for an attractive input material for direct hydrometallurgical processing. To make hydrometallurgical processing viable, the tailings must first undergo physical upgrading to increase the concentration of valuable elements. The physical upgrading trials were run by our project partners at Luleå University of Technology (LTU), Sweden. Their goal was to maximise the REE and P content in a concentrate via grinding and flotation.

Grinding is one of the main technologies for size reduction of materials. Size reduction has two main objectives: achieving a specific particle size distribution and enabling the separation of multicomponent materials. Reducing a material to a specific particle size is important, as it affects various properties of the material (e.g. colour intensity in pigment, leachability of ores, etc.). Grinding also enables the separation of multicomponent systems by breaking apart agglomerated components into discrete individual pieces. When each component is no longer physically connected to the others, efficient separation becomes possible.

Grinding is done by feeding the material into a drum filled with a grinding medium and then agitating said drum. The feed material is trapped between the grinding media (traditionally steel balls, rods or bars) and is ground by the motion imparted by the drum [6]. The tailings were ground in a stainless-steel rod mill for 10 min, which led to a d_{90} of 50 μm (90 % of all particles have a particle diameter smaller than 50 μm).

Flotation is one of the key techniques in the mineral separation and upgrading field. The principle behind this technique is based on the hydrophilic and hydrophobic behaviour of particles in an aqueous environment. Hydrophilic particles are wetted by water, while hydrophobic particles are wetted by oils and bubbles. Thus, if bubbles are introduced into an aqueous suspension of particles, the bubbles will adhere to the hydrophobic particles and carry them to the surface of the suspension.

Most minerals are hydrophilic by nature but can be made hydrophobic through the addition of chemicals. (e.g. calcite ($CaCO_3$) can be made hydrophobic when treated with sodium oleate ($C_{17}H_{33}COONa$).) These chemicals are termed *flotation reagents* and fall into 4 categories: collectors, frothers, depressants and activators.

Collectors are the compounds that make minerals hydrophobic, as well as improve the adhesion of the minerals to air bubbles and/or oil droplets. *Frothers* are compounds that create a metastable froth phase at the surface of the suspension. This froth collects of the floated minerals, allowing for easy recovery. *Depressants* are used to suppress the hydrophobic behaviour of minerals and/or prevent the collectors from affecting certain minerals. This allows for a measure of selectivity when separating minerals through flotation. Finally, *activators* are used to promote the adhesion of reagents to minerals (e.g. sphalerite (ZnS), which cannot be made hydrophobic by xanthates (collector) unless Cu^{2+} ions are present in the suspension, thus $CuSO_4$ is used as an activator for sphalerite.). [7]

The flotation of the tailings was performed at LTU at a pH between 9 and 11, using *Atrac 1563* as a collector and Na_2SiO_3 as a depressant [8]. The end product is a concentrate that represents 11.9 wt.% of the original feed material and contains 62 % of the total P_2O_5 content of the tailings. This translates

to a concentrate with a reported 32 wt.% of P_2O_5, which implies an approximate upgrade of 5x over the original tailings. In terms of REEs the concentrate contains approximately 5000 ppm, which is an upgrade factor of 4 compared to the tailings before upgrading.

After this upgrading process the obtained concentrate was shipped to TU Delft for hydrometallurgical processing.

3.3.2. Characterisation of the upgraded mine tailings

3.3.2.1. Phase analysis

Before a hydrometallurgical process could be developed, the upgraded tailings from LTU were characterised. The first step in characterising the concentrate is a phase analysis using XRD and a chemical analysis using XRF. The phase analysis, see Figure 3.2, shows that the major components of the upgraded tailings are apatite [$Ca_5(PO_4)_3(OH,F)$], calcite [$CaCO_3$] and dolomite [$CaMg(CO_3)_2$]. Quartz and magnetite were also detected as minor phases, as well as various magnesiosilicates. None of the major REE bearing minerals were detected during analysis, which indicates that none of these minerals are present in a concentration that exceeds the detection limit of the XRD, which is approximately 1 wt.%.

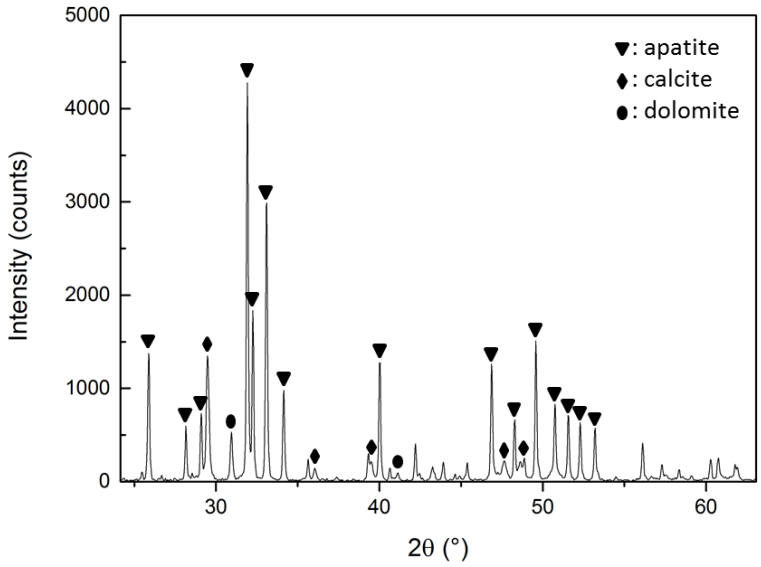

Figure 3.2: XRD spectrum section (20°-60°) of the upgraded mine tailings

3.3.2.2. Chemical analysis

With the primary phases of the upgraded tailings now known, XRF is used to determine of the chemical composition. The XRF analysis was performed on 11 samples taken from the material and the results are averaged in Table 3.1.

Table 3.1: XRF analysis of the upgraded tailings, concentrations are given in wt.% and were averaged over 11 measurements

	Ca	P	F	Fe	Mg	Si	Ce	Nd	Y	La
wt.%	34	10.3	2.0	1.14	0.96	0.54	0.11	0.09	0.059	0.05
σ	1.5	0.7	0.8	0.08	0.08	0.07	0.01	0.03	0.004	0.03

The chemical analysis shows that Ca and P are the major elements present in the concentrate. However, the obtained results do not compare well to the reported chemical composition we received from LTU, which was measured with ion chromatography (IC) (see Table 3.2 and 3.3). Also, the XRF analysis reports the presence of only 4 of the 17 REE (the detection limit XRF is 100 ppm). To improve the accuracy of the chemical analysis and obtain a more detailed view on the REE composition, the chemical analysis was repeated using ICP-OES for comparison.

Table 3.2: Chemical composition (wt.%) major elements of the upgraded tailings provided by LTU, measured with IC

	Ca	P	Fe	Mg	Si	Al
wt.%	37.4	15.5	0.93	0.75	0.8	0.1

Table 3.3: Chemical composition (ppm) REEs of the upgraded tailings provided by LTU, measured with IC

	Ce	La	Nd	Y	Pr	Sm	Gd
ppm	1950	885	835	570	216	136	124
	Dy	**Er**	**Eu**	**Ho**	**Tb**	**Tm**	**SUM**
ppm	90.3	51.1	19.1	18.8	16.4	6.71	5009

16 samples of the upgraded tailings were digested using the borax fusion method and were measured via ICP-OES. The results were averaged and reported in Table 3.4 for the major elements and in Table 3.5 for the REEs.

Table 3.4: ICP-OES analysis of major elements, concentrations given in wt.% and were averaged over 16 measurements

	Ca	P	Fe	Mg	Si	Al
wt.%	37	14.1	0.9	0.68	0.64	0.16
σ	1.5	0.6	0.1	0.02	0.02	0.03

Table 3.5: ICP-OES analysis of REEs, concentrations given in ppm and were averaged over 16 measurements

	Ce	Nd	La	Y	Sm	Pr
ppm	1763	892	563	517	385	148
σ	229	73	177	89	99	65
	Eu	**Gd**	**Ho**	**Dy**	**Er**	**SUM**
ppm	139	137	92	87	51	4775
σ	152	11	30	22	8	368

The obtained results using ICP-OES better match those of LTU for the major elements. The calculated uncertainty does suggest that REE distribution within the material is not fully homogeneous. The measured REE values from LTU do mostly fit within the uncertainty range of our results, but the uncertainty of the LTU analysis was unavailable. Still it is clear that Ce is the major REE within the concentrate, followed by La and Nd. This means that the apatite concentrate is primarily a source for light REEs. There are some noteworthy heavy REEs, (i.e. Y, Dy and Er) present in the apatite concentrate

whose behaviour will be monitored. Y is present in a higher concentration than average compared to other light REE resources and Dy is quite valuable. The analysis of Er has quite a low uncertainty (amongst the heavy REEs), which makes it a useful indicator for the behaviour of the heavy REEs. Therefore, these elements will be used to track the behaviour of heavy REEs during processing.

The ICP-OES at TU Delft analysis did not detect Lu, Tb, Tr and Yb, which were detected in the LTU analysis. To verify their presence a sample was sent to Utrecht University for ICP-ms analysis. The results of that analysis are shown in Table 3.6. The analysis confirms the presence of Lu, Tb, Tr and Yb, however due to the low concentration and considerable uncertainty, these elements will not be considered further during this work.

Table 3.6: ICP-ms analysis of missing REEs, concentrations given in ppm and were averaged over 2 measurements

	Yb	Tb	Tm	Lu
ppm	45	19	7	5
σ	7	3	1	1

Based on the obtained chemical composition and the identified phases an approximate mineral composition can be established. Assuming all phosphorous is contained in apatite (no other P based minerals were detected with XRD, thus no other P based minerals have a concentration above 1 wt.%) and all Mg in dolomite (same reason as P), then the phase fractions are: 77% apatite, 13% calcite and 5% dolomite. The remaining 5% of the minerals consists mainly out of quartz and magnetite, and some other refractory minerals. From this we can conclude that the upgrading was quite effective, and the upgrading process produced an apatite concentrate.

3.3.2.3. Identifying the REE bearing compounds

Chemical analysis confirms the presence of REEs within the apatite concentrate. However, the mineral(s) associated with the REEs cannot be identified with XRD. This suggests that either the fraction of REE bearing mineral in the concentrate lies below the detection limit of the XRD or that the REEs are dispersed in the detected mineral phases. As further analysis and leaching results will show, it is both.

To identify the REE phases in the apatite concentrate, the material was analysed with SEM and EDS. Using Back Scattered Electron (BSE) imaging, it is possible to trace particles which are composed of heavy elements. Heavier elements are more likely to cause backscattering of electrons, making them appear brighter on the detector than lighter elements [9]. As lanthanides have atomic numbers ranging from 57 (La) to 71 (Lu), this makes particles that contain them appear brighter than the Ca (atomic number 20) containing particles. Using this principle, it is possible to detect REE-rich particles within the concentrate on the SEM image and analyse their composition with EDS, see Figure 3.3.

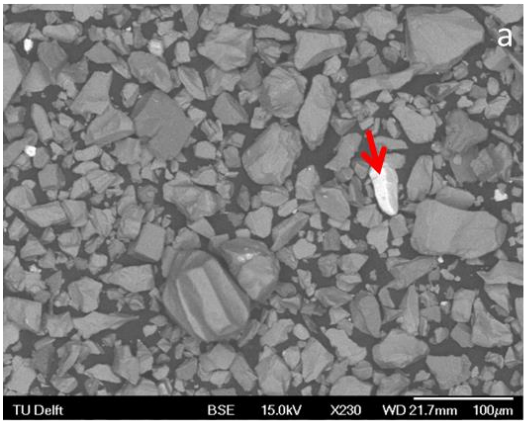

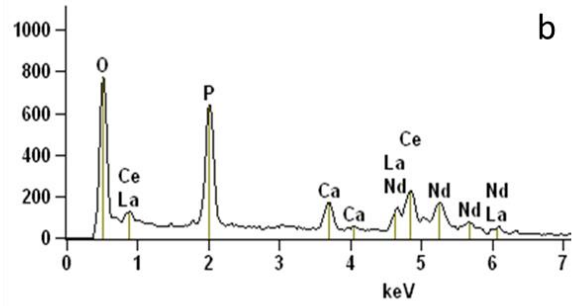

wt.% measured with EDS					
O-K	P-K	Ca-K	La-L	Ce-L	Nd-L
28.9	13.9	5.04	11.17	30.61	10.4

Figure 3.3: **(a):** SEM image of the apatite concentrate using BSE imaging; **(b):** EDS analysis of indicated particle (red arrow)

The EDS analysis of the indicated particle in Figure 3.3 (a) identifies it as a REE-rich mineral (see Figure 3.3 b). Its chemical composition suggests that this mineral is of the monazite ($(Ce,La,Nd,\ldots)PO_4$) family, which agrees with the mineralogical study performed by Pålsson et al. [8]. Further analyses of other bright particles show similar EDS spectra.

The leaching experiments in Chapter 4.4. will show that monazite is not the only REE mineral present within the apatite concentrate. Apatite itself is also a REE containing mineral, with REEs substituting for Ca in the apatite crystal lattice. The REE contrition is apatite is low, thus EDS does not detect it. The leaching experiments also show that the REE distribution is not homogeneous, rather the light REEs concentrate mainly in the monazite and the heavy REEs concentrate mainly in the apatite.

3.4. WEEE and its upgraded fractions

3.4.1. Origin of the WEEE and physical upgrading

The raw material for the WEEE recycling used in this research originates from the WEEE shredder at INDUMETAL RECYCLING, Spain [10]. A generalised version of their shredder flowsheet is shown in Figure 3.4, where the WEEE is separated into several fractions after shredding, first magnetically and then via eddy current.

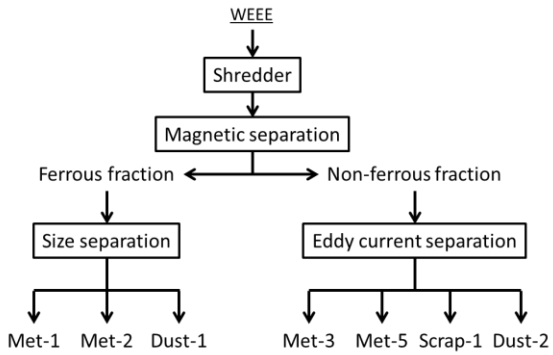

Figure 3.4: Overview of the INDUMETAL shredder flowsheet

A survey of all end streams from their WEEE shredder products shows that 88% of recovered Nd is present in the ferrous end stream (without taking the Nd lost in the shredder into account, as due to

their magnetic properties NdFeB magnet particles often remain stuck inside the shredder equipment), while the remaining 12% is distributed over various non-ferrous and dust fractions. Since the Nd present in the WEEE is, in all likelihood, in the form of NdFeB magnet particles, it is not surprising that the Nd concentrates in the ferrous fraction of the WEEE shredder. After magnetic separation the ferrous fraction is separated in a coarse (*Met-1*) and fine fraction (*Met-2*). The majority of the Nd present in the ferrous fraction (94%) reports to the coarse *Met-1* fraction (but with low concentration), while only 6 % reports to the fine fraction (but with high concentration). This is due to the fact that, while NdFeB is brittle, it also possesses a very strong magnetic field. This means that even small particles attach themselves to the large iron fragments and will not be detached by mechanical means. An overview of the end stream compositions is shown in Table 3.7.

Table 3.7: INDUMETAL shredder end streams, fractions and compositions, measured with ICP-OES

	Met-1	Met-2	Met-3	Met-5	Scrap-1	Dust-2	Total*
Shredder fraction (%)	64.9	0.9	8.9	0.22	0.00024	1.89	76.8
Nd concentration (ppm)	489	2111	0	17	19067	2359	381
Nd distribution (%)	83	5	0	<0.1	<0.1	12	100
Concentration other elements in the shredder end streams							
Fe (%)	99	66.5	0.42	2.05	64.8	35.6	65.6
Al (%)	0.05	0.24	67.2	6.74	0.3	2.77	6.1
Cu (%)	0.011	1.58	11.8	18.72	0.54	8.37	1.3
Zn (%)	0.5	4.49	0.41	2.51	0.1	2.63	0.5

*Not all shredded fractions are reported, thus total < 100%. Nd distribution is calculated on the assumption that no Nd is present in the non-reported fractions

The compositions and mass fractions of the end streams of the shredder offer an interesting choice when it comes to Nd recycling. If the primary goal is to recover as much Nd as possible, then Met-1 is the obvious choice, as it contains the majority of the Nd. However, the overall concentration of Nd in this stream is low, only 489 ppm. Physically upgrading this material to a level where it is recyclable will require a substantial amount of energy and will likely to be detrimental to the Fe value of the stream. *Met-2* on the other hand, while being only a minor stream, does have a more manageable Nd concentration to work with. It is also only a minor stream in the flowsheet, and it contains a high fraction of Cu (detrimental to Fe recycling, and Fe is detrimental to Cu recycling), meaning that the inherent value of this stream is low. Both streams offer advantages and disadvantages for recycling Nd and both are taken into consideration when developing a recycling process.

Before either stream can be effectively recycled hydrometallurgically it must first be physically upgraded, which was again done by our project partners at LTU. The physical upgrading process [11] has two main components: demagnetisation, followed by grinding and sieving. The demagnetisation serves to break the magnetic connection between the Fe and the NdFeB magnet particles, allowing them to be separated from one another. This is achieved by heating the material to 500°C for 1 h, since the Curie temperature of NdFeB magnets typically lies between 300 and 400°C, depending on the Dy content, [12]. This heat treatment will remove the magnetic field from the NdFeB magnet particles, causing them to detach from the steel components. After demagnetisation the material is fed into a knife mill to further separate the ferrous and magnet particles. NdFeB is quite brittle, which causes them to undergo significant size reduction during milling. When the milled material is sieved the NdFeB magnet particles will report to the smallest size fraction.

Table 3.8: Sieving results Met-1 after demagnetisation. "*-d*" indicates particles smaller than *d*, "*+d*" indicates particles larger than *d*.

	Mass		Nd	
	(g)	(%)	Concentration (wt.%)	Distribution (%)
Feed	34515	100	0.01	100
Heat loss	62.3	0.2	0	0
Demagnetized	34452	99.8	0.01	100
+9.5 mm	33940	98.3	0	0
-9.5 mm	494	1.4	0.65	94.4
-4.75 mm	18.5	0.1	1.03	5.6

Table 3.8 shows the sieving of the demagnetised Met-1 stream, as expected the Nd reports to the smaller size fractions of the sieving process. The −9.5 mm fraction of the sieving only contains 1.4 % of the total mass flow of *Met-1*, yet it contains all the Nd (if not sieved further to −4.75 mm). This results in an upgrade factor of 13 (from 489 ppm to 6498 ppm). A higher-grade material can be achieved by sieving again to 4.75 mm, which leads to a feed material with a Nd concentration of 10309 ppm. However, only 5.6 % of the total Nd would report to this −4.75 mm fraction. As such the −9.5 mm fraction is the most interesting one for recycling. A major drawback of this upgrade process is that a large amount of material that must be heated, for only 1.4 % to be useable for recycling.

When sieving demagnetised and ground *Met-2* similar results were obtained as with the sieving of *Met-1*: the Nd concentrates in the smaller size fractions. However, unlike *Met-1*, the Nd fully reports to the −1.75 mm fraction instead of the −9.75 mm fraction. This is because *Met-2* was cryo-milled, whereas *Met-1* was not, due to the presence of hard and large components, which the cryo-mill could not process. The cryo-grinding reduced the size of the magnet particles considerably, allowing them to be sieved down to −1.75 mm. The −1.75 mm sieve fraction was further sieved on a 75 µm sieve, see Table 3.9, to produce the final upgrade. (Note that in Table 3.9 the Fe distribution value in the +75 µm fraction is the sum of Fe in this fraction and all coarser fractions) The −75 µm fraction represents 7.69 wt.% of the *Met-2* stream and contains 55.2 % of its Nd, and only 10.9% of its Fe. This is the upgraded product that will be utilised for hydrometallurgical recycling. The +75 µm fraction was utilised by NTNU for their pyrometallurgical experiments.

Table 3.9: Distribution and concentration of Fe and Nd at the final sieving step for Met-2

	Met-2			
	Concentration (wt.%)		Distributions (%)	
	Nd	Fe	Nd	Fe
–75 µm (TUD)	0.99	57.8	55.2	10.9
+75 µm (NTNU)	0.11	64.1	44.8	89.1*

*sum of Fe from all sieving fractions

Of all streams that were upgraded, it was decided that the *Met-2* −75 µm stream was the most valuable stream to perform experimental research on. This stream contains a sufficiently high Nd concentration to properly observe it behaviour during hydrometallurgical processes, yet still contain sufficiently high levels of impurities to make the results valuable for process development. Thus, this stream will serve as the focus for the research of this work.

3.4.2. Characterisation of the Met-2 –75 µm shredded WEEE stream

3.4.2.1. Phase analysis

The phase composition of the upgraded *Met-2* –75 µm material was determined via XRD. The results of the analysis are shown in Figure 3.5.

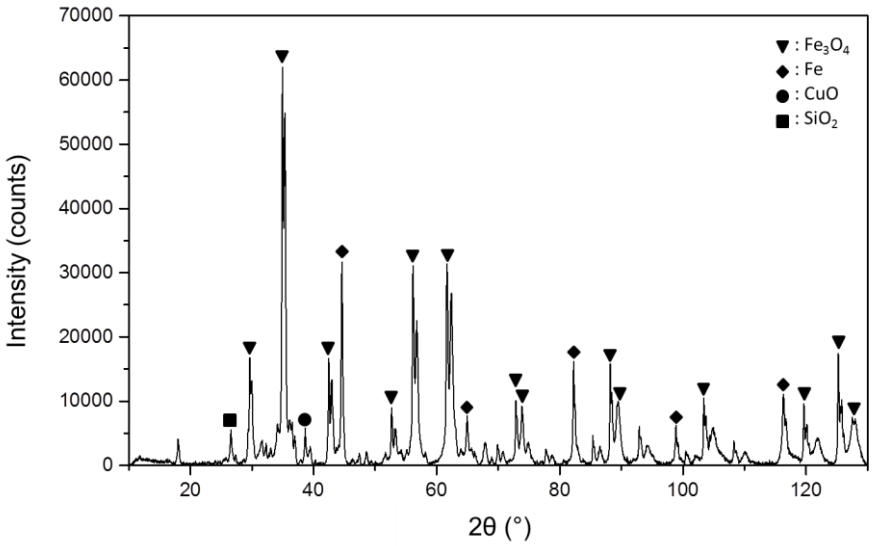

Figure 3.5: Phase analysis of the upgraded WEEE using XRD with the most abundant phases marked

The XRD analysis shows that the most abundant phases are Fe_3O_4, Fe, CuO and SiO_2. Note that the Fe_3O_4 peaks in the spectrum are split and are a combination of both Fe_3O_4 peaks and peaks of a phase where Zn and Mn partially replace Fe in the Fe_3O_4 lattice ($Zn_{0.18}Mn_{0.80}Fe_{2.02}O_4$, concluded based on the spectrum and the ICP-OES chemical analysis in Table 3.10). This indicates the possible presence of galvanised steel in the WEEE. From this analysis it is possible to conclude that a large fraction of the Fe in the WEEE has been oxidised during the demagnetisation pre-treatment.

3.4.2.2. Chemical analysis

Chemical analysis was performed using ICP-OES and the samples were dissolved using the borax fusion method described above. Aqua Regia dissolution was also tested, and while it rapidly digested the majority of the material, some residue remained. To ensure a full dissolution the borax fusion method was required. The results of the chemical analysis are shown in Table 3.10.

Table 3.10: Elemental composition in wt.% of the upgraded WEEE analysed with ICP-OES, average over 4 samples

Element	Fe	Zn	Mn	Ca	Cu	Ni	Si
Average concentration (wt.%)	58	7.5	3.12	2.4	2.0	1.16	1.00
Standard deviation (σ, wt.%)	2	0.2	0.04	0.2	0.1	0.03	0.06
Element	**Nd**	**Al**	**Pb**	**Mg**	**Pr**	**Sm**	**Dy**
Average concentration (wt.%)	0.99	0.55	0.5	0.260	0.16	0.07	0.030
Standard deviation (σ, wt.%)	0.01	0.02	0.5	0.003	0.01	0.04	0.002

The analysis shows that the accuracy of the ICP-OES analysis is reasonably high, with a relative standard deviation for most elements less than 5% (exceptions are Sm and Pb which have relative standard

deviations above 50%). The analysis was performed on 4 samples (measured in triplicate) taken at different times, which suggests that the material is fairly homogeneous. The major elements identified are Fe, Zn and Mn, which suggests that (galvanised) steel is the main component, which is expected for a ferrous WEEE fraction. The main impurities are Cu, Ni, Ca and Si. The main REE component is Nd with a concentration of 0.99 wt.%, which shows that the upgrading process by LTU increased the Nd concentration with a factor of 5 and was thus successful in delivering a material with an acceptable REE concentration. Pr and Dy are also present, as they are common alloying elements for NdFeB magnets. Trace amounts of Sm are detected as well (originating from SmCo magnets), but its concentration is very low.

3.4.2.3. Identifying the REE bearing compounds

The chemical analysis, as well as the nature of the material, suggests that the REE bearing compound of the upgraded shredded WEEE are NdFeB magnet fragments, that attached themselves to the iron components during shredding. Confirmation of this with SEM/EDS has proven challenging, however, since the average atomic weight of the upgraded WEEE is higher than that of the tailings. This negatively impacts the contrast of the image under BSE imaging. Figure 3.6, BSE image of the upgraded shredded WEEE, shows plenty of particles that are bright, however most contain no REEs. This is further complicated by the presence of Pb, which is heavier than Nd, meaning that the brightest (most noticeable) particles do not contain Nd, but Pb instead. Nevertheless, some NdFeB particles were found using EDS, see Figure 3.7, but overall the SEM/EDS analysis is not very reliable for this material.

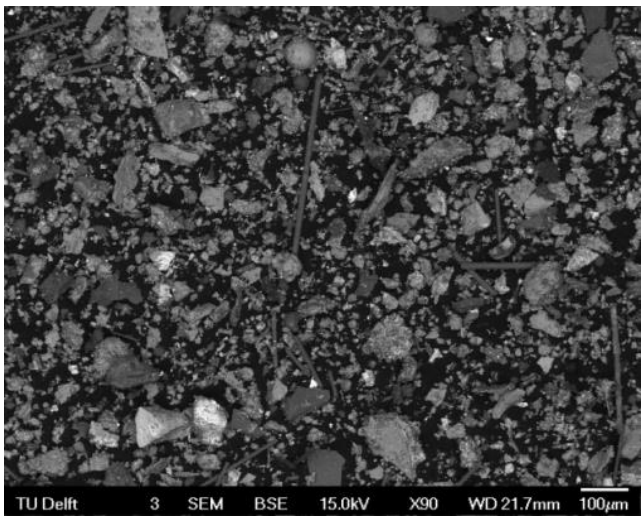

Figure 3.6: BSE image of the upgraded shredded WEEE

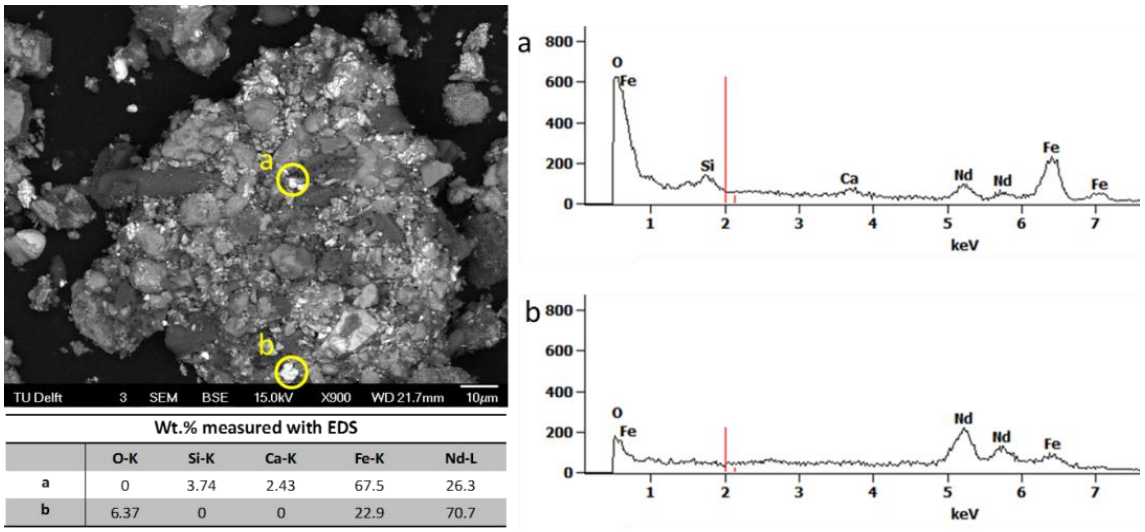

Wt.% measured with EDS

	O-K	Si-K	Ca-K	Fe-K	Nd-L
a	0	3.74	2.43	67.5	26.3
b	6.37	0	0	22.9	70.7

Figure 3.7: EDS identification of NdFeB particles attached to a larger Fe particle

3.5. Pyrometallurgically treated WEEE and the produced slags

3.5.1. Origin of the pyrometallurgical slags

As was mentioned above, one of the drawbacks of the physical upgrading of the ferrous shredded WEEE is the energy consumption of the demagnetisation step. Large amounts of energy are required to demagnetise the ferrous fraction of the WEEE, while only a small fraction of recyclable material is produced (1.4 % for *Met-1*, 7.69 % for *Met-2*), meaning that the energy is largely wasted. Also, the oxidation of the iron during demagnetisation negatively impacts its recyclability, as oxidised Fe cannot be used in the BOF (basic oxygen furnace) during steel making. In an effort to circumvent this, an alternative upgrading process was developed by our project partners at the Norwegian University of Science and Technology (NTNU) and Tecnalia, Spain. This pyrometallurgical process utilises the extremely high oxygen affinity of Nd to create a Nd-rich slag, by smelting the ferrous WEEE in a graphite crucible at 1650°C ±30°C. This process produces a metallic iron ingot, which can be used in steel making, and a Nd-rich slag for hydrometallurgical REE recovery. NTNU and Tecnalia both produced slags for recycling; NTNU utilised non-upgraded coarse *Met-1* stream to produce slags and Tecnalia utilised non-upgraded fine *Met-2* stream. Both slags were sent to TU Delft for hydrometallurgical processing to extract the REEs.

3.5.2. Characterisation of the slags

3.5.2.1. Phase analysis

The phase composition of both slags was determined via XRD measurement. The result of the analysis of the NTNU *Met-1* slag is shown in Figure 3.8.

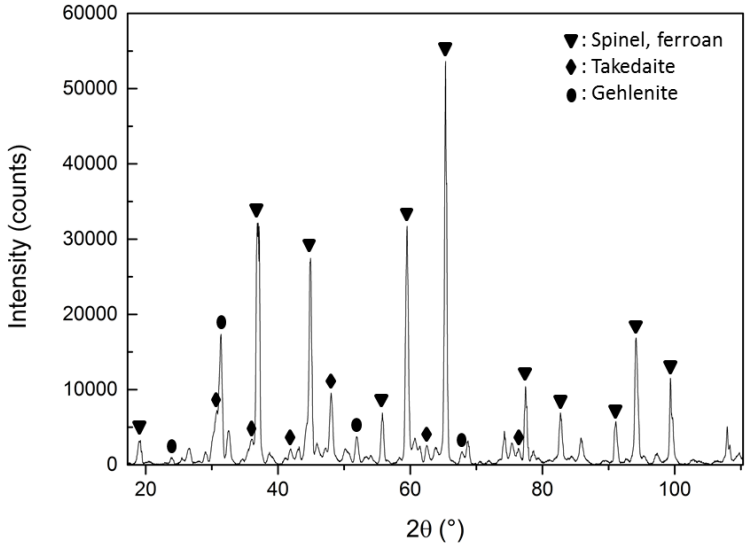

Figure 3.8: Phase analysis of the NTNU *Met-1* slag using XRD with the most abundant phases marked. For the chemical composition of the phases refer to Table 3.11

The XRD analysis shows the presence of three major phases: $Mg_{0.7}Fe_{0.23}Al_{1.97}O_4$ (Spinel, ferroan), $Ca_3B_2O_6$ (Takedaite) and $Ca_2Al_2SiO_7$ (Gehlenite). The Ca, Mg and Al that make up these phases are present in the WEEE before smelting, while the B however was added as $Na_2B_4O_7$ flux. This flux was chosen based on the success of the borax fusion during digestion for chemical analysis with the aim to create an easily soluble slag.

The result of the XRD analysis of the Tecnalia Met-2 slag is shown in Figure 3.9.

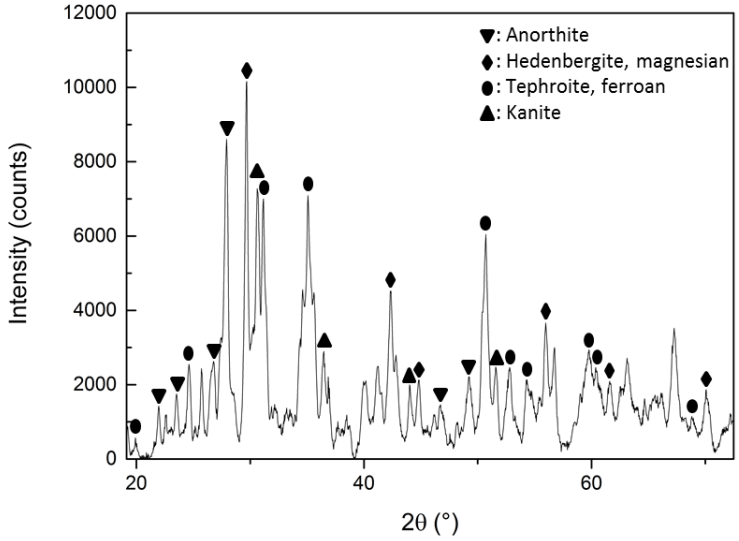

Figure 3.9: Phase analysis of the Tecnalia *Met-2* slag using XRD with the most abundant phases marked. For the chemical composition of the phases refer to Table 3.11

Unlike the NTNU slag this slag phase was created without the use of any flux (to serve as a contrast). All elements that comprise the slag originate from the shredded WEEE. A detailed overview of the identified phases can be seen in Table 3.11.

Table 3.11: Detailed phase composition of the slags

Met-1 slag NTNU	
Spinel, ferroan	$Mg_{0.7}Fe_{0.23}Al_{1.97}O_4$
Takedaite	$Ca_3B_2O_6$
Gehlenite	$Ca_2Al_2SiO_7$
Met-2 slag Tecnalia	
Anorthite	$Ca(Al_2Si_2O_8)$
Kanoite	$(Mn^{(2+)},Mg)_2(Si_2O_6)$
Hedenbergite, magnesian	$CaMg_{0.34}Fe_{0.66}Si_2O_6$
Tephroite, ferroan	$Mn_{1.4}Fe_{0.6}(SiO_4)$

3.5.2.2. Chemical analysis

Chemical analysis was performed using ICP-OES and the samples were dissolved using the borax fusion method. Aqua Regia dissolution was also tested, and while it rapidly digested the majority of the NTNU slag, some residue remained. For the Tecnalia slag Aqua Regia dissolved less than half of the slag. To ensure full dissolution of the slags the borax fusion method was required. The results of the chemical analysis are shown in Table 3.12.

Table 3.12: Elemental composition in wt.% of the slags analysed with ICP-OES

		Al	Mg	Ca	Fe	Mn	Nd	Pr	Dy
Met 1 slag NTNU	**wt.%**	23.0	9.3	8.9	1.17	0.06	1.3	0.2	0.001
	σ	1.5	0.5	0.5	0.05	0.02	0.1	0.1	0.001
Met 2 slag Tecnalia	**wt.%**	7.35	2.9	3.8	1.6	17.6	1.4	0.2	0.05
	σ	0.5	0.2	0.1	0.1	0.2	0.1	0.1	0.01

Chemical analysis shows that the slags produced via the pyrometallurgical upgrading have a slightly higher Nd concentration compared to the physically upgraded WEEE (1.25-1.43 vs 0.99 wt.%). What stands out is the fact that the Fe content in the slags is considerably lower in the slags compared to the physically upgraded WEEE. The impact of this lower Fe content will be discussed in later chapters.

References

[1] "Bruker D8 Advance diffractometer." [Online]. Available: https://www.bruker.com/products/x-ray-diffraction-and-elemental-analysis/x-ray-diffraction/d8-advance/overview.html. (retrieved 28/02/2018)

[2] "X-RAY DIFFRACTION FACILITIES at the department of Materials Science & Engineering." [Online]. Available: http://labs.tudelft.nl/index.php?action=instrument&id=122. (retrieved 28/02/2018)

[3] "Panalytical Axios Max WD-XRF." [Online]. Available: http://www.panalytical.com/Axios-FAST.htm. (retrieved 28/02/2018)

[4] "SPECTRO ARCOS ICP-OES." [Online]. Available: http://www.spectro.com/products/icp-oes-aes-spectrometers/arcos-inductively-coupled-plasma. (retrieved 28/02/2018)

[5] "JEOL JSM 6500F." [Online]. Available: http://labs.tudelft.nl/index.php?action=instrument&id=137. (retrieved 28/02/2018)

[6] Ullmann's Encyclopedia of Industrial Chemistry, Volume B2 Unit Operations I., pp. 5-1 – p5-31, ISBN: 0-89573-537-7, 1988.

[7] Ullmann's Encyclopedia of Industrial Chemistry, Volume B2 Unit Operations I., pp. 23-1 – p23-30, ISBN: 0-89573-537-7, 1988.

[8] B. Pålsson, O. Martinsson, C. Wanhainen, and A. Fredriksson, "Unlocking Rare Earth Elements from European apatite-iron ores," in Proceedings of the 1st European Rare Earth Resources Conference (ERES 2014), Milos (Greece), pp. 211–220, 2014.

[9] D. H. Krinsley, K. Pye, J. Sam Boggs, and N. K. Tovey, Backscattered Scanning Electron Microscopy and Image Analysis of Sediments and Sedimentary Rocks. Cambridge University Press, 1998.

[10] "Indumetal recycling." [Online]. Available: http://www.indumetal.com/. (retrieved 28/02/2018)

[11] B. Pålsson and C. Wanhainen, "Recovery of Rare Earth Elements from Electronic Waste by Cryo-grinding," presented at the Conference in Minerals Engineering 2015, Luleå, pp. 65–79, 2015.

[12] Y. Matsuura, S. Hirosawa, H. Yamamoto, S. Fujimura, and M. Sagawa, "Magnetic properties of the $Nd_2(Fe_{1-x}Co_x)14B$ system," Appl. Phys. Lett., vol. 46, no. 3, pp. 308–310, 1985.

Chapter 4: Hydrometallurgical recovery or REE from apatite concentrate

Abstract

The rare earth elements present in the Kiruna iron ore mine tailings represent a possible new REE resource for the EU. These tailings, after physical upgrading, contain approximately 5000 ppm of rare earth elements, concentrated in apatite and monazite minerals. To economically extract the REEs from these tailings, the phosphorous contained in the apatite must also be extracted and the waste generation of the process should be minimal. To achieve the extraction of REEs and phosphorous, HCl and HNO_3 were investigated as possible leaching agents. After leaching, solvent extraction using P350 was investigated for separation of REEs from Ca and H_3PO_4. Based on the results a leaching process using HNO_3 is proposed. By controlling the concentration of HNO_3 the proposed process can either co-dissolve 99% of the P and 75-100% of the heavy REEs (high concentration of HNO_3) or concentrate the heavy and light REEs into the leach residue (low concentration of HNO_3). If the REEs are co-dissolved with the P, solvent extraction is used to purify both the H_3PO_4 solution and the REEs. If the REEs are concentrated in the residue, the residue is treated with NaOH to convert the monazite to $REE(OH)_3$, which are then leached with HNO_3. Both routes produce a H_3PO_4 solution from the apatite, as well as $Ca(NO_3)_2$ as a by-product. Using a low concentration HNO_3 solution has proven to be the superior method. The developed flowsheet is shown in Figure 4.1.[4]

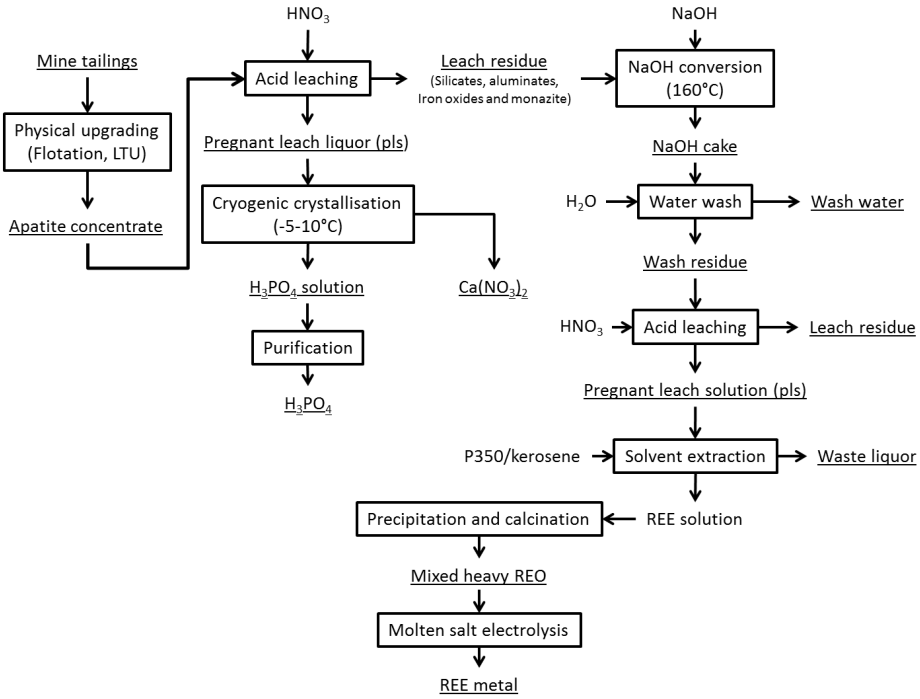

Figure 4.1: Developed flowsheet for the recycling of the Kiruna mine tailings

[4] **Remark:** This chapter is based on the published paper: S. Peelman, Z. H. I. Sun, J. Sietsma, and Y. Yang, "Hydrometallurgical extraction of rare earth elements from low grade mine tailings," in Rare Metal Technology, editors: Alam, S., Kim, H., Neelameggham, N., Ouchi, T., Oosterhof, H., TMS, Springer, pp. 17–29, 2016.

4.1. Introduction

This chapter will discuss the hydrometallurgical recycling processes that were developed in order to recover the REE contained within the apatite concentrate produced by LTU from the LKAB mine tailings. The focus of the process development was not solely on the REEs. As the phosphorous content of the apatite concentrate is considerable and phosphorous is also considered a critical raw material, all the developed recycling processes also co-extract the P.

We will discuss where the inspiration for the developed process was drawn and how the chosen processes were selected. Then the individual processes will be discussed, to see how the REEs behave during the process and how effective the developed processes are for recovering REEs and P. Finally, we will discuss how each of these processes fits in an overall recycling flowsheet and what the challenges are to realise an effective recycling process.

4.2. Identifying potential process routes

As each process was developed with the co-extraction of P in mind, inspiration was primarily drawn from the phosphorous industry. As apatite is one of the primary raw materials for the production of phosphorous, various established processes already exist. The most common process uses H_2SO_4 to dissolve the apatite to form H_3PO_4, while the Ca precipitates out as $CaSO_4$, also known as gypsum. The main advantage of this process is the easy separation of Ca and P, as Ca is removed from the system as $CaSO_4$ while the phosphorous remains in solution. Reviewing the literature shows that the behaviour of REEs in this process has been investigated in the past. Previous research shows that during the precipitation of the $CaSO_4$ 80% of the dissolved REEs get incorporated in the $CaSO_4$ lattice and are lost to the gypsum (see chapter 2 REE recovery in the phosphoric acid industry). Although this is not beneficial to the recycling of REE from mine tailings, it has in fact sparked the interest for the recycling of waste gypsum for REEs [1], but this falls outside of the scope of this project.

The formation of $CaSO_4$ means that the traditional phosphorous production process will not be effective in recovering both phosphorous and REEs from the apatite concentrate. However, it does offer a basic concept to work on, namely acid digestion to form H_3PO_4. As an alternative to H_2SO_4, HCl and HNO_3 could also be used to digest the apatite and form H_3PO_4:

$$Ca_5(PO_4)_3F_{(s)} + 10\,HCl \rightarrow 5\,CaCl_2 + 3\,H_3PO_4 + HF_{(g)} \quad (4.1)$$

$$Ca_5(PO_4)_3F_{(s)} + 10\,HNO_3 \rightarrow 5\,Ca(NO_3)_2 + 3\,H_3PO_4 + HF_{(g)} \quad (4.2)$$

Additionally, the expected by-products, i.e. $CaCl_2$ and $Ca(NO_3)_2$, are soluble compounds, unlike $CaSO_4$. Thus, there are no potential REE losses to a precipitating Ca phase. However, this does mean that the REE and Ca both exist in the leach solution and they will need to be separated from one another, and from the H_3PO_4, in a separate process step.

To separate two compounds in solution, solvent extraction is the one of the most effective techniques. Solvent extraction is a process in which two immiscible phases, traditionally an aqueous and an organic phase, are mixed. (For this work only the aqueous-organic system will be considered.) The organic phase is loaded with chemicals called extractants, and they are the key to solvent extraction. The purpose of the extractants is to form complexes with the elements that we wish to extract. The formed complexes will no longer be water soluble, instead they become soluble in the organic phase. Thus,

when the aqueous and organic phases separate after mixing, the elements which formed complexes will be present in the organic phase and the elements which did not will remain in the aqueous phase. There are three main types of extractants: neutral, acidic and basic, each of which has their own complexation reaction. In this work only acidic extractants were used, their complexation reaction takes the general form

$$M^{n+}_{(aq)} + nHX_{(org)} \rightleftarrows MX_{n\,(org)} + H^{+}_{(aq)} \quad (4.3)$$

This reaction (4.3) is subjected to chemical equilibrium, thus solvent extraction is traditionally carried out in several stages, where each stage partially extracts the target element. Of course, having the element in the organic phase is not the end of the solvent extraction process. The next step is removing the element from the organic phase back into an aqueous phase. This is done via a process called stripping. Stripping requires reversing the complexation reaction, for acidic extractants (see reaction 4.3) this is achieved by mixing the organic phase with a strong (clean) acid. This returns the extracted elements to the strip solution, and at the same time also regenerates the extractant in the organic phase. For this process a solvent extraction process will be designed to separate the REEs from Ca and H_3PO_4. The separation of Ca and H_3PO_4 is also necessary to valorise the H_3PO_4, but this falls outside of the scope of this project.

Thus, the first recycling process will explore the extraction of REEs and phosphorous from the apatite concentrate through an acidic leaching process with HCl and/or HNO_3. The resulting leach liquor will be used to develop a solvent extraction process to separate REE from H_3PO_4.

Next to an acidic leaching process, an alkaline processing route will also be investigated. As opposed to the acidic leaching route, which was based on phosphorous production, the alkaline process is based on the commercial primary REE production technology. As monazite was identified as one of the REE bearing components of the apatite concentrate, the alkaline conversion process, which is used to process monazite ore in primary industry, serves as the inspiration to develop an alkaline based recycling process for recovering REEs and phosphorous.

The alkaline conversion process applied to the apatite concentrate is expected to follow the following reactions:

$$REEPO_{4(s)} + 3NaOH \rightarrow REE(OH)_{3(s)} + Na_3PO_4 \quad (4.4)$$

$$Ca_5(PO_4)_3(OH,F)_{(s)} + 10\,NaOH \rightarrow 5\,Ca(OH)_2 + 3\,Na_3PO_4 + Na(OH,F) \quad (4.5)$$

$$CaCO_{3(s)} + 2\,NaOH \rightarrow Ca(OH)_2 + Na_2CO_3 \quad (4.6)$$

$$CaMg(CO_3)_{2(s)} + 4\,NaOH \rightarrow Ca(OH)_2 + Mg(OH)_2 + Na_2CO_3 \quad (4.7)$$

Reaction (4.4) is the main conversion reaction where the monazite is converted into REE hydroxides and reactions (4.5)-(4.7) are side reactions. What makes this a potentially interesting process is the solubility of the different by-products of these reactions in different media. Na_3PO_4 and Na_2CO_3 are water soluble compounds, meaning that the P of the apatite concentrate can be extracted, and separated from the REEs, by washing the residue of the apatite conversion with water. $Ca(OH)_2$ is soluble in weak acids and $REE(OH)_3$ is soluble in strong acids, as such Ca and REEs could be separated

by sequential leaching steps. This means that a three-stage washing - leaching of the alkaline conversion residue would yield a separate P, Ca and REE stream.

4.3. Experimental setup

The acidic leaching experiments were performed in a 1 litre glass reactor, shown in Figure 4.2 (a), equipped with a glass paddle stirrer and submerged in an oil bath for heating. The stirring rate was kept constant for all experiments at 600 rpm. A condenser was used for high temperature experiments to prevent solvent loss. Leaching experiments were run with 50 g batches of the apatite concentrate to minimise the influence of the heterogeneity of the concentrate. Leach residues were filtered using a Buchner filter with Whatman 52 filtration paper (7 µm) and washed with demineralized water. Filtered leach residues were dried in a drying oven at 105°C for 24 h. All experiments were performed under normal atmosphere and using conventional equipment. High temperature (above 100°C) and high pressure leaching in autoclaves was not considered for acidic leaching, as the value contained within the apatite concentrate is too low to justify the use of such equipment on an industrial scale.

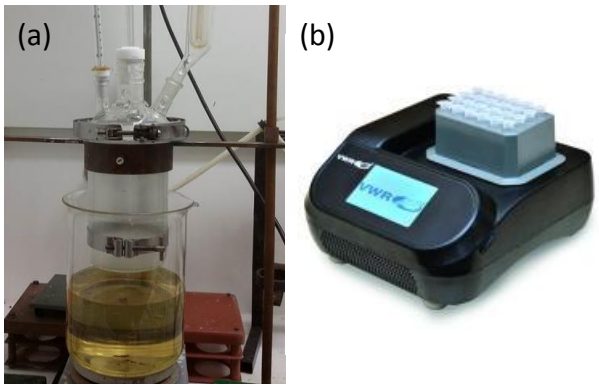

Figure 4.2 (a) Setup for acidic leaching **(b)** VWR® Thermal Shake Touch

Solvent extraction experiments were run using a VWR® Thermal Shake Touch [2] (see Figure 4.2 (b)), in 1.5 ml polymer Eppendorf phials. Solvent extraction tests were performed at room temperature and with a mixing time of 6 h at a shake speed of 800 rpm. The phases were allowed to separate and settle overnight to ensure full separation of the phases. Overall experiment time per sample was 24 h. Chemical analysis was performed on the aqueous phase before and after solvent extraction, the organic phase was not analysed as the necessary equipment for this was not available. As such it is assumed that the chemical composition of the organic phase is the difference in composition of the aqueous before and after solvent extraction.

The alkaline conversion experiments were performed in 500 ml Teflon reactors equipped with overhead stirring for experiments below 100°C. For experiments above 100 °C Ni crucibles were used, and the crucibles were placed in an oven and left overnight at the set temperature without agitation. Due to the nature of the alkaline solvent no glass reactors can be used safely. Residues were filtered using a Buchner filter with Whatman 52 filtration paper (7 µm) and washed with demineralized water. Filtered leach residues were dried in a drying oven at 105°C for 24 h.

4.4. Acidic leaching process for the upgraded mine tailings

The goal of the acidic leaching process is to dissolve the REE in the apatite concentrate and at the same time produce H_3PO_4. To this end the dissolution behaviour of the REEs is investigated as the apatite concentrate is leached with HCl and HNO_3.

4.4.1. HCl leaching

To observe the behaviour of the REEs in concentrate the material is first leached with solutions of increasing concentration of HCl. This is done to establish reactivity of the REE compounds in relation to the compounds in the apatite concentrate. In Chapter 3 it was established that monazite is present in the apatite concentrate and from literature we know that monazite is a mineral that is difficult to dissolve. However, we do not know if monazite is the only REE bearing compound in the apatite concentrate.

The apatite material was leached with 250 ml HCl solutions of increasing concentration. The concentrations used were 0.3 M, 1.5 M, 2.1 M, 4.2 M and 6.3 M HCl. A liquid solid ratio (L/S) of 5 was maintained for these experiments. The experiments were run for 6 h at room temperature. The results of these experiments are displayed on Figure 4.3 (a) and Figure 4.3 (b).

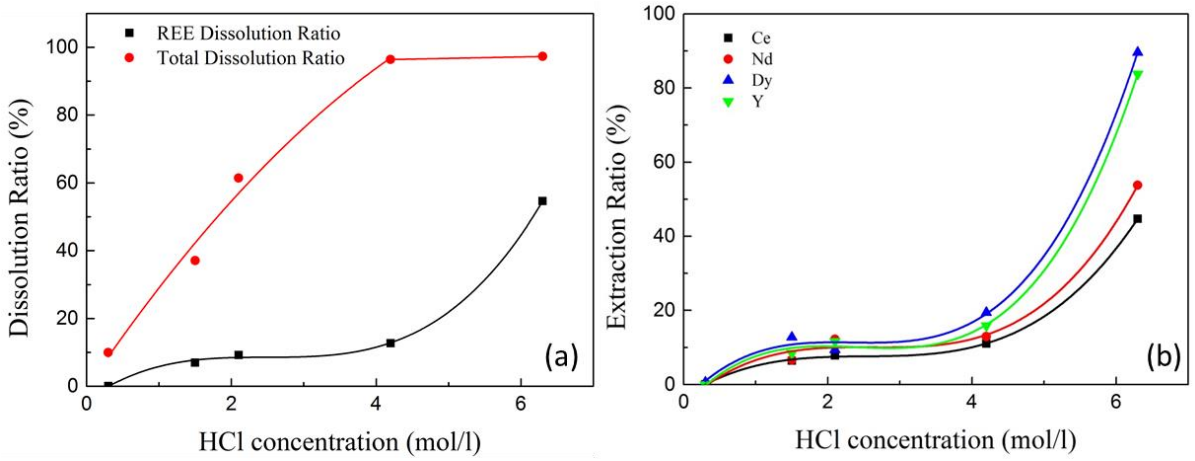

Figure 4.3: (a): HCl leaching profile - total dissolution and REE dissolution; **(b):** individual REE extraction ratios as a function of HCl concentration

The results show that REE extraction is limited as long as there is undissolved apatite. Only when all Ca compounds (i.e. calcite, dolomite and apatite) of the apatite concentrate have dissolved, does the REE extraction ratio increase from 10-15% to about 55% (see Figure 4.3 (a)). This clearly shows that the apatite, calcite and dolomite are far more reactive than the REE minerals, i.e. monazite. This means that after leaching with a 4.2 M HCl solution (10% excess over the required amount for stoichiometry based on the Ca compounds) 85-90% of the REEs in the apatite concentrate report to the remaining 5 wt.% of the leach residue. To extract any significant amount (more than 50%) of REEs to the leach liquor a large excess of acid (more than 50%) is required.

Figure 4.3 (b) shows the extraction behaviour of some individual REEs. A clear difference in extraction ratios is observed when comparing the heavy REEs (here Y at 84% and Dy at 90%) to the lighter REEs (Ce at 45% and Nd at 54%) when leaching with a large excess of acid. This behaviour is also observed at the lower acid concentrations, albeit in far smaller amounts (Ce at 11% and Dy at 20%). This could be attributed to the marginally higher solubility of the heavy REEs [3] or could indicate that the heavy

REE and light REE are associated with different minerals within the apatite concentrate, meaning it is possible that monazite is not the only REE bearing compound. Literature shows that monazite is a light REE mineral and that primary monazite processing requires very aggressive reaction conditions to dissolve the monazite [4]. A possibility of the other REE mineral is the apatite itself. Previous studies have shown that the apatite mineral can also contain REEs [5]. Through substitution of Ca, REEs can be incorporated in the apatite lattice. Thus, as the apatite dissolves the REEs in its lattice will co-dissolve.

However, at first glance, this behaviour is not observed in the HCl leaching profile (Figure 4.3 (a) and 4.3 (b)). The REE extraction ratio remains virtually constant as the apatite dissolution ratio increases until full apatite dissolution (4.2 M) is achieved. The REE extraction ratio only increases when all the apatite has been dissolved and an excess of acid is present (6.3 M). However, there is a side reaction that should be taken into account, the REE phosphate precipitation:

$$\mathrm{REE}^{3+} + \mathrm{PO_4}^{3-} \rightarrow \mathrm{REE(PO_4)_{(s)}} \tag{4.8}$$

REE phosphates are insoluble, as shown by the equilibrium constant K (inverse of the solubility product K_{sp}) of reaction (4.8), approximately $K = 10^{22}$ [6].

This reaction occurs when the formed H_3PO_4, from the apatite digestion (reaction (4.1)), dissociates to PO_4^{3-} anions. These anions will react with the dissolved REE^{3+} cations and re-precipitate as $REE(PO_4)$. This becomes more likely when the pH of the solution increases, as the level of dissociation of H_3PO_4 is tied to the pH [5], i.e. a higher pH will lead to more available PO_4^{3-}. During the leaching process the apatite dissolution consumes the available HCl, naturally increasing the pH of the solution. This means that if no excess acid is used, the increasing pH will enable any dissolved REEs to re-precipitate as REE phosphates, thereby lowering the overall extraction ratio. Using an excess of acid keeps the pH of the solution low enough to suppress the H_3PO_4 dissociation and prevents the precipitation reaction, yielding higher extraction ratios. Considering this, it is likely that apatite is indeed the second REE mineral in the apatite concentrate and that it's a source of the heavy REEs.

The residues of the leaching experiments were analysed with XRD, and SEM/EDS to identify the minerals resistant to dissolution. XRD analysis of the 4.2 M HCl leach residue (Figure 4.4) confirms that all apatite, calcite and dolomite have dissolved. It has also identified the major refractory minerals that were not detected on the XRD analysis of the material prior to leaching. Most of these refractory minerals are magnesio-silicates and iron oxides.

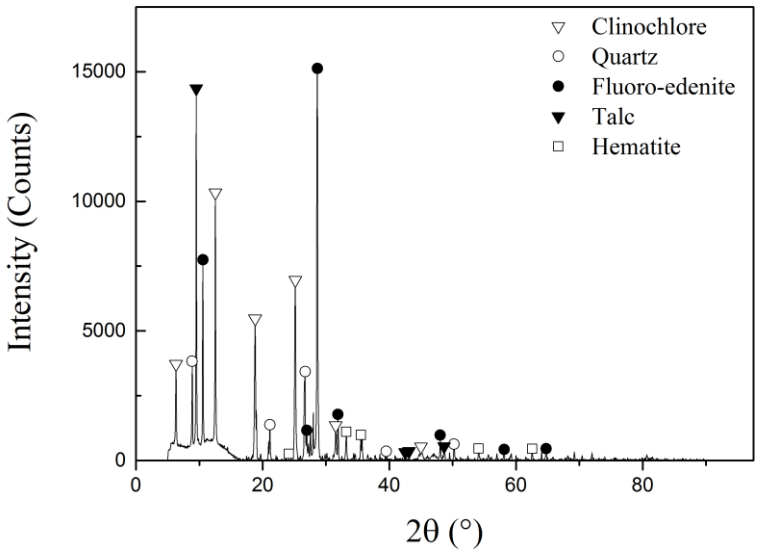

Figure 4.4: XRD spectrum 4.2 M HCl leach residue

SEM/EDS analysis of the 6.3M HCl (Figure 4.5) and the HNO_3 (presented in section 4.4.2, Figure 4.7) leaching residues reveals the presence of a substantial fraction of monazite.

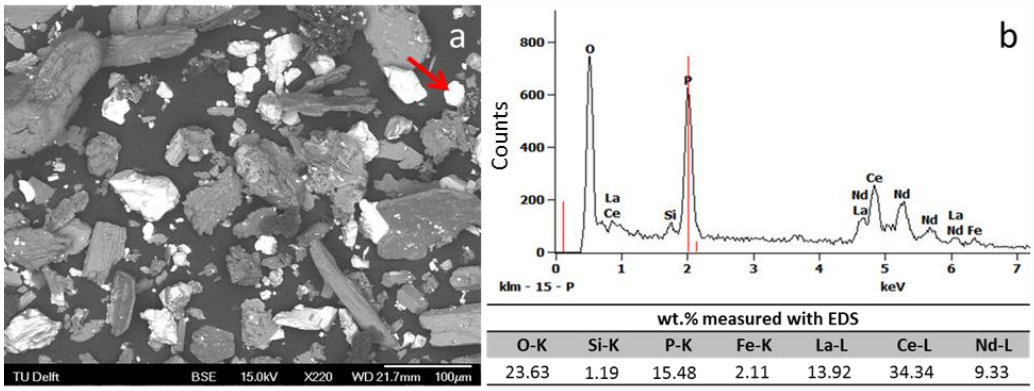

wt.% measured with EDS

O-K	Si-K	P-K	Fe-K	La-L	Ce-L	Nd-L
23.63	1.19	15.48	2.11	13.92	34.34	9.33

Figure 4.5: (a): SEM analysis of the 6.3 M HCl leach residue; **(b):** EDS analysis of the particle indicated by the red arrow

The monazite particles in the leach residue appear smooth and show no sign of partial dissolution. The observable particles have an approximate particle size between 10 and 50 µm, the same size as the observed particles in the material prior to the leach (Chapter 3, Figure 3.3a). This indicates that the monazite is not dissolving under these leaching conditions. Given that monazite is known to be an REE mineral that mainly contains light REEs [4], it is possible to conclude that the heavy REEs that were extracted during the HCl leaching experiments are not associated with the monazite.

4.4.2. HNO_3 leaching

The leaching experiments using HCl show that the REE extraction is only significant when the apatite concentrate is leached with a large excess of acid. Considering this HNO_3 can be used to achieve even higher levels of acidity due to its higher solubility in H_2O (65 wt.% vs HCl at 37 wt.%). Leaching with a concentrated HNO_3 solution can offer additional insights to the REE extraction behaviour. Additionally, to maximise the potential REE extraction the HNO_3 leaching experiments were performed at elevated temperatures (60-70°C) to enhance the leaching kinetics.

Table 4.1: REE extraction ratios (%) of HNO_3 leaching experiment at 70°C using L/S=5

Y	La	Ce	Pr	Nd	Sm	Eu	Gd
64.7	38.3	43.3	49.2	52.6	65.9	78.9	76.9
Tb	**Dy**	**Ho**	**Er**	**Tm**	**Yb**	**Lu**	**Total REE**
94.0	92.7	100	97.8	100	100	100	51.0

Table 4.1 shows the results of the leaching experiment using HNO_3. The obtained extraction ratios do not differ much from the ones obtained when leaching with HCl. Overall the extraction ratios are about 5 % lower than those of HCl, but that does lie within the variance of data. This means that the additional acidity did not contribute to a better REE extraction, supporting the theory that the excess acid only functions to suppress the phosphate precipitation reaction (reaction 4.8). This indicates that there are at least 2 different REE phases in the apatite concentrate: one which is rich in heavy REEs (apatite) and is dissolved by both HCl and HNO_3 and the other is rich in light REEs (monazite) and is not dissolved by either acid.

As both HCl and HNO_3 yield similar REE extraction rates, the choice of acid is determined by the next process steps. Solvent extraction prefers HNO_3, because HCl can decompose the organic phase more easily. While this is important, there is another, more valuable, reason to use HNO_3 over HCl and that is the possibility of controlled $Ca(NO_3)_2$ precipitation. The Norsk Hydro process [7] utilises this principle to valorise the Ca as $Ca(NO_3)_2$, which is a resource for the fertilizer industry [8]. This improves the economy of the process and also benefits the recovery of REEs from the solution at a later stage, as most of the Ca will have been removed already. Taking the precipitation of $Ca(NO_3)_2$ into account additional experiments with lower liquid solid ratios were conducted. A lower liquid solid ratio will increase the Ca concentration in the liquor making subsequent precipitation easier.

Table 4.2: REE extraction ratios (%) of HNO_3 leaching experiment at 70°C using L/S=2

La	Ce	Pr	Nd	Sm	Eu	Gd	Tb
37.8	26.1	45.2	46.9	59.3	66.5	68.3	73.2
Y	**Dy**	**Ho**	**Er**	**Tm**	**Yb**	**Lu**	**Total REE**
73.6	79.1	89	75.9	100	80.6	100	43.0

Table 4.2 shows the extraction ratio of REEs when the apatite concentrate is leached with HNO_3 at a L/S of 2. The lower L/S does appear to have a negative impact of the extraction of the REEs. However, this does lead to a richer leach solution, 1.14 g/L REE vs the 0.53 g/L REE at L/S = 5. This increased REE concentration, combined with lower acid excess, increases the driving force of the $REEPO_4$ re-precipitation. This is likely the cause of the decreased REE extraction for the leaching experiment with L/S = 2. Nevertheless, the REE losses are not substantial and the overall economics of the system would benefit from the lower liquid solid ratio.

XRD analysis of the HNO_3 leach residue (Figure 4.6) identifies additional refractory minerals, as well as detecting monazite as part of the residue. This proves that the observed particles with SEM are indeed monazite and that monazite is resistant to acid digestion under atmospheric conditions.

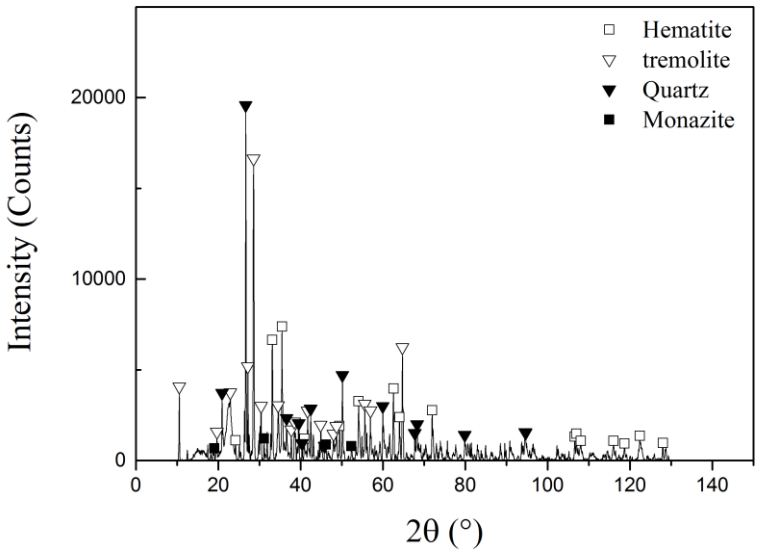

Figure 4.6: XRD spectrum HNO_3 leaching residue

SEM/EDS analyses of the HNO_3 leaching residues, see Figure 4.7, show the same behaviour as those of the HCl leach residues. The residue is rich in monazite particles which have the same apparent size as those found in the concentrate before leaching. Additionally, the monazite particles show no clear signs of reaction, again suggesting that the monazite is completely unaffected by the leaching process.

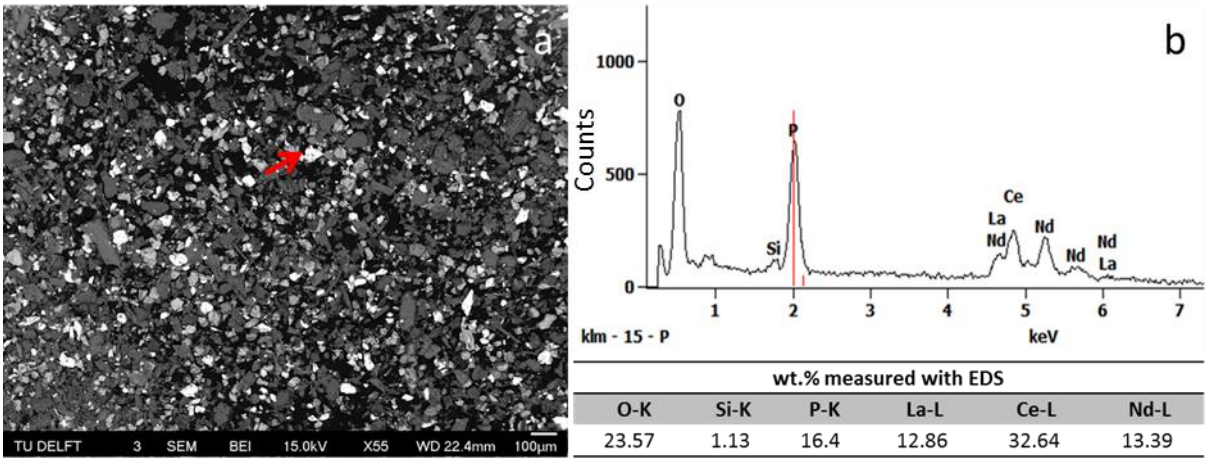

wt.% measured with EDS

O-K	Si-K	P-K	La-L	Ce-L	Nd-L
23.57	1.13	16.4	12.86	32.64	13.39

Figure 4.7: (a): SEM analysis of the HNO_3 leach residue; **(b):** EDS analysis of the particle indicated with the red arrow

4.4.3. Ca removal from the leach liquor

Now that the apatite concentrate has been leached, both the phosphorous and the heavy REEs have been extracted to the leach liquor. However, before they can be separated, first the large amount of co-dissolved Ca must be addressed. As Ca is considered an impurity in both H_3PO_4 and REO it must be removed from both streams. As discussed previously, in traditional H_3PO_4 production this was done via the precipitation of $CaSO_4$, however, due to the REE capturing nature of $CaSO_4$, this not an option here.

For the HCl leach liquor the Ca removal is challenging as $CaCl_2$ is a highly soluble compound that is not easily precipitated. This means that the Ca would have to be removed using a solvent extraction process. This has the added complication that HCl is harmful to most of the common organic phases that are used in solvent extraction. While these challenges can be managed, the HNO_3 leach liquors do

not have the same complications and as the HNO_3 process is not inherently inferior to the HCl process it is more realistic to continue with the HNO_3 leach liquors than try and overcome the complications the HCl process poses.

Based on an existing H_3PO_4 production process by Norsk Hydro, that uses HNO_3 instead of H_2SO_4 [7], $Ca(NO_3)_2$ can be precipitated from the leach liquor by cooling the liquor to −5°C. To confirm this behaviour, 20 ml samples of the HNO_3 leach liquors were cooled, by means of a freezer, to −20°C for 24 h. The behaviour of the REEs was also monitored to see if the precipitation captured any REEs.

The initial tests failed to precipitate any $Ca(NO_3)_2$ after cooling for 24 h. In order to facilitate the precipitation, the experiments were repeated with a small amount of $Ca(NO_3)_2 \bullet 4H_2O$ seed crystals (1g). As a result of the seeding considerable precipitation was observed after the solution was chilled. The exact amount of precipitation is difficult to determine. Due to high moisture content the crystals begin to re-dissolve when they are separated from the leach liquor and traditional drying methods (e.g. oven drying at 105°C) are unusable due to the low melting point of $Ca(NO_3)_2 \bullet 4H_2O$ (42.7°C). This makes the determination of the mass of the precipitated crystals challenging. To measure the effectiveness of the precipitation process, the concentration of Ca in the liquor before and after precipitation is measured with ICP-OES instead. The ICP-OES analysis shows that the precipitation process removes about 65% of the Ca present from the leach liquor. It should be noted that these were simple experiments and that with specialised equipment (e.g. good agitation, homogeneous seeding, greater temperature control, etc.) the Ca removal is expected to be higher. Still, 65% removal is not insignificant and will put less strain on the subsequent solvent extraction processes.

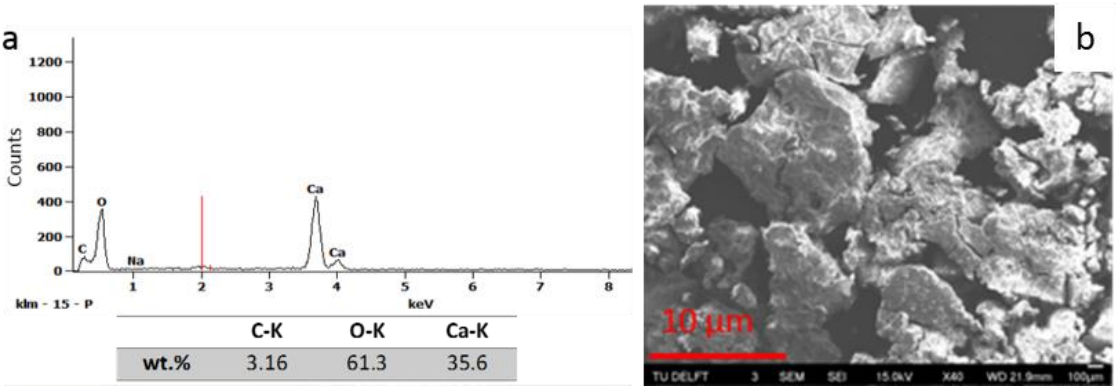

Figure 4.8: (a): EDS analysis of the precipitated crystals; **(b):** SEM analysis of the collected crystals

A small sample of the precipitated crystals was analysed with SEM/EDS to analyse the formed crystals. The results, as seen in Figure 4.8 (a), show that the crystals are quite pure. The nitrogen (signal peak K_α at 0.392 eV) cannot be accurately measured with the EDS due to the need to carbon coat the material (C signal peak K_α at 0.277 eV). The carbon coating is also the reason C is detected as a component of the spectrum. No traces of REE were detected with EDS. Some phosphorous contamination was detected (red line on the EDS spectrum), but it was minor.

It should be noted that $Ca(NO_3)_2$ is not a waste product, but rather a marketable by-product. This means that the Ca removal not only simplifies the subsequent process steps, but also helps with the economic viability of the process.

4.4.4. Extraction of REEs from the leach liquor through solvent extraction

The final step of this process is the solvent extraction, in which the REEs are recovered from the H_3PO_4 solution. This has the additional benefit of purifying the H_3PO_4 solution, yielding another valuable product stream. The organic phase of the solvent extraction uses P350, $CH_3P(O)(OC_8H_{17})_2$, as an extractant, which reacts, with kerosene as the solvent, via [9]

$$REE^{3+}_{(aq)} + NO^{-}_{3\,(aq)} + 3P350_{(org)} \rightleftarrows REE(NO_3)_3 \bullet 3(P350)_{(org)} \quad (4.9)$$

The solvent extraction presented here is still in development and the results shown here serve as a proof of concept. In order to show the robustness of the method the solvent extraction was performed on the leach liquor before the cryogenic Ca removal.

In order to successfully extract the REEs, the H_3PO_4 leach liquor is first neutralised with NH_4OH to a pH of 0.4 and mixed with KNO_3 as a salting agent. To determine the effectiveness of the salting agent trials were run with and without a salting agent. In order to show the effectiveness of the solvent extraction the concentration of the main elements before and after extraction was compared and the extraction ratios were calculated after a single step of extraction. The concentration of the main elements before extraction can be seen in Table 4.3. For clarity only 4 REEs were monitored. For the discussion below, this is considered the aqueous phase.

Table 4.3: Concentration of the main elements (ppm) of the prepared solution before solvent extraction

Ca	PO_4^{3-}	Mg	Fe	Ce	Nd	Y	Dy
51900	47700	776	357	121	62	71	10

The solvent extraction trials were run with varying amounts of aqueous leach liquor, organic solvent and extractant. The results of the solvent extraction trials can be seen in Figure 4.9. The results show that, in order to achieve single step REE extraction ratios higher than 50%, the aqueous:extractant ratio (A:E) must be greater than 1. Lower solvent volumes also appear to improve extraction rate, which can be most likely attributed to the higher relative extractant concentration in the solvent. The influence of the salting agent is also clear; the addition of a salting agent increases the extraction ratios of the REE by 5-10%.

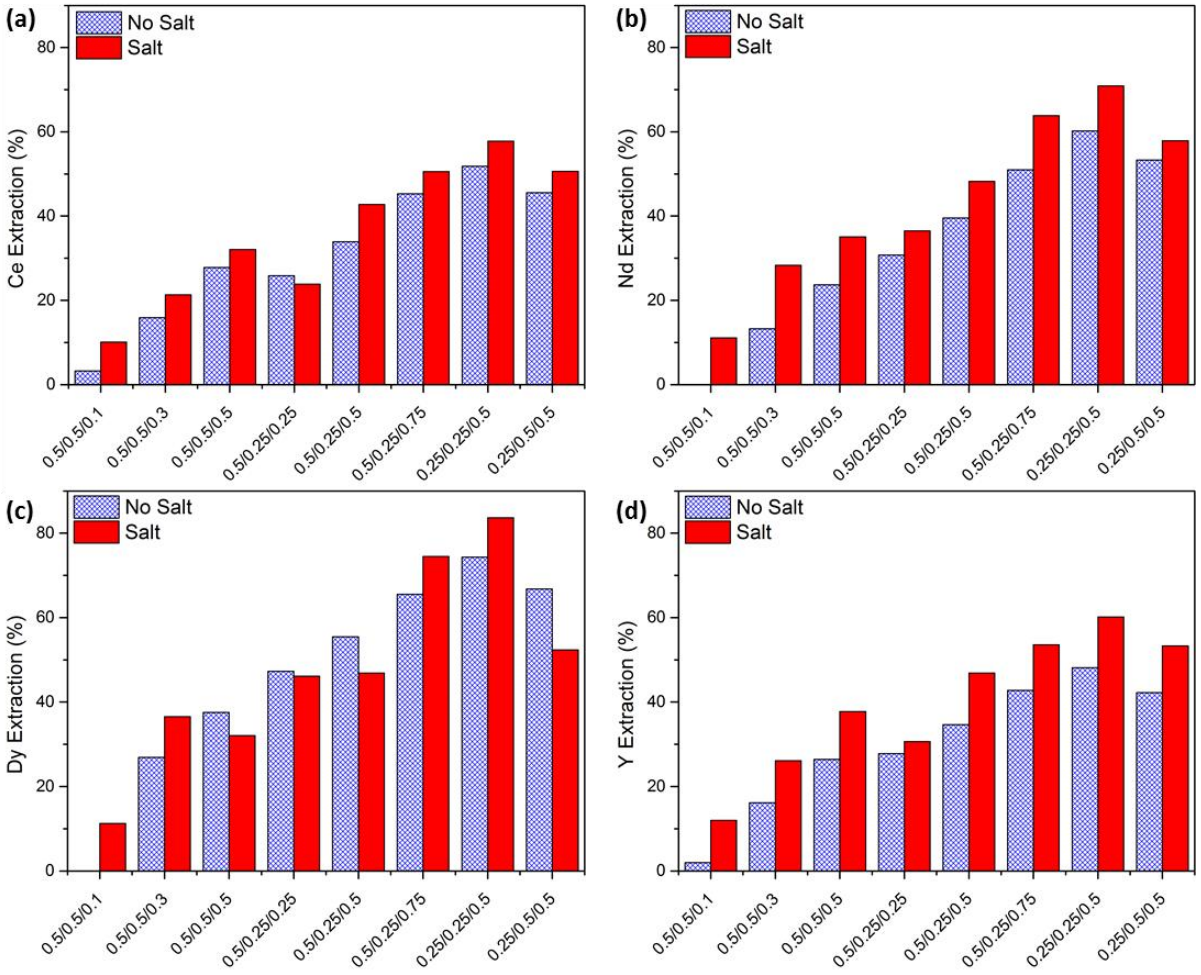

Figure 4.9: Extraction ratios of **(a)** Ce, **(b)** Nd, **(c)** Dy and **(d)** Y after a single stage extraction with P350. The extraction conditions are given as the labels on the x-axis, expressed as aqueous/kerosene/P350 volume in ml.

The optimal single step results were obtained when running the extraction with 1:3 to 1:4 aqueous:organic (A:O) ratio (organic = solvent + extractant), and a 1:2 (A:E) ratio. The detailed extraction ratios obtained at these conditions for both REEs and non-REEs can be seen in Table 4.4.

Table 4.4: Extraction ratios (%) of a single step P350 solvent extraction using varying solvent and extractant to aqueous ratios (resp. A:O and A:E) and salt concentrations (salt conc.).

(A:O)	(A:E)	Salt conc.	Extraction ratio (%)							
			Ca	PO_4^{3-}	Fe	Mg	Ce	Nd	Y	Dy
1:3	1:2	0	6.9	2.8	7.5	0	51.8	60.2	48.1	74.3
1:3	1:2	10%	9.9	6.6	15.9	12.4	57.8	70.9	60.1	83.7
1:4	1:2	0	11.9	9.9	4.9	0	45.5	53.3	42.2	66.8
1:4	1:2	10%	7.0	4.0	8.2	11.7	50.6	57.9	53.3	52.4

The use of a salting agent improves the extraction of the REEs, but also those of the impurity elements.

After the extraction experiments the REEs were stripped from the REE-loaded organic phases, using a 0.01 M HNO_3 solution and a 1:1 ratio of stripping solution to loaded organic. The stripping ratios can be seen in Table 4.5.

Table 4.5: Stripping ratios (%) of a single step P350 solvent extraction using a 1:1 ratio stripping solution to loaded organic. A:O, A:E and Salt conc. define the conditions of the extraction stage

(A:O)	(A:E)	Salt conc.	Stripping ratio (%)							
			Ca	PO_4^{3-}	Fe	Mg	Ce	Nd	Y	Dy
1:3	1:2	0	28.9	64.0	0	0	100	100	100	76.2
1:3	1:2	10%	12.6	15.7	0	0	88.7	84.3	81.9	66.6
1:4	1:2	0	8.1	7.7	0	0	99.5	100	96,3	66.9
1:4	1:2	10%	10.1	10.3	0	0	76.0	76.4	71.4	75.9

The results show that the use of a salting agent, added during the extraction stage, has an adverse effect on the stripping behaviour, as the stripping rates of all elements are reduced when using a salting agent. The absence of a salting agent allows for over 95% of the REEs (except Dy) to be stripped from the organic phase.

Analysing the concentration of the aqueous strip solution, shown in Table 4.6, reveals that, while the Ca and PO_4^{3-} concentrations are greatly reduced (initial Ca concentration was 51900 ppm and $PO4^{3-}$ 44700 ppm), Ca and PO_4^{3-} are still the main components of the strip solution. This shows that single stage solvent extraction is not sufficient to achieve separation and that multistep extraction will be necessary. Single stage extraction is effective in achieving separation from Fe and Mg.

Note that after stripping the extracted Fe and Mg remain bonded to the organic phase. While this does not influence the extraction and stripping of REEs, it does mean that these elements will need to be removed from the organic phase to regenerate it. The regeneration of the organic phase was not investigated here, but will be a point of interest for future upscaling studies.

Table 4.6: Concentrations of elements (ppm) in the end solution after stripping

(A:O)	(A:E)	Salt conc.	Final concentrations in stripping solution (ppm)							
			Ca	PO_4^{3-}	Fe	Mg	Ce	Nd	Y	Dy
1:3	1:2	0	1030	852	0	0	63.9	41.5	34.7	5.8
1:3	1:2	10%	614	468	0	0	63.2	43.5	38.0	6.0
1:4	1:2	0	501	361	0	0	55.0	42.6	29.0	4.6
1:4	1:2	10%	352	185	0	0	47.4	32.1	29.3	4.3

Before considering multistep extraction, first the optimal combination of extraction and stripping must be determined. This is done by combining the results of the single stage extraction and stripping experiments into a final extraction ratio for each element. These combined results as can be seen in Table 4.7.

Table 4.7: Final extraction ratios (%) of the combined extraction and stripping of the single stage solvent extraction process

(A:O)	(A:E)	Salt conc.	Final recovery ratios (%)							
			Ca	PO_4^{3-}	Fe	Mg	Ce	Nd	Y	Dy
1:3	1:2	0	1.99	1.79	0	0	52.8	66.9	48.9	57.9
1:3	1:2	10%	1.18	0.98	0	0	52.2	70,1	53.5	59.9
1:4	1:2	0	0.97	0.76	0	0	45.4	68.7	40.8	45.7
1:4	1:2	10%	0.68	0.39	0	0	39.2	51.8	41.3	42.8

From these results the optimal extraction and stripping conditions found during the experiments were an A:O of 1:4 and an A:E of 1:2, without using a salting agent. These parameters yield a separation process which has relatively high (single stage) REE extraction, while keeping the relative impurity level minimal. While running the solvent extraction with a salting agent has higher extraction rates during extraction, the negative impact of the salting agent on the stripping step outweighs the added extraction from the aqueous phase.

As single step extraction does not achieve the level of separation that is required to produce a high quality REE product, multistage extraction must be considered. The effect of multistage extraction can be extrapolated from the single stage data. Using

$$(Q_{aq})_n = (\frac{c_{aq,1}}{c_{aq,0}})^n \tag{4.10}$$

where $c_{aq,1}$ is the concentration of an element in the aqueous phase after 1 stage of extraction and $c_{aq,0}$ is the concentration of an element in the aqueous phase before extraction, it is possible to calculate the theoretical distribution Q_{aq} of an element in the aqueous phase before and after n stages of extraction.

Applying this formula to the data of optimal conditions found in the single stage extraction experiments and setting $(Q_{aq})_n$ to 0.001 (=99.9% extraction rate) gives the n-values for the REEs given in Table 4.8.

Table 4.8: Theoretical number of stages required to achieve 99.9% REE extraction, rounded up to the nearest integer

Ce	Nd	Dy	Y
6	5	4	7

These values show that 7 stage extraction would be required to extract 99.9% of all REEs from the leach liquor for a solvent extraction process using P350, with parameters (A:E) = 1:2 and (A:O) = 1:4 and no salting agent. Taking into account the stripping efficiency these conditions would also lead to a Ca extraction of 4% and a P extraction of 3.5%. Due to the high Ca and P concentration in the leach liquor however this still represents a considerable Ca and P concentration in the end liquor (2076 ppm and 1670 ppm respectively). The solvent extraction process of 7 stages and 1 stripping stage should be repeated 4 times to reduce the Ca and P concentration to less than 1 ppm (0.13 ppm Ca and 0.07 ppm P).

Based on these results a multi-stage solvent extraction process can be built to separate and recover the REE from the H_3PO_4 solution with little loss to the PO_4^{3-}. This method also shows good selectivity towards Ca separation, even at high Ca concentrations. This means that, while valuable, the cryogenic Ca removal is not required to separate the REEs from the Ca and H_3PO_4.

4.4.5. Constructing the process flowsheet for the acidic leaching process

4.4.5.1. The flowsheet

The final step is linking all these process steps together and constructing a flowsheet to represent the REE recycling process from start to finish. The constructed flowsheet is shown in Figure 4.10, with the process steps discussed above highlighted with the dashed box. The processes leading to the dashed box were developed by LTU as discussed in chapter 3 and the processes following the dashed box are to be further developed by our project partner at TU Delft for the production of REE metal.

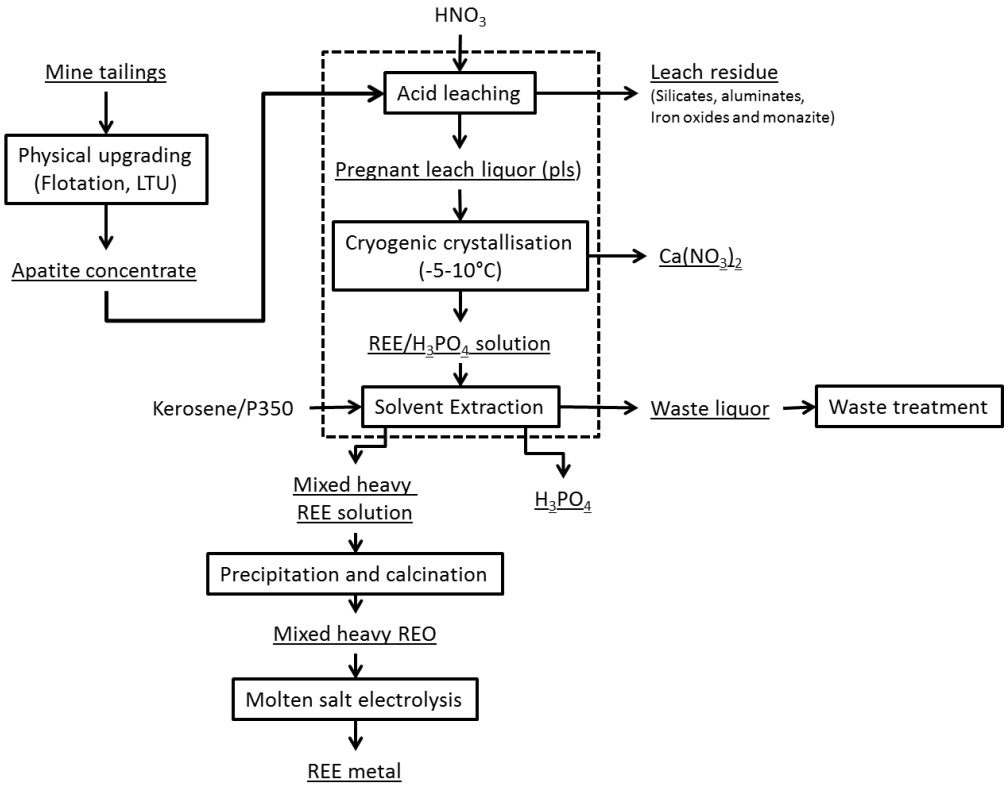

Figure 4.10: Flowsheet from the REE recycling process using the acidic leaching approach

The proposed flowsheet offers a process which effectively recovers the heavy REEs and the phosphorous from the mine tailings. Starting from physical upgrading with flotation, the REEs and phosphorous are collected in an apatite concentrate. This concentrate is then digested in acid to transfer the heavy REEs and phosphorous into solution from which they can then be separated through solvent extraction. The REE solution is then sent for further processing to produce REE metal, through precipitation and calcination to form REO and finally molten salt electrolysis to convert the REO to REE metal.

One remaining challenge this process faces is the light REEs that are not extracted during the acidic leaching process. While the light REEs do not have the inherent value of the heavier ones, it would be prudent to not discard them. As it stands, the process produces a leach residue that represents 5 wt.%

of the concentrate, which contains the majority of the light REEs in the form of monazite. This residue can, in the future, serve as a REE resource and should thus be stockpiled properly. As monazite is an ore which the primary industry works with the technology to extract REE from monazite exists, but at present the value contained with the residue does not warrant its use.

4.4.5.2. Waste management

Consideration must also be given to the management of the waste products that are produced during the hydrometallurgical part of the flowsheet (dashed box in Figure 4.10). Two main waste streams are being produced: (1) the leach residue and (2) the waste liquor from the solvent extraction. The leach residue can be managed in one of two ways: either it is stockpiled as a monazite resource for later processing or it is dumped back into the tailings pond. Stockpiling would be the ideal solution, however, this does place an economic burden on the process that may not yield returns in the short term. Dumping the leach residue back into the tailings pond is also viable, as no new pollutants are introduced to this residue compared to the original tailing (assuming the residue was washed properly, and no residual acid remains).

Managing the waste liquor of the solvent extraction will pose a greater challenge. This solution still contains a considerable amount of HNO_3 (25 g/L) and Ca (50 g/L), as well as minor amounts of Fe and Mg. The high concentration of Ca and HNO_3 prevents the use of traditional waste water treatment. Two potential routes can be investigated to manage this waste liquor: (1) an additional solvent extraction step to remove all metal cations from the HNO_3 and (2) crystallising the solution to produce impure anhydrous $Ca(NO_3)_2$.

By adding more solvent extraction steps to the process to remove the metal cations from the solution a pure HNO_3 solution is retained, which can be re-used in the leaching operation. This does leave an organic phase loaded with Ca, Fe, and other trace elements. The organic must be regenerated in order to be re-used, and the metal cations must therefore be stripped from it. This stripping should be performed with a large volume of wash water, thereby minimising the concentration of metal cations is the resulting waste water. This waste water can then be sent to water treatment together with the other wash waters (this will be discussed below).

For the crystallisation, first stoichiometry should be established between Ca and NO_3^- (this can be done by adding either $Ca(OH)_2$ or HNO_3). Then, the solution should be heated to above 151°C (the decomposition temperature of $Ca(NO_3)_2 \bullet 4H_2O$ at 101.3 kPa [10]). This will boil off the water of the solution and produce anhydrous $Ca(NO_3)_2$ crystals, which be lightly contaminated with Fe and Mg. This process will be quite energy intensive, but will also decrease the load of the water treatment. It will also produce another possible marketable by-product (assuming the contamination of Fe and Mg are not too high).

Besides these two main waste streams there is also the wash water that is used in the filtration of both the leach residue and $Ca(NO_3)_2$ to consider. Wash waters are generally highly diluted streams with low levels of hazardous components. For hydrometallurgical processes these hazardous components are most commonly leftover acid and metal cations. Traditionally this waste water is processed by: (1) neutralisation the leftover acid, (2) precipitation the metal cations (e.g. via hydrolysis with NaOH or CaO or via sulphide precipitation with H_2S or NaHS), (3) sedimentation of the insoluble compounds in large settling basins and (4) filtration of the overflow of the basins to obtain water clean enough to be discharged into the environment [11]. This general waste water processing strategy should be

applicable to the wash water produced during this process, but the presence of HNO_3 requires attention. The nitrate anions require a specific treatment: biological denitrification. Biological denitrification is a process in which heterotrophic organisms assist in the decomposition of nitrates via

$$6NO_3^- + 5CH_3OH \rightarrow 3N_{2(g)} + 6OH^- + 5CO_{2(g)} + 7H_2O \quad (4.11)$$

in the presence of a biodegradable organic compounds (e.g. acetic acid, methanol, etc.) and in anaerobic conditions [12]. This reaction (4.11) breaks down the nitrate anions and removes nitrogen from the system as N_2 gas. The necessity of the biological waste treatment process makes the waste treatment more complex, as well as more time consuming (it can take more than 30 days to reduce the nitrate concentration to dischargeable levels (more than 10 mg/L) [13]). Besides the biological denitrification, the other tradition waste water treatment steps should suffice for the produced wash water.

4.5. Alkaline conversion process for the upgraded mine tailings

The acid-based process route was developed based on a phosphorous production process, thus the achieved phosphorous recovery was high (over 95%, with ~4% loss during solvent extraction). However, only the heavy REEs responded well to the acidic process, and more than half the light REEs were not recovered (see figure 4.3). Because of this an alternative process route was investigated, based on the REE production process used in primary industry. The goal of this process is to use NaOH to convert the monazite, which does not dissolve during the acid process, to REE hydroxide (equation 4.4). The formed REE hydroxides are known to easily dissolve in strong acids, making more efficient recovery of the REEs possible. As discussed in section 4.2, the expected side reactions (equations 4.5-4.7) would also make it possible to recover the phosphorous with a water washing after alkaline conversion before the REE hydroxides are leached with a strong acid. A weak acid pre-leach after washing should selectively dissolve the Ca compounds, simplifying the REE purification in the following process steps.

As the primary industry uses very aggressive conditions during the NaOH conversion (60-70 wt.% NaOH / 200 °C / 3 bar), the preliminary tests were done using a 50 wt.% NaOH solution, a process temperature of 105°C and a reaction time of 24 h. These conditions are near the limit of what can be achieved under atmospheric conditions with non-specialised equipment. After conversion the residue was filtered and dried. It should be noted that the filtration was quite challenging, as the end solution was very “thick” and viscous sludge. XRD analysis of the residue shows the following new phases: $Ca(OH)_2$, Na_3PO_4, Na_2CO_3 and Na_2HPO_4, which indicates that the predicated side reactions (equations 4.5-4.7) did take place. Some leftover apatite was still detected, meaning that the conversion was not 100% complete.

SEM analysis of the residue, see Figure 4.11, reveals a new REE phase in the form of needles. These needles appear to be imbedded/covered by a Ca phase. EDS analysis of the needles show that they contain REEs, oxygen, and no phosphorous, which suggests that these needles are REE hydroxides.

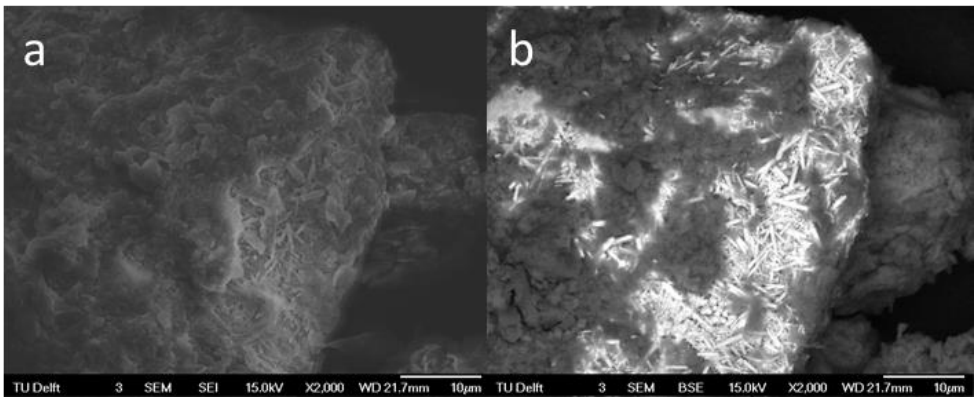

Figure 4.11: SEM NaOH conversion residue. **(a):** SEI mode; (**b):** BSE mode

When this residue is washed with water at 75°C about 60% of the residue dissolves. XRD analysis of the wash residue shows that all Na compounds have been washed away, but also reveals a substantial apatite signal. This combined with the chemical analysis of the wash water shows that not all P has been extracted and suggests that the apatite fraction after conversion is not insignificant.

After the water wash the residue is pre-leached with 50 vol.% CH_3COOH to remove the $Ca(OH)_2$. The pre-leach successfully removes the $Ca(OH)_2$ from the wash residue and the XRD analysis shows that the primary phase left is apatite. The SEM analysis of the residue is shown in Figure 4.12. It indicates that the Ca-phase that surrounded the REE hydroxide is now removed, revealing clusters of needles and nodules. An interesting observation is that the nodules and needles have a slightly different composition; the needles contain primarily Ce, while the nodules contain La and Nd.

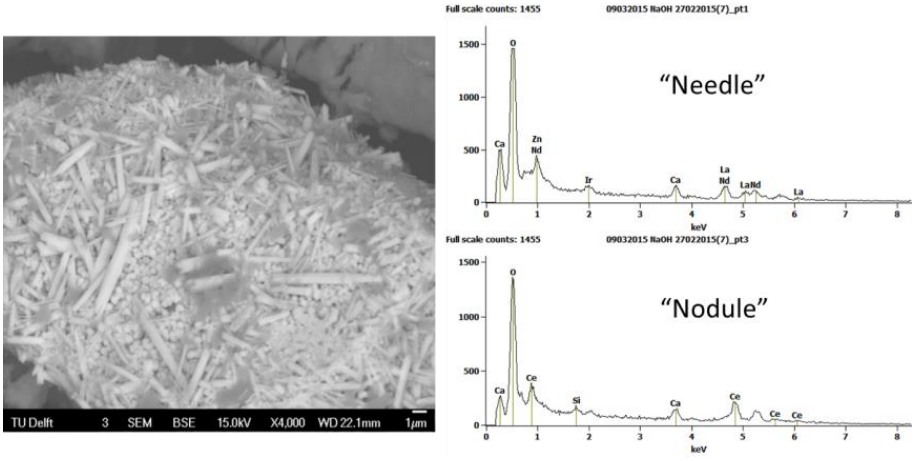

Figure 4.12: SEM BSE image of residue after CH_3COOH pre-leach

Finally, the pre-leach residue is leached with HNO_3 to digest the REE hydroxides. Analysing the leach residue shows that only 30-35% of the REE have been recovered by this leach process, which was unexpected. SEM analysis (Figure 4.13) of the residue reveals the reason for this: there still exists monazite in the residue, meaning that the conversion was incomplete.

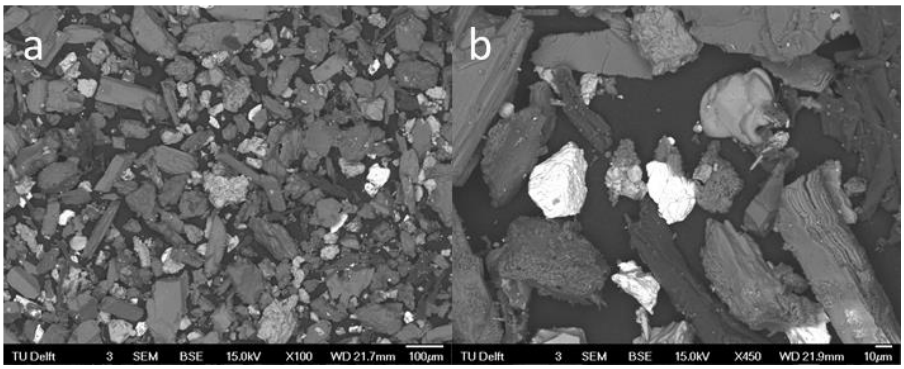

Figure 4.13: SEM BSE image residue after HNO_3 leaching. **(a):** overview; (**b):** zoom on REE particle

However, no monazite was initially observed during the analysis of the other residues. Re-analysing the pre-leach residue reveals the reason for this. Figure 4.14 shows a fractured REE particle observed during the analysis of the pre-leach residue. This particle shows that the formed REE hydroxides adhere to the surface of the monazite particles, effectively forming a barrier which reduces the rate of reaction. As these $REE(OH)_3$ scales completely envelop the monazite this explains why no monazite was found initially, but once the REE hydroxides were dissolved by the HNO_3 the underlying monazite is revealed.

This means that the NaOH conversion is not very effective under these conditions. Due to the scale formation on the monazite particles the reaction kinetics are extremely slow. The presence of apatite introduces a lot of additional complications, and a vast amount of NaOH and energy are required to fully convert the residue. Overall the potential for success with this process route is low and it will not be further explored in this form.

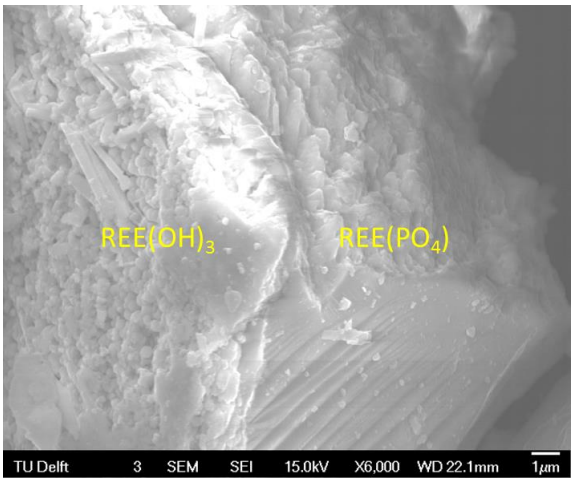

Figure 4.14: SEM image fractured particle from the CH_3COOH pre-leach showing the formation of a $REE(OH)_3$ scale on a monazite particle

4.6. Combination of the acidic and alkaline processes

While the NaOH conversion process applied to the apatite did not yield satisfactory results, the fact remains that monazite conversion is possible with NaOH. We also know that we can produce a monazite concentrate without apatite through the developed acidic process, see figure 4.3. While the monazite residue produced during the acidic process is depleted of its heavy REE, that is only the case

when the apatite concentrate is leached with a large excess of acid. If the acid leaching process is modified to leach with a stoichiometric amount of HNO_3 most of the REEs would report to the residue (see Figure 4.3), while the phosphorous is still extracted as H_3PO_4. The residue that would be produced now would only represent 5 % of the input mass, yet it would contain nearly all REEs. This reduction in mass also means that more aggressive methods can now be employed to convert the monazite, as the energy consumption per kg of apatite concentrate would be drastically lower than the previous conversion process. The acid economy of the overall process would also be improved, as no large excess of acid would be required.

4.6.1. Producing the monazite concentrate

The first step in the combined process is the leaching of the apatite concentrate with HNO_3 to extract the phosphorous and produce a REE rich residue. The goal is to minimise the amount of co-extracted REE, thus the apatite concentrate was leached with a slightly less than stoichiometric (based on the available Ca: 137.5 ml HNO_3/100 g apatite concentrate) amount of HNO_3. The process was performed with 200 g of apatite concentrate that was leached with a 600 ml (27.1% HNO_3) solution at room temperature.

The analysis of the leach liquor shows that under these conditions only 2.5-5% of the REEs was leached from the apatite concentrate. This shows that the pre-treatment was successful in concentrating the REE in the remaining residue. Analysis of the residue, see Table 4.9, shows a significant upgrade in REE concentration, between 14 and 16 times, in the residue, which was the goal of the process. The other major component in Fe which originates from the traces of magnetite left in the tailings.

Table 4.9: chemical composition (wt.%) residue after HNO_3 pre-leach

	Fe	Si	PO_4	Ca	Mg	Al	Cu
wt.%	21.5	14.8	7	7	5.6	2	0.37
σ	1.4	0.5	0.8	0.3	0.2	0.2	0.07
	Ce	**Eu**	**La**	**Nd**	**Pr**	**SUM REE**	
wt.%	2.9	0.61	0.93	1.2	0.34	6.0	
σ	0.4	0.06	0.03	0.3	0.03	0.5	

4.6.2. NaOH conversion of the monazite concentrate in a furnace

The next step in the combined process is converting the monazite in the leach residue to $REE(OH)_3$. As the previous experiments have shown, this is a kinetically unfavourable reaction. Thus, in order to overcome the inhibiting effect of the scaling more reactive conditions were utilised.

A 2 g batch of leach residue was mixed with 6.5 g of NaOH and 3.5 ml of water to form a 65 wt.% NaOH solution. This mixture was transferred into a Ni crucible and placed in an oven at 160°C for 12 hours. This creates reaction conditions which more closely resemble the conditions under which monazite is processed in primary industry.

Figure 4.15: Ni crucible used in NaOH conversion process after conversion

When the crucible was removed from the furnace (Figure 4.15) a solid mass is recovered. It proved difficult to remove the mass from the crucible, thus the crucible and the mass within were placed in a water vessel to wash away Na compounds. The water wash was performed with 100 ml H_2O at room temperature for 24 h. Analysis of the wash water (Table 4.10) shows that Al, Si and P are partially removed during the washing stage (Na was not analysed due to its extremely high concentration). No other elements were detected in the wash water.

Table 4.10: ICP-OES analysis of wash water

	Si	PO_4	Al
g/L	0.34	0.16	0.060
σ	0.02	0.04	0.004

4.6.3. Leaching the converted monazite concentrate

After washing, the remaining residue is leached with concentrated HCl (37 wt.%) at L/S = 10 for 6 h at room temperature (HNO_3 was unavailable for this experiment, but results are expected to be the same). Chemical analysis and the calculated extraction ratios of the resulting leach liquor are shown in Table 4.11 and 4.12.

Table 4.11: Chemical composition (g/L) of the leach liquor

	Fe	Si	PO_4	Ca	Mg	Al	Cu
g/L	16.1	0.01	0.8	4.1	3.4	0.5	0.26
σ	0.4	0.005	0.1	0.1	0.1	0.2	0.01
	Ce	**Eu**	**La**	**Nd**	**Pr**	**SUM REE**	
g/L	2.3	0.559	0.705	6.4	0.253	10.2	
σ	0.2	0.001	0.005	0.01	0.001	0.2	

Table 4.12: Extraction (%) of main elements after acid leach

	Fe	Si	PO_4	Ca	Mg	Al	Cu
Extraction (%)	75	0.07	12	59	60	29	72
σ	5	0.04	2	3	3	10	13
	Ce	**Eu**	**La**	**Nd**	**Pr**	**SUM REE**	
Extraction (%)	80	92	76	53	80	381	
σ	12	9	3	12	7	21	

The analysis shows that the new conversion conditions are greatly improved over the previous ones, yet the REE extraction is not a 100%. This could be attributed to the presence of other REE minerals that were not yet previously identified. Mineralogical studies conducted on the apatite concentrate by our project partners at LTU [14] have recently uncovered two other minor REE phases: allanite and titanite. The behaviour of these two phases is currently unknown, but they could account for the leftover REE in the residue.

SEM/EDS analysis of the REE particles present in the final residue, see Figure 4.16, reveals that the presence of allanite, $(REE,Ca)_2(Al,Fe^{3+})_3(SiO_4)_3(OH)$, is a strong possibility. As XRD on individual particles is not possible the identification was based on the elements identified with EDS analysis.

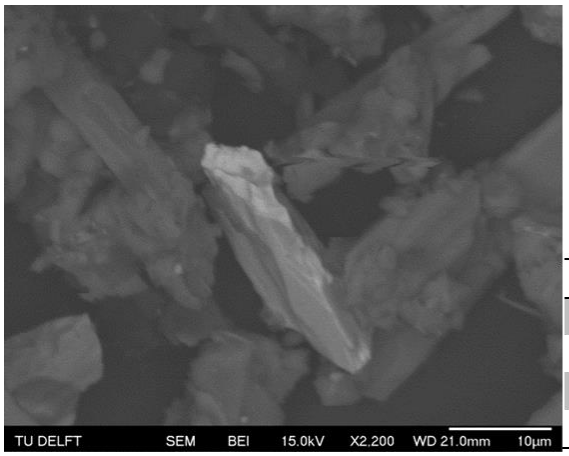

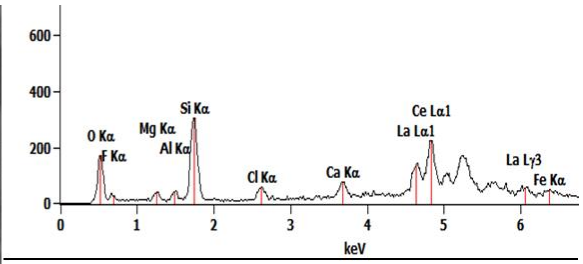

Wt.% measured with EDS				
O-K	**F-K**	**Mg-K**	**Al-K**	**Si-K**
8.77	0.85	1.34	1.11	12.2
Cl-K	**Ca-K**	**Fe-K**	**La-L**	**Ce-L**
1.92	2.22	3.21	16.1	52.4

Figure 4.16: SEM/BSE image and EDS analysis a probable allanite particle (bright particle in the image) present in the final leach residue after HCl leaching.

The observed allanite particle appear unaffected by both the NaOH conversion and the HCl leaching process, lending strength to theory that there is a second REE phase that is not extracted with the NaOH conversion process. The other possible phase, titanite, was not detected during the analysis.

Further SEM/BSE analysis of the leach residue reveals the allanite particles are not the sole remaining REE particles. Figure 4.17 reveals the presence of quite large, partially reacted, REE phosphate particles.

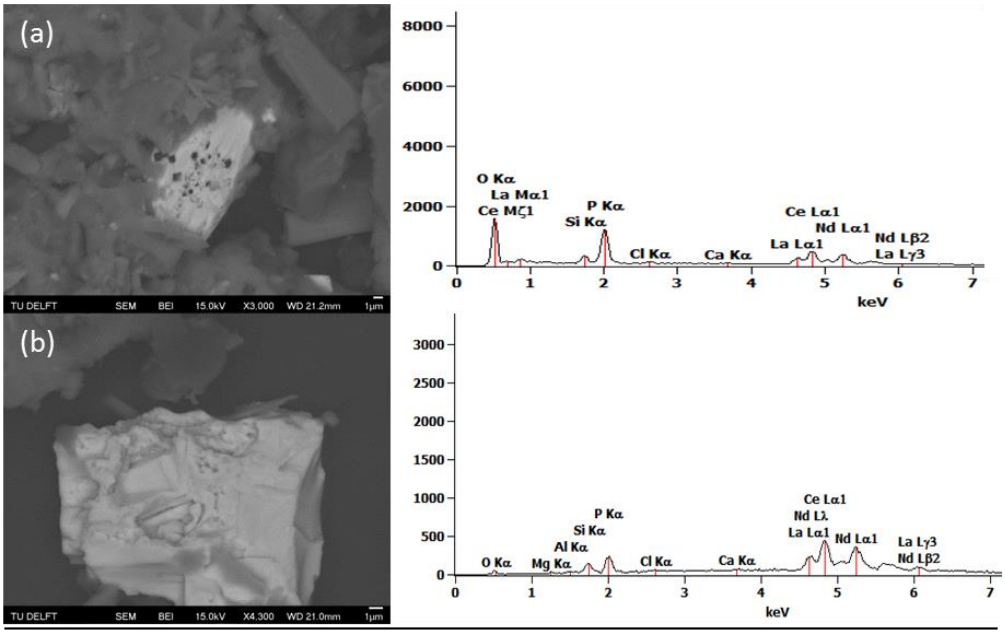

Wt.% measured with EDS

	O-K	Mg-K	Al-K	Si-K	P-K	Cl-K	Ca-K	La-L	Ce-L	Nd-L
a	24.3	0.0	0.0	2.68	14.8	0.83	0.47	10.8	38.0	8.22
b	1.51	0.58	0.21	3.01	5.95	0.62	0.64	16.5	54.9	16.1

Figure 4.17: SEM/BSE image and EDS analysis of large, partially reacted, REE phosphate particles present in the final leach residue after HCl leaching.

Ordinarily REE phosphates would be identified as monazite. However, EDS analysis does show the presence of Si in all remaining REE particles found in the residue. Si is not an element that is associated with monazite and its presence may have an influence on the conversion and dissolution behaviour of the REE particles present in the monazite residue. Reviewing literature on REE minerals no clear candidate was found for the identity of a Si bearing REE phosphate (or P bearing REE silicate). Based on the images (Figure 4.17 (a) and (b)) of the surface of these particles, it is clear that these particles have undergone at least partial dissolution. This indicates that Si likely has an inhibiting effect on the NaOH conversion.

Next to the REEs, the other extracted components are primarily Ca, Mg and Fe. The extraction of these elements means that a solvent extraction process will be required to further purify the REEs.

4.6.4. Constructing a combined flowsheet

4.6.4.1. The flowsheet

Although the REE recovery of the new conversion process is not 100%, the process does recover 75-80% of the REEs in the monazite concentrate, meaning that when looking at total REE recovery it is superior to the acidic process. Also, in terms of phosphorous recovery less acid per kg of concentrate is required to produce the H_3PO_4. The primary advantage of this process is that the energy and chemical intensive processes now only need to be performed on 5% of the input material. The process itself is also less influenced by the REE market, because the REE residue can be easily stockpiled for later processing, while H_3PO_4 production is maintained.

The flowsheet for the proposed combined process is shown in Figure 4.18.

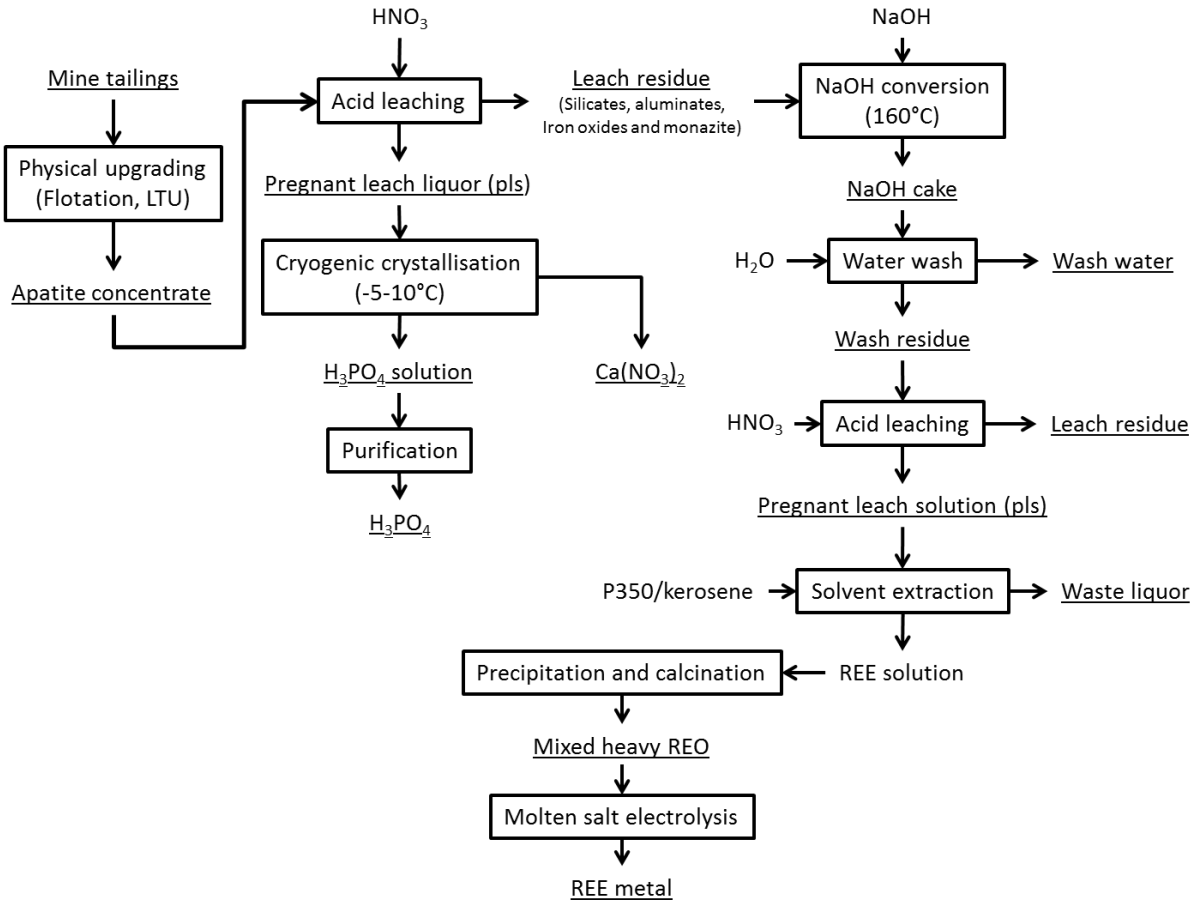

Figure 4.18: Flowsheet that combines acidic and alkaline processes to extract H_3PO_4 and REEs from the apatite concentrate

4.6.4.2. Waste management

For the waste management of the combined acid-alkaline process, the waste treatment options proposed for the acidic flowsheet (see section 4.4.5.2) are also valid, with some modifications. This process has two types of wash water, one nitrated and one alkaline. The nitrated wash water from the solvent extraction step should be treated as was discussed in 4.4.5.2., i.e. by biological denitrification followed by traditional water treatment.

The alkaline wash water can be eliminated as waste stream by a small modification of the process flowsheet. The water used to prepare the initial NaOH solution (for the conversion process) evaporates in the furnace. With a condenser setup added to the furnace the evaporated water can be recovered and used for the washing process. After washing, the water can be used to prepare the NaOH solution for the next batch operation. This has the added benefit of recuperating part of the NaOH that has been dissolved into the wash water after washing. Figure 4.19 shows of the proposed modification to the flowsheet shown in Figure 4.18.

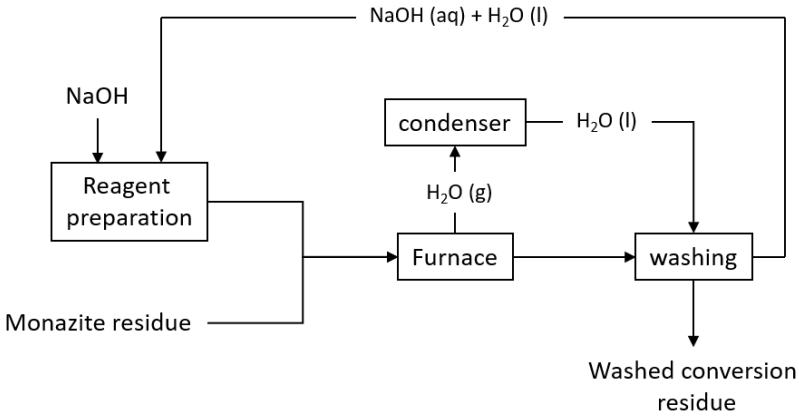

Figure 4.19: Proposed modification to the first and second step in the alkaline part of the combined acid-alkaline flowsheet to minimise the amount of alkaline waste water

Further research is required to validate the proposed modification, with a focus on the water balance of the process and the influence accumulation of impurities in the wash water.

For the solvent extraction waste liquor, the option of running additional solvent extraction processes to produce reusable HNO_3 is more viable than the crystallisation of anhydrous $Ca(NO_3)_2$. This is due to the drastically lower Ca content in this part of the flowsheet.

4.7. Conclusions

Based on the analyses of the obtained experimental results the following conclusions can be drawn:

- At least two REE phases are present within the apatite concentrate: apatite and monazite. A small amount of REE particles that have chemical composition similar to allanite were found as well.
- Full apatite dissolution can be achieved through acid leaching with either HCl or HNO_3. This leads to near total (more than 99%) phosphorous recovery from the apatite as H_3PO_4.
- The REEs associated with the apatite are only extracted if a large excess (150%) of acid is used. Otherwise the dissolved REEs re-precipitate due to reaction with PO_4^{3-}.
- The monazite dissolves in neither concentrated HCl nor HNO_3 under atmospheric conditions.
- The REEs associated with the apatite have a higher fraction of heavy REEs than those associated with the monazite.
- The choice of acid (HCl or HNO_3) does not influence the REE extraction behaviour. HNO_3 is chosen as the leachant for the developed flowsheet due to the possibility of $Ca(NO_3)_2$ recovery and easier solvent extraction.
- 65 % of the dissolved Ca can be recovered as $Ca(NO_3)_2$ by cooling the solution to −20°C, without incurring REE losses.
- Solvent extraction using P350 successfully recovers the REEs from the leach liquor. To achieve 99.9% REE recovery 7 extraction stages and one stripping stage are required. To reduce the impurities (Ca, P) to less than 1 ppm the entire process (7 extraction stages and 1 stripping stage) should be repeated 4 times.
- The alkaline conversion route is not successful in recovering the REEs. The cause is attributed to the formation of $REE(OH)_3$ scales on the monazite surface, effectively passivating the monazite.

- A combined acid - alkaline leaching process proved to result in the highest REE recovery. By leaching the apatite concentrate with diluted HNO_3 it is possible to concentrate the REEs into the leach residue, while recovering the phosphorous as H_3PO_4. This leach residue can be treated with NaOH at 160°C in a furnace to convert the monazite to $REE(OH)_3$ which can be dissolved in concentrated HNO_3 (or HCl).
- NaOH conversion at 160°C has a high conversion rate, but Si containing REE phosphates and possible allanite particles were detected in the final leach residue.

References

[1] A. Jarosiński, J. Kowalczyk, and C. Mazanek, “Development of the Polish wasteless technology of apatite phosphogypsum utilization with recovery of rare earths”, J. Alloys Compd., Vol. 200, pp. 147–150, 1993.

[2] “VWR® Thermal Shake Touch.” [Online]. Available: https://us.vwr.com/store/product/9146319/vwr-thermal-shake-touch-with-1-5ml-block#. (retrieved 28/02/2018)

[3] B. S. Hopkins, “Chemistry of the rarer elements”, D.C. Heath and company, 1923

[4] N. Krishnamurthy and C. K. Gupta, “Extractive metallurgy of rare earths”, CRC press, 2004.

[5] A. M. T. S. Bandara and G. Senanayake, “Leachability of rare-earth, calcium and minor metal ions from natural Fluorapatite in perchloric, hydrochloric, nitric and phosphoric acid solutions: Effect of proton activity and anion participation”, Hydrometallurgy, vol. 153, pp. 179–189, 2015.

[6] D. Beltrami, G. J.-P. Deblonde, S. Bélair, and V. Weigel, “Recovery of yttrium and lanthanides from sulfate solutions with high concentration of iron and low rare earth content,” Hydrometallurgy, 2015.

[7] F. T. Nielsson, “Manual of Fertilizer Processing”, New York: Marcel Dekker inc., 1987.

[8] S. Peelman, Z. H. I. Sun, J. Sietsma, and Y. Yang, “Leaching of rare earth elements: review of past and present technologies”, in *Rare Earths Industry technological, economic and environmental Implications,* Elsivier, pp 319-334, 2016.

[9] H. Li, F. Guo, Z. Zhang, D. Li, and Z. Wang, “A new hydrometallurgical process for extracting rare earths from apatite using solvent extraction with P350,” J. Alloys Compd., vol. 408–412, pp. 995–998, 2006.

[10] Ullmann’s Encyclopedia of Industrial Chemistry, Volume A 17 Naphthalene to Nuclear Technology, pp. 278, ISBN: 0-89573-167-3, 1988.

[11] European IPPC-Bureau, “Best Available Techniques in the non-ferrous metals industries”, Gent, Academia Press, 2001.

[12] Ullmann’s Encyclopedia of Industrial Chemistry, Volume B 8 Environmental protection and industrial safety II, pp. 34, ISBN: 3-527-20138-6, 1995.

[13] S. E. Jørgensen, “Industrial Waste Water Management”, Studies in Environmental Science 5, Elsevier, ISBN: 0-444-41795-8, 1979.

[14] C. Wanhainen, B. I. Palsson, and O. Martinsson, “Rare earth mineralogy in tailings from Kiirunavaara iron ore, northern Sweden: Implications for mineral processing,” Miner. Metall. Process., vol. 34, no. 4, pp. 189–200, 2017.

Chapter 5: Microwave-assisted pressure leaching of the apatite concentrate

Abstract

In order to develop a process to efficiently extract the REEs from the undissolved monazite of the apatite concentrate, microwave-assisted leaching was explored. Microwave-assisted leaching has found success in the processing of other difficult to leach minerals, such as gold ore and chalcopyrite, and can offer new process routes for the extraction of REEs from monazite. Both acidic and alkaline leaching systems were investigated and the acidic leaching system using H_2SO_4 has proven to be more effective.

However, based on observations during the leaching experiments it was concluded that the improved leaching of REEs from monazite was not primarily caused by the microwave irradiation. Rather the improved leaching behaviour is attributed to the achieved temperature and pressure in the reaction vessel.

By utilising the rapid heating of the microwave reactor, leaching conditions of 200°C and 9 bar internal pressure were achieved in the leaching vessel within minutes and by maintaining these conditions for 2 h REE extraction rates of 80 to 90% were achieved. This makes the microwave-driven autoclave process superior to the alkaline conversion process, not only in REE extraction, but in process time and energy consumption as well. Based on the findings a redesigned flowsheet can be proposed as shown below.

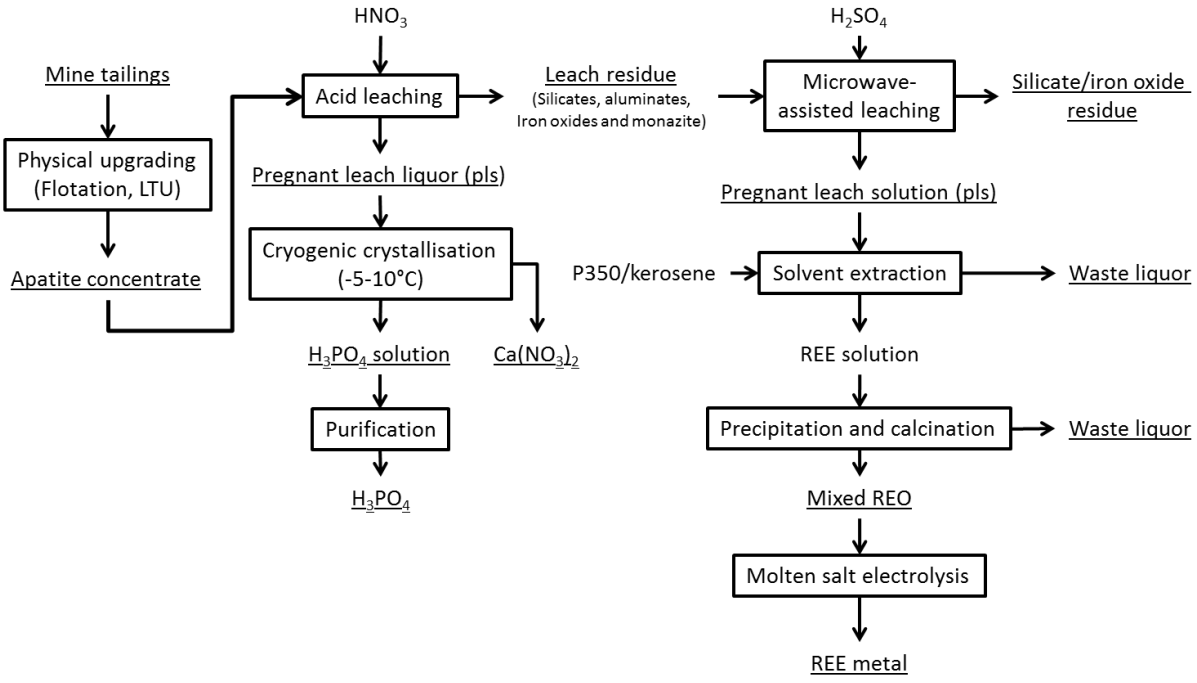

Figure 5.1: Redesigned flowsheet employing microwave-assisted pressure leaching to extract the REE from the leach residue produced by the H_3PO_4 production step

5.1. Introduction

Microwave-assisted leaching is, as the name implies, a leaching system in which the heating method is microwave irradiation. Microwaves are a form of electromagnetic radiation, with a frequency between 300 MHz and 300 GHz, which can be reflected, transmitted or absorbed by materials. How a material interacts with microwaves is determined by its dielectric properties, i.e. its dielectric constant ε_r and its loss tangent $tan(\delta)$. The dielectric constant determines how transparent a material is to microwaves (i.e. whether they transmitted or absorbed) and the loss tangent characterises a material's ability to store and release energy as heat. These two parameters are often combined as the dielectric loss factor ε'', which is defined as $\varepsilon'' = \varepsilon_r tan(\delta)$. The higher the dielectric loss factor the more the material absorbs microwaves and releases the absorbed energy as heat. This heat is the result of the dipolar molecules of the material continuously aligning themselves with the rapidly varying electrical field of the microwaves, which causes friction within the material and produces heat. The generated temperature increase ΔT can be related to absorbed power density P_d via

$$P_d = k * f * E_0^2 * \varepsilon^{"} \tag{5.1}$$

with $k = 2\pi\varepsilon_0$ a constant (ε_0 is the permittivity of vacuum), f the frequency of the microwaves and E_0 the magnitude of the electric field of the microwaves. Only ε'' is a material property, and it determines the degree in which a material can be heated with microwaves [1]–[6]. The absorbed power density related to the absorbed energy E via

$$E = P_d * t \tag{5.2}$$

and the absorbed energy relates to temperature via

$$E = m * c_p * \Delta T \tag{5.3}$$

Thus the absorbed power density can converted into a temperature increase via

$$\Delta T = \int \frac{P_d}{m * c_p} * t * \mathrm{d}t \tag{5.4}$$

What are the benefits of microwave-assisted leaching? First and foremost, it is an efficient and fast method of suppling heat to the leaching system. Microwave heating only heats the leaching solution and the input material, no energy is wasted on heating the reaction vessel, the equipment or the environment. Even without the other potential benefits, this makes microwave-assisted leaching a technique to be investigated. Next to being an efficient heating technique, microwave heating is reported to have two major effects on the leaching of minerals: (1) heterogeneous heating of mineral particles, and (2) breaking of reaction product layers (or scales) formed during reaction through thermal stresses.

The heterogeneous heating refers to the fact that different materials have different ε'' and thus are heated differently by microwaves. General gangue minerals like silicates have a low ε'' and are thus heated slowly (or not at all), while metal-bearing minerals[5] (e.g. Fe_2O_3) can have high ε'' and are heated rapidly. This difference in heating rate can lead to locally very high temperature (and thus high leaching

[5] Metal-bearing mineral both refers to minerals with metallic inclusions (like gold) and minerals that are formed from (transition)metals, such as hematite (Fe_2O_3). This discussion centers around the second type.

rates) around the metal-bearing particles, without wasting energy on heating the gangue minerals unnecessarily. This effect was observed in the leaching of gold-bearing minerals [5].

The breaking of reaction product layers (or scales), through thermal stresses, is an effect that is observed during the leaching of Cu from chalcopyrite. This leaching process is generally slow, due to the formation of a sulphur layer on the ore particles [2], which acts as a barrier to reaction. Due to the different heating rate of the ore and the product layer thermal stresses are generated between them, which can crack and break the inhibiting sulphur layer and allowing for it to be washed away by the agitation of the leach liquor.

How will these effects influence the leaching behaviour of the monazite residue? The residue that is left after apatite dissolution consists mainly of silicates, which are quite transparent to microwaves. Unfortunately, monazite is reported to also be quite transparent to microwaves [5], with a $\varepsilon_r = 12.34$ and $tan(\delta) = 1.19*10^{-4}$, which is only marginally higher than those of silicates [6]. This means that heterogeneous heating is unlikely to occur and that the bulk of the microwave energy will be absorbed by the liquor phase. For this reason, another potential application of microwave, the dry microwave pre-treatment, was not considered for monazite. The dry microwave pre-treatment is a process in which minerals are irradiated with microwaves before they are leached [2]. The purpose of this pre-treatment is to introduce thermal stresses and cracks into the minerals to improve their leachability. This process relies on the minerals having a high ε_r and $tan(\delta)$, however, as monazite does not have those, this pre-treatment was not considered.

The microwave effect that is of greater interest, is the scale breaking effect. The presence of the $REE(OH)_3$ scale during NaOH conversion of monazite significantly slows down the conversion process and its removal would greatly benefit the rate of the conversion process. Whether this effect will occur cannot be predicted, as there is no dielectric data available for $REE(OH)_3$ in literature.

This chapter will explore the possibilities of microwave-assisted leaching to recover the REEs from the apatite concentrate. The focus will be on the monazite residue left after apatite dissolution, as monazite is the mineral of interest for this method. Several leaching experiments will be discussed, which investigate the influence of microwaves on the extraction of REE from the monazite residue. The tested systems include acidic leaching with HNO_3 and H_2SO_4 and alkaline conversion with NaOH.

5.2. Experimental setup and equipment

The microwave-assisted leaching experiments were performed using the Anton Paar Monowave 300 microwave synthesis reactor [7]. The Monowave 300 is equipped with magnetic stirring and utilises 10 ml borosilicate glass reaction vessels, sealed with PEEK caps. When the reactor is sealed, a pressure sensor is placed on top of the phials to monitor possible pressure build-up. The pressure sensor also serves to make the phials air tight. The glass vessels are irradiated with microwaves (frequency around 2455 MHz) from the side. A glass sleeve is inserted through the PEEK cap of the phials, see figure 5.2

(c), to house and protect the "Ruby" temperature sensor [8]. The reactor and vessel assembly are shown in Figure 5.2.

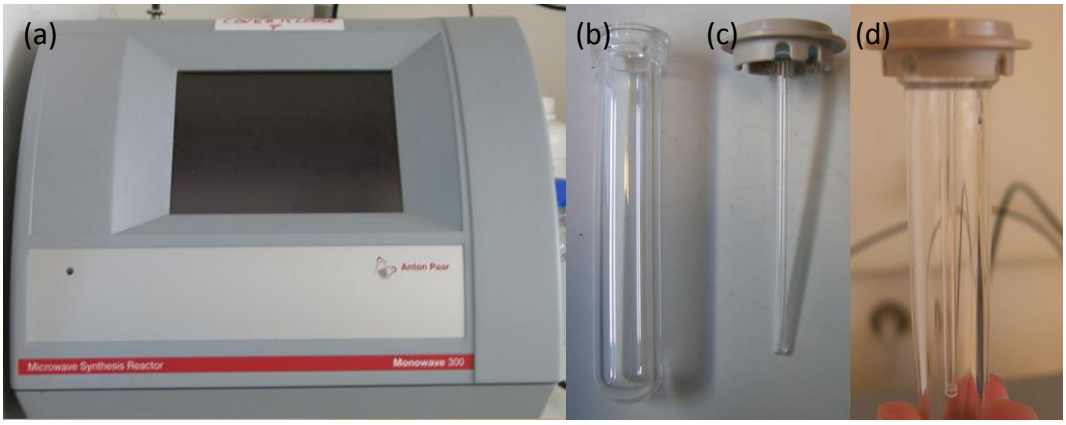

Figure 5.2: **(a)** Monowave 300 microwave reactor. **(b)** 10 ml borosilicate reaction phial. **(c)** PEEK cap with glass sleeve for Ruby temperature sensor. **(d)** assembled reaction vessel.

For the alkaline experiments the glass reaction vessel was replaced with a Teflon one. The reason for this was the large degree of damage that was observed on a glass phial after the NaOH experiment (see figure 5.4(a) in section 5.3.2). Considering that the internal pressure in the phial can reach upwards to 9 bar, the level damage that was incurred on the glass reaction vessel is unacceptable. Thus, the glass reaction vessels are considered unsuitable for NaOH based reactions in the microwave reactor. The risks associated with operating the Monowave 300 at high temperatures under these conditions are too high. To continue performing NaOH conversion experiments in the microwave reactor, the glass phials were replaced with Teflon (which is also transparent to microwaves, $\varepsilon_r = 2.1$) ones. The Teflon phials were machined to the exact dimensions of the glass phials, see figure 5.4 (b), to ensure compatibility with the Monowave 300.

5.3. Incompatibility of the microwave equipment with the leaching system

While performing the microwave experiments, it became clear that the Monowave 300 was not the correct appliance to investigate the influence of microwave-assisted leaching of monazite. This manifested itself as a result of two factors: (1) non-continuous microwave irradiation and (2) location of the microwave focus point.

5.3.1. Non-continuous microwave irradiation

When analysing the data logs of the microwave experiments it became clear that the microwave irradiation during the experiments was limited to a high intensity burst in the beginning of the reaction. After this initial burst, only low power microwaves were intermittently supplied to the system to maintain the temperature to the set point. Figure 5.3 shows two data logs from the experiments discussed in 5.4.2. For both, a 2 h experiment (Figure 5.3 (a)) and a 10 min experiment (Figure 5.3 (b)), the logs show that the reaction vessel is only exposed to a burst of high energy (900 W) microwaves in at the start of the reaction. After this initial burst of microwaves, only low energy (5-10 W) microwaves are required to maintain the target temperature.

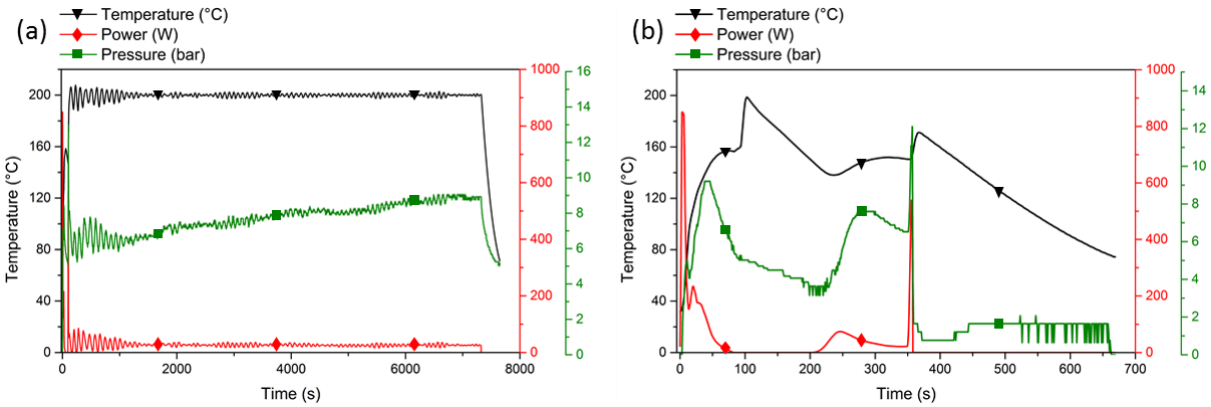

Figure 5.3: Data acquisition graph of the Monowave 300, showing phial temperature and pressure as well as power supplied to the system during **(a)** experiment at 200°C (2 h) and **(b)** experiment at 200°C (10 min)

This means that the possible beneficial effects of microwave irradiation (heterogeneous heating and inducing thermal stresses) only occur in a very small time window (± 10 s) of the experiment. Therefore, distinguishing the microwave effects from the enhanced reactivity due to high temperature and pressure is impossible.

The high vessel pressure is an unexpected, yet beneficial, observation. For the reaction at 200°C the internal pressure is measured at 6 to 9 bar. When reviewing the pressure for the other experiments, pressures of 3.5 bar were detected during the HNO_3 experiments and 4.5 bar for the H_2SO_4 experiments at 90°C. This internal pressure likely originates from water evaporation during leaching, as the reaction vessel is gas tight. Based on this observation, combined with the high temperatures under which these experiments were performed, it would be more apt do consider the Monowave 300 as a highly efficient autoclave, instead of a microwave reactor.

5.3.2. Location of the microwave set point

During the NaOH conversion experiments (see 5.5.1), severe damage was observed to the glass reaction vessel, after the alkaline conversion microwave experiment. The reaction between glass and NaOH is well known, which is the reason the fragile glass sleeve housing the temperature sensor was replaced with Teflon. However, the attack of glass by NaOH is normally a slow reaction [14]. The thickness loss of glass is approximately 1.4 µm/h at 100°C for 1 M NaOH [15], and therefore the thick walls of the glass phial (± 2 mm) should have lasted for more than 100 hours. Indeed, the glass reaction vessel that was heated conventionally showed no observable damage and weighing it before and after reaction showed a glass loss of approximately 0.01%. In contrast, the glass loss for the microwave phial is approximately 2%, which is considerably higher. What is also interesting is that the damage is localised near the top of the phial, see the red arrow in Figure 5.4 (a).

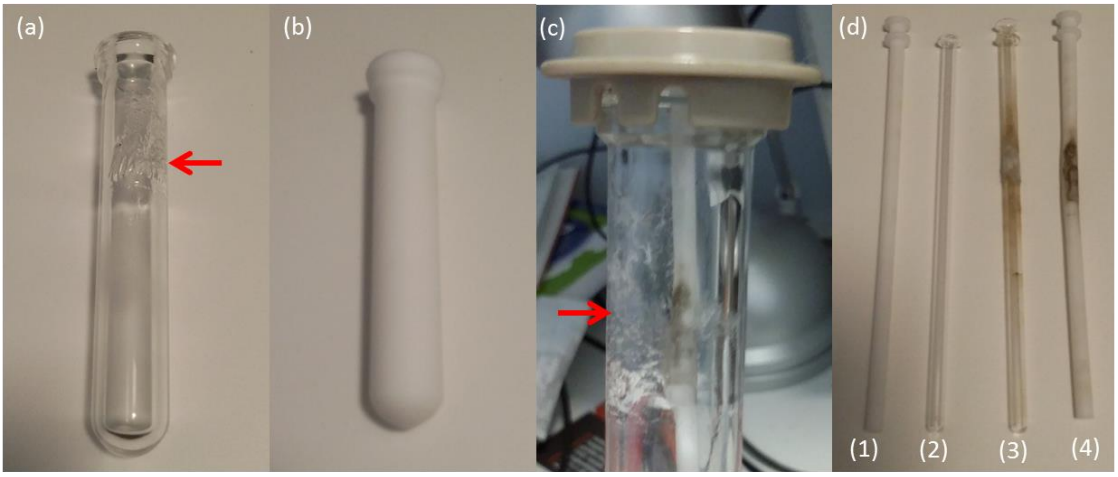

Figure 5.4: (a) Damaged glass reaction vessel due to reaction with NaOH during microwave heating; **(b)** Teflon replacement phials for high temperature microwave NaOH conversion; **(c)** Burnt Teflon sleeve inserted in damaged glass phial to highlight height match; **(d)** protective sleeves for the temperature sensor: (1) undamaged Teflon, (2) undamaged glass, (3) glass with $CaSO_4$ residue and (4) burnt Teflon sleeve

The area where the glass damage was observed is significant. During high temperature NaOH experiments (see section 5.5.2), using the Teflon phials, burn marks were observed on the Teflon sleeves that house the temperature sensor. These burn marks were located on the same height as the damaged area on the glass phials, indicated by the red arrow in Figure 5.4 (c). Additionally, upon examining the glass sleeves of the acidic leaching experiments (see section 5.4.2.2.), it became clear that the $CaSO_4$ deposition was also concentrated at this location, as shown in Figure 5.4 (d)(3)-(4). From these observations, it can be concluded that the chemical reactions are most vigorous in this area of the phial. This, combined with the observed burn marks, leads to the conclusion that the microwaves generated by the Monowave 300 are primarily focussed on this location. This means that only a small fraction of the solid particles, i.e. only those particles that are suspended high enough via agitation, is effectively being irradiated during the leaching operation. Thus, it is unlikely that the microwaves affect the solid particles to a meaningful extent for extended periods of time. This means that the effects described in literature, e.g. heterogeneous heating and induced thermal stresses, likely do not occur when using this setup.

5.3.3. Monowave 300 interpreted as autoclave

Based on both observations (non-continuous irradiation and high focus point) it is difficult to attribute any of the observed positive influences to direct interaction of microwaves and monazite. Considering the process conditions, the influence of high temperatures and pressure is likely to mask any influence that the microwave may have on the system. That is not to say that the microwaves have not influence on the system, but isolating the influence of microwaves from the influence of temperature and pressure is not possible in this system.

Nevertheless, it should be noted that even if the microwaves themselves are not contributing to the dissolution of monazite, the microwave reactor is still a very effective and efficient reactor to achieve extreme leaching conditions, as opposed to a furnace and/or autoclave that are traditionally used for pressure leaching. Creating more aggressive leaching conditions was the original intent behind using microwave and they were achieved, albeit not in the predicted manner. And the more aggressive leaching conditions do have an observable positive influence of the leaching behaviour of monazite. As such, the Monowave 300 may not be suitable for microwave-assisted leaching, it does perform

excellently as an autoclave. Therefore, the results that were obtained during testing are valuable for the purposes of process development.

Based on the above discussion, the experimental work will be discussed and evaluated not as microwave-assisted leaching, but as microwave-driven autoclave leaching.

5.4. Pre-treatment of the apatite concentrate

As was done in section 4.6. for the combination of acidic and alkaline processes of the apatite concentrate, a pre-treatment was first performed on the apatite concentrate to remove the apatite and create a monazite residue. This was done by leaching 200 g of apatite concentrate with 600 ml of 27.1 wt.% HNO_3 (identical to the conditions in section 4.6.2.). The chemical composition of the resulting residue is given in Table 5.1. Please note that for this measurement, and those further in the chapter, the PO_4 content was not measured, as it was deemed unimportant for the discussion of microwave leaching.

Table 5.1: Concentration of major elements and REEs of the monazite residue after HNO_3 pre-treatment, measured with ICP-OES

	Fe	Si	Ca	Mg	Al	Cu	Total REE	
wt.%	21.5	14.8	7	5.6	2	0.37	5.4	
σ	1.4	0.5	0.3	0.2	0.2	0.07	0.5	
	Ce	**Nd**	**La**	**Sm**	**Y**	**Ho**	**Gd**	**Dy**
wt.%	2.9	1.2	0.93	0.11	0.1	0.1	0.05	0.03
σ	0.4	0.3	0.03	0.02	0.01	0.01	0.01	0.01

5.5. Microwave-driven autoclave leaching using acidic media

For the acidic leaching experiments HNO_3 and H_2SO_4 were investigated as possible leaching agents. These two acids were selected in order to compare the microwave-driven system to conventional leaching (HNO_3) and to explore the possibilities of leaching under more aggressive (temperature higher than 100°C) conditions (H_2SO_4).

The HNO_3 leaching system has been proven to be ineffective in dissolving monazite in section 4.4, where it was shown that with a conventional leaching setup monazite reports to the residue after leaching. By running the HNO_3 leaching system using microwave heating it is possible to observe if the more reactive conditions enable the dissolution of monazite.

The H_2SO_4 leaching system on the other hand has not been tested under conventional conditions. This is because for the apatite concentrate, H_2SO_4 was rejected as a possible leaching agent, due to the precipitation of $CaSO_4$ and the associated REE losses (see section 4.2). However, the monazite residue contains much less Ca than the apatite concentrate (7 wt.% vs 37 wt.%), which may allow for the use of H_2SO_4 without having major problems with $CaSO_4$ precipitation. The advantage of using H_2SO_4 as a leaching agent is that more aggressive leaching conditions can be achieved, compared to HNO_3. The boiling point of a 95-98 wt.% H_2SO_4 solution lies between 290 and 300°C, while a 65 wt.% HNO_3 solution has a boiling point of approximately 121°C [10]. The microwave reactor allows for experiments to be

performed at temperatures of 200°C and higher, in a controlled and safe way. This, as will be shown below, will be beneficial in decomposing the monazite.

5.5.1. Microwave-driven autoclave leaching with HNO_3

Figure 5.5 shows the influence of the conditions induced by microwave heating on the HNO_3 leaching system, by comparing the extraction of the major elements and REEs of a HNO_3 leaching system heated through conduction and heated by microwave. The conventional heating experiment was conducted using the VWR® Thermal Shake Touch (the same one used in section 4.4.4. to run the solvent extraction trials), equipped with a sample block that is compatible with the microwave phials. This allows us to compare the microwave heating to conventional heating, using the same reactor vessel. The leaching system was operated at 90°C for 2 h, with a stirring/shaking speed of 600 rpm, using a 65 wt.% HNO_3 solution and a L/S ratio of 10 (0.5 g of sample on 5 ml solution).

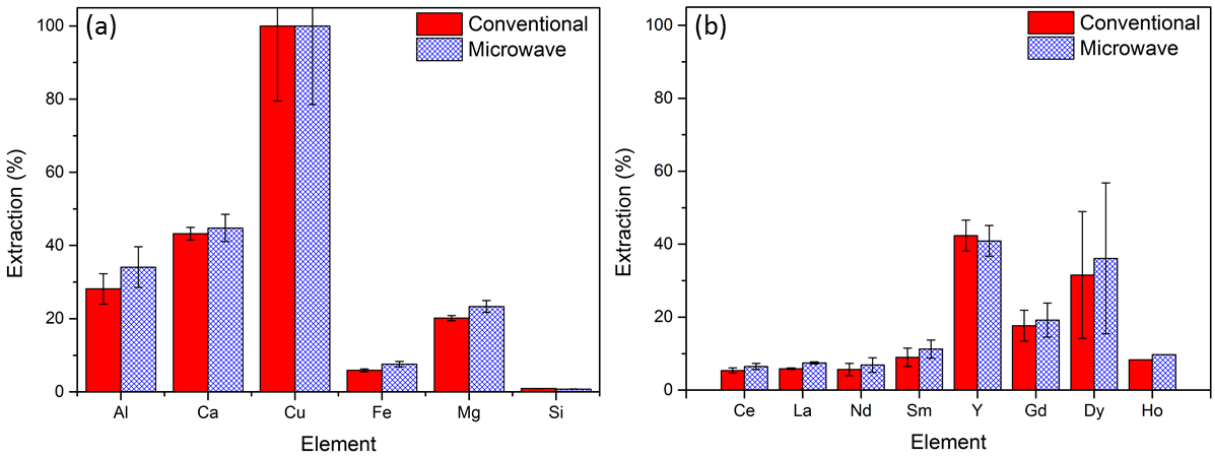

Figure 5.5: Comparison of HNO_3 leaching extraction at 90°C under conventional and microwave heating **(a)** major elements and **(b)** REEs

Without the presence of the pressure sensor the glass phials are not gas tight. Thus, the pressure within the phial is assumed to be 1.013 bar (1 atm) during the conventional heating experiments. The measured pressure in the phial during the microwave experiments was averaged at 3.5 bar.

The difference in observed extraction, between conventional heating and microwave heating, is minimal and is smaller than the uncertainty of the system. From these observations we can conclude that, for the HNO_3 leaching system, the influence of increased pressure within the reaction vessel on REE dissolution is insignificant. The presence of microwaves in the system also does not affect the REE dissolution.

What can be noted however, is the increased extraction of Y and Dy compared to those of Ce and La, irrespective of microwave assistance. As was discussed in chapter 4, Y and Dy are primarily associated with apatite, not monazite, and thus co-dissolved during the apatite leaching. Y and Dy then re-precipitated as YPO_4 and $DyPO_4$, because the acidity of the leaching solution was insufficient to supress reaction 4.8. These results show that the formed YPO_4 and $DyPO_4$ precipitates, while having a chemical formula similar to that monazite [$(REE)PO_4$], do not have the same resistance to acid dissolution as monazite.

5.5.2. Microwave-driven autoclave leaching with H_2SO_4

5.5.2.1. Comparison with HNO_3

Before investigating the influence of the extreme leaching conditions that can be achieved with H_2SO_4, first the differences between the HNO_3 and H_2SO_4 leaching system under similar conditions must be investigated. The two leaching agents are compared by analysing the extraction of elements after microwave-driven autoclave leaching at 90°C for 2 h with a 14.6 M HNO_3 solution (65 wt.%) (same as above), a 7.3 M H_2SO_4 solution (equal H^+ concentration to HNO_3) and a 17.8 M H_2SO_4 solution (95 wt.% H_2SO_4). Figure 5.6 shows the results of this analysis.

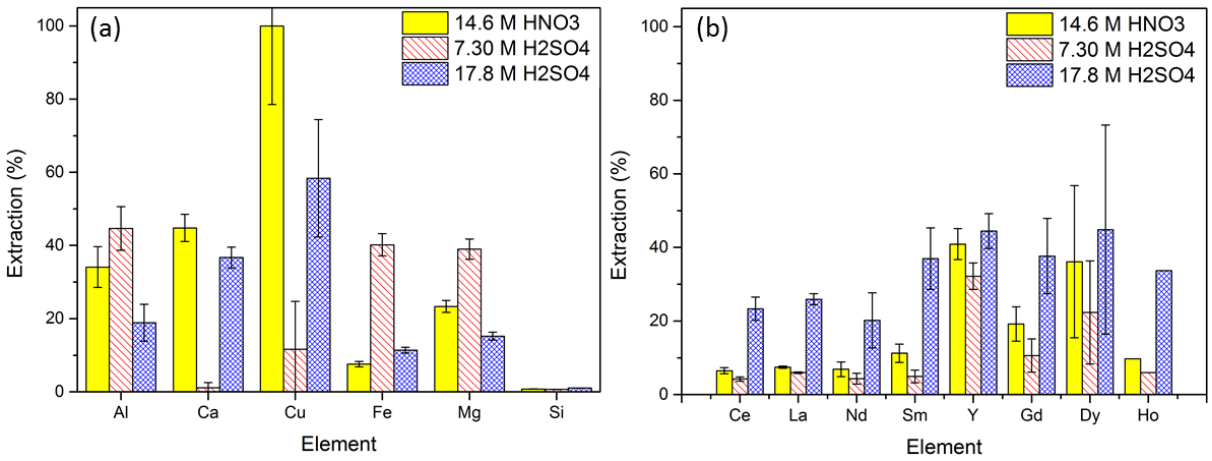

Figure 5.6: Comparison of microwave-driven autoclave extraction between HNO_3 and H_2SO_4 for **(a)** major elements and **(b)** REEs

The measured phial pressures were: 3-3.5 bar for the HNO_3 experiment and 4.5 bar for both H_2SO_4 experiments.

The influence of the H_2SO_4 concentration in the leaching agent on the extraction of the major elements differs for each element. Al, Fe and Mg show a higher extraction for the 7.30 M H_2SO_4 solution, but a lower extraction for the 17.8 M solution. This effect is attributed to the decreased solubility of their respective sulphate salts in highly concentrated sulfuric acid [11]-[12]. The differences in extraction of Ca are likely caused by the $CaSO_4$ precipitation. Depending on the water content of leaching liquor $CaSO_4$ can precipitate as either $CaSO_4 \bullet 2H_2O$, $CaSO_4 \bullet ½H_2O$ or $CaSO_4 \bullet 0H_2O$. For the current situation $CaSO_4 \bullet 2H_2O$ and $CaSO_4 \bullet ½H_2O$ are considered to have the same precipitation behaviour (as $CaSO_4 \bullet ½H_2O$ is an intermediary for $CaSO_4 \bullet 2H_2O$). The hydrated forms of $CaSO_4$ precipitate relatively easily and form quickly if water is available. The anhydrous form however, precipitates more slowly and requires higher temperatures [13]. This means that the water content of the leaching agent determines whether or not the Ca has a chance to precipitate. Because the water content in 95 wt.% H_2SO_4 is minimal, the Ca did not precipitate out during the 17.8 m H_2SO_4 leaching experiment, leading to higher Ca extraction. The behaviour of Cu is difficult to explain, as the XRD analysis was unable to detect which Cu mineral phase was present in the feed. As the extraction is the lowest for the leaching agent with the lowest acid strength (see reaction (5.2) and (5.3)), it is likely that the Cu phase requires a certain level of acidity to dissolve. The reasons behind the influence of the acid type (HNO_3 vs H_2SO_4) on the extraction of major elements are unclear and require more study. However, this lies beyond the scope of this chapter.

The influence of leachant on the extraction of REEs is more uniform than for the major elements, which is not surprising, as all REEs have similar chemical properties. There is also the fact that the overall concentration of REE is low, implying that solubility limits are unlikely to be a limiting factor. The strong increase in extraction ratio for the 17.8 M H_2SO_4 leaching solution suggests that the reaction for REE dissolution is primarily controlled by the acidity of the leaching solution and not the acid type. This is shown by the slightly lower extraction ratios of the 7.3 M H_2SO_4 system, since the H^+ activity of the 14.6 M HNO_3 and 7.3 M H_2SO_4 solutions is not equal, whereas the H^+ concentration is. H_2SO_4 is a diprotic acid, which reacts via

$$H_2SO_4 \rightarrow H^+ + HSO_4^- \quad (5.5)$$

$$HSO_4^- \rightarrow H^+ + SO_4^{2-} \quad (5.6)$$

However, only reaction (5.5) is a complete dissociation ($K_a = 1*10^3$). This means that H_2SO_4 is a strong acid, but HSO_4^- ($K_a = 1*10^{-2}$) is not. When considering the dissociation of sulphuric acid in water, reaction (5.6) contributes less than 0.01 M to the H^+ concentration. This leads to an overall lower H^+ activity, compared to HNO_3, which explains the minor decrease in extraction for REE when leaching with 7.3 M H_2SO_4. As general rule of thumb, H_2SO_4 only contributes half its H^+ cations when used in excess, thus the H^+ activity will be proportional to the molarity of H_2SO_4 and not twice the molarity. (consumption of H^+ will of course prompt further dissociation via reaction (5.6)).

The observed extraction of REEs after leaching with a 17.8 M H_2SO_4 solution is higher than those of a 14.6 M HNO_3 solution, which is expected as the acid strength of this solution is much higher (K_a HNO_3= $2.4*10^1$). This shows that more extreme leaching conditions do have a positive influence on REE extraction, and that monazite is not entirely immune to acid leaching.

5.5.2.2. Leaching at increased temperatures

The next step is to validate that further increasing the reactivity of the system leads to higher levels of monazite dissolution. This is done by running leaching experiments at temperature above the limit of traditional aqueous systems (100°C) and using concentrated H_2SO_4 (98 wt.% / 17.8 M). The temperatures that were investigated were 100°C, 150°C and 200°C. The L/S ratio was keep at 10 and the leaching time was maintained at 2 h, as this is the limit of the Monowave300. The results are shown in Figure 5.7.

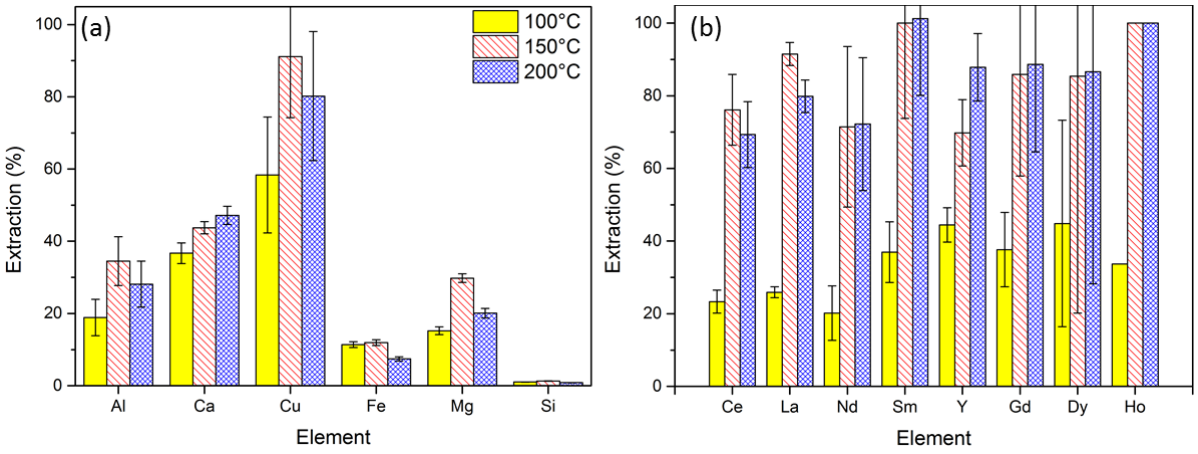

Figure 5.7: Influence of temperature on leaching extraction of **(a)** major elements and **(b)** REEs (colour legend is the same as for the major elements), during microwave leaching with 98 wt. % (17.8M) H_2SO_4

The results clearly show that the increased leaching temperature has a strong effect on the extraction of REEs (Figure 5.7 (b)). Each REE has an extraction that is approximately 2-3 times higher at 150°C and 200°C, compared to 100°C. The measured pressure at 150°C was 4.5 bar, while the pressure measured at 200°C varied between 8 and 12 bar. The pressure did not increase between the 100°C and 150°C experiments, the REE extraction did. This indicates that temperature has much stronger influence on the monazite dissolution, compared to pressure. This observation is expected as the gas phase does not participate in the reaction. The main positive influence the pressure build-up has in this system, is increasing the boiling point of the solution, allowing for leaching at high temperatures.

The increased REE extraction shows that acidic dissolution of the monazite contained within the apatite tailings is possible, if the reactivity of the system is high enough. Thermodynamically the possibility of monazite digestion is not dependant on temperature, as shown by the Gibbs free energy for the reaction

$$2\,\mathrm{CePO_{4(s)}} + 3\,\mathrm{H_2SO_4} \rightarrow \mathrm{Ce_2(SO_4)_3} + 2\,\mathrm{H_3PO_4} \tag{5.7}$$

which is negative between 20°C to 200°C (−140 kJ at 20°C and −123 kJ at 200°C, calculated with HSC 6, using $CePO_4$ as a representative compound for monazite). The thermodynamic data also shows that the reaction is exothermic (ΔH = −208 kJ at 20°C), meaning that a higher temperature, thermodynamically, does not benefit the reaction. Thus, an increased temperature only influences the rate of the reaction (kinetics) and not the reaction extent. This indicates that monazite dissolution reaction is either kinetically slow or has a high activation energy (or both).

An additional experiment was conducted at 200°C for only 10 min instead of 2 h, with the extraction of the major elements and REEs are shown in Table 5.2.

Table 5.2: Extraction of major elements and REEs after 10 min 200°C H_2SO_4 microwave leaching

	Fe	**Si**	**Ca**	**Mg**	**Al**	**Cu**	**Total REE**	
%	8.7	0.88	47	22	27	90	60	
σ	0.6	0.04	3	2	7	21	1	
	Ce	**La**	**Nd**	**Sm**	**Y**	**Gd**	**Dy**	**Ho**
%	57	64	53	89	79	**81**	81	83
σ	9	6	17	20	9	**24**	53	n.a.

The extraction of the major elements is approximately equal between 10 min and 2 h, which indicates that the dissolution of the non REE minerals reaches equilibrium quickly. For the REEs the extraction is between 10 and 20 % lower for 10 min than it is for 2 h, which indicates that the monazite dissolution is a slower reaction.

However, this also means that 80-90% of the observed monazite dissolution occurs within the first 10 min of the leaching experiment. This may be an indication that the initial burst of high intensity microwaves (see Figure 5.3 b) does have a positive effect on the leaching system. If it is assumed that the monazite dissolution reaction has a high activation energy, the initial microwave burst may imbue the system temporarily with enough energy to overcome the activation energy and dissolve part the monazite. When the microwave burst ends, this addition energy disappears, leading to a significant reduction is dissolution rate.

This is however only a hypothesis, which cannot be verified with the equipment available. The Monowave 300 has a built-in safety that does not allow for sample access before the device has sufficiently cooled down (which takes between 10 and 20 min), nor does the Monowave 300 allow for the system to be exposed to high intensity microwaves for an extended time, due to its temperature and pressure safeguards.

Further increasing the reactivity of the system was not tested. While it is theoretically possible to further increase the reaction temperature up to 290°C (the boiling point of a 95% H_2SO_4 solution), for safety purposes this was not attempted. Therefore, 200°C was considered the upper limit for the reaction conditions during leaching. Under these conditions the REE extraction was not complete, thus the residue was analysed to verify if there is still unreacted monazite, or if there is another REE phase present that does not react with H_2SO_4.

5.5.2.3. Analysis of the high temperature leach residues

Figure 5.8 shows the SEM/BSE analysis of both the pre-treated material before microwave leaching (a) and the residue after leaching at 200°C for 2h (b). Comparing both SEM/BSE images shows that the bright particles are missing from the residue after microwave leaching, compared to the original residue. The only particles that have a higher BSE intensity than the background silicates are iron oxide particles. The absence of bright, i.e. REE, particles suggests that the dissolution of monazite was complete and that there is no other REE phase present in the leach residue. However, the ICP-OES analysis does not validate this assumption. While it can be argued that SEM/EDS is a localised analysis method, the surface area that was analysed was large enough to be considered representative for the entire residue. SEM analysis of the material before leaching showed a fairly homogeneous spatial distribution of REE particles.

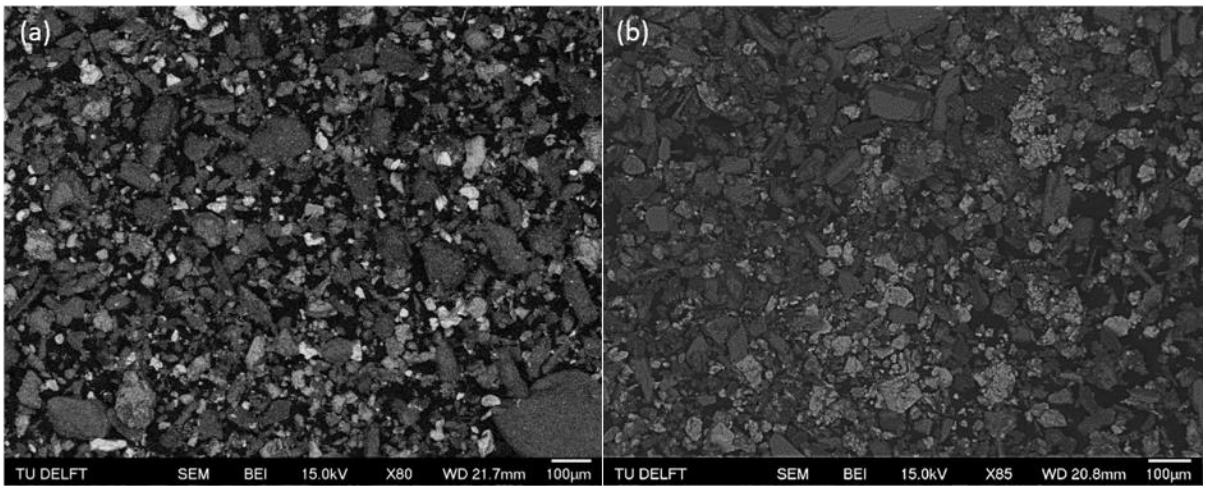

Figure 5.8: SEM/BSE analysis of the **(a)** un-leached residue and **(b)** residue after 200°C H_2SO_4 leach

An explanation for these contradictory observations lies with the reaction product that forms on the walls of the reaction vessel: $CaSO_4$. After microwave leaching with H_2SO_4 at 200°C, a hard and white phase forms on the glass walls of the reaction vessel and on glass sensor sleeve that houses the temperature sensor (see Figure 5.4 (d)(3)). Analysis of this phase with EDS shows it is $CaSO_4$ (recovered amount was too low for XRD analysis, and XRD is unable to identify $CaSO_4$ as a separate phase when the entire residue is measured). $CaSO_4$, as mentioned above, is known to capture REEs during its formation. However, confirming this capture with EDS was not possible, as the detection limit of EDS

is too high (approx. 0.1 wt.%). When $CaSO_4$ precipitates it does not encapsulate REE particles, rather REEs are built into the $CaSO_4$ lattice as substitutional elements for Ca. This means that there are no areas within the formed $CaSO_4$ where the REEs could locally concentrate, rather the REEs are uniformly distributed through the lattice of $CaSO_4$. This makes it impossible for the EDS to resolve a REE concentration, or for BSE to observe any bright areas.

Because of this, the presence of the non-recovered REE in the $CaSO_4$ phase has yet to be confirmed. However, based on observation and literature, the $CaSO_4$ formation is the most likely explanation for the incomplete REE recovery. To conclusively confirm the presence of REE, the $CaSO_4$ phase needs to be digested and its chemical composition measured with ICP-OES. However, we have not been able to recover and separate a sufficient amount of the $CaSO_4$ phase to perform this analysis. Since the formation of the $CaSO_4$ on the glass components is very detrimental to the equipment, the experiments were not continued to produce extra $CaSO_4$.

Despite the incomplete REE recovery, the high temperature H_2SO_4 leaching experiments prove to be the most effective method for monazite digestion that was found during this work. They prove that acidic dissolution of monazite is possible. The challenge now becomes the minimisation of the amount of Ca in the monazite residue, so that the $CaSO_4$ precipitation side reaction is prevented as much as possible. This optimisation falls outside of the scope of this chapter, but serves as an excellent starting point for future research.

5.6. Microwave-driven autoclave leaching using alkaline media

Section 4.5 showed that the more aggressive leaching conditions (160°C for 24 h) induced by the furnace had a positive influence on the conversion of monazite to $REE(OH)_3$. However, the energy requirement of this system is quite substantial. Microwave-driven autoclave leaching may be a more energy efficient alternative to the furnace to reach the required aggressive conversion conditions.

Next to better energy efficiency, the ability of microwave-assisted leaching to break up of layers of formed reaction products, through inducing thermal stresses between the reacting particles and the forming product layer (see section 2.4.3 microwave leaching of chalcopyrite), is also of interest for this process. While it is unlikely to occur given the microwave conditions, it should not be discounted off hand.

5.6.1. Comparison between microwave heating and conventional heating

As with the acidic leaching systems, the first experiments serve to compare microwave heating to conventional heating, under similar leaching conditions. The leaching system was run for 2h at 100°C with a stirring/shaking speed of 600 rpm in glass reaction vessels. 0.5 g of monazite residue was treated with 5 ml 60 wt.% NaOH solution.

After the alkaline conversion tests, 0.1 g of the obtained solids was leached with 1 ml 65 wt.% HNO_3 for 2 h at room temperature in the shaker at 1000 rpm. The extraction of major elements and REEs of this combined conversion and leaching was determined through ICP-OES analysis of the leach liquor.

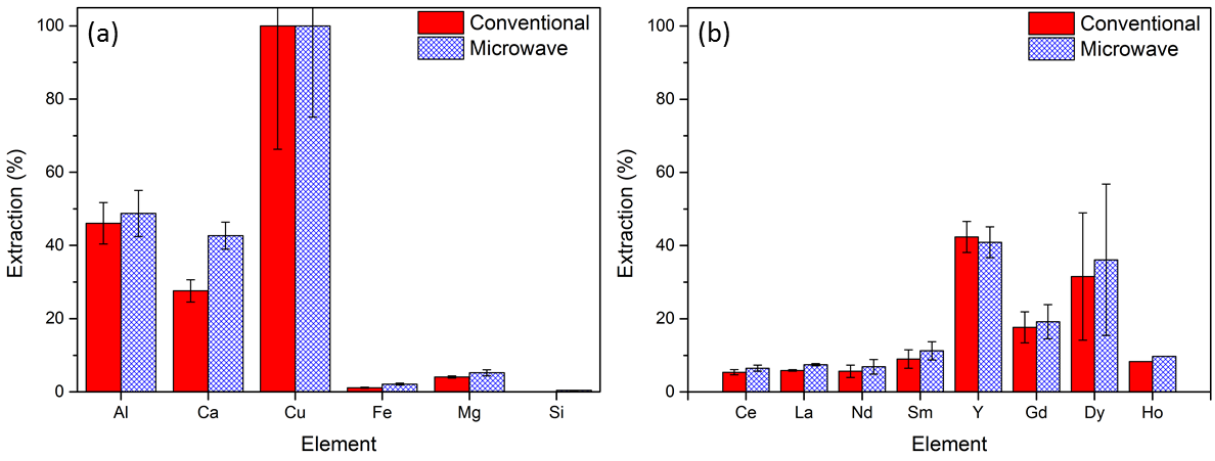

Figure 5.9: Comparison NaOH pre-treatment with conventional and microwave heating for (a) major elements and (b) REEs

Figure 5.9 shows the comparison of extraction for major elements (a) and REEs (b). Similar to the acidic leaching experiments, there is a minor increase in extraction between conventional and microwave heating. The increased extraction lies outside of the experimental uncertainty, but not by much. This makes it difficult to attribute the observed increase to the use of microwaves or the increased pressure (4.5 bar). Analysis of the converted material (before HNO_3 leaching) with SEM/BSE, see Figure 5.10 (a) and (b) shows that the needle like scale of $REE(OH)_3$ is still present on both the conventional and microwave conversion process. However, more solitary needles are observed in the microwave residue (Figure 5.10 b), which may be an indication for scale breakage. But, due to the uncertainty associated with the Monowave 300's microwave field, no concrete conclusions could be drawn from this observation. To validate the scale breaking effect of microwaves on monazite more specialised microwave equipment is required.

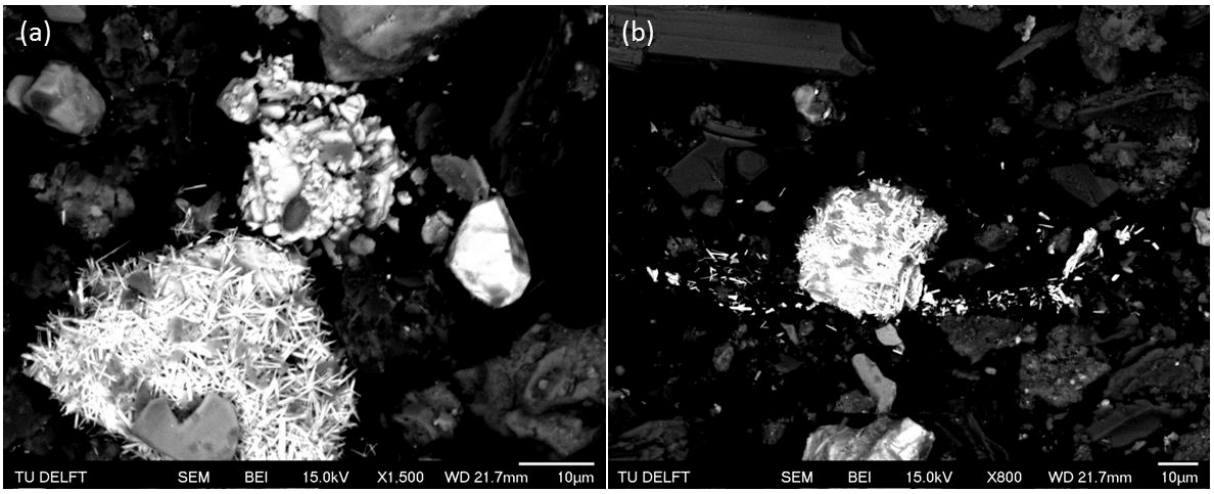

Figure 5.10: SEM/BSE analysis of alkaline conversion residues of **(a)** conventional heating and **(b)** microwave heating; Image illustrates monazite particles covered with a scale of $REE(OH)_3$ needles

5.6.2. Alkaline conversion at higher temperatures

The question now becomes if it is possible to achieve REE extraction on the same level as the alkaline conversion in the furnace shown in section 4.5 using the microwave reactor.

The Teflon reaction vessels were used to perform the NaOH conversion at 120°C and 140°C. 140°C proved to be the limit at which the experiments could be performed, without damaging the phials due to overly high pressure.

As before, after alkaline conversion, 0.1 g of the converted solids were leached with 1 ml of 65 wt.% HNO_3 and the leach liquor analysed with ICP-OES and the extraction rates calculated. The resulting extraction rates are shown in Figure 5.11.

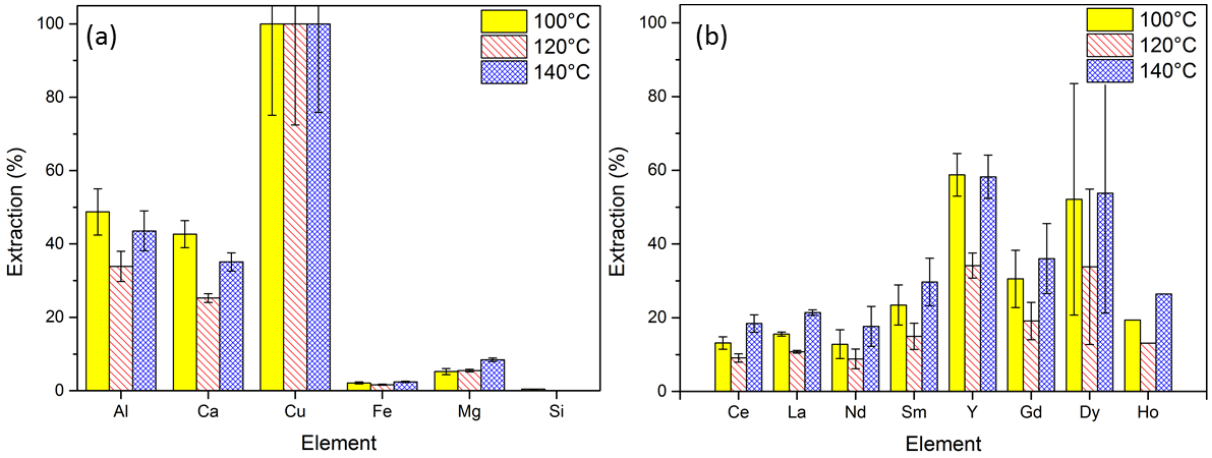

Figure 5.11: Influence of temperature on leaching extraction of **(a)** major elements and **(b)** REEs, during microwave NaOH conversion in Teflon vessel at higher temperatures (note that the 100°C results were taken from Figure 5.9, which was performed in a glass vessel)

The extraction results show that the use of the Teflon tubes affects the leaching rate of both the major elements and the REEs. Teflon is less transparent to microwave than glass [4], and also has a poorer thermal conductivity. Both factors, combined with the fact that the thermal sensor is placed in a Teflon sleeve, makes the temperature readout of the Monowave 300 less reliable. It is likely that the temperatures of 120°C and 140°C were not reached during the reactions and that the conditions during the 140°C experiments in the Teflon vessel were similar to the 100°C experiment in the glass phial and that the conditions at the set temperature of 120°C in actually did not exceed 100°C. (Please note that the 100°C data in Figure 5.9. is the data from the glass vessel experiment.)

No pressure increase was measured during the high temperature NaOH experiments. The Teflon phial was unable to remain gas tight due to a poor seal with the PEEK cap. Thus, for these experiments there is no autoclave effect. From this we conclude that the Teflon phials are unusable for this type of experiment.

This means that using the current microwave setup, the extraction levels of the NaOH conversion in the furnace were superior. However, this is in large part due to the limitation of the Monowave 300 and the Teflon vessels. Sturdier vessels and a lower microwave focus point would both greatly benefit the microwave process and enable a more effective and efficient alkaline conversion process. However, this would require an entirely new reactor, which was not available for the present study.

5.7. Modifying the apatite concentrate flowsheet

5.7.1. The flowsheet

As it stands, it can be concluded that for dissolving the REEs of the monazite residue, the microwave-driven autoclave leaching using H_2SO_4 and operating at 150-200°C is the superior process option. This process surpasses the furnace alkaline conversion in both REE recovery and energy efficiency. This means that the final flowsheet of chapter 4, see Figure 4.18, can be modified to include a microwave extraction process instead of the alkaline conversion. The modified flowsheet can be seen in Figure 5.12.

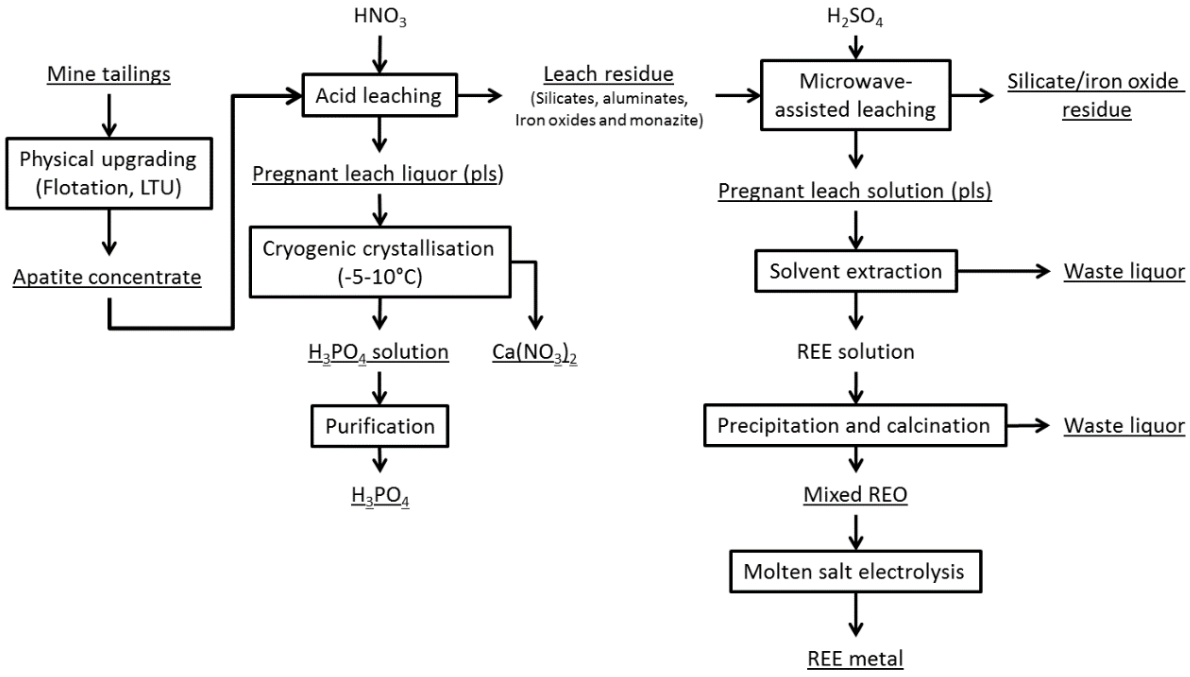

Figure 5.12: Modified flowsheet employing microwave-driven autoclave leaching, in place of alkaline conversion, to extract the REE from the leach residue produced by the H_3PO_4 production step

With the change of leaching reagent from HNO_3 to H_2SO_4 the previously developed P350 solvent extraction system may no longer yield the required separation efficiency. Further research is required to develop a solvent extraction process which extracts the REEs in sulphate media. Based on literature D2EPHA may be potential extractant for this system [16].

5.7.2. Waste management

As the flowsheet of figure 5.12 is a modification of those developed in chapter 4, the waste management strategy proposed there translates to this flowsheet as well. The use of H_2SO_4 during the microwave step of the process does simplify the treatment of the waste streams produced in the microwave segment of the flowsheet and in the subsequent steps. As was discussed in chapter 4 the neutralisation of a sulphuric acid waste stream with lime (CaO) creates large volumes of gypsum sludges. The tendency of gypsum to capture other metal cations during its precipitation greatly benefits the purification process, as it collects all waste products into a single solid waste [17]. This means that the traditional waste treatment strategy for hydrometallurgical waste water described in section 4.4.5.2. (neutralisation, precipitation, sedimentation and filtration) should work for the waste waters produced by the microwave-driven autoclave leaching process.

5.8. Conclusions and suggestions

Based on the experimental results of the microwave experiments the following conclusions can be drawn.

- At this point it is not clear if microwave irradiation does not influence monazite due to its relatively low dielectric constant or if the microwave setup simply could not irradiate the solid phase properly due to a too high microwave focus point.
- The irradiation time of the Monowave 300 is mainly limited to a short high intensity burst at the start of the process. Once the target temperature is achieved minimal irradiation was required to maintain the target temperature.
- The increased REE extraction observed due to microwave heating is likely due to the more extreme leaching conditions achieved within the vessel, i.e. temperatures of 150-200°C and higher and internal pressures of 4.5 to 9 bar. This makes this setup more comparable to an autoclave.
- The phenomenon of breaking of reaction product layers, due to thermal stress induced by microwave irradiation, was not observed during alkaline conversion.
- Microwave-driven autoclave leaching using HNO_3 offers no benefits to REE extraction, as the extreme conditions mentioned in the previous point cannot be achieved with this leaching medium.
- Microwave-driven autoclave leaching with H_2SO_4 at 150-200°C can successfully dissolve monazite and offers a more energy efficient alternative to the alkaline conversion process described in chapter 4.
- The current setup was not able to provide a more energy efficient alternative to the furnace alkaline conversion. However, this was due to limitations of the Monowave 300 and the Teflon reaction vessel and sensor sleeve.

Based on the obtained data it is clear that microwave-driven autoclave leaching has potential, even if only as an efficient alternate to traditional autoclave pressure leaching. Further study into a more suitable reaction vessel for alkaline processes would benefit the development of alkaline based monazite dissolution. Also, an investigation on the proper placement of the microwave focus point would offer more insight into the influence of microwave irradiation on the dissolution of monazite, for both the acidic and alkaline process routes.

References

[1] Microwave Processing of Materials. Washington, D.C.: National Academy Press, 1994.

[2] M. Al-Harahsheh and S. W. Kingman, “Microwave-assisted leaching—a review,” Hydrometallurgy, vol. 73, no. 3, pp. 189–203, 2004.

[3] D. A. Jones, T. P. Lelyveld, S. D. Mavrofidis, S. W. Kingman, and N. J. Miles, “Microwave heating applications in environmental engineering—a review,” Resour. Conserv. Recycl., vol. 34, no. 2, pp. 75–90, 2002.

[4] S. Horikoshi, R. F. Schiffmann, J. Fukushima, and N. Serpone, Microwave Chemical and Materials Processing: A Tutorial. Springer, 2017.

[5] K. E. Haque, “Microwave energy for mineral treatment processes—a brief review,” Int. J. Miner. Process., vol. 57, no. 1, pp. 1–24, 1999.

[6] R. H. Church, W. E. Webb, and J. B. Salsman, “Dielectric Properties of Low-Loss Minerals,” Bureau of Mines, Report of Investigations 9194, 1988.

[7] “Anton Paar Monowave 300 synthesis reactor.” [Online]. Available: https://www.anton-paar.com/corp-en/products/details/microwave-synthesis-monowave-400200/. (retrieved 28/02/2018)

[8] “Anton Paar Ruby Thermometer.” [Online]. Available: https://www.anton-paar.com/corp-en/products/details/ruby-thermometer/. (retrieved 28/02/2018)

[9] C. O. Kappe, “Microwave dielectric heating in synthetic organic chemistry,” Chem. Soc. Rev., vol. 37, no. 6, pp. 1127–1139, 2008.

[10] R. H. Perry, D. W. Green, and J. O. Maloney, Eds., Perry’s chemical engineers’ handbook, 7th ed. New York: McGraw-Hill, 1997.

[11] N. Imura, A. Sonohara, and I. Hirasawa, “The Solubility Characteristics of Aluminum Sulfate in Sulfuric Acid Aqueous Solution in the Presence of Oxalic Acid,” J. Chem. Eng. Jpn., vol. 50, no. 7, pp. 516–520, 2017.

[12] M. E. Wise et al., “Solubility and freezing effects of Fe^{2+} and Mg^{2+} in H_2SO_4 solutions representative of upper tropospheric and lower stratospheric sulfate particles,” J. Geophys. Res. Atmospheres, vol. 108, no. D14, p. 4434, 2003.

[13] D. M. K. Al-Gobaisi, “Seawater Desalination by large Multistage Flash Plants,” in “History, Development and Management of Water Resources- Volume II”, EOLSS Publications, 2010.

[14] F. R. Bacon and O. G. Burch, “Effect of time and temperature on accelerated chemical durability tests made on commercial glass bottles,” J. Am. Ceram. Soc., vol. 23, no. 1, pp. 1–9, 1940.

[15] “Technical Glasses Physical and Technical Properties”. Schott AG, 2015.

[16] F. Xie et. al. , “A critical review on solvent extraction of rare earths from aqueous solutions.”, *Minerals Engineering,* vol. 56, pp. 10-28, 2014.

[17] European IPPC-Bureau, “Best Available Techniques in the non-ferrous metals industries”, Gent, Academia Press, 2001.

Chapter 6: Hydrometallurgical recycling of WEEE

Abstract

A three-step process was developed for the hydrometallurgical recycling of the ferrous fraction of shredded WEEE. First the upgraded ferrous WEEE fraction is oxidised by means of water corrosion. Secondly the oxidised WEEE is leached with diluted H_2SO_4 to selectively extract Nd and other non-ferrous elements. Finally the leach liquor is treated with Na_2SO_4 to precipitate the Nd from the liquor and recover it as the double sulphate $(Nd,Na)(SO_4)_2$. The oxidation process oxidises 93% of the metallic iron to $Fe(OH)_3$, leaving 7% of the iron un-oxidised. The leaching process dissolves between 70% and 99% of the Nd, depending on the temperature and liquid/solid ratio (L/S); this is accompanied by an iron co-extraction between 9% and 20%. The subsequent precipitation recovers 92% of the leached Nd. The purity of the obtained precipitates is dependent on the pH at which the precipitation takes place. A pH below 0.5 is required to prevent Fe contamination and a pH below 0 reduces the Ca contamination to below 1 wt.%. The developed process provides an effective and low-cost method to recycle Nd from a shredded WEEE stream with an overall Nd recovery of over 90%. The developed process can be implemented in a WEEE recycling flowsheet, as indicated by the boxed area in Figure 6.1, to create a viable Nd recycling process.[6]

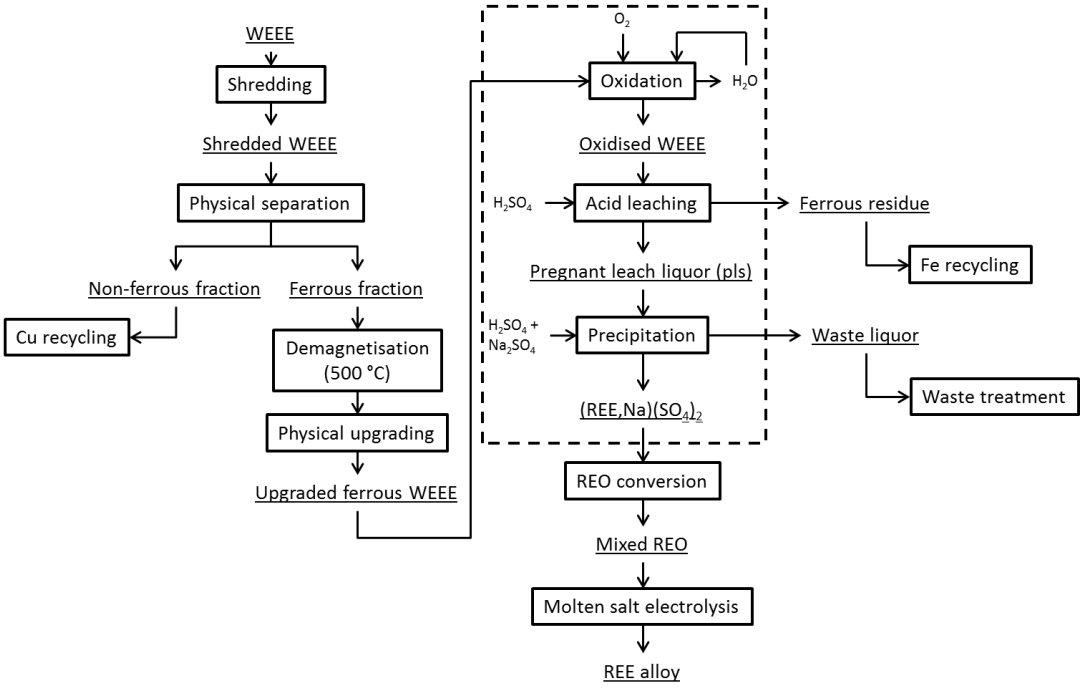

Figure 6.1: Recycling flowsheet for REE from WEEE, the developed hydrometallurgical process highlighted by the boxed area

[6] **Remark:** This chapter is based on the published paper: S. Peelman, J. Sietsma & Y. Yang, Recovery of Neodymium as $(Na,Nd)(SO_4)_2$ from the Ferrous Fraction of a General WEEE Shredder Stream, Journal of Sustainable Metallurgy, vol. 4, pp.276-287, 2018.

6.1. Introduction

The rare earth elements or REEs, a collection of 17 chemical elements (15 lanthanides plus yttrium (Y) and scandium (Sc)) are becoming increasingly important in modern day technology. With applications in electrical and electronic devices (e.g., capacitors, phosphors and high strength magnets), chemical industry (e.g., catalysts) and green energy (e.g., batteries and windmills) [1]–[5], they are becoming an increasingly critical resource for many industries. However, to meet this increasing demand, the EU is entirely dependent on REE imports from China [6], as there are currently no active REE mines, nor production, in the EU [7]. This dependency, combined with the recent instability of the REE market [8], has driven the EU to consider recycling end-of-life (EoL) REE-containing products in order to reduce this dependency and to ensure the availability of the most critical REEs in the future.

Neodymium (Nd) is one of the most critical REEs that the EU wishes to recycle. This element is a key component of Neodymium-Iron-Boron (NdFeB) high strength magnets. These magnets are approximately 2000 times stronger than traditional ferrite magnets and are used in a variety of applications, ranging from miniature magnets in high tech devices (such as hard disk drives (HDDs) and speakers) to large 2 ton windmill magnets. A stable supply of Nd is crucial to ensure the future production and development of such applications within the EU.

The recycling of Nd is currently limited to the recycling of production scrap and separately collected large EoL magnets (such as those from windmills). The methods for recycling the magnets from these waste streams are well established [9]. Most involve dissolving the magnet in acid and extracting the Nd via either precipitation or solvent extraction. However, these methods have only been proven to work on discrete magnets. This has limited the overall recycling of NdFeB magnets, as collecting and separating the magnets from their devices is a very labour intensive and expensive endeavour. Although some automated disassembly methods have been developed recently (e.g., the Hitachi process for HDDs [10]), the presence of small NdFeB magnets in electronic and high-tech devices is still largely being ignored and they end up mixed in with a general “Waste Electrical and Electronic Equipment” (WEEE) stream, from which Nd is not recycled.

Many elements are recycled from WEEE. Iron, copper and aluminium, as well as gold, silver and palladium, are selectively extracted from this complex waste stream [11]. This is done by first shredding the WEEE and further processing in a physical separation plant. This plant then separates the WEEE into various streams based on their main component (magnetic separation yields a ferrous and a non-ferrous stream, eddy current methods separate copper from aluminium, etc.). Each stream is then sent to either a hydrometallurgical or pyrometallurgical plant for further processing and refining. However, little research has been done to also extract Nd from shredded WEEE streams. The amount of Nd in WEEE is steadily increasing, as is the importance of Nd to the EU, and therefore efforts are now being made to also recycle Nd from this waste stream.

The goal of this study is to develop a hydrometallurgical process to extract Nd from shredded WEEE and then implement this process into a complete WEEE recycling flowsheet developed in a recent EU funded project REEcover [12], as is shown in Figure 6.2. To do so, first the most appropriate stream coming from the WEEE physical separation plant must be selected. The Nd magnets will naturally follow the steel within WEEE, see chapter 3.4.1, and thus will end up in the ferrous stream after magnetic separation. Therefore, the ferrous stream is the focus of this work. Once the shredded ferrous WEEE stream has been collected and properly upgraded (to maximise the Nd content) a

hydrometallurgical process can be developed to recover the Nd. When this is achieved the recovered Nd compounds can either be used directly or converted its pure metallic form through conversion and molten salt electrolysis.

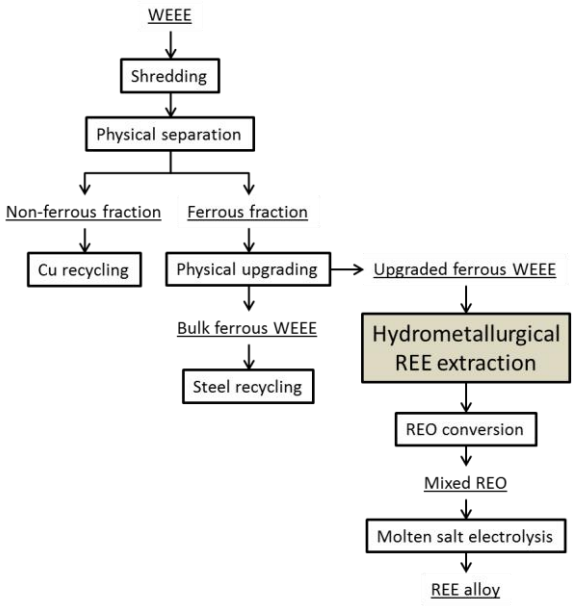

Figure 6.2: Insertion of a hydrometallurgical REE recover process in a WEEE recycling flowsheet

6.2. Exploratory leaching of the upgraded WEEE

Before a process could be designed several exploratory leaching experiments were run of the upgraded shredded WEEE in order to gain understanding on how the material responds to acidic leaching. The upgraded WEEE was first leached with a small amount of HCl to determine its most reactive components. Please note that the exploratory leach was not run with *Input2-Met2*, which was characterised in chapter 3, but was run on a similar material also originating from the shredder at INDUMETAL, *Input3-Met2*, which was sent in advance. This input material was obtained by feeding collected hard drives (HDDs) through the shredder instead of regular WEEE. This material has a higher Nd content than the WEEE feed material and contains fewer elements in general, which is useful for observing the behaviour of Nd. Only the exploratory leaches were performed with this material.

The HCl leach was performed with a HCl volume that corresponds with the stoichiometric requirement for full Nd dissolution, which for this experiment corresponds with 0.02 mole of HCl. A small excess (20%, 0.024 mole) of HCl was added to account for variation, which leads to a HCl volume of 2ml/20g of input material. The results of the exploratory leach can be seen in Table 6.1. The three main elements that leached from the upgraded WEEE were Fe, Nd and Zn.

Table 6.1: Results of exploratory leach of Input3-Met2 using HCl

Exploratory leach Input3-Met2				
	Input (wt.%)	**Liquor (wt.%)**	**Extraction (%)**	**HCl consumed (mole)**
Nd	4.91	0.08	8.01	0.002
Fe	50.3	0.38	3.80	0.02
Zn	2.92	0.04	7.53	0.001

The leaching results show that the reactivity of the WEEE is relatively high, as all HCl supplied was consumed (the extraction of minor elements account for the missing 0.001 mole). Based on the extraction rates it can be estimated that Nd and Zn have similar reaction rates and that Fe reacts at about half that rate. None the less, this slower reaction rate is not enough to prevent most of the acid being consumed in the Fe dissolution reaction, as the Fe represents over half the composition of the WEEE. This means that in order to achieve selective leaching, either the leaching conditions must be altered to favour the more rapid reactions, or the reactivity of the Fe must be suppressed.

A way to favour the faster reactions in the system is by leaching with weaker acids or at lower temperatures. Both aim to reduce the overall kinetics of the reactions, which should favour the fastest reactions. As the exploratory HCl leaching was performed at room temperature, it is unlikely that lower temperatures will have any significant influence on the reaction rates. Considering this, a next set of exploratory leaching experiments was performed with the weak acid CH_3COOH (acetic acid). The results of the weak acid leaching can be seen in Table 6.2.

Table 6.2: Extraction of Fe, Nd and Zn for Input3-Met2 CH_3COOH leaching

Leaching solution			Extraction (%)		
acid:water	**acid concentration (M)**	**pH_0**	**Nd**	**Fe**	**Zn**
100:0	17.4	n.a.	16	5.6	16
50:50	8.7	1.91	100	47	32
10:90	1.7	2.66	72	24	20

The initial pH of the solution (pH_0) is calculated using $K_a = 1.76*10^{-5}$ for acetic acid. Note that the 100:0 solution does not contain water, thus its pH cannot be calculated, as the acetic acid cannot dissociate.

The weak acid leaching shows that lowering the reactivity of the leaching solution does favour the Nd dissolution reaction, but only when the reactivity is decreased significantly. The least reactive conditions, [10:90] or 10% acetic acid, show that the extraction rate difference between Fe and Nd increases to a factor 3, from 2 with HCl, implying that the Nd reaction under these conditions is about three times faster than that of Fe. This increase in reaction rate difference is not observed in the more reactive leaching solution of [50:50] experiment. Here the reaction rate difference between Fe and Nd is approximately 2, the same factor as with the HCl experiments, even though the reactivity of this solution, based on H^+ concentration, should be approximately 20x lower than that of the HCl solution. This shows that the decrease in reactivity has to be considerable for the Nd reaction to be favoured over that of Fe. The [50:50] experiment also shows that complete extraction of Nd from the WEEE is possible and does not require aggressive leaching media. The challenge presented here is the selectivity of the extraction, as even mild leaching agents such as acetic acid dissolve almost 50% of the Fe present in the WEEE. The extraction rates of the [100:0] experiments are low for all elements, which likely means that the formed acetates are insoluble in acetic acid (no water present to dissolve in).

The exploratory leaching experiments show that 100% extraction of Nd from the WEEE is possible and that it does not require aggressive leaching media, nor does it require high temperatures or high pressures. The challenge lies with the high reactivity of the other components of the WEEE, mainly Fe

and Zn. To achieve any measure of selectivity during the leaching process a pre-process must be developed in order to reduce the reactivity of these components.

6.3. Improving selectivity of Nd over Fe

The goal of this research is to extract Nd from upgraded ferrous WEEE stream and do so as selectively as possible. The selectivity is important, as it will reduce the number of process steps required to obtain a pure rare earth oxide (REO) phase, which will reduce the overall costs of recycling. It also allows for the residual WEEE to be further recycled for its Fe.

A pre-treatment is proposed to reduce the Fe co-extraction, by reducing the reactivity of Fe and thus enhancing the selectivity. The pre-treatment aims to oxidise the Fe present within the WEEE to its Fe^{3+} state, which is unstable in solution when the pH is higher than 1, for Fe concentration higher than 1 M, and begin to precipitate as $Fe(OH)_3$ (see the E-pH diagram of Fe in Figure 6.3). This, in combination with appropriate leaching conditions which allow for the pH to increase naturally, as the reaction progresses, should decrease the degree of Fe co-extraction. This is the same principle used in magnet recycling when the magnets are roasted where the metallic Fe is converted into its more inert oxides [13]. However, roasting is an energy intensive and costly operation, and additionally the upgraded ferrous WEEE does not lend itself well to roasting due to its small particle size, which could cause sintering or even ignition of fine Nd particles as they are pyrophoric.

As an alternative we propose a water-based corrosion process to oxidise Fe, which is a lot less energy intensive than roasting. The required reaction time for the corrosion is expected to be short, due to the small particle size of the material. If all Fe can be successfully oxidised, diluted acid leaching can be used to extract Nd from the oxidised WEEE while leaving the majority of the Fe behind as solid residue.

From the iron-poor leach liquor Nd can now be extracted through precipitation, instead of having to resort to solvent extraction. With this in mind, the leach acid chosen for this work is H_2SO_4, as it is relatively cheap and is readily available. It also allows for easy double sulphate precipitation of the Nd after leaching. Double sulphate precipitation is the reaction of Na with Nd given as

$$\mathrm{Na^+ + Nd^{3+} + 2SO_4^{2-} \rightarrow (Na, Nd)(SO_4)_{2(s)}} \qquad (6.1)$$

in a sulphate environment. The Na can be provided by either NaOH or Na_2SO_4. This precipitation reaction offers an alternative to the traditional oxalate precipitation, which is more expensive [14].

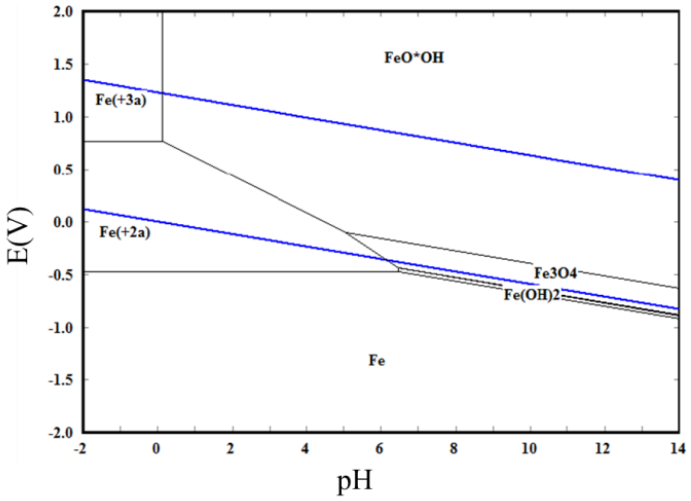

Figure 6.3: E-pH diagram of iron in water at 25°C calculated with HSC 6

6.4. Experimental setup

6.4.1. Oxidation setup

The oxidation pre-treatment was performed in a 1 litre glass reactor equipped with oil bath, condenser and O_2 injection. 100 g batches of upgraded WEEE Input2-Met2, which was characterised in chapter3, were stirred in 500 ml demineralised water under three different conditions (6 h at 80°C, 24 h at 80°C and 24 h at 45°C), while 40 l/h of O_2 was bubbled through the reactor. After the oxidation the WEEE was filtered with a vacuum filter on a 4 µm filtration paper. The oxidised material was then dried overnight at 105°C to remove moisture. The dried samples were analysed with XRD to determine the level of oxidation by comparing their spectra to the base spectrum (see also Figure 3.5). The samples of the conditions that yielded the highest oxidation ratio were selected for leaching experiments.

6.4.2. Leaching setup

Leaching experiments were performed in 100 ml glass reactors for room temperature (21-23°C) experiments and in 250 ml reactors for experiments at elevated temperatures (see Figure 6.4). The diameter of both reactors is identical. The reactors are equipped with overhead stirring, and the 250 ml reactor is also equipped with a condenser and oil bath. Leaching experiments were performed on 20 g batches of the oxidised WEEE. Note that the oxidation pre-treatment results in a dilution of all elements present in the 20 g batches due to mass increase incurred by oxidised Fe.

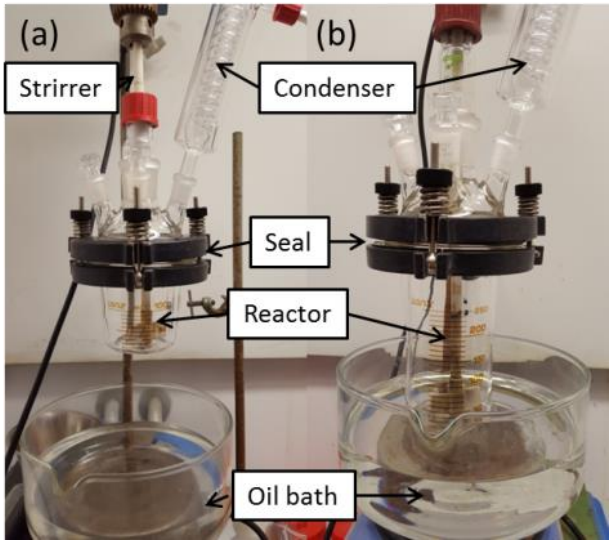

Figure 6.4: Setup of the two reactors used for leaching experiments: **(a)** 100ml; **(b)** 250ml

The leaching conditions were chosen such that only the required amount of acid (stoichiometrically) is supplied to the system to dissolve the reactive non-ferrous elements. Due to the minimal amount of acid that is required, this will allow for the pH of the solution to increase over time, removing most of the Fe that would have been extracted from the leach liquor. Based on the chemical composition of the upgraded WEEE 0.043 mole of H_2SO_4 would be required to dissolve all non-ferrous elements, which (including a 25 % excess) translates to 3 ml of 98.08 wt.% H_2SO_4.

The investigated leaching parameters were temperature and liquid/solid ratio (L/S). The investigated temperatures were 21°C (room temperature), 45°C and 70°C at a constant L/S of 5 and the investigated L/S at room temperature were 2 and 5. For the investigation of the L/S dependence two different approaches were explored: leaching with a constant acid volume and leaching with a constant acid concentration. This is done to account for the stoichiometry of the reactions, as leaching at a lower L/S while maintaining the same acid concentration as at L/S=5 will result in an acid deficit for all nonferrous elements, yet should still supply enough acid for the Nd dissolution.

During leaching the liquor was sampled at times 1, 5, 10, 15, 30, 45, 60, 90, 120, 240 and 360 min. The samples taken were immediately syringe filtered (0.45 µm) to quickly remove the solids from the sample and prevent further reaction. They were diluted with 3 wt.% HNO_3 to ensure that no precipitation takes place in the sample before the analysis. The samples were analysed in triplicate with ICP-OES.

The chemical composition of Met-2 material used in the leaching experiments is shown in Table 6.3. (identical to Table as Table 3.10 in chapter 3.4.2.2.)

Table 6.3: Elemental composition in wt.% of the upgraded WEEE analysed with ICP-OES, average over 4 samples

Element	Fe	Zn	Mn	Ca	Cu	Ni	Si
Average concentration (wt.%)	58	7.5	3.12	2.4	2.0	1.16	1.00
Standard deviation (σ, wt.%)	2	0.2	0.04	0.2	0.1	0.03	0.06
Element	**Nd**	**Al**	**Pb**	**Mg**	**Pr**	**Sm**	**Dy**
Average concentration (wt.%)	0.99	0.55	0.5	0.260	0.16	0.07	0.030
Standard deviation (σ, wt.%)	0.01	0.02	0.5	0.003	0.01	0.04	0.002

6.4.3. Precipitation setup

The precipitation experiments were performed in a glass beaker on a hot plate equipped with magnetic stirring. Leach liquors were re-acidified prior to precipitation to control the pH during the reaction and to prevent undesired side reactions. The precipitation agents used were Na_2SO_4 and NaOH. Both of these precipitation agents were also compared to the classical $H_2C_2O_4$ to observe their effectiveness.

Precipitation was performed at 70°C, as the solubility of $(Na,Nd)(SO_4)_2$ decreases with increasing temperature [15]. Precipitation experiments were run for 24 h with a large excess of precipitation agent (25 times the stoichiometry). The initial pH of the solution was set at 0, 0.5 and 1 to determine its influence on the purity of the precipitates. The precipitates were recovered on a 4 µm filtration paper and dried at 105°C. Afterwards they were analysed with XRD and SEM/EDS, followed by re-dissolution in HNO_3 for ICP-OES analysis to measure their purity.

6.5. Results and discussion

6.5.1. Oxidation pre-treatment

The results of the XRD analysis of samples taken from the three oxidation conditions can be seen in Figure 6.5.

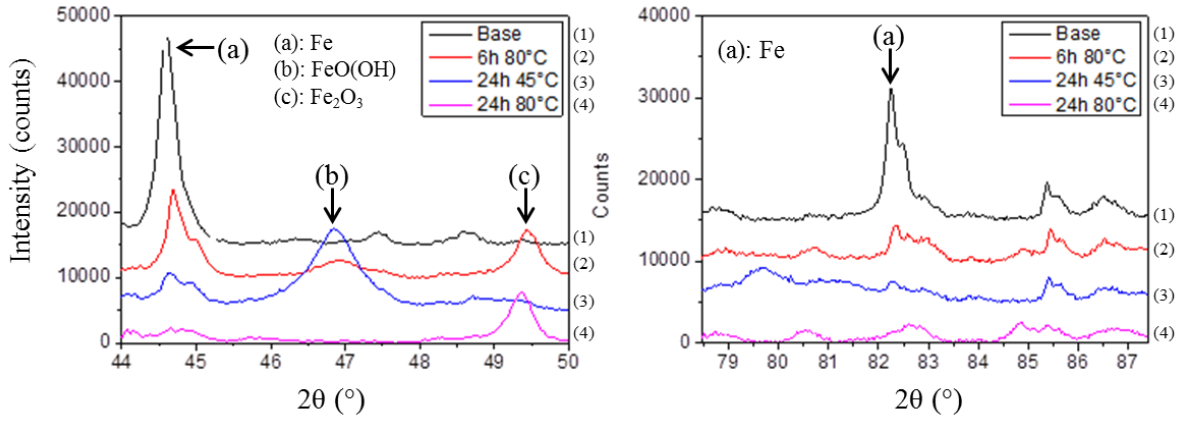

Figure 6.5: Approximation of the degree of Fe oxidation by comparison of the metallic Fe peak intensity in the XRD spectra of the three oxidation conditions (24h at 45°C, 6h at 80°C and 24h at 80°C) to the base spectrum (Figure 3.5) at 2θ 44°…50° and 2θ 79°…87°

By comparing the spectra and evaluating the difference in intensity of the metallic Fe peaks a measure for the degree of oxidation can be calculated by taking the ratio of the intensity of the metallic Fe peak before and after oxidation, see Table 6.4. For the conditions [24 h at 45°C], [6 h at 80°C] and [24 h at 80°C], this yields oxidation ratios of 83%, 59% and 93% respectively.

Table 6.4: Peak intensities of the measured Fe peaks of the XRD spectra and the calculated oxidation ratios

	Base	24h 45°C	6h 80°C	24h 80°C
Peak intensity (counts)	33000	5760	13500	2380
σ	182	76	116	49
Oxidation ratio (%)		83	59.1	93

σ	1	0.9	2

This shows that the condition of 24 h and 80°C is the optimum of the tested cases, suggesting that the oxidation takes some time to complete. It should be noted that none of the three conditions leads to a total oxidation of the Fe, which indicates that some of the Fe is likely stainless steel, a common component of WEEE. This would also explain the presence of Ni (Table 6.3), which does not show up as a separate component in the XRD spectra. The oxidation ratios show that time has a greater influence than temperature on the level of oxidation, as higher oxidation rates are achieved in 24h at 45°C than in 6h at 80°C. Temperature determines which oxidation product is formed. At 45°C the main oxidation product formed is FeO(OH), while at 80°C it is Fe_2O_3. As the highest oxidation ratios were achieved at 24 h and 80°C this oxidation condition was chosen to produce the samples for the leaching experiments.

The oxidation pre-treatment also has an influence on the particle size distribution, shown in Figure 6.6, of the upgraded WEEE. As iron corrodes the oxidation product ($Fe(OH)_3$/Fe_2O_3) only loosely adheres to the surface of the iron and can be easily stripped away through the agitation induced by the stirring of the oxidation tank. This both ensures that fine particles are formed in the residue and also ensures that the oxidation process can continue unhindered by a forming product layer (as was the case in the NaOH conversion of monazite).

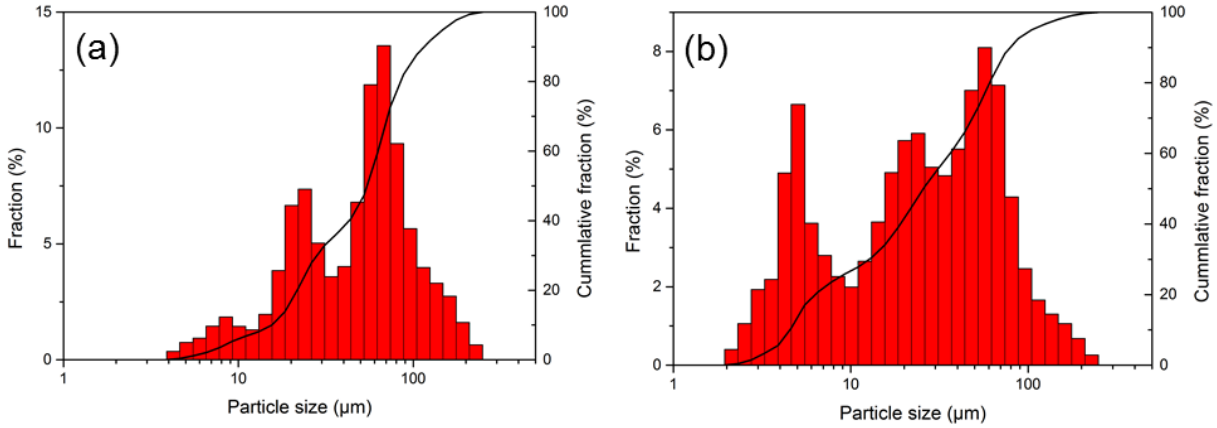

Figure 6.6: PSD plot of the **(a)** non-oxidised WEEE and **(b)** the oxidised WEEE

To quantify the change in particle size distribution, the d_{25}, d_{50} and d_{90} of the non-oxidised and oxidised WEEE are compared. The d_x value of a powder stands for the x % of particles that have a size smaller or equal to the d_x value (e.g. a d_{90} of 80 µm means that 90 % of particles have a particle size of 80 µm or less).

Table 6.5: Change in particle size (µm) measured in function of d_{25}, d_{50} and d_{90}

	Particle size (µm)	
	Non-oxidised	**Oxidised**
d_{25}	25	9
d_{50}	55	26
d_{90}	124	80

By comparing the d_{25}, d_{50}, and d_{90} of the non-oxidised and oxidised WEEE, see Table 6.5., it becomes

clear that the oxidation process resulted into a substantial decrease in average particle size. If the d_{50} value is considered the average particle size (i.e. 50% of particles are this size or smaller), then the oxidation process halves (55 µm vs 26 µm) the average particle size of the upgraded shredded WEEE.

6.5.2. Leaching results

6.5.2.1. Leaching at room temperature

The extraction profile of Nd and Fe at room temperature with L/S=5 is presented in Figure 6.7. The extraction profile shows a relatively rapid overall reaction which stabilises after about 90 min. Nd extraction is significant with a final extraction ratio of 90% under the current conditions. During the initial 30 min the reaction appears to be quite unstable due to the great sensitivity to the sampling time. The extraction of Fe was not fully prevented, but was limited to 21% (opposed to the 50-80% without oxidation).

To verify the consistency of the leaching setup the room temperature experiments was run in triplicate and the samples taken were also measured in triplicate. Analysis of the results shows that the variance observed between the samples of a single experiment is of the same magnitude as the variance observed between the samples of the three experiments. This shows that considering the analysis variance the leaching setup is quite consistent and that in the interest of reliable results it is more important to measure each sample in triplicate than it is to run each experiment in triplicate. As it is not feasible to measure 9 samples per data point priority was given to measuring in triplicate instead of running each experiment in triplicate.

Based on the observed pattern of the data points an interpolation based on inverted exponential decay was applied to quantify the leaching characteristics of Nd and Fe. The base formula of the interpolation takes the form

$$R_x = \alpha * (1 - \exp(-\beta * t)) \tag{6.2}$$

where R_x (x = Nd/Fe) is the extraction ratio of Nd or Fe in % and t the time in min. The coefficients α and β give a measure for the final extraction ratio (α) of the element and its rate of extraction (β). Applying this interpolation, using OriginPro 9, to the data points yields α = 89.6% and 20.7%, and β = 0.91 min^{-1} and 0.08 min^{-1} for Nd and Fe respectively.

$$R_{Nd} = 89.6\% * (1 - \exp(-0.91\ min^{-1} * t)\ ) \tag{6.3}$$

$$R_{Fe} = 20.7\% * (1 - \exp(-0.08\ min^{-1} * t)) \tag{6.4}$$

Based on these expressions and the extraction profile it is clear that Nd reacts faster than Fe. Defining that the total process has stabilised when the Fe extraction ratio reaches 95% of its final value we obtain a necessary reaction time of 37 min. Theoretically the reaction does not have to stabilise, and if we determine the time required for Nd extraction to reach 95% of its final value a greater selectivity of Nd can be achieved. Based on the interpolations Nd extraction reaches 95% of its final value in 3.3 min, at which time the Fe extraction is calculated to be only 4.8% instead of its maximum extraction ratio of 21%.

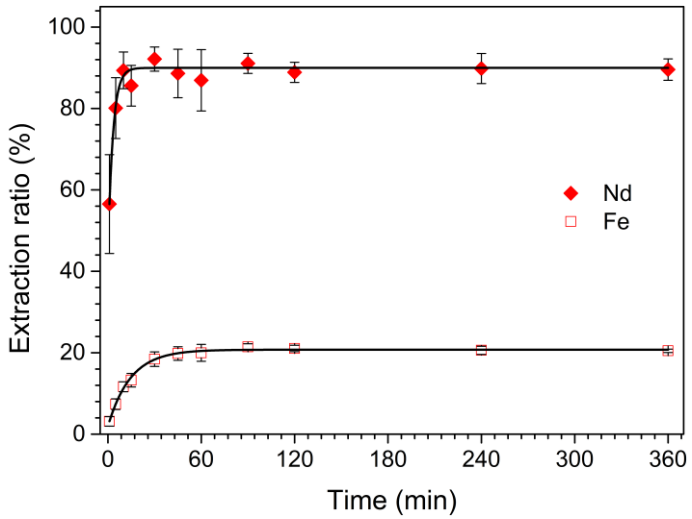

Figure 6.7: Extraction profile of Fe and Nd for room temperature leaching at L/S = 5. Some error bars of the Fe profile are smaller than the mark of the data point

All final extraction ratios of the leached elements after a reaction time of 360 min are listed in Table 6.6. All REEs associated with NdFeB magnets (Nd, Pr and Dy) show high extraction ratios, while the Sm extraction ratio is only 21%. The other elements (other than Fe) with considerable extraction ratios are Cu and Zn, however these two elements can potentially be removed with a prior ammonia leaching. Despite the extraction of other elements, it is clear that this leaching process with oxidative pre-treatment has a relatively high selectivity for Nd (and other REE present in the magnet particles). The concentration of Nd in the leach liquor after leaching under these conditions is 1.77 g/L.

Table 6.6: Extraction ratios of all extracted elements at room temperature leach conditions and L/S = 5, after 360 min

	Nd	Dy	Pr	Cu	Sm	Fe	Zn	Ca
Extraction (%)	90	90	62	47	20	20.8	15	13
σ	3	40	7	6	16	0.7	2	3

6.5.2.2. Influence of temperature

The influence of temperature is observed by comparing the extraction profiles of Fe and Nd at 45°C, 70°C and room temperature, and the results are shown in Figure 6.8. For clarity the error bars of the room temperature profile are not shown, however this profile is identical to that shown in Figure 6.7 and the level of error shown there is representative.

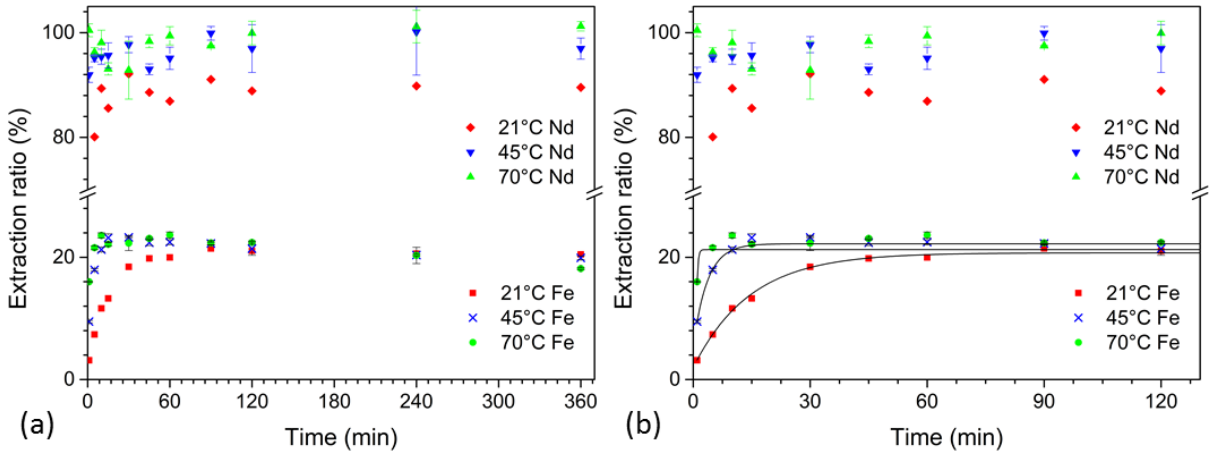

Figure 6.8: (a): Comparison of extraction profiles of Fe and Nd for 21°C, 45°C and 70°C; **(b):** Enhanced view of the first 100 min of the experiments with interpolation curves for Fe, some error bars are smaller than the mark of the data point. For clarity a break was placed on the y-axis and the error bars for the 21°C data points were removed

The increase in leaching temperature has two clear effects; first it increases the overall reaction rate. Applying the same exponential fitting used for the room temperature experiments (Figure 6.7) shows that the Fe dissolution reaction reaches 95% completion at 6.7 min at 45°C (α = 22.06% and β = 0.45 min^{-1}) and 2.2 min (α = 21.25% and β = 1.39 min^{-1}) at 70°C, which is a considerable decrease from the 37 min required at room temperature. The Nd profiles cannot be fitted to interpolation equation (2), which indicates that at elevated temperatures this reaction finishes before the first sample (at 1 min) can be taken. This also means that increasing the selectivity reaction by stopping the reaction early becomes more challenging at higher temperatures as reaction times will be shorter than 1 min.

The second effect is that the Nd extraction has been driven to near total extraction with 95% at 45°C and 99% at 70°C. The maximum Fe extraction on the other hand has not increased; although the Fe extraction reaches 20% more quickly at higher temperature, it does not exceed it, in fact after 360 min it even decreases to 19% at 70°C. This decrease in Fe concentration over time suggests the possibility of precipitation of Fe^{3+}. However, this cannot be verified due to inability to differentiate between precipitated $Fe(OH)_3$ and the undissolved $Fe_2O_3/Fe(OH)_3$ formed during the oxidation pre-treatment.

The minor decrease in Fe extraction of time and minor overall increase of Nd extraction shows that the temperature only has a minor influence of the system. The most prominent effect temperature has is the rate at which equilibrium is achieved.

The extraction ratios of all extracted elements are displayed in Table 6.7. With increasing temperature higher extraction ratios of the Cu, Pr, and Dy are also observed, while Zn, Sm and Ca appear relatively unaffected.

Table 6.7: Extraction ratios of all extracted elements during leaching at 45°C and 70°C

All extraction ratios 45°C leach								
	Ca	Cu	Dy	Fe	Nd	Pr	Sm	Zn
Extraction (%)	12	54	100	19.9	95	67	20	13.0
σ	1	3	27	0.6	2	6	12	0.4
All extraction ratios 70°C leach								
	Ca	Cu	Dy	Fe	Nd	Pr	Sm	Zn

Extraction (%)	14	54	100	18.5	99	73	20	13.4
σ	2	3	50	0.5	1	8	12	0.6

6.5.2.3. Influence of liquid/solid ratio

The influence of the liquid/sold ratio is observed by comparing the extraction profiles of both the constant acid volume, Figure 6.9 (a), and the constant acid concentration, Figure 6.9 (b), approaches at L/S = 2 to the extraction profile at L/S = 5 at room temperature.

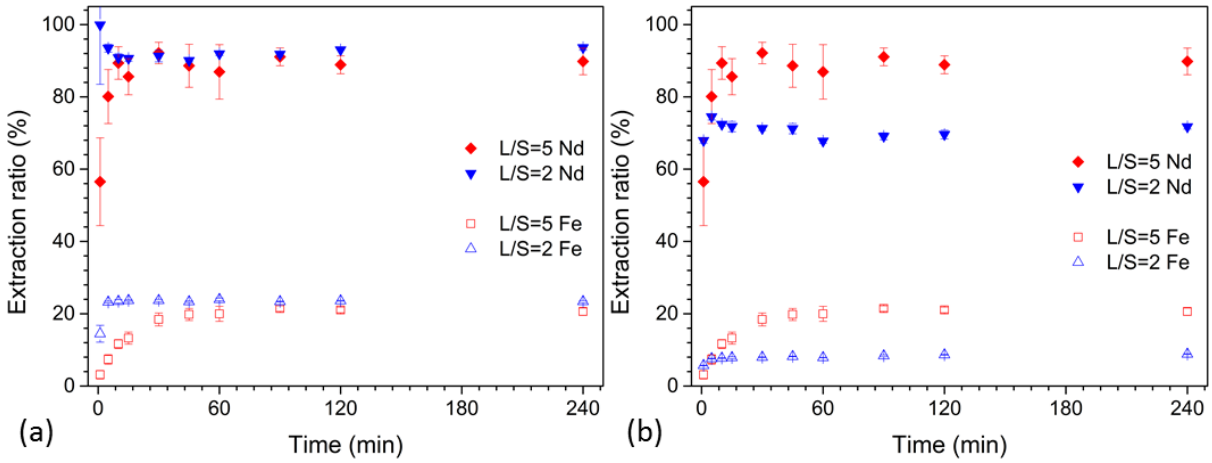

Figure 6.9: (a): Extraction profile L/S=2 vs L/S=5 using constant acid volume; **(b):** Extraction profile L/S=2 vs L/S=5 using constant acid concentration, both at room temperature

When leaching with a constant acid volume (Figure 6.9 (a)) a decrease in L/S from 5 to 2 manifests as an increase in leaching rate. The decreased L/S combined with the same acid volume translates to leaching at a higher acid concentration (0.53 M to 1.325 M), leading to increased leaching kinetics. For the process this means that stability is reached quickly and fitting shows that the time required for Fe dissolution to reach 95% completion is 3.3 min (α = 23.48% and β = 0.92 min^{-1}) opposed to the 42.3 min at L/S = 5. This shows that kinetically the increased acid concentration has a similar effect as raising the temperature to 70°C. However, other than increasing the leaching rate the liquid/solid ratio does not affect the stabilised extraction ratios (as they were at higher leaching temperatures), meaning that increasing the temperature leads to superior results, compared to decreasing the L/S (using the same acid volume).

When the acid concentration is kept constant (Figure 6.9 (b)) for leaching at L/S = 2 the differences in leaching behaviour are more pronounced. Both Nd and Fe extraction ratios are considerably lower than they were at L/S = 5, 72% vs 90% for Nd and 9% vs 21% for Fe. This indicates that the other nonferrous elements, in combination with the reaction of Fe, consume too much of the available acid to ensure a high Nd extraction ratio. A summary of the major extracted elements for both approaches can be seen in Table 6.8. From these results it can be observed that Zn and Fe dissolution decreases more rapidly with a lower acid volume than that of Nd. Cu does not dissolve at all under these conditions, showing that for this system Nd is more reactive than these elements and that a lower acid volume leads to higher leaching selectivity for Nd. The Ca extraction ratio however has not been negatively affected, implying that Ca is the most reactive element in this system. It also clearly shows that the acid volume is the determining factor for the level of Fe extraction; acid concentration does not contribute to the Fe extraction ratio. Considering this, to ensure an efficient Nd recovery the

initially proposed acid volume (enough to ensure stoichiometry for the nonferrous elements) is necessary. Lower acid volumes, while improving selectivity, do not yield sufficient Nd extraction.

Table 6.8: extraction ratios of the major elements during leaching at L/S=2, using constant acid volume and using constant acid concentration

	L/S= 2 with constant acid volume				
	Ca	Cu	Fe	Nd	Zn
Extraction (%)	11	45	23.8	94	15.5
σ	1	3	0.7	1	0.5
	L/S= 2 with constant acid concentration				
	Ca	Cu	Fe	Nd	Zn
Extraction (%)	17	0.0	8.9	72	8.8
σ	5	0.7	0.3	1	0.2

The reduced L/S does lead to a higher concentration of Nd in the leach liquors, 4.6 g/L and 3.5 g/L respectively. However, as the results of the next section will show, this increase is not necessary to ensure high Nd recovery rates. The achieved concentration of 1.7 g/L at L/S = 5 is sufficient for recovery.

6.5.3. Precipitation results

6.5.3.1. NaOH vs Na_2SO_4 vs $H_2C_2O_4$

Table 6.9 shows the effect of NaOH, Na_2SO_4 and $H_2C_2O_4$ on the purity of the obtained precipitates, when they are used as a precipitation agent to recover Nd. The precipitation agent was added to a pregnant leach liquor at 70°C for 24 h, with only minor re-acidification of the solution. From these results it becomes clear that, under the present conditions, NaOH and $H_2C_2O_4$ are not suitable as precipitation agents, as the precipitates are heavily contaminated with Fe. For NaOH this is due to the increasing pH that occurs due to the addition of the NaOH, which leads to the formation of $Fe(OH)_3$ and $Fe(OH)_2$ by-products during the precipitation process. The use of NaOH also eliminates any possibility of recovering the acid from the leach liquor. $H_2C_2O_4$ has an affinity for Fe and can form iron oxalates at 70°C if the pH is not sufficiently suppressed, which leads to the Fe contamination observed in the recovered oxalates. Na_2SO_4 on the other hand shows a far lower, but still considerable, Fe contamination and was thus selected as the precipitation agent for further experiments.

Table 6.9: Comparison in purity of precipitates formed with NaOH, Na_2SO_4 and $H_2C_2O_4$

	Fe	**Nd**	**Zn**	**Cu**
	wt.%	wt.%	wt.%	wt.%
Na_2SO_4	3.26	19.1	0.23	0
NaOH	22.5	14.5	1.68	0
$H_2C_2O_4$	24.6	7.0	8.0	8.3

6.5.3.2. Influence of starting pH

The influence of the starting pH is shown in Table 6.10. It is clear that, when the leach solution is heavily re-acidified, it is possible to fully remove the Fe contamination from the formed double sulphates. This is most likely due to the increased solubility of Fe^{3+} (see the E-pH diagram in Figure 6.3) at these low levels of pH. The major contaminants still remaining in the precipitates are Zn (unaffected by pH) and

Ca, which decreases with pH, but is not eliminated. The Nd recovery as double sulphate at pH=0 is 92%, implying that not all Nd is recovered using this method.

Table 6.10: Chemical analysis of precipitates formed at pH 0, 0.5 and 1 after precipitation with Na_2SO_4

	Ca	Fe	Dy	Nd	Pr	Zn
	wt.%	wt.%	wt.%	wt.%	wt.%	wt.%
pH=0	0.88	0.00	0.39	30.3	3.11	0.28
pH=0.5	1.61	0.00	0.28	17.8	1.86	0.29
pH=1	1.62	13.8	0.14	14.7	1.54	0.31

As lowering the pH has a positive influence on the purity of the double sulphates, its effects on purity of Nd oxalates is also investigated. The results are shown in Table 6.11.

Table 6.11: Chemical analysis of precipitates formed at pH 0.15 after precipitation with $H_2C_2O_4$

	Ca	Fe	Dy	Nd	Pr	Zn	Cu
	wt.%	wt.%	wt.%	wt.%	wt.%	wt.%	wt.%
pH=0.15	0.0	0.0	0.7	23.6	1.9	0.9	26.6

By performing the precipitation at a pH of approx. 0 (measured value 0.15) the co-precipitation of Fe and Ca can be eliminated, however the co-precipitation of Cu and Zn cannot. Based on these results it is concluded that Na_2SO_4 is the optimal precipitation agent for this system. However, the argument can be made that if Zn and Cu are removed from the system via a pre-processing step (i.e. ammonia leaching, see chapter 6.7.1), then oxalic acid becomes a viable alternative to Na_2SO_4.

6.5.3.3. Precipitate characterisation

SEM analysis, illustrated in Figure6.10 (b), of the obtained precipitates shows that they form needles with an average length of 5-7 µm and a thickness approximately 1 µm. Due to this fine size complete capture of the precipitates is challenging. XRD analysis, Figure6.10 (a), of the precipitates reveals two phases: $(Na,Nd)(SO_4)_2$ (unmarked peaks) and $Ca(OH)_2$ (peaks marked with red arrows). No Zn phase was detected with XRD.

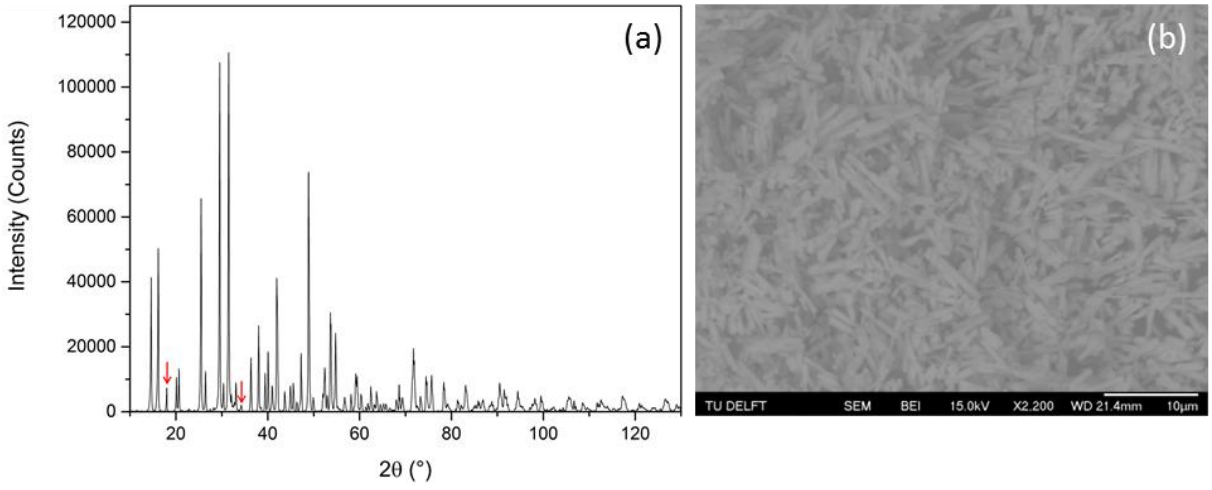

Figure 6.10: (a): XRD analysis of formed precipitates, all peaks (save those marked with red arrows) belong to the $(Nd,Na)(SO_4)_2$ spectrum, the marked peaks are of the $Ca(OH)_2$ spectrum; **(b):** SEM image of the formed precipitates, showing that they take a needle shape

6.6. Construction of a process flowsheet

6.6.1. The flowsheet

Based on the results obtained from the experiments a flowsheet for the hydrometallurgical recovery of Nd can be constructed. The established flowsheet and its implementation into a general WEEE recycling process are illustrated in Figure 6.11. The process design interlinks the oxidation and leaching steps by oxidising the upgraded ferrous WEEE at the required liquid/solid ratio and then adding a small volume of concentrated acid to initiate the leaching step when oxidation has been completed. This conserves the heat of the oxidation and eliminates a filtration step. The preserved heat allows for rapid leaching (1-5 min), after which the pregnant leach solution is filtered and transferred to a precipitation tank. While oxidation experiments were run with pure O_2, this should not be required for a larger scale process. With proper mixing and reactor design, air is expected to work just as well as the oxidising agent. With proper isolation to conserve heat during filtration it should be possible to run the entire process without any external heating and solely use the heat produced due to oxidation of the Fe during the oxidation process. Based on the obtained results this process yields an 91% overall Nd extraction and Nd is recovered as $(Na,Nd)(SO_4)_2$ crystals with minor impurities of Ca (8800 ppm) and Zn (2800 ppm).

The $(Na,Nd)(SO_4)_2$ crystals are considered the end product of the process proposed in this work. Currently the traditional method of converting these double sulphates to oxides involves dissolution, and then re-precipitating them as oxalates and then calcining the oxalates. Alternatively, the double sulphates can also be converted to NdF_3 for further metal production. More work will be done in the future to find an energy and cost-effective method to convert the double sulphates to oxides and/or fluorides.

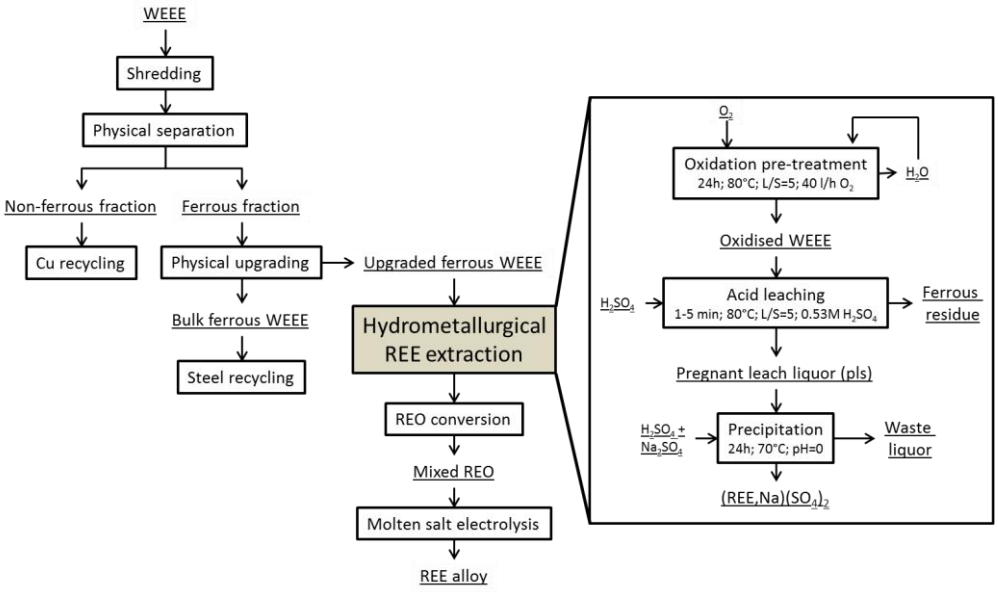

Figure 6.11: Flowsheet for the hydrometallurgical Nd recovery process based on the results of the performed experiments and insertion of the process in the overall flowsheet

6.6.2. Waste management

The waste management strategy for this flowsheet differs from the one proposed for the mine tailings processes in two ways: (1) greater amounts of solid waste and (2) sulphate-based waste waters.

The greater amount of solid waste is a result of the selectivity for Nd over Fe in the proposed flowsheet. Based on the experimental work only 25% of the input material is dissolved and the rest is left as an $Fe(OH)_3$ residue. This only considers the residue left after leaching, during the waste water treatment the co-dissolved Fe will also precipitate out as $Fe(OH)_3$. Together, this leads to almost 90% of the input being discarded as $Fe(OH)_3$ residue. Landfilling this residue is an option, but the presence of heavy metals (e.g. 0.5 wt.% of Pb) in the residue means that caution must be exercised when taking this route. A more effective method of dealing with this waste would be utilising it in Fe production. Although there is currently no desire from the recycling industry to process this type of material, it may be a useful Fe resource in the future.

The sulphate-based waste waters on the other hand are easily treated with traditional water treatment. As discussed in chapter 5.6.2, adding lime (CaO) to sulphate-based waste water both neutralises the left-over acid and removes the heavy metals. This results in a gypsum solid waste product and waste water that can be processed by municipal waste water treatment. There is one waste water stream for which an additional process step is required: the waste liquor after precipitation. This waste liquor has a high Na concentration (±50 g/L), which does not precipitate during lime neutralisation, as the reaction

$$Na_2SO_4 + Ca(OH)_2 \rightarrow CaSO_{4(s)} + 2\,NaOH \tag{6.5}$$

has a Δ*G* of +83 kJ/mol (at 20°C calculated with HSC 6.0). This means that the sulphates associated with the Na cannot be precipitated as $CaSO_4$ and remain in solution. A potential solution to this problem is to add HCl to the system. The reaction

$$Na_2SO_4 + 2\,HCl + Ca(OH)_2 \rightarrow CaSO_{4(s)} + 2\,NaCl + 2\,H_2O \tag{6.6}$$

has a Δ*G* of −144 kJ/mol (at 20°C calculated with HSC 6.0), thus enabling the sulphate removal. This option does not remove the Na, but a NaCl solution can be discharged to marine environments (provided the other contaminants, such as the dissolved heavy metals are removed). Na_2SO_4 cannot be discharged this way.

An alternative solution for the high Na concentration is recuperating it as crystallised Na_2SO_4. As shown by eq. (6.5) Na_2SO_4 does not precipitate due to lime addition. This does not prevent the neutralisation with lime from removing the other contaminants and the free acid. This means that after lime neutralisation a relatively pure Na_2SO_4 solution should be retained. This solution can be evaporated to crystallise the Na_2SO_4 and recover it as a solid material. It can then be re-used in the $(Nd,Na)(SO_4)_2$ precipitation process. The evaporated water can be condensed and used again in the oxidation process.

This solution also compensates for a weakness in the precipitation process: the large amount of excess Na_2SO_4 required to precipitate the $(Nd,Na)(SO_4)_2$. The experiments have shown that an excess 25 times is required, and most of this Na_2SO_4 is lost to the waste stream. If this Na_2SO_4 is recovered at a sufficient purity, the actual consumption is reduced to the stoichiometric requirement for $(Nd,Na)(SO_4)_2$

precipitation. The waste water and gypsum production would also be decreased if the Na_2SO_4 is recovered this way. Figure 6.12 shows the theoretical expansion of the flowsheet to reduce Na_2SO_4 consumption and minimise waste water generation

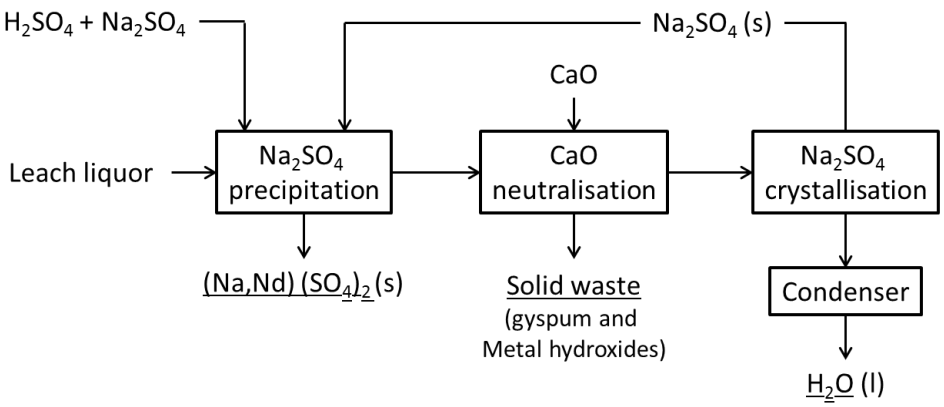

Figure 6.12: Theoretical expansion of the flowsheet to reduce Na_2SO_4 consumption and minimise waste water generation

6.6.3. Further development of the flowsheet: Cu and Zn recovery through ammonia pre-leaching

Ammonia leaching is mature technology that can recover up to 90% of the Cu and 70% of Zn in traditional WEEE recycling [16]. It could potentially be added to the developed process in order to both valorise the Cu present and also remove Zn to reduce the impurities levels in the final precipitates. The use of ammonia would not incur much extra cost chemical wise, as the ammonia can be recovered during the electrowinning of Cu. However, the inclusion of ammonia leaching would require the use of an extensive washing step, to be placed between the ammonia leaching and the H_2SO_4 leaching of Nd. No ammonia should be present during the H_2SO_4 leaching as ammonia, like Na_2SO_4, can serve as a precipitation agent for $(NH_4,Nd)(SO_4)_2$ double sulphates, which can negatively impact the extraction of Nd during leaching.

In case an ammonia leaching step proves beneficial, the question becomes where in the flowsheet in the process should be inserted. It must naturally be placed before the H_2SO_4 leaching step, but whether it should be placed before the oxidation step or after remains to be investigated. Placing the ammonia leaching step before the oxidation step means that the washing step needed to remove the ammonia could be combined with the oxidation process, thereby eliminating a process step. Placing the ammonia leach after the oxidation step could facilitate the Cu extraction as it is likely that the Cu has been (partially) oxidised already during the oxidation process, thereby reducing the amount of oxidising agent required for extraction.

An exploratory leach using a 0.75M NH_4OH / 0.75M $(NH_4)_2CO_3$ solution (which is about 2x the stoichiometric requirement), at room temperature and with air bubbling (70 L/h), was performed on both oxidised and non-oxidised WEEE. The results of this leach are shown in Figure 6.13.

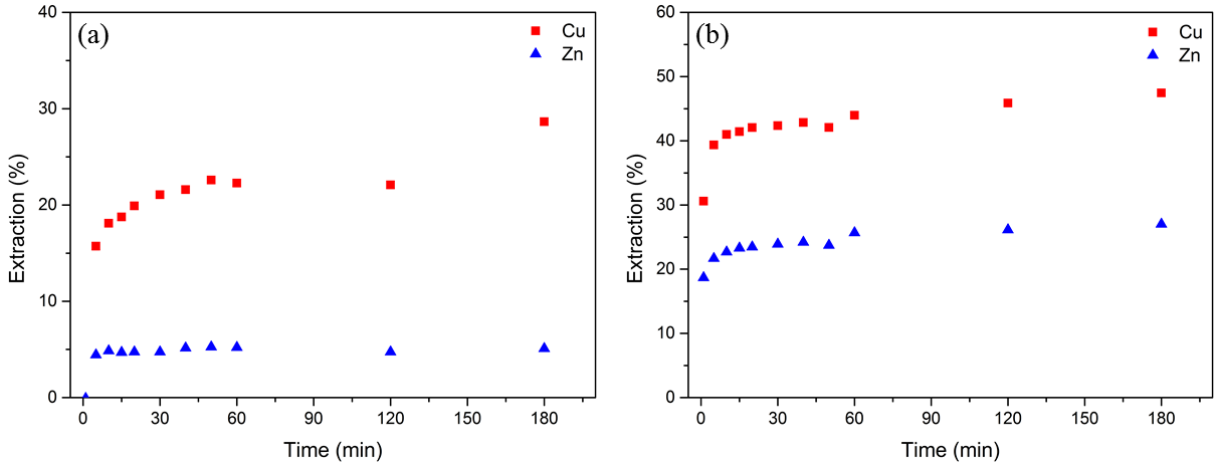

Figure 6.13: Exploratory ammonia leaching results of (a) oxidised WEEE and (b) non-oxidised WEEE, showing Cu and Zn extraction

The results show that, even with two times the required amount of ammonia, the extraction rates of Cu and Zn are low, both for the non-oxidised WEEE and the oxidised. However, the extraction rates for the non-oxidised WEEE (Figure 6.13 (b)) are higher than those of the oxidised WEEE, which indicates that should an ammonia leach be included in the process it is best placed before the oxidation process. The reason for this difference in unknown at this time, but could serve a starting point for future research.

There is of course also the argument of combining the oxidation process and the ammonia leaching process into one process step. However, the exploratory leaching tests quickly showed that this is not possible. The required process time and temperature for Fe oxidation are not compatible with ammonia leaching. Analysis after 24 h of oxidation at 70°C with ammonia shows less than 5% of Cu extraction was extracted.

6.7. Conclusions

Based on the obtained experimental results the following conclusions can be drawn:

- Nd is a very reactive component in the upgraded ferrous WEEE and can be successfully leached even with weak acids like CH_3COOH. However, Fe also shows a high reactivity which results in high co-extraction rates.
- Oxidation of the Fe in the upgraded ferrous WEEE is necessary to achieve a good leaching selectivity towards Nd.
- The Fe can be successfully oxidised using a water corrosion process. To achieve an oxidation ratio of more than 90% the WEEE should be stirred in water for 24 h at 80°C while providing an O_2 supply (through bubbling) of 40 l/h. (At industrial scale air is a viable alternative to O_2.)
- Nd can be successfully leached from the oxidised WEEE by supplying the minimal amount of H_2SO_4 that meets the stoichiometric requirements for dissolution of all nonferrous elements present in the upgraded ferrous WEEE.
- The temperature of the leaching process strongly affects the rate of the dissolution of both Fe and Nd. Increasing temperature decreases the time required to reach stability (maximum recovery) from 37 min at room temperature to 6 min at 45°C and to 2 min at 70°C.

- Selectivity towards Nd can be increased by halting the reaction before the Fe reaction reaches stability, however this becomes increasingly difficult as temperature increases.
- The influence of temperature on the total metal extraction is less pronounced, but still important. While 90% Nd extraction can be achieved at room temperature, the total Nd recovery can be increased to 99% at 70°C. While the total dissolution rate of Fe decreases from 21% at room temperature to 18.5% at 70°C.
- A decrease in liquid/solid ratio (L/S) from 5 to 2 while maintaining the required acid volume only increases the rate of the reaction; it does not increase the final extraction of Nd or Fe.
- A decrease in liquid/solid ratio (L/S) from 5 to 2 while maintaining the same acid concentration, thus leaching with an acid deficit, increases the selectivity of the leaching process towards Nd, by reducing the dissolved Fe from 21% to 9%. However, this is accompanied with a decrease of the Nd extraction to 72% compared to 90% achieved at L/S=5.
- The supplied acid volume based on the stoichiometric requirement is the key factor that determines the Nd and Fe extraction, while temperature and acid concentration have only a minor influence.
- The Nd can be recovered from the leach liquor via addition of Na_2SO_4. For optimal recovery and precipitate purity, the leach liquor must be re-acidified with H_2SO_4 to a pH of at least 0. This allows for the recovery of 92% of the Nd in the leach liquor as $(Na,Nd)(SO_4)_2$ with minimal impurities of Ca (8800 ppm and Zn (2800 ppm).
- The consumption of Na_2SO_4 can be minimised by crystallising the waste liquor after removing the impurities with lime.
- The obtained experimental results allow for the construction of a process flowsheet with a projected Nd recovery of over 90%.
- An ammonia-based pre-process to extract Cu and Zn could potentially be added to the flowsheet. Should it be included, it would need to be placed before the oxidation step as the oxidation process has a negative influence on the extraction rate of Cu and Zn.

References

[1] K. Binnemans et al., “Recycling of rare earths: a critical review,” J. Clean. Prod., vol. 51, pp. 1–22, 2013.

[2] S. Hoenderdaal, L. Tercero Espinoza, F. Marscheider-Weidemann, and W. Graus, “Can a dysprosium shortage threaten green energy technologies?”, Energy, vol. 49, pp. 344–355, 2013.

[3] F. Cardarelli, “Materials Handbook: A Concise Desktop Reference,” in Materials Handbook: A Concise Desktop Reference, Springer Science & Business Media, p. 224, 2013.

[4] M. A. Alam, L. Zuga, and M. G. Pecht, “Economics of rare earth elements in ceramic capacitors,” Ceram. Int., vol. 38, no. 8, pp. 6091–6098, 2012.

[5] C. Tunsu, T. Retegan, and C. Ekberg, “Sustainable processes development for recycling of fluorescent phosphorous powders–rare earths and mercury separation: A literature report,” Chalmers University of Technology, 2012.

[6] M. Humphries, “Rare Earth Elements: the global supply chain,” Congressional Research Service, CRS Report for Congress, 2013.

[7] S. Peelman, Z. H. I. Sun, J. Sietsma, and Y. Yang, “Hydrometallurgical extraction of rare earth elements from low grade mine tailings,” in Rare Metal Technology 2016, Springer, pp. 17–29, 2016.

[8] S. Massari and M. Ruberti, “Rare earth elements as critical raw materials: Focus on international markets and future strategies,” Resour. Policy, vol. 38, no. 1, pp. 36–43, 2013.

[9] J. W. Lyman and G. R. Palmer, “Recycling of Neodymium Iron Boron Magnet Scrap”, Bureau of Mines US, 1993.

[10] K. Baba, Y. Hiroshige, and T. Nemoto, “Rare-earth Magnet Recycling,” Hitachi Rev., vol. 62, no. No. 8, pp. 452–456, 2013.

[11] C. Hagelüken, “Recycling of Electronic Scrap at Umicore’s Integrated Metals Smelter and Refinery,” World Metall. - ERZMETALL, vol. 59, pp. 152–161, 2006.

[12] “REEcover.” [Online]. Available: https://cordis.europa.eu/project/rcn/110976_en.html (retrieved 09/09/2018)

[13] T. Vander Hoogerstraete, B. Blanpain, T. Van Gerven, and K. Binnemans, “From NdFeB magnets towards the rare-earth oxides: a recycling process consuming only oxalic acid,” RSC Adv., vol. 4, no. 109, pp. 64099–64111, 2014.

[14] Y. M. Khawassek, A. A. Eliwa, E. A. Gawad, and S. M. Abdo, “Recovery of rare earth elements from El-Sela effluent solutions,” J. Radiat. Res. Appl. Sci., vol. 8, no. 4, pp. 583–589, 2015.

[15] M. Tanaka, T. Oki, K. Koyama, H. Narita, and T. Oishi, “Chapter 255 - Recycling of Rare Earths from Scrap,” in Handbook on the Physics and Chemistry of Rare Earths, vol. Volume 43, Jean-Claude G. Bünzli and Vitalij K. Pecharsky, Ed. Elsevier, pp. 159–211, 2013.

[16] Y. Xiao et al., “Hydrometallurgical recovery of copper from complex mixtures of end-of-life shredded ICT products,” Hydrometallurgy, vol. 140, no. Supplement C, pp. 128–134, 2013.

Chapter 7: Recovery of REEs from pyrometallurgical slags

Abstract

In parallel to the development of the hydrometallurgical recycling process for WEEE, discussed in chapter 6, a pyrometallurgical process was developed as well. This pyrometallurgical process was developed by our project partners at NTNU and is based on the high oxygen affinity of the REEs. The pyrometallurgical process aims to produce REE-rich and low Fe-content slags that are highly upgraded, up to 25 times in REE concentration to serve as an alternative to the thermal demagnetisation upgrading process. The produced slags are investigated at TU Delft for hydrometallurgical processing to extract the REEs.

At TU Delft a combined pyro-hydrometallurgical process was developed in co-operation with NTNU and Elemetal to recover the REEs from the ferrous stream of the shredded WEEE. In the process the ferrous shredded WEEE is smelted at 1650°C to form a molten iron phase and a REE-rich slag phase. The smelting process requires the use of a $Na_2B_4O_7$ flux to create a slag mineralogy from which the REEs can be leached. The formed slag phase is hydrometallurgically leached with a 2 M HNO_3 solution to extract 99% of the REEs. Solvent extraction, using D2EHPA and kerosene, extracts the REEs from the leach liquor, and separates the REEs from the impurities (Al, Ca, Mg, and Mn). Finally, oxalic acid precipitation is used to recover the REEs as oxalates, followed by calcination to convert them to pure REO. The developed flowsheet is shown in Figure 7.1.

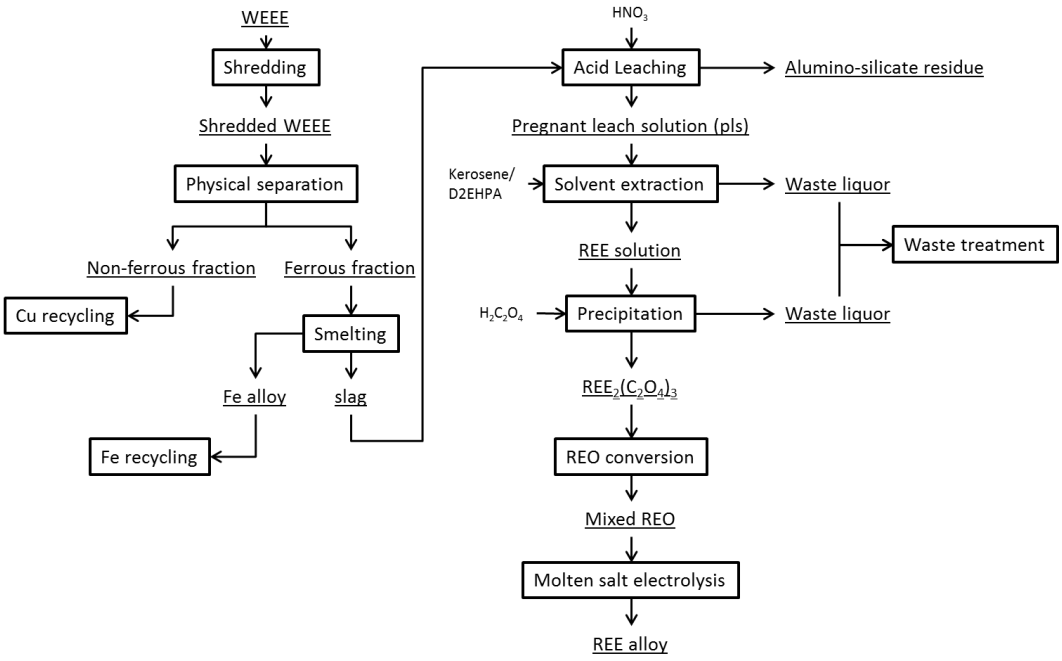

Figure 7.1: Flowsheet for the combined pyro-hydrometallurgical process to recycle REEs from WEEE

7.1. Introduction

The goal of the REEcover project was to develop recycling processes to recover REEs from secondary resources. To achieve this, both hydrometallurgical and pyrometallurgical processing routes were investigated by the different project partners. The hydrometallurgical processing was investigated at Delft University of Technology (TU Delft), while the pyrometallurgical processing was investigated at the Norwegian University of Science and Technology (NTNU). The two processing routes were developed in parallel.

The theory behind the pyrometallurgical process route is based on the high stability of the REE oxides (REO). The stability of the REOs makes the reduction of REO to REE metal a challenging process, requiring high temperature molten salt electrolysis [1]. Conversely, this also means that the oxidation of REE metals to their oxides is very easy. This means that under virtually any pyrometallurgical smelting process the REEs will be oxidised to REO and will form a slag (oxide) phase.

Based on this behaviour, the pyrometallurgical separation process was designed as a non-oxidising smelting operation. The conditions were chosen such that Fe oxidation is prevented during the process. The oxidation of REEs on the other hand, cannot be prevented during the smelting operation. This leads to a metallic Fe phase and a Fe-free oxide phase containing the REEs, thus achieving separation between Fe and REEs. Additionally, as Fe is the primary component of the ferrous WEEE, the produced slag volume is expected to be very low. This low slag volume leads to a substantially upgraded REE concentration in the slag phase, which benefits the subsequent process steps. Note that by oxidising only the REEs, this process also separates the Fe that is part of the NdFeB magnet alloy from the REEs (Nd, Pr and Dy), meaning that this process is also applicable to scrap magnets. Also, no prior physical upgrading is required for the pyrometallurgical smelting process to be effective. The magnetic NdFeB particles and steel components do not need to be separated prior to smelting and the driving force (reaction with oxygen) for REE oxidation during smelting is high enough to not require a high input concentration of REEs. Another advantage is that the Fe can now be recovered as steel scrap, which is easily recycled, as opposed to the $Fe_2O_3/Fe(OH)_3$ waste produced during the hydrometallurgical recycling of the shredded ferrous WEEE developed in chapter 6.

Of course, the ferrous shredded WEEE is not just a Fe-REE system, and many other elements are also present and some (e.g. Ca and Al) also form very stable oxides. To determine which elements will report to the slag phase the Ellingham diagram is used (see Figure 7.2 [2]). Using this diagram, it is possible to estimate which elements will remain part of the Fe phase and which will be oxidised and form the slag.

The smelting process is performed at 1650°C (±30°C) in graphite crucibles, using an induction furnace open to air [3]. These graphite crucibles react with the air in the furnace to form CO, which serves as the main reducing agent during the smelting process. The reducing potential of CO can be read on the Ellingham diagram, indicated by the red line in Figure 7.2. For a given temperature any element that lies above the red CO line will be reduced by CO, those below will not. At a 1650°C Fe lies well above the CO line, thus it will not be oxidised during the smelting process. The REEs lie well below the line, see Figure 7.2 (b), and will thus be oxidised.

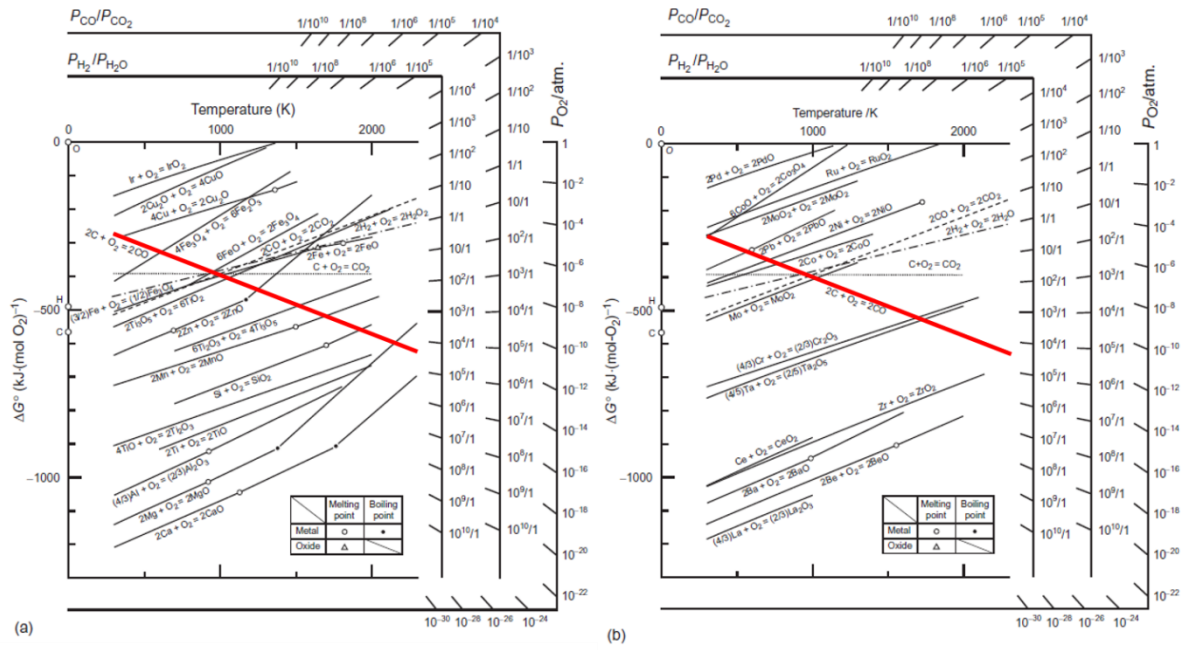

Figure 7.2: Ellingham diagrams, (a) common elements and (b) less common elements [2]

Based on the smelting conditions and the Ellingham diagram, Mn and all elements with a lower oxide formation Gibbs energy (i.e. all elements with equilibrium lines below that of Mn on the Ellingham diagram) will report to the slag phase. Thus, Ca, Si, Al and Mg are expected to report to the slag, based on the chemical composition of the ferrous WEEE, see section 3.4.2.2. As the free energies of oxide formation of the REEs are lower than that of Al (see Figure 7.2 b), the REE are also expected to report to the slag.

Cu, Ni and Pb will remain part of the Fe phase, while Zn will evaporate under the smelting conditions. The presence of Cu in the Fe phase does pose a challenge for this process route, as it severely degrades the quality of the generated scrap iron. Cu concentrations in steel as low as 0.1 wt.% [4] can result in surface cracks during hot rolling, severely degrading the quality of the produced steel. Scrap iron with high Cu content must be diluted with Cu free production scrap in order to be recycled. This limits the volume of scrap that can be processed in a single operation. The challenge of reducing the Cu content in the iron phase falls outside of the scope of the REEcover project.

The smelting process does not yield a pure REE slag phase, but a mixture of Ca, Si, Al, Mg and REEs, thus further processing is required to recover the REEs. However, the separation of REEs from the other elements in the slag is not possible with pyrometallurgy. Firstly, achieving reducing conditions able to reduce these stable oxides is extremely difficult, as is demonstrated by the need for molten salt electrolysis for the reduction of elements like Al (Hall-Héroult process [5]) and REEs. Secondly, the difference in Gibbs free energy of oxide formation between Al, REE and Ca is too small to achieve any significant degree of separation between these elements, even if the appropriate reducing conditions could be reached. Thus, in order to recover the REEs that are concentrated in the slag phase, hydrometallurgical processing is required.

This chapter will detail the hydrometallurgical processes that were developed to extract the REEs from the slags produced during the development of the pyrometallurgical REE recycling process for the ferrous WEEE stream. The developed hydrometallurgical process involves three steps: (1) a leaching

step using a diluted HNO_3 solution which partially dissolves the slags and extracts the REEs, followed by (2) a solvent extraction step to separate the REEs from the co-dissolved Ca, Mn, Mg and Al using D2EHPA, and finally (3) a precipitation step with $H_2C_2O_4$ to recover the REEs from the strip solution as mixed REE oxalates. The oxalates are then calcined in a furnace to produce REO.

The slags that were hydrometallurgically processed in this study originate from the *Met-1* (coarse) and *Met-2* (fine) ferrous fractions of the WEEE shredder at INDUMETAL, without prior physical upgrading. They were smelted by NTNU (*Met-1*) and Tecnalia (*Met-2*) and their characterisation can be found in section 3.5.2., Table 3.11 and Table 3.12.

Before discussing the developed final processes, first an overview will be given of exploratory leaching experiments that were performed on intermediate slags. These intermediate slags were produced during the exploration phase of the pyrometallurgical process and were created with physically upgraded WEEE. These experiments give insight into the influence of the mineralogy of a slag on its leaching behaviour. These insights were used to develop the finalised pyrometallurgical smelting process.

7.2. Exploratory leaching

7.2.1. Leaching with HCl and H_2SO_4

As part of the development of the pyrometallurgical process several test slags were produced at NTNU. In order to explore possible leaching options, these test slags were used to perform preliminary leach tests. These slags are not representative for the slags that were produced during the final smelting process. Nonetheless, they do offer valuable insights into the leaching behaviour of Nd in a slag phase.

The slag used in these preliminary tests was produced from highly upgraded *Met-1* (manually collected magnetic clusters from the sieving screens), without the addition of any fluxing agents during smelting. This led to a small amount of slag with a very high Nd content (over 60 wt.%). The chemical composition was measured using XRF. The elements with a concentration over 0.5 wt.% are listed in Table 7.1. Due to small amount of slag received it was not feasible to take multiple measurements on each sample to establish the uncertainty. Therefore, a conservative estimation on the uncertainty was made.

Table 7.1: XRF analysis of the high-Nd *Met-1* test slag, using a conservative estimate of the deviation

	Nd	Pr	Sr	Si	Ba
wt.%	62	7	3.4	2.8	2.8
σ	2	1	0.5	0.5	0.5
	Al	**Dy**	**Ca**	**Mn**	**Mg**
wt.%	2.6	2.1	1.4	1.3	0.8
σ	0.5	0.5	0.5	0.5	0.5

The chemical analysis shows that the Nd content of this slag is very high (over 60 wt.%) and that the major impurities are the elements that are less noble than Fe, i.e. elements whose equilibrium lines lie below that of Fe on the Ellingham diagram (see Figure 7.2). The Fe content of these slags is very low (less than 0.5 wt.%), which shows that the theory behind the forming an REE-rich slag phase to separate REE from Fe is sound.

To explore the leaching behaviour 10 g samples of this slag were leached with 50 ml (L/S = 5) of H_2SO_4 and HCl solutions with varying concentrations at room temperature for 18 h. Both diluted and more concentrated solutions were used to investigate the reactivity of the slag components. The results of this exploratory leaching are shown in Figure 7.3.

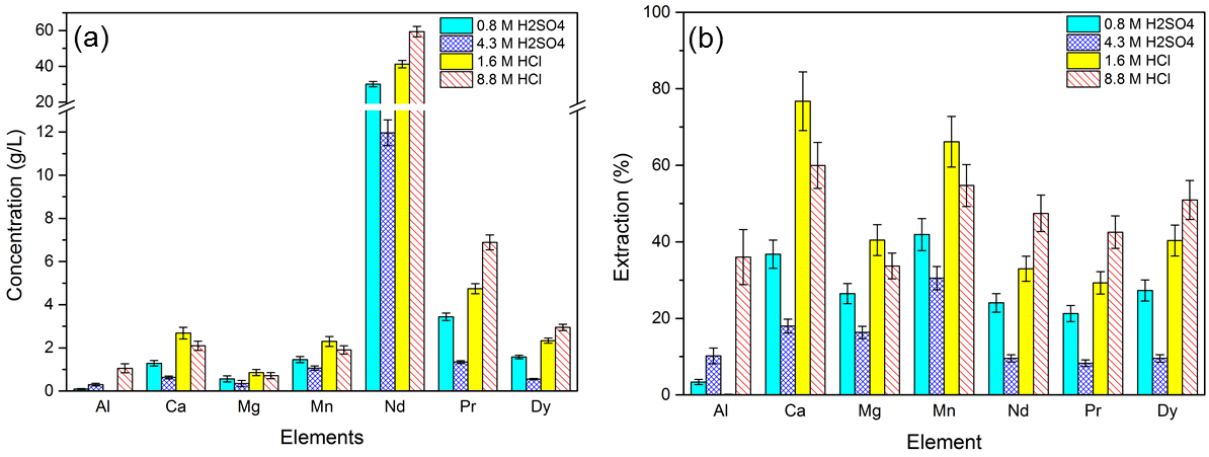

Figure 7.3: (a): Concentration (in g/L) of elements in leach liquor after exploratory leaching; **(b):** Extraction of elements (in %) based on measured concentrations in solution

The results of the exploratory leaching show that HCl is a superior leaching agent compared to H_2SO_4, for both the diluted and more concentrated solutions. This can be attributed to two factors: the solubility of $Nd_2(SO_4)_3$ and the presence of Ca, Sr and Ba. The solubility of $Nd_2(SO_4)_3$ at room temperature in sulphuric acid is low [6], which was not an issue when leaching WEEE in chapter 6 where the Nd content in the leach liquor never exceeded 5 g/L. However, with the high concentration of Nd in the slags, the low extraction indicates that the solubility limit is exceeded. This also explains why the 4.3 M H_2SO_4 leach has lower extraction rates than the 0.8 M H_2SO_4 leach, as the higher concentration of SO_4^{2-} benefits the precipitation reaction. XRD analysis of the residue left after the 4.3 M H_2SO_4 leaching confirms the precipitation, as the majority of the residue is characterised as $Nd_2(SO_4)_3$.

7.2.2. Residue analysis

The presence of Ca, Sr and Ba can result in the formation of sulphate precipitates in the H_2SO_4 leaching system. The formation of $CaSO_4$ is a problem that has been discussed in chapters 4 and 5, where $CaSO_4$ was found to capture REEs from the leach solution, leading to lower extraction of REEs. Sr and Ba also form an insoluble sulphate, similar to Ca ($SrSO_4$ and $BaSO_4$), and they can also form mixed sulphates: $(Ca,Sr,Ba)SO_4$. Analysis of the 0.8 M H_2SO_4 leach residue with SEM/EDS, Figure 7.4, shows that these sulphates do form and that they capture REEs when they form, resulting in low REE extraction.

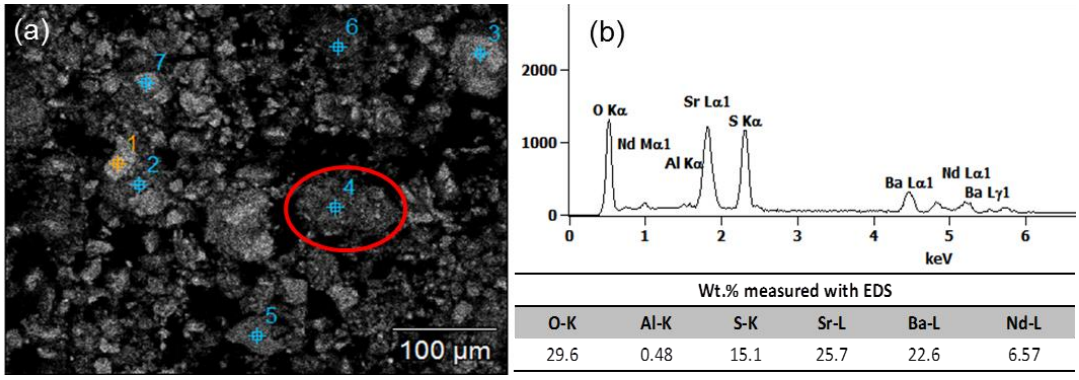

Wt.% measured with EDS					
O-K	Al-K	S-K	Sr-L	Ba-L	Nd-L
29.6	0.48	15.1	25.7	22.6	6.57

Figure 7.4: (a): SEM analysis of the 0.8 M H_2SO_4 leach residue, **(b):** EDS analysis of the particle indicated by the red circle, showing the presence of Nd in a $(Sr,Ba)SO_4$ particle

The HCl leaching system is not faced with these precipitation side reactions, since the associated chlorides have a high solubility. This is reflected in the increased extraction of all elements compared to the H_2SO_4 leaching system. However, even without these side reactions the extraction of Nd is not complete.

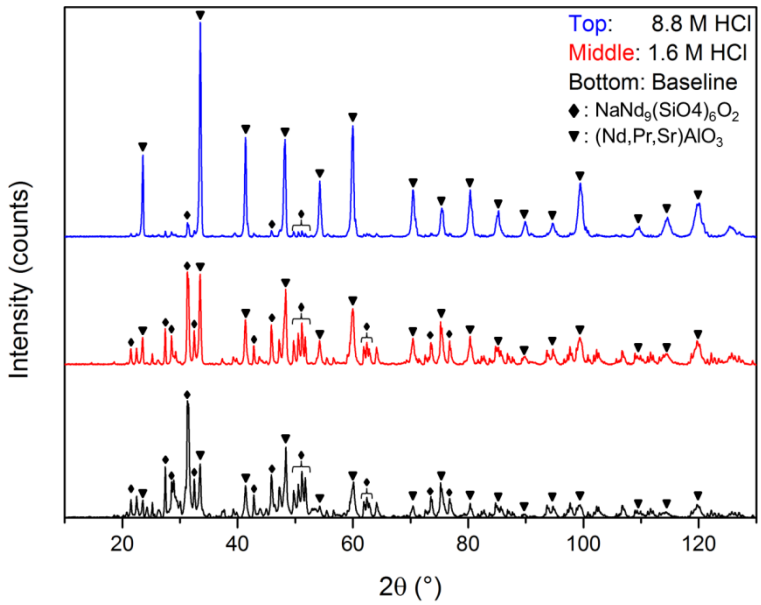

Figure 7.5: XRD spectrum comparison of the HCl leached residues to the baseline spectrum of the input material

The XRD analysis of the residues after HCl leaching, see Figure 7.5, reveals that there are two main phases present in the slag, a Nd silicate ($NaNd_9(SiO_4)_6O_2$) and a Nd aluminate ($(Nd,Pr,Pr)AlO_3$). When comparing the XRD spectra of the un-leached material to those of the leach residues, it becomes clear that the intensity of the silicate phase peaks has reduced in the 1.6 M HCl residue spectrum and the peaks have disappeared in the 8.8 M HCl residue spectrum. On the other hand, the intensity of the peaks of aluminate phase in the spectra of the leached residues has increased, which indicates that the concentration of it in the residue is increasing. Thus, it is clear that the silicate is more reactive and dissolves to a greater degree during HCl leaching, compared to the aluminate which is more resistant to dissolution and thus remains in the residue.

7.2.3. Leaching with Aqua Regia

In an effort to achieve the full dissolution of the slag, a leaching experiment using concentrated Aqua Regia (3/1 vol.%, using 37 wt.% HCl and 65 wt.% HNO_3) was performed. The experiment was run for 5 h at 60°C, using an L/S ratio of 10. The results of this experiment are shown in Table 7.2. The results indicate that Aqua Regia is also not capable to fully dissolve the slag and that it is only moderately more effective than HCl with regard to Nd extraction (from 47% with 8.8 M HCl to 58% with Aqua Regia).

Table 7.2: Results of the Aqua Regia leach of the Nd rich slag

	Al	Ca	Mn	Mg	Fe	Nd	Pr	Dy
Concentration (g/L)	1.4	1.2	1.1	0.53	0.33	36	4.3	1.8
σ	0.3	0.1	0.1	0.05	0.03	2	0.2	0.1
Extraction (%)	97	70	64	50	57	58	53	62
σ	20	7	0.6	5	6	6	5	6

Note that for the higher L/S ratio the concentrations of elements in the Aqua Regia leach solution are half that of the results in the previous tests. Based on the results of both the HCl and Aqua Regia leaching experiments, it is possible to conclude that the mineral phases in the slag, formed during the smelting process, greatly influence the slags leaching behaviour. The success of the hydrometallurgical processing, to recover the REEs from the slags, will strongly depend on the ability of the pyrometallurgical process to control the mineralogy of the produced slag and prevent the formation of insoluble phases like $((Nd,Pr,Pr)AlO_3)$.

One method that is often used to control the mineralogy of the slag during pyrometallurgical processes is the addition of fluxing agents. Fluxing agents are added to a slag during smelting to manipulate its properties, such as its melting point and viscosity, so that it can be more easily handled during processing. These fluxing agents will also play a role in determining the mineralogy of the slag once it cools down and crystallises.

With the idea to create an easily dissolvable slag, $Na_2B_4O_7$ (borax) was suggested as a fluxing agent. Borax is the compound that was also used in the Borax fusion method applied throughout this work to dissolve solid samples for ICP-OES analysis. Based on the effectiveness of this method in decomposing refractory minerals, borax was recommended as a fluxing agent. As Borax is a well-known fluxing agent [7], NTNU agreed to run the smelting process with borax as the fluxing agent. The addition of a fluxing agent does increase the slag volume produced and consequentially lowers the concentration of REEs in the slag, but as will be shown below the increased leachability more than compensates for this decrease in REE concentration.

7.3. Leaching of the slags from the pyrometallurgical processes

The exploratory leaching tests offered substantial insight into the leaching behaviour of Nd containing slags, but the high Nd content of those slags is not representative for the slags produced by the final pyrometallurgical process. In order to develop a viable hydrometallurgical recovery process, representative slags must be studied. To this end NTNU and Tecnalia supplied batches of their final slag product produced from the non-upgraded *Met-1* (NTNU) and *Met-2* (Tecnalia) WEEE shredder fractions. NTNU prepared their slag with a borax flux to increase the leachability of their slag. The slags

produced by Tecnalia were prepared without flux, since analysis of the input material showed a high Si and low Al concentration. The exploratory leaching experiments show that the silicates are more soluble than the aluminates, thus the use of flux may not be required to leach the REEs from the produced slags. However, as the experiments below will show, this is not the case. The characterisation of these slags can be found in Chapter 3.5.

7.3.1. Leaching of the fluxed NTNU Met-1 slags

The exploratory leaching experiments have shown that increased acidity is beneficial to the leachability of the REEs. Therefore, for the leaching experiments undiluted HCl (37 wt.%) and HNO_3 (65 wt.%) solutions were used as leaching agents. H_2SO_4 was not considered as a leachant, based on the presence of Ca, Sr and Ba in the slags and the observed negative impact these elements have in the H_2SO_4 system. A summary of the concentrations of the main elements in the fluxed Met-1 NTNU slags is given in Table 7.3 (recapitulated from section 3.5.2). As the slags are oxides the remainder of the mass is assumed to be oxygen.

Table 7.3: Summary of the main element concentrations in the fluxed *Met-1* NTNU slags, measured with ICP-OES

	***Met-1* slag NTNU**							
	Al	**Mg**	**Ca**	**Fe**	**Mn**	**Nd**	**Pr**	**Dy**
wt.%	23	9.3	8.9	1.17	0.06	1.3	0.2	0.001
σ	1.5	0.5	0.5	0.05	0.02	0.1	0.1	0.001

The slags were leached at 80°C, using a L/S = 5, for 6 h. The obtained extraction of the main elements is shown in Figure 7.6.

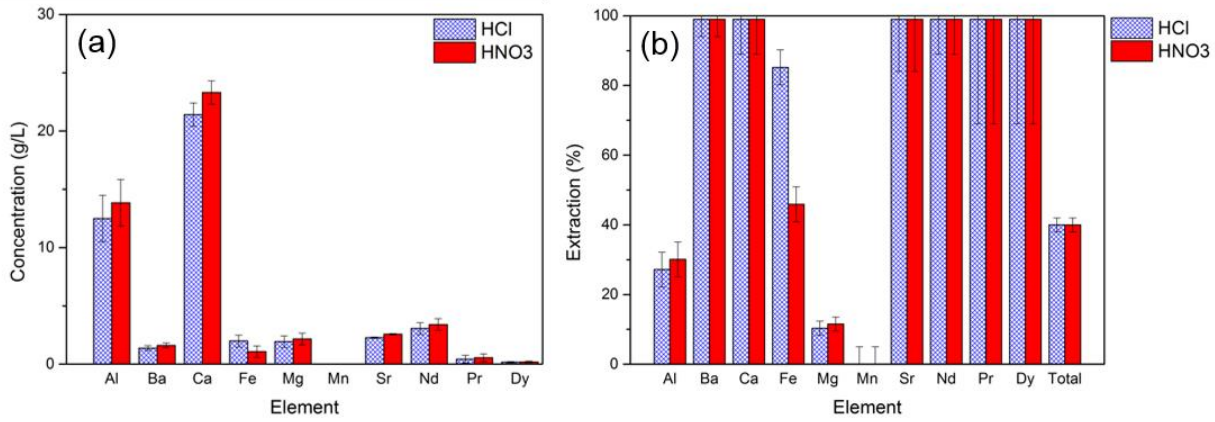

Figure 7.6: Extraction of elements (in **(a)** g/L and **(b)** %) of the Met-1 slag when leached with undiluted HCl and HNO_3

The results clearly show that the *Met-1* slags prepared with a borax flux have very high (over 99%) extraction for the REEs, as well as for Ca and Ba, in both the HCl and HNO_3 leaching system. This shows that the addition of the flux has a very positive influence on the extraction of REEs. Overall 40% of the slags were dissolved during the leaching experiments (indicated by the bar labelled total in Figure 7.6 (b)). Analysis of the *Met-1* leach residues, see Figure 7.7, shows that the boron phase Takedaite ($Ca_3B_2O_6$), that was originally present (see Table 3.12), has fully dissolved, while the Al spinel phase ($Mg(Al_2O_4)$) makes up the majority of the residue. From this we can derive that the REE were primarily associated with the boron phase and not with the Al spinel phase. This means that it is not necessary to fully digest the entire slag to completely extract the REEs and that the REEs associate with a specific

phase, instead of being homogeneously dispersed. The Gehlenite ($Ca_2Al_2SiO_7$) minor phase also appears to have dissolved, which would account for fractional Al extraction. One additional phase was detected in the residue and was identified as graphite. This is attributed to fragments of the graphite crucibles used to prepare the slags.

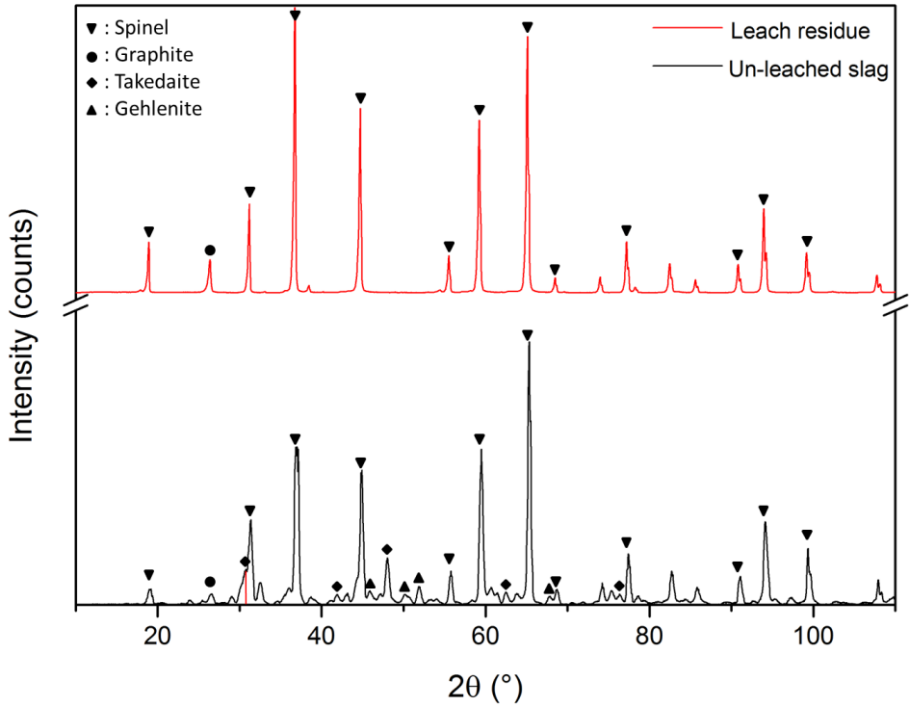

Figure 7.7: Comparison of XRD spectrum for the un-leached *Met-1* NTNU fluxed slag and the leach residue of the HCl leaching experiment

The leaching behaviour of the *Met-1* slag does not differ greatly between HCl and HNO_3. This suggests that the REE phase is readily soluble in acidic media and that the increased acidity of undiluted (65 wt.%) HNO_3 over HCl (37 wt.%) is not required for dissolution. The leaching behaviour of the non-REE is also similar, except that of Fe. However, this is likely due to heterogeneously distributed metallic Fe fragments which were not fully separated from the slag and has no bearing on the slag leaching behaviour. We conclude that both HCl and HNO_3 are equivalent options with regard to *Met-1* fluxed slag leaching and the choice of acid will depend on the further process steps.

7.3.2. Leaching of the non-fluxed Tecnalia slags

The same leaching experiments were performed with the non-fluxed *Met-2* slags produced by Tecnalia. A summary of the concentrations of the main elements in the non-fluxed Met-2 Tecnalia slags is given in Table 7.4 (recapped from section 3.5.2). As the slags are oxides the remainder of the mass is assumed to be oxygen, however, analysis with XRF also showed the presence of upwards of 20 wt.% of Si. The presence of Si was not verified with ICP-OES, as it was deemed not relevant. The slags were leached at 80°C, using L/S = 5, for 6 h using undiluted HNO_3 and HCl solutions. The results of the experiments are shown in Figure 7.8.

Table 7.4: Summary of the main element concentrations in the non-fluxed *Met-2* Tecnalia slags, measured with ICP-OES

***Met-2* slag Tecnalia**								
	Mn	**Al**	**Ca**	**Mg**	**Fe**	**Nd**	**Pr**	**Dy**
wt.%	17.6	7.35	3.8	2.9	1.6	1.4	0.2	0.05
σ	0.2	0.5	0.1	0.2	0.1	0.1	0.1	0.01

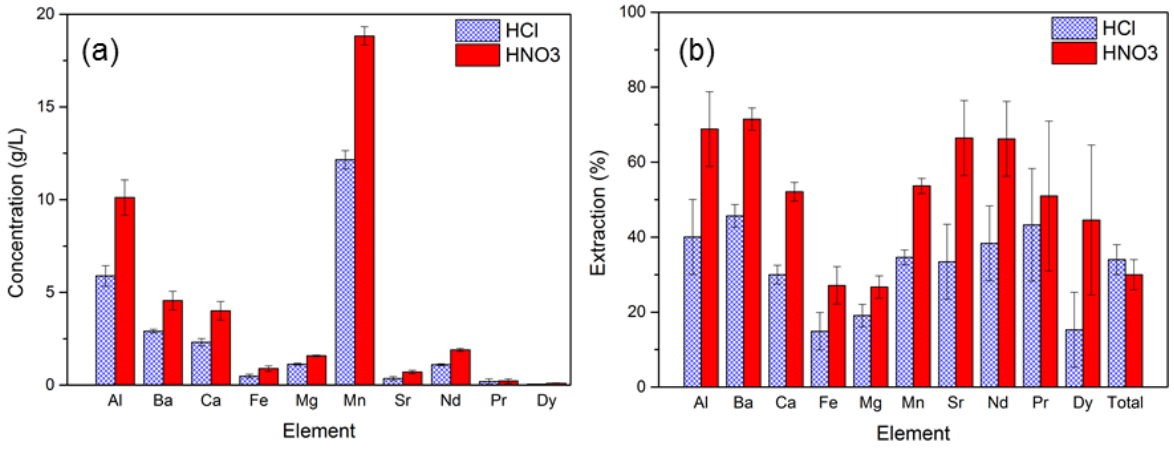

Figure 7.8: Extraction of elements (in **(a)** g/L and **(b)** %) of the *Met-2* slag when leached with undiluted HCl and HNO_3

The results show that the non-fluxed *Met-2* slag does not respond as favourably to leaching as the fluxed Met-1 slags. While the achieved extraction of REEs is moderately high (66 %), it is significantly less than the achieved extraction (above 99 %) of the *Met-1* slags. Also, unlike the results from the fluxed *Met-1* leaching experiments, HNO_3 is clearly more effective in dissolving the *Met-2* slag components. This suggests that the formed mineralogy during slag production is not favourable to acidic leaching and require a greater acidity for even partial dissolution.

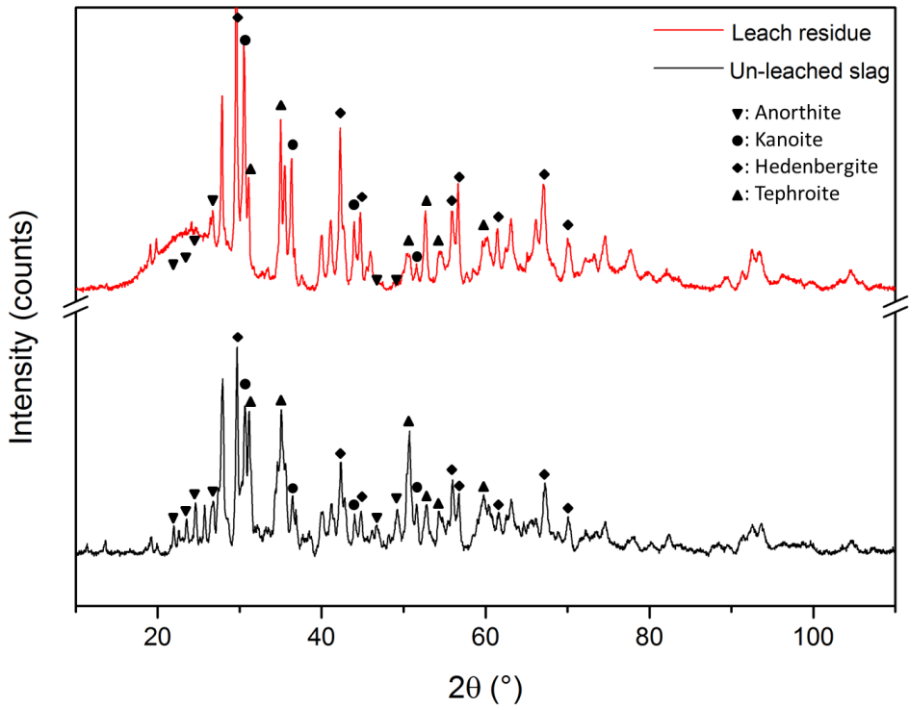

Figure 7.9: XRD spectrum comparison of the un-leached Met-2 Tecnalia non-fluxed slag and the leach residue of the HCl leaching experiment

Comparing the XRD spectra of the HCl leach residue to the un-leached Tecnalia slag, see Figure 7.9, shows that there is little change in the mineralogy. The only phase has dissolved more selectively is the Anorthite ($Ca(Al_2Si_2O_8)$) phase, however this may be an artefact due to broad signal between 2θ of 20° and 30°. This broad signal indicates the formation of an unknown amorphous phase, likely a type of silica gel. The main mineral phases in the slag are still present in the leach residue, which indicates that there is very little preferential leaching. The soluble silicates present in the high-Nd slag used during the exploratory leaching experiments are clearly not representative for the silicates formed during the pyrometallurgical smelting of non-upgraded *Met-2*.

SEM-EDS analysis shows that the REEs do not form a single distinct phase, rather the REEs are part of the overall mineral phases, (Nd,Mn,Mg,Al,Si)(O), and thus homogeneously distributed in the slag. However, the REE extraction rate is higher than the total slag dissolution. This means that there is at least one REE-bearing phase that is more soluble compared to the other slag phases.

Comparing the results of the leaching experiments on the fluxed *Met-1* and non-fluxed *Met-2* slags shows that the addition of the borax flux to the pyrometallurgical process is beneficial to the REE recovery and also leads to an overall greater dissolution rate (25% higher) of the entire slag.

7.4. Recovery of REEs through multistep precipitation

7.4.1. Theoretical evaluation of multistep precipitation

After leaching, the REEs must be recovered from the leach liquor. Precipitation is the easiest and most cost-effective route. However, the co-dissolved elements, for both the *Met-1* and *Met-2* leach liquors, make the use of the precipitation method challenging. Due to the presence of Ca, Ba and Sr double

sulphate precipitation is impossible, due to the likelihood of gypsum formation. They also form insoluble oxalates, preventing the use of oxalic acid as a precipitation agent.

This means that selective, one step, REE precipitation is not possible in this system. However, multistep hydroxide precipitation may offer a viable alternative. Hydroxide precipitation of metals can be expressed by the reaction

$$\mathrm{M^{x+} + x\,OH^- \rightleftarrows M(OH)_x} \tag{7.1}$$

which shows that the precipitation can be driven forward by increasing the OH^- concentration, or in other words increasing the pH. The solubility of various common metal hydroxides is shown in Figure 7.10. This figure shows that by gradually increasing the pH, metal species can be precipitated in stages. Fe^{3+} can be removed selectively by increasing the pH to 3, followed by Al^{3+} at pH = 5. Precipitating Ca^{2+} with this method would require a pH of above 12. Note that Fe^{3+} is the expected form of Fe in solution when leaching with HNO_3, due to the oxidising nature of HNO_3.

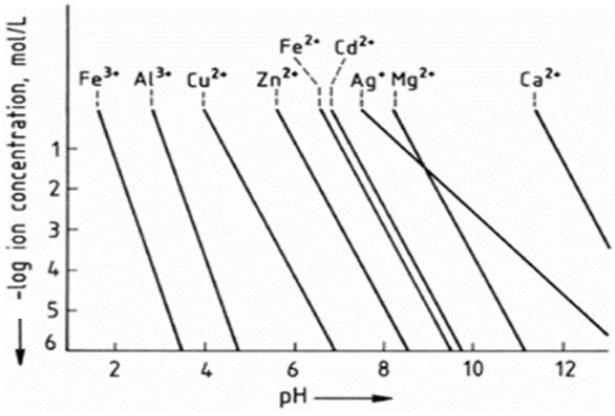

Figure 7.10: Solubility of metal hydroxides, expressed as metal cation concentration as a function of pH [8]

The solubility of $Nd(OH)_3$ is not shown on Figure 7.10 and must thus be calculated. The equilibrium constant *K* of $Nd(OH)_3$ formation in a nitrate media is approximately $3.1*10^{-21}$ [9]. From this value and the equations

$$K = \frac{1}{[\mathrm{Nd^{3+}}]*[\mathrm{OH^-}]^3} \tag{7.2}$$

$$[\mathrm{H^+}] * [\mathrm{OH^-}] = 10^{-14} \tag{7.3}$$

and the expression

$$\log([\mathrm{Nd^{3+}}]) = 20.5 - 3 * pH \tag{7.4}$$

are derived, which gives the concentration of Nd^{3+} in solution in function of pH.

Using eq. 7.4, the concentration of Nd^{3+} at various values of pH can be calculated. Table 7.5 shows the results for pH 3 (Fe precipitation), 5 (Al precipitation) and 9.

Table 7.5: Calculated Nd^{3+} concentration in mol/L and g/L at pH 3, 5 and 9 using expression 7.4

	Nd^{3+} concentration		Remarks
pH	mol/L	g/L	
3	n.a.	n.a.	End $Fe(OH)_3$ precipitation
5	n.a.	n.a.	End $Al(OH)_3$ precipitation
7	3.2×10^{-1}	4.6×10^{1}	Start $Nd(OH)_3$ precipitation
9	3.2×10^{-7}	4.6×10^{-5}	End $Nd(OH)_3$ precipitation

The maximum solubility of $Nd(NO_3)_3$ in nitrate media is 1.42×10^3 g/L. Thus, the interpolation expression (7.4) is only valid at pH 6.5 (calculated solubility 1.44×10^3 g/L) and above [10]. The calculated Nd^{3+} concentrations show that $Nd(OH)_3$ precipitation requires a pH of 9 to remove the majority of the Nd^{3+} in solution. This, combined with high solubility at pH 3 and 5, means that theoretically multistep precipitation is possible. Fe will be removed first at pH 3, followed by Al at pH 5 and Nd at pH 9, whereas Ca (Sr and Ba) will remain in solution.

7.4.2. Multistep precipitation Experiments

To validate the multistep precipitation a solution containing Al and Nd was neutralised from pH 0 to 9 using NH_4OH. The solution was sampled and the Al and Nd concentrations at pH 0, 3, 5 and 9 are shown in Table 7.6.

Table 7.6: Stage wise neutralisation of an Al/Nd-Cl solution, using NH_4OH

	Al (g/L)	Nd (g/L)
pH=0	10.5	7.66
pH=3	3.95	3.26
pH=5	0.00	1.76
pH=9	0.00	0.00

The results show that the theoretically predicted behaviour does not occur. Rather, upon the start of Al precipitation the Nd co-precipitates to some degree. This behaviour does not appear to be previously observed in literature for Al, but it may be similar to the observed behaviour of Fe^{3+} and Nd^{3+}, where the precipitation of $Fe(OH)_3$ induces the co-precipitation of $Nd(OH)_3$ [11].

Based on these observations we can conclude that multi step precipitation is not a viable method to recover the REEs from the leach solution. This means that to achieve separation between the REEs and the other elements a different method is needed. Solvent extraction was chosen as an alternative to precipitation.

7.5. Recovery of REEs through solvent extraction

7.5.1. Modifying the leaching system for solvent extraction

The use of solvent extraction imposes some additional boundary conditions on the leaching process. Most organic phases can be damaged by HCl, which means that HNO_3 is a preferred leaching agent. Solvent extraction is also very sensitive to pH, thus suppling leach solutions with pH below 0, as is the case when leaching the slags with undiluted HNO_3, is not workable for the solvent extraction process. This means that the leach solution must be partially neutralised before solvent extraction becomes

possible. Neutralising a mostly undiluted HNO_3 solution consumes a large amount of reagent, which is unfavourable. However, the necessity of leaching with an undiluted HNO_3 solution is not yet proven. Full REE extraction was achieved with undiluted HNO_3, but the less concentrated HCl achieved the same results. Thus, a leaching experiment on the fluxed *Met-1* NTNU slags, using a diluted HNO_3 solution, was performed. A 2 M HNO_3 solution (8.9 wt.%) was prepared and the slags were leached using the same leaching conditions as the concentrated experiments i.e. 80°C, L/S = 5 and 6 h. The results of this experiment are shown in Table 7.7.

Table 7.7: Extraction of main elements of the fluxed *Met-1* NTNU slag after diluted HNO_3 (2M) leaching experiment

	Al	Ca	Fe	Mg	Mn	Nd	Pr	Dy
Extraction (%)	31	100	20	23	82	100	100	100
σ	3	10	2	3	8	5	5	5
Concentration (g/L)	14.4	17.9	0.5	4.3	0.1	2.5	0.4	0.002
σ	1.5	1.8	0.05	0.4	0.05	0.3	0.2	0.001

The results show that even with a diluted (2 M) HNO_3 solution full REE extraction is achieved, Thus the REE phase in the slag is highly soluble. This means that a more realistic solution can be supplied to solvent extraction, which can more easily be neutralised to the appropriate pH and with less reagent consumption. These results also show a very high Ca co-extraction, which supports our claim that the REEs are associated with the $Ca_3B_2O_6$ phase. These milder leaching conditions were used to prepare the solution for the solvent extraction experiments that were performed by our project partners at Elemetal, the Netherlands [12].

7.5.2. Solvent extraction experiments in cooperation with Elemetal

In section 4.4.4. solvent extraction was discussed as the method to separate the REEs from H_3PO_4 to produce two separate purified product streams. There, P350 was used as an extractant, which is specific for the REE-P system [13]. The slag leaching system does not contain P, thus a specialised extractant will not be necessary. Instead the more conventional extractant D2EHPA ($(C_8H_{17}O)_2PO_2H$) was selected as the extractant of choice. D2EHPA is an extractant often used in solvent extraction and its use in REE extraction has been established [14]. Acidic organic extractants (HOrg) like D2EHPA react with Nd^{3+} (and other metallic cations) via the reaction

$$Nd^{3+} + (m+3)HOrg \rightleftarrows Nd(Org)_3(HOrg)_m + 3H^+ \quad (7.5)$$

where Nd^{3+} replaces 3 protons from the organic phase. As this is an equilibrium reaction, it progresses better at a higher pH (lower concentration of H^+), transferring more Nd^{3+} to the organic phase. Conversely, the reaction can be reversed by lowering the pH, i.e. increasing the H^+ concentration, releasing the extracted Nd from the organic phase. Thus, the REEs are stripped from the organic phases by mixing it with a "clean" (free of impurities) acid.

In co-operation with Elemetal a solvent extraction process was developed to recover the REEs from the slag leaching liquors. The developed flowsheet is shown in Figure 7.11.

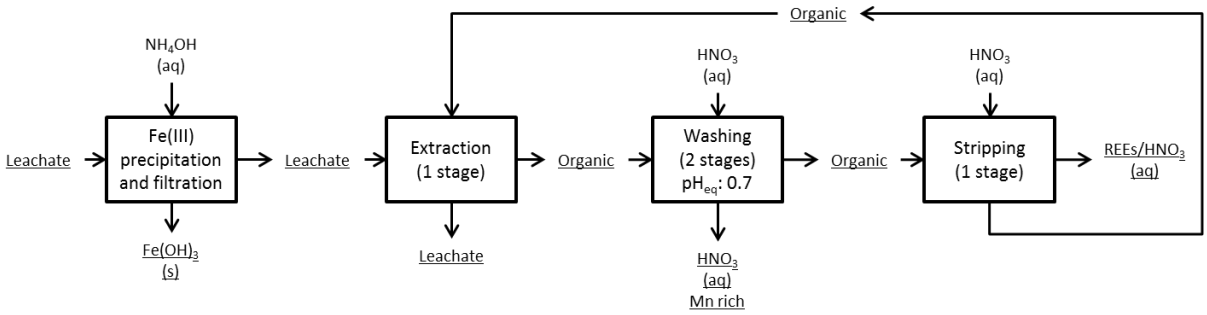

Figure 7.11: Solvent extraction flowsheet developed by Elemetal for the recovery of REEs form slag leaching liquors

The solvent extraction was designed based on the composition of the slag leaching liquor, thus the elements from which the REEs must be separated are Ca, Al, Fe, Mg and Mn. For purposes of discussion Sr and Ba are assumed to behave similarly to Ca. Mn was included as an impurity in an effort to make the process more robust. While the Mn concentration in the *Met-1* slags is low (0.06 wt.%), the *Met-2* slags have a much higher concentration of Mn (17.6 wt.%). Ideally these two input streams will be treated together in the pyrometallurgical process, implying that the expected Mn content in future slags (and thus in the leach liquor) will be considerably higher than the one in Table 7.5. As such, the solvent extraction experiments were conducted with the synthetic solution. The chemical composition of the synthetic solution is shown in Table 7.8, which was prepared based on the chemical composition of both slags. The Fe content was also increased to account for metal-slag separation problems or possible metallic inclusions with the slag.

Table 7.8: Chemical composition of the input solution for the solvent extraction experiments

	Mn	Al	Fe	Mg	Ca	Nd	Pr	Dy
Concentration (g/L)	7	6.5	5	5	2	2.4	0.3	0.1

The solvent extraction experiments were performed using D2EHPA as extractant and with kerosene (ShellsolD100) as the solvent. Preliminary test showed that a high D2EHPA concentration resulted in higher extraction rates, thus the D2EHPA concentration of 500 g/L was used for the process design.

D2EHPA is a well-known extractant for REEs, but next to a strong affinity for REEs, D2EHPA also has a strong affinity for Fe^{3+}. While the presence of Fe does not impact the separation process of the REEs, it does irreversibly load into the organic phase, resulting into Fe build-up. Removing the Fe from the solvent requires stripping with concentrated HCl, which causes the organic phase to break down. Thus, in order to run the solvent extraction efficiently, the Fe must first be removed from the input solution. As the slags were leached with HNO_3, most of the dissolved Fe will be in its 3+ state. In order to remove the traces of Fe^{3+}, the pH of the solution is first increased to 2 by adding NH_4OH (25 wt.% NH_3). In this way Fe^{3+} is precipitated as $Fe(OH)_3$. Only minimal losses of REEs were observed during Fe precipitation. After filtration the solution is fed into a solvent extraction circuit which contains 1 extraction stage, 2 wash stages and 1 stripping stage. All stages were used a 1:1 aqueous to organic volume ratio and the pH of the input solution was 2.

Of the elements shown in Table 7.5, only the REEs, Ca and Mn are extracted from the leach liquor into the organic solution, Al and Mg are not extracted under these conditions. Both Ca and Mn can be removed from the organic phase by implementing two washing stages before stripping. The extraction

and washing behaviour of the REEs and Mn (Ca behaves similar to Mn) is shown in Figure 7.12.

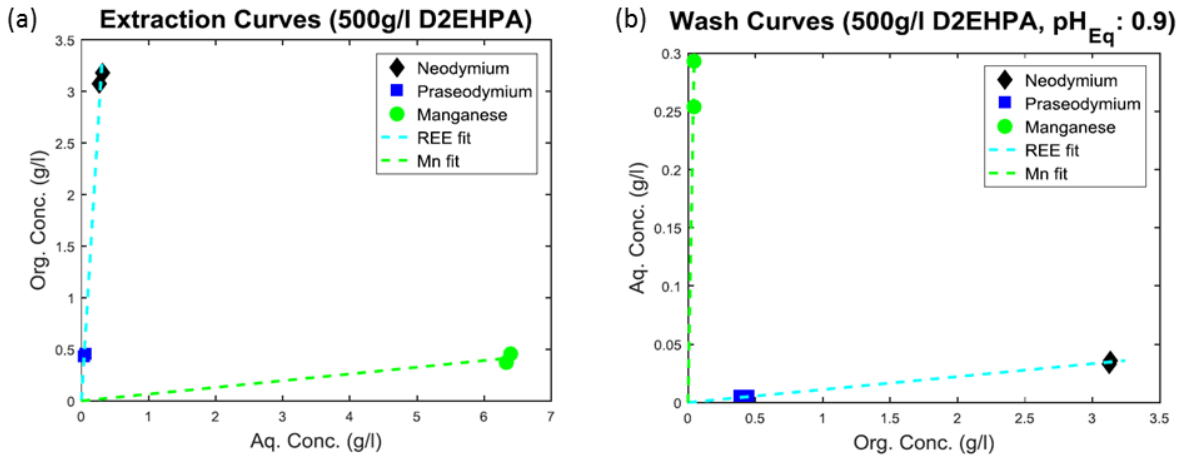

Figure 7.12: (a): Extraction curves of Mn, Nd and Pr after a single stage extraction with 500 g/L D2EHPA, showing the distribution of elements between aqueous and organic phase in g/L. **(b):** Washing curves of Mn, Nd and Pr after single stage washing with a pH 0.9 HNO_3 solution, showing the distribution of elements between aqueous and organic phase in g/L. Data and graph supplied by Elemetal

Figure 7.12 (a) shows that the REEs strongly concentrate in the organic phase (≈ 3.2 g/L in organic phase and ≈ 0.3 g/L left in the aqueous phase), while the Mn only partially reports to the organic (≈ 6.5 g/L in the aqueous phase and ≈ 0.5 g/L in the organic phase). This shows that the extraction behaviour of D2EHPA favours the REEs, but the contamination of Mn must be washed out prior to stripping. Figure 7.12 (b) shows that washing the loaded organic phases at pH of 0.9 leads to the removal of virtually all Mn from the organic phase (less than 0.06 g/L = 60 ppm left in the organic phase), while the concentration of REEs in the organic phase is virtually unchanged (≈ 3.2 g/L).

The washing stages were performed using a pH of 0.9 (A:O = 1), which successfully removed the Mn and Ca from the organic phase. The pH of the aqueous phase which is leaving the final wash stage (pH_{eq}) is controlled to a value of 0.7. A lower pH results in a loss of REEs and a higher pH results in a less efficient removal of Ca and Mn. Once the Ca and Mn are removed from the organic phase, the REEs can be stripped using a 35 wt.% HNO_3 solution (pH < 0). The low pH was required to achieve a REE stripping efficiency of 100%. For A:O = 1 this yielded an end solution of ≈3.2 g/L Nd.

As a final step of the process the REEs are recovered in a solid form through precipitation. At room temperature a stoichiometric amount of oxalic acid is added to the purified REE-rich solution from the stripping stage of the solvent extraction circuit. This precipitated the REEs as REE oxalates and yielded precipitation ratios of 94% for Nd, 89% for Pr and 95% for Dy. This results in the precipitation of REE oxalates, which are subsequently calcined in order to produce REOs. The calcination was performed in an electric furnace without additional air supply. The oxalates were calcined at a 1000°C for 8 h. A mass loss of 46.7% was observed due to the evolution of CO_2 as a result of the thermal decomposition of the oxalates via the equation

$$REE_2(C_2O_4)_3 \xrightarrow{\Delta T} REE_xO_y + CO_2 \qquad (7.6)$$

The theoretical mass loss for the calcination of $Nd_2(C_2O_4)_3$ is 39%. This indicates that some residual solution was retained in the filter cake after precipitation. The compositions of the resulting rare earth oxide mixture are shown in Table 7.9. The total composition of the oxides does not add up to 100%.

This can be explained by residual carbon and nitrogen (originating from the retained leach solution), which are not completely removed during calcination and cannot be measured with ICP-OES. By increasing the calcination temperature and/or the residence time in the calcination furnace, these elements can be completely removed. A trace amount of Mn is present in the final oxides, but its concentration does not exceed 500 ppm.

Table 7.9 - Composition of the mixed REOs produced with the demo pyro-hydrometallurgical flowsheet (concentrations measured by ICP-MS after dissolution of the mixed REOs in aqua regia, the oxygen content is calculated by assuming that the REEs are present in the forms as shown in the table). Data supplied by Elemetal.

Composition of the mixed REOs (%)			
Nd_2O_3	Pr_6O_{11}	Dy_2O_3	Total
81.5	9.0	3.6	94.2

7.6. Concluding remarks

Processing the slags has shown that the pyrometallurgical smelting of the WEEE is a viable method of recovering the REEs from the ferrous fraction of the WEEE shredder streams. Through pyro- and hydrometallurgical processing a pure mixed oxide of Nd, Pr and Dy can be obtained from the WEEE. This combined approach can be summarised in the flowsheet shown in Figure 7.13 (the same as in Figure 7.1).

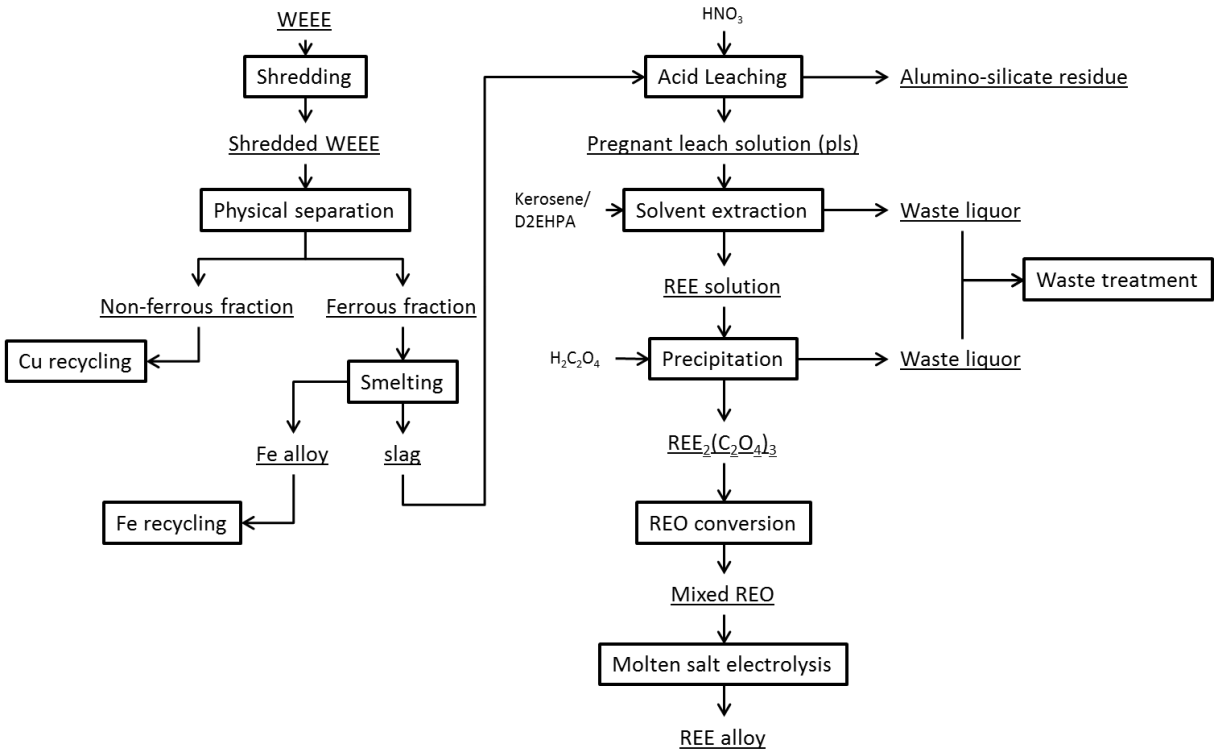

Figure 7.13: Developed pyro-hydrometallurgical flowsheet for recycling REEs from ferrous WEEE

When this process is compared to the pure hydrometallurgical process described in chapter 6, several advantages and disadvantages can be observed. The advantages over the pure hydrometallurgical approach are: the recyclability of the Fe is maintained, it avoids the thermal demagnetisation step and it produces REO as its end-product.

The maintained recyclability of the Fe is important, especially on a larger scale. Fe recycling is what these shredder fractions are currently used for and the ability to maintain this recycling stream is beneficial to the overall viability of the REE recycling process. By producing metallic iron phase after smelting, the Fe can still be utilised for steelmaking, which is what the Met-1 is currently being used for, and the REE recycling only has to account for the process costs.

The thermal demagnetisation process is overall very energy inefficient, as only a small fraction of the heated bulk is actually useful for REE recycling. But the main issue is the combustion of the small amounts of plastics present in the ferrous WEEE. Combustion of these plastics at a temperature of 500°C will produce several harmful gasses, like dioxins [13]. These gasses require the installation and upkeep of gas treatment facilities to ensure safety and limit environmental pollution. The ability to remove the thermal demagnetisation from the flowsheet is a major advantage of the combined pyro-hydrometallurgical process. The production of REO means that the REE are immediately useable in molten salt electrolysis, as opposed to the double sulphates that are produced during the pure hydrometallurgical process.

In terms of solid waste management this process route is also strong. The bulk of the Fe is contained in the iron ingot, which is not a waste. The leftover slag phase after leaching is a good material to produce concrete, as it no longer contains any elements that would leach to the environment due to exposure.

There are also disadvantages to the combined pyro-hydrometallurgical process, compared to the pure hydrometallurgical process. The main ones are: high consumption of energy and chemicals, and the necessity for solvent extraction and the loss of Cu.

The energy and chemical consumption is much higher for this process than the purely hydrometallurgical process. The purely hydrometallurgical process can run on only the heat produced by the oxidation reaction and only requires a diluted H_2SO_4 solution to leach, making it a considerably more economical process. Although the thermal demagnetisation is energy inefficient, it does require considerably less total energy than the smelting operation. This is further exacerbated by the need for solvent extraction to purify the REEs after leaching.

The waste management of the waste waters is also more complex as they are nitrated waste waters instead of sulphate-based ones. Thus, biological denitrification is required, see chapter 4.4.5.2.

The loss of Cu is a minor, yet potentially impactful disadvantage. While recovering the Cu in the hydrometallurgical process was not fully explored it was proven to be possible, giving the purely hydrometallurgical process another possible revenue stream. However, the loss of Cu valorisation is not the main issue, rather the degradation in quality of the metallic Fe phases due to the presence of Cu poses the greater limitation. The presence of Cu in the metallic Fe phase has a negative influence on the recyclability of the Fe, reducing its value as steel scrap.

Overall the combined pyro-hydrometallurgical process has its advantages and disadvantages, but it is a viable process and a valid alternative to the pure hydrometallurgical process. Further research into this process can prove to be very valuable, especially the influence of boron flux on the formation of leachable REE slag phases. Further development with regard to removing the Cu prior to smelting can also greatly improve the economics of this process.

References

[1] N. Krishnamurthy and C. K. Gupta, “Extractive metallurgy of rare earths”, CRC press, 2004.

[2] M. Hasegawa, “Chapter 3.3 Ellingham Diagram”, in *Treatise on Process Metallurgy. Volume 1: Process Fundamentals.*, Red. Boston, pp. 507-516, 2013.

[3] B. Vinje, “Recovery of REE from WEEE”, Norwegian University of Science and Technology, 2016.

[4] K. E. Daehn, A. Cabrera Serrenho, and J. M. Allwood, “How Will Copper Contamination Constrain Future Global Steel Recycling?”, Environ. Sci. Technol., vol. 51, nr. 11, pp. 6599–6606, 2017.

[5] G. E. Totten and D. S. MacKenzie, Red., “Handbook of aluminum”, New York, Basel: M. Dekker, 2003.

[6] M. Tanaka, T. Oki, K. Koyama, H. Narita, and T. Oishi, “Chapter 255 - Recycling of Rare Earths from Scrap”, in Handbook on the Physics and Chemistry of Rare Earths, vol. Volume 43, Jean-Claude G. Bünzli and Vitalij K. Pecharsky, Red. Elsevier, pp. 159–211, 2013.

[7] “Borax | chemical compound”, Encyclopedia Britannica. [Online]. Available on: https://www.britannica.com/science/borax-chemical-compound. (retrieved 28/02/2018)

[8] B. Yarar and R. B. Richter, “Flotation”, in Ullmann’s Encyclopedia of Industrial Chemistry, Wiley-VCH Verlag GmbH & Co. KGaA, Red. Weinheim, Germany: Wiley-VCH Verlag GmbH & Co. KGaA, pp. 1–56, 2016.

[9] R. S. Tobias and A. B. Garrett, “The Thermodynamic Properties of Neodymium Hydroxide $Nd(OH)_3$, in Acid, Neutral and Alkaline Solutions at 25°; the Hydrolysis of the Neodymium and Praseodymium Ions, Nd^{3+}, Pr^{3+}”, J. Am. Chem. Soc., vol. 80, nr. 14, pp. 3532–3537, 1958.

[10] D. L. Perry, Handbook of Inorganic Compounds. CRC Press, pp. 285, 2016.

[11] M. A. R. Önal, C. R. Borra, M. Guo, B. Blanpain, and T. Van Gerven, “Hydrometallurgical recycling of NdFeB magnets: Complete leaching, iron removal and electrolysis”, J. Rare Earths, vol. 35, nr. 6, pp. 574–584, 2017.

[12] “Home | Elemetal B.V.” [Online]. Available on: http://www.elemetal.eu/. (retrieved 28/02/2018)

[13] H. Li, F. Guo, Z. Zhang, D. Li, and Z. Wang, “A new hydrometallurgical process for extracting rare earths from apatite using solvent extraction with P350”, J. Alloys Compd., vol. 408–412, pp. 995–998, 2006.

[14] F. Xie, T. A. Zhang, D. Dreisinger, and F. Doyle, “A critical review on solvent extraction of rare earths from aqueous solutions”, Miner. Eng., vol. 56, pp. 10–28, 2014.

[15] N. Ortuño, J. A. Conesa, J. Moltó, and R. Font, “Pollutant emissions during pyrolysis and combustion of waste printed circuit boards, before and after metal removal”, Sci. Total Environ., vol. 499, pp. 27–35, 2014.

Chapter 8: Conclusions and recommendations

8.1. Conclusions

8.1.1. The mine tailings

The development of the recycling process for the mine tailings was fully determined by the two major REE components: apatite and monazite. The apatite proved to be the source for the majority of the heavier REEs (as well as phosphorous), while monazite contained the majority of the lighter REEs. Through physical upgrading (grinding and flotation) it was possible to collect all the apatite from the mine tailings into a concentrate, which accounts for 12% of the mine tailings. The flotation process also collected the majority of the monazite, as it is also a phosphate mineral. The produced concentrate served as the input material for the two developed hydrometallurgical extraction processes.

The key parameter of the hydrometallurgical leaching process is the acidity of the leaching solution. A high acidity (more than 6.5 M of H^+) leads to a high extraction rate (75-100%) of the heavier REEs (those associated with apatite), while a low acidity (4.2 M of H^+) leads to a minor extraction of REEs (less than 10%). This phenomenon is attributed to the interaction of the dissolved REEs and the formed H_3PO_4. The reaction between the dissolved REEs and PO_4^{3-} has a very high equilibrium constant ($K = 10^{22}$) and leads to insoluble REE phosphate precipitate ($REEPO_4$). This reaction can be prevented if the dissociation of H_3PO_4 is suppressed by lowering the pH of the solution; which is what occurs when using a high acidity leaching solution. This shows that the REE extraction is fully controlled by the acidity of the leach solution. The acid type proved to be unimportant with regard to the leaching mechanics, as long as it is a strong acid. However, H_2SO_4 was dismissed as a possible leachant, as it would result in an unfavourable side reaction, $CaSO_4$ precipitation. HCl and HNO_3 both proved to be viable as leaching agents, but HNO_3 has the added advantage of $Ca(NO_3)_2$ recovery, as well as being the preferred acid for solvent extraction. As such HNO_3 was chosen as the leach acid for the final developed process.

Regardless of the acidity of the leaching solution all P is co-extracted as H_3PO_4, which shows that apatite is a very soluble mineral. This is beneficial to the overall recycling flowsheet, as phosphorous is a critical resource as well. It does mean however that a separation process is required to separate the dissolved REEs from the H_3PO_4. This was achieved with solvent extraction, using P350 $[CH_3P(O)(OC_8H_{17})_2]$ as the extractant and kerosene as the solvent. Solvent extraction experiments show that optimal separation rates are achieved with (A:E) = 1:2 and (A:O) = 1:4 and that under these conditions the theoretically seven stages are needed to extract 99.9% of all REEs from the aqueous solution, while only co-extracting 3.5% of the P. This allows for the REEs and H_3PO_4 from the apatite to be separated from each other and yield two separate recycling end products.

In contrast to the easily soluble apatite the monazite does not dissolve under any of the tested leaching solution, preventing the full extraction of REEs in a single leaching step. This shows that monazite is a very stable mineral, resistant to acidic dissolution under atmospheric conditions. To digest the monazite and extract its REEs a high temperature (160°C) NaOH conversion process was applied to the

residue of the leaching process that dissolved the apatite. This high temperature process does not fully extract the REEs from the residue, but does achieve REE recovery rates of 70%. For total extraction a process similar to the one used for monazite digestion in the primary industry would likely be required (200°C / 3bars). While running such a process on a large scale can be an economic (as well as environmental) challenge, the fact that it could be applied to a leach residue (which represents less than 5% of the concentrate, which in turn represents only 12% of the mine tailings) means that the high temperature conversion process can be run on a much smaller scale than the overall process.

Still the high temperature NaOH conversion process is not the optimal solution for the recovery of the REEs from the monazite. In an effort to develop an alternative, microwave-assisted leaching was explored to dissolve the monazite in the leach residue. Microwave-assisted leaching is an emerging technology that has seen previous successes with other difficult to leach materials like Cu and Au ore. Applying it to the leach residue has had mixed results, ranging from less than 60% extraction when using NaOH conversion to near total REE extraction using H_2SO_4 at 200°C. The less than optimal results when using NaOH shows that the expected effect of microwave irradiation (the cracking of reaction product layers) does not occur and that microwave irradiation has no meaningful contribution to the mechanics of the conversion system. However, the efficient heating that can be achieved with microwave heating does provide the possibility to easily leach at high temperatures and with the appropriate leaching vessels at high pressures as well. This was demonstrated when the residue was leached with H_2SO_4, where temperatures of 200°C and pressures of 10 bar were achieved in a measure of minutes. Under these conditions the monazite decomposes completely and near total REE extraction is achieved. The only losses of the REEs are attributed to the $CaSO_4$ precipitation side reaction which could not be prevented, but due to the fact that most of the Ca had already been removed from the system by the apatite leaching, this was a minor loss.

In the end no conclusions could be drawn on the effect of microwave irradiation on the mechanics of monazite dissolution, other than the fact that the extreme leaching conditions (regarding temperature and pressure) are beneficial to the dissolution. This is in part due to the limitation of the equipment that was used.

From the developed processes a final recycling flowsheet can be constructed to recover the REEs and the phosphorous from the mine tailings. Through diluted HNO_3 leaching 95% of the phosphorous is recovered as H_3PO_4, while 95% of the REEs report to the leaching residue. This leaching residue is then treated with H_2SO_4 in a microwave reactor, which dissolves 80-100% of the REEs. Using solvent extraction to remove the impurities the REEs can then be recovered as precipitates. The detailed flowsheet can be found in chapter 5.6., Figure 5.12.

8.1.2. The shredded WEEE

The recycling process developed for the shredded WEEE was vastly different from of the mine tailings. With the mine tailings the main challenge lay with the difficult dissolution of monazite, while with the shredded WEEE the main REE phase (NdFeB) proved to be very soluble. The main challenge presented by the shredded WEEE was limiting the co-dissolution of Fe and obtaining a REE product free of impurities, while working within the limits of economic viability.

Before the shredded WEEE can be recycled the NdFeB magnet particles must first be concentrated from the bulk ferrous scrap of the shredded WEEE. This was achieved by LTU through thermal demagnetisation (which detached the magnetic particles from the bulk steel), grinding (which reduced

the particle size of the brittle magnet particles) and sieving (which separates the fine magnet particles into a concentrate). Once upgraded the shredded WEEE was sent for hydrometallurgical recycling.

The key process in achieving a selective REE extraction from the shredded WEEE is the Fe oxidation process. In order to suppress the Fe co-dissolution, the Fe has to be oxidised to its 3+ state. In this state it is less reactive and is also unstable in solution at a pH above 1.5. The fact that the oxidation of Fe is necessary is a well-established knowledge in NdFeB magnet recycling, where the oxidation is traditionally achieved through oxidative roasting. However, roasting is not an option for the shredded WEEE for two reasons: it is not economically viable to roast a large batch of material for the little REE that is present and the small particle size (less than 75 µm, due to the physical upgrading) of the material would impose severe complications into the process, such as sintering or potentially even explosions (Nd is pyrophoric). An alternative process to roasting was required, one that is not as energy intensive and does not change the morphology of the material. The solution that was found is water-based corrosion. Due to the small particle size of the material full oxidisation of the Fe in 24 h is possible through corrosion. By placing the shredded WEEE in an aerated water tank at 80°C for 24 h it is possible to oxidise 92% of Fe. Doing this requires far less energy than roasting and (as the oxidation is exothermic) is self-sustaining.

Once oxidation of the Fe is achieved the REEs can be leached from the shredded WEEE through leaching with diluted (3%) H_2SO_4. The extraction of REEs is over 90% regardless of the leaching conditions (temperature, L/S, time), but due to the oxidation the dissolution of Fe is limited to 20% after 6 h of leaching. However, analysis of the leaching kinetics shows that the REE dissolution reaction is substantially faster than the Fe dissolution reaction, which means that by running the leaching reaction for limited time (1-5 min at room temperature) drastically reduces the Fe co-dissolution (down to 7%), thereby improving the leaching selectivity towards the REEs.

Reducing the Fe co-dissolution not only lowers the acid consumption of the recycling process, it also enables the use of double sulphate precipitation as a means for recovering the REEs. By adding Na_2SO_4 and H_2SO_4 to the leach liquor it is possible to precipitate 92% of the REEs as double sulphate precipitates [$(Na,Nd)(SO_4)_2$] with minor impurities (8800 ppm Ca and 2800 ppm Zn). This allows for the elimination of solvent extraction as a required process step, greatly improving the economic viability of the recycling process.

These three process steps have been combined into the process flowsheet that is shown is chapter 6, see Figure 6.11.

Finally, a pyrometallurgical process was developed by NTNU as an alternative to the thermal demagnetisation process. This process was able to separate the REEs from the Fe through reductive smelting. This produces a metallic Fe phase and a REE-rich slag phase, achieving separation rates of over 95% between Fe and the REEs. The produced slags are then hydrometallurgically processed to recover the REEs.

The smelting process created slags with complex mineralogy, each with its own leachability with regards to the REEs. Through experimentation it became apparent the presence of B (added via $Na_2B_4O_7$ flux) is key in creating leachable slags from which 99% of the REEs can be extracted. The presence of B leads to a slag from which all REEs can be leached with diluted (2 M) HNO_3. Without B less than 60 % of the REEs can be leached from the slags, even using undiluted Aqua Regia.

The presence of B leads to highly soluble REE phases in the slags, but it also leads to the co-dissolution of several other elements. To separate the REEs from these elements a solvent extraction process was developed together with Elemetal, using D2EHPA and kerosene. The developed solvent extraction process requires 1 extraction, 2 washing and 1 stripping stage to separate the REEs from the other elements with a 99 % efficiency. The REEs are recovered as oxides with oxalic acid precipitation and calcination of the resulting oxalates.

These processes were combined in a complete flowsheet that is described in Chapter 7, see Figure 7.13.

8.2. Recommendations

8.2.1. Mine tailings

While a viable recycling strategy was developed for the mine tailings, further research into finding a less energy- and chemicals-intensive method for dissolving monazite would greatly benefit the recycling process. In-depth research on how to handle the produced waste streams, especially the nitrated ones, will also be crucial in translating the developed flowsheets into actual industrially viable processes.

A more in-depth study on the influence of microwaves on the acidic dissolution and alkaline conversion behaviour of monazite would certainly yield more conclusive results than those found in this work. Isolating the effects of microwave irradiation would require equipment which can control over the microwave focus point, wave frequency and power output. Comparing the leaching systems, with those performed with apolar solvents would also yield more information on the heterogeneous heating potential of the microwave irradiation.

8.2.2. The shredded WEEE

It is believed that the developed hydrometallurgical recycling process described in chapter 6 forms a viable basis for the development of a small scale industrial process. To achieve this, the process needs to be tested and optimised on a pilot scale in order to observe whether or not the lab scale results can be replicated on a larger scale.

Further optimisation studies on the recovery of Cu and Zn prior to the Nd recovery would also greatly improve the hydrometallurgical recycling process. This can also improve the combined pyro-hydrometallurgical process as well as it would solve the challenge of Cu in steel scrap.

For the combined pyro-hydrometallurgical recycling process, additional research into the effect of B on the leachability of Nd from slags is needed. The underlying mechanism of the influence of B is not known at this time and would serve as an excellent starting point for further research into the development of combined pyro-hydrometallurgical extraction of REEs.

Summary

The rare earth elements (REEs) are a material group that is becoming increasingly important in modern day technologies, with applications in electronics (e.g. FeNdB magnets and luminescent phosphors), chemical industry (e.g. REE catalysts), energy industry (e.g. NiMH batteries and windmills) and medicine (e.g. Gd MRI contrast fluid).

Considering the importance of REEs, a steady and secure supply is essential. However, the European Union does not have any domestic production of these elements and is reliant on import from China to meet its REE demand. With the volatility of the REE market and potential Chinese export restrictions, the EU has begun exploring secondary low-grade resources to mitigate a potential shortage of REEs.

The possibility of extracting REEs from two such resources: (1) mine tailings from LKAB (Luossavaara-Kiirunavaara Aktiebolag) iron ore mine at Kiruna, Sweden, and (2) the ferrous fraction of the shredded WEEE from the WEEE shredder at INDUMETAL RECYCLING, Spain is investigated in this thesis. These resources share the characteristic that they are available in high volumes and have a minor fraction of assorted REEs. The mine tailings consist of various gangue minerals, of which apatite and monazite are the REE-bearing minerals of interest. Apatite is one of the primary resources in the production of phosphoric acid and monazite is one of the primary resources of REEs. The ferrous fraction of shredded WEEE is a primarily metallic material, mainly composed of steel scrap fragments. The REEs in this resource are present as NdFeB magnet particles adhering to the steel fragments.

The development of the flowsheets for the mine tailings focusses on the recovery of both the REEs and the phosphorous. To achieve this, processes from the phosphoric acid industry and the primary REE industry are combined. Three flowsheets were developed to achieve this: (1) an acidic flowsheet (see section 4.4.5.), (2) a combined acid-alkaline flowsheet (see section 4.6.4.) and (3) a microwave-driven autoclave flowsheet (see section 5.6.). Each of these flowsheets has the same initial process step, a nitric acid leach to dissolve the apatite and produce a H_3PO_4 solution.

In the acidic process a highly concentrated HNO_3 solution is used to co-dissolve the heavy REEs associated with the apatite and prevent their re-precipitation through reaction with H_3PO_4. Then the REEs and phosphorous are separated through solvent extraction to yield two end-product streams. In the combined acid-alkaline flowsheet a low concentration nitric acid solution is used during the leaching step, which concentrates both light and heavy REEs in the leach residue. Then the leach residue is treated with NaOH in a furnace to convert the $REEPO_4$ to $REE(OH)_3$ similar to primary REE industry. The $REE(OH)_3$ is then dissolved and selectively re-precipitated as $REE2(C_2O_4)_3$. This precipitate is then calcined to form the REO end-product. The microwave-driven autoclave flowsheet is an adaptation of the combined acid-alkaline flowsheet, where the alkaline conversion process is replaced with the microwave-driven autoclave process. In the microwave process microwave heating is used to efficiently heat a concentrated H_2SO_4 solution to 200°C to dissolve the leach residue of the HNO_3 leaching step. This dissolves over 80 % of the REEs which are then recovered and concentrated via solvent extraction.

The development of the flowsheets for the shredded WEEE focusses on selectivity of the REE extraction over that of Fe. This selectivity is enabled in two ways: (1) oxidation of the Fe through water corrosion (see section 6.6) and (2) oxidation of REEs through pyrometallurgical slagging (see section 7.6).

The water corrosion process converts the metallic Fe to $Fe(OH)_3$, which allows the REEs to be selectively leached with diluted H_2SO_4. From the resulting leach liquor the REEs are recovered via precipitation with Na_2SO_4. This results in recovery of REEs as $(REE,Na)(SO_4)_2$ without the need for solvent extraction. The pyrometallurgical slagging concentrates the REEs into an iron free slag phase, from which they are then leached with HNO_3. To enable full extraction the REEs from the slags borax is required as a fluxing agent during the slagging process. The REEs are recovered from the resulting leach liquor via solvent extraction with D2EHPA and precipitated with $H_2C_2O_4$.

The development of these flowsheets shows that the possibility exists for recovering REEs from low-grade secondary resources. The experimental work performed for this thesis, combined with the proposed flowsheets, provide a first step into the development of an industrial REE-recovery process within the EU.

Samenvatting

De “rare earth elements (REEs)” (zeldzame-aardelementen) zijn een grondstof die steeds crucialer wordt in de ontwikkeling van moderne technologieën, met toepassingen in elektronica (b.v. FeNdB magneten en luminescente fosfor), de chemische industrie (b.v. REE-katalysatoren), de energie industrie (b.v. NiMH batterijen en windmolens) en in de medische wereld (b.v. Gd MRI contrast vloeistof).

Gezien het belang van de REEs, is een stabiele en constante bevoorrading van deze elementen essentieel. De Europese unie heeft echter geen binnenlandse productie van REEs en is dus geheel afhankelijk van Chinese import om aan zijn REE noden te voldoen. Door de volatiliteit van de REE markt en de mogelijke restricties van China op hun export, is de EU begonnen aan het verkennen van mogelijke alternatieve bronnen van REEs. Hiervoor wordt gekeken naar grondstoffen van een mindere kwaliteit die in grote volumes beschikbaar zijn.

Deze thesis onderzoekt de mogelijkheid om REEs te extraheren uit twee van zo’n grondstoffen: (1) mijnafval van de LKAB (Luossavaara-Kiirunavaara Aktiebolag) ijzerertsmijn in Kiruna, Zweden en (2) de ijzerfractie van versnipperd WEEE afkomstig van de WEEE versnipperaar van INDUMETAL RECYCLING, Spanje. Beide grondstoffen zijn beschikbaar in grote volumes en bevatten een kleine fractie van verscheidene REEs. Het mijnafval bestaat uit verschillende ganggesteenten, waarvan apatiet en monaziet de mineralen zijn die REEs bevatten. Apatiet is een van de voornaamste grondstoffen in de productie van fosforzuur en monaziet is een van voornaamste mineralen waar industrieel REEs uit gewonnen worden. De ijzerfractie van versnipperd WEEE is een hoofdzakelijk metallisch materiaal, bestaande uit voornamelijk ijzeren fragmenten. De REEs in deze stroom zijn NdFeB magneetfragmenten die magnetisch gebonden zijn aan het ijzer.

De ontwikkeling van flowsheets voor het mijnafval focust zich op het winnen van zowel het fosfor uit het apatiet als de REEs uit het monaziet. Om dit te bereiken zijn processen van de fosforzuurindustrie gecombineerd met processen van de REE-industrie. Dit heeft geleid tot de ontwikkeling van drie flowsheets: (1) een zuur gebaseerde flowsheet (zie sectie 4.4.5.), (2) een flowsheet met zowel zuur als alkalisch milieu (zie sectie 4.6.4) en (3) een flowsheet die gebruik maakt van een microgolf-autoclaaf systeem (zie sectie 5.6.). Elk van deze flowsheets start met hetzelfde proces, een loging met salpeterzuur om het apatiet op te lossen en een fosforzuuroplossing te creëren.

De zuurgebaseerde flowsheet gebruikt een hoog geconcentreerde HNO_3 oplossing om de zware REEs, die met het apatiet geassocieerd zijn, ook in oplossing te brengen. De hoge zuurconcentratie voorkomt ook dat de opgeloste REEs terug neerslaan via reactie met H_3PO_4. Na loging worden het H_3PO_4 en de REEs van elkaar gescheiden door middel van solvent extractie. Hierdoor worden twee eindproductstromen gecreëerd. De gecombineerde zuur-alkalische flowsheet gebruikt daarentegen een HNO_3-oplossing van lage concentratie tijdens de loogstap. Dit concentreert zowel de lichte als de zware REEs in het loogresidu. Het loogresidu wordt dan behandeld met NaOH in een oven om het $REEPO_4$ om te zetten in $REE(OH)_3$. Het gevormde $REE(OH)_3$ kan dan opgelost worden om vervolgens selectief te worden neergeslagen als $REE_2(C_2O_4)_3$. Als laatste stap wordt het precipitaat gecalcineerd tot het REO eindproduct. De microgolf-autoclaaf flowsheet is een aanpassing van de zuur-alkalische flowsheet, waar het NaOH conversie proces is vervangen door het microgolf-autoclaaf proces. Dit proces gebruikt microgolven om efficiënt een geconcentreerde H_2SO_4 oplossing tot 200°C te brengen,

om zo het loog residu van de HNO_3 loging in oplossing te brengen. Dit proces extraheert meer dan 80% van de REEs in het residu, waarna ze gewonnen worden via solvent extractie.

Bij de ontwikkeling van de flowsheets voor versnipperd WEEE wordt de selectiviteit van de extractie van REEs over die van ijzer vooropgesteld. Deze selectiviteit wordt gehaald via twee manieren: (1) oxidatie van Fe door corrosie (zie sectie 6.6) en (2) oxidatie van de REEs via pyrometallurgische verslakking (zie sectie 7.6).

Het corrosieproces converteert het metallische Fe tot $Fe(OH)_3$, hetgeen mogelijk maakt om de REEs selectief te logen met een verdunde H_2SO_4-oplossing. De REEs worden neergeslagen uit de resulteerde loogoplossing door reactie met Na_2SO_4. Dit maakt het mogelijk om de REEs selectief te winnen als $(REE,Na)(SO_4)_2$ zonder de nood aan solventextractie. Het pyrometallurgisch verslakkingsproces concentreert de REEs in een ijzer-vrije slakfase, waaruit ze dan geloogd worden met een HNO_3-oplossing. Om volledige REE-extractie uit de slakken te garanderen moet borax gebruikt worden als flux-middel tijdens het verslakkingsproces. De REEs worden gewonnen uit de loogoplossing via solventextractie met D2EHPA en worden vervolgens neergeslagen met $H_2C_2O_4$.

De ontwikkeling van deze flowsheets toont aan dat het mogelijk is om REEs te winnen uit grondstoffen van mindere kwaliteit. Het experimenteel werk uitgevoerd voor deze thesis, samen met de voorgestelde flowsheets, voorzien een basis waarop een industrieel REE-winningsproces kan worden ontwikkeld voor de EU.

Acknowledgements

Firstly, I would like to thank my daily supervisor and promotor Yongxiang Yang. His tireless effort and guidance were invaluable during my research. He helped me find my way in the field of hydrometallurgy and the chemistry or rare earths. Just as important was the help and advice of my second promotor Jilt Sietsma. His experience and outside viewpoints were extremely helpful.

Secondly, I would like to thank my colleagues Prakash Venkatesan, Aida Abbasalizadeh, Xiaoling Guo, Dharm Jeet Gavel and Zhi Sun. Our endless discussions, about work and otherwise, were the highlights of my research. Prakash especially made the times in the lab an absolute joy. Zhi also deserves special mention as his efforts as the resident post doc allowed me to hit the ground running and made sure everything was done right. I would also like to thank our lab supervisor Sander van Asperen. He made it possible for all of us to work efficiently and without worry. He was always ready to help and his enthusiasm was infectious. A special thank you is also in order for Kees Kwakernaak, Ruud Hendrikx and Michel van den Brink. The endless amounts of analyses they ran for me were instrumental for the completion of this thesis.

Finally, I would like to thank my friends and family. Their support during these four years cannot be overstated. My parents, Christine Van Marcke and Dirk Peelman, especially made sure that nothing stood in my way to achieve my goals.

To all of you: thank you.

I also want acknowledge the financial support under the EU Project FP7 REEcover (Project ID: 603564), and thank the project partners at INDUMETAL RECYCLING, Spain, for providing the ferrous WEEE input material; the Luleå University of Technology, Sweden for providing and physically upgrading both the tailings and the WEEE; NTNU, Norway for providing the slags of the smelted WEEE; and Elemetal for conducting the solvent extraction of the leached slags.

List of Publications

S. Peelman, D. Kooijman, J. Sietsma & Y. Yang "Hydrometallurgical Recovery of Rare Earth Elements from Mine Tailings and WEEE", Journal of Sustainable Metallurgy, vol.4, pp. 367-377, 2018.

S. Peelman, J. Sietsma & Y. Yang, "Recovery of Neodymium as $(Na,Nd)(SO_4)_2$ from the Ferrous Fraction of a General WEEE Shredder Stream", Journal of Sustainable Metallurgy, vol. 4, pp.276-287, 2018.

S. Peelman, Z. H. I. Sun, J. Sietsma, and Y. Yang, "Hydrometallurgical extraction of rare earth elements from low grade mine tailings". In: Alam S., Kim H., Neelameggham N.R., Ouchi T., Oosterhof H. (eds) Rare Metal Technology 2016.

S. Peelman, Z. H. I. Sun, J. Sietsma, and Y. Yang, "Leaching of rare earth elements: review of past and present technologies", in *Rare Earths Industry technological, economic and environmental Implications,* Elsivier, pp 319-334, 2016.

S. Peelman, Z. H. I. Sun, J. Sietsma, and Y. Yang, "Leaching of Rare Earth Elements: Past and Present", in *the proceedings of ERES 2014: 1st European Rare earth resources Conference,* pp 446-456, Greece 2014.

Curriculum Vitae

Personal information:

Sebastiaan Peelman

Born in Ghent 24-12-1990

Work experience:

05/2018 – present: project manager hydrometallurgy at Umicore R&D

Education:

02/2014 – 02/2018:	PhD researcher at Delft University of Technology, department of Materials Science and Engineering, group Material Production, Refining and Recycling.
09/2013 – 11/2013:	PhD researcher at University of Ghent (terminated due to lack of funding).
09/2011 – 02/2013:	Master of Science in Materials Engineering: Metallurgy at the University of Ghent.
09/2008 - 02/2011:	Bachelor in Chemical and Material Engineering at the University of Ghent.